UNIVERSITY OF WALES, TRINITY SAINT DAVID

From Practice to Theory: Computational Studies on Fluorescence Detection and Laser Therapy in Dermatology

by

Nick van der Beek, LL.M, M.Sc

Director of Studies: Prof. Kelvin Donne

Second Supervisor: Dr. Owen Williams

A thesis submitted in partial fulfilment for the degree of Doctor of Philosophy

in the

Faculty of Architecture, Computing and Engineering

School of Applied Computing

October 8th, 2017

Abstract

Computational studies on light-tissue interactions in medical treatment and diagnosis have offered deeper insights in the processes underlying laser treatments and fluorescence measurements. I apply this approach in the study of fluorescence detection and of laser therapy.

First, I investigate three methods of fluorescence detection and the reported contrast between healthy skin and malignant tissue. I varied the concentration of haemoglobin in the target, the concentration of melanin in the epidermis, the scattering of light in the skin, the depth at which the target is located in the skin, the width of the target, the thickness of the target, the concentration of photosensitizer in the target, and the concentration of photosensitizer in the skin. My findings confirm previous clinical studies in that the auto-fluorescence corrected fluorescence detection method generally shows a higher contrast than the other methods. The results support earlier clinical studies and are in accordance with expert experience.

Second, I study laser therapy for psoriasis. In a series of simulations, I analyse three types of pulsed dye laser systems and one IPL system. The investigated biological effects are heat shock proteins, hyperthermic tissue damage and vasoconstriction of the microvasculature. The changes in the skin concern blood volume, blood oxygenation and scattering in the epidermis. The calculations show that there are some notable differences in the effect changes in the composition of psoriatic tissue has on the efficacy of laser and IPL therapy. Still, Inter-device variance was more prominent than intra-geometry variance.

My study adds to the understanding of fluorescence detection of keratinocyte skin cancers, as well as that of laser therapy for psoriasis. Additionally, it offers potential avenues for increasing the efficacy and efficiency of these therapies.

(T)he only way in which a human being can make some approach to knowing the whole of a subject, is by hearing what can be said about it by persons of every variety of opinion, and studying all modes in which it can be looked at by every character of mind. No wise man ever acquired his wisdom in any mode but this; nor is it in the nature of human intellect to become wise in any other manner.

John Stuart Mill, in On Liberty, 1859

The sciences do not try to explain, they hardly even try to interpret, they mainly make models. By a model is meant a mathematical construct which, with the addition of certain verbal interpretations, describes observed phenomena. The justification of such a mathematical construct is solely and precisely that it is expected to work.

John von Neumann, in the Unity of Knowledge, 1955

Table of contents

List of figures

List of tables

1. Introduction

1.1 Context of the Problem

Of all organs of the human body, the skin is among the most accessible. Easy to touch and directly observable, we'd expect it to divulge all its secrets at first notice. Alas, in reality both the limitations of our clinical research methods and the complexities of the skin have made the quest for knowledge on the conditions of the human skin rather difficult. Subtle neurological or immunological responses to internal and external triggers are not susceptible to direct observations, making the "easy access" to the skin rather misleading.

In practice dermatologists, like so many other researchers, have to resort to scientific methods in order to better understand the diseases and conditions that affect the normal functioning of our skin. The best-known method to do so is the clinical trial: treat patients with what one think works and see how their condition improves. Methodological refinements have increased the accuracy of this tool. We now are used to strict randomization and blinding in order to prevent deliberate or implicit bias. But the essence remains the same: Treat a large number of patients and see what happens. Or at least test a large number of people, as in the case of epidemiological studies.

This is not the only way we can investigate the skin. Laboratories are filled with specially crafted mice and other test animals, which literally sacrifice their lives for science. In some cases, it is possible to construct a phantom. The collection and testing of tissue samples as well as the use of in vitro experiments are similar in approach. We do not look at the patient, but at some real-world alternative which, at least we hope, sufficiently approaches the human body / skin.

A third way in which the human skin can be studied, at least for some applications is mathematical modelling. Assuming that sufficient data is available, we can use the lessons learned in chemistry, physics, biology, any many other fields to create a quite abstract but detailed representation of the skin. Abstract in the sense that the model often leaves out a lot of details, detailed because each variable can be studied at every moment or location.

This distinction to our opinion is not unique to medicine or dermatology. In economics too we see the use of large sets of empirical data, the application of laboratories and questionnaires, and the use of abstract logical methods of analysis including the application of mathematical models. That is, econometrics collect tremendous amounts of data on firms, industries and countries and thereby try to elucidate "what works". Behavioural economists and game theorists love inviting oblivious students to play their games, learning more and more about how rational human economic decisions really are. But the best-known instruments in economics rely on abstract theories and mathematical models, applied to explain the best macro-economic policy, build a foundation for the regulation of markets by governments, or the decision by an individual to start working on a Ph.D.

In the work presented below, I apply mathematical models in order to better understand the way certain clinical dermatological methods work or can be improved. At the outset, we know that these therapeutic and diagnostical methods are effective. The clinical trials have been conducted, even when the level of rigor can often be increased. But these trials haven't explained how certain methods work and others do not. As we shall see below, the level of detail and control that can be achieved with the mathematical modelling cannot reasonably be achieved in a clinical setting, or at least not within reasonable financial and time limits. Let us introduce the two dermatological techniques that will now be considered for further analysis.

In chapter three I model the fluorescence detection of keratinocyte skin cancers (KSC). Fluorescence and phosphorescence describe variants of the phenomenon that certain molecules emit visible light when irradiated using an appropriate light source (1). To be precise, I analyse a system for fluorescence detection that is used in clinical practice called the DyaDerm Expert. It comprises of a detector head containing white light LEDs, 409 nm LEDs and a CMOS chip, which are controlled through a trigger box which itself is connected to a personal computer running Microsoft Windows. The front of the detector head is visible in figure 1. The image is captured using the sensor mounted in the centre of the head. The outer ring contains the LEDs: The smaller circles are the white light emitting LEDs and the larger circles belong to the 409 nm LEDs. Figure 2 illustrates the situation during a measurement. In a darkened room the patient is positioned in front of a blue or black background. The detector head, here mounted on

a robot, is positioned in front of the area to be investigated and the measurements are performed. The LEDs emit pulsed light (1Hrz) and the images are captured in between the pulses.

A common misconception is that these systems are best used to diagnose a suspicious lesion. More conventional techniques such as dermatoscopy are better suited for that purpose. Rather fluorescence detection is intended to discover areas which have a high likelihood of containing a KSC, i.e. the stage prior to making a diagnosis. This way a clinician can find lesions that are not readily observed with the naked eye (2). The rationale for using such a device is that earlier treatment is associated with higher cure rates: commonly applied treatments for KSC such as 5-fluorouracil have a modest clearance rate of 70% after one year (3,4). Because these systems are intended to detect lesions at the earliest opportunity, it is important to understand their limitations. Using a parametric study, I investigate the effect of optical and morphological changes on the ability of three methods of fluorescence detection to detect the presence of a tumour based on the difference in emitted fluorescence from the target and the surrounding healthy skin. These parameters are the scattering coefficient of light in the skin, blood content of the target, melanin content of the epidermis, width, thickness and location of the target, and concentration of fluorophore in the target and surrounding tissue.

Figure 1: Detector head of the DyaDerm Expert fluorescence detection system.

Figure 2: Situation when performing fluorescence detection.

The fourth chapter is dedicated to psoriasis, a chronic and burdensome skin condition which is characterized by the presence of red and scaly lesions, which are often accompanied by persistent itching. Psoriasis can have a considerable negative impact on the quality of life of the patients, and if so, is treated using a wide range of therapeutic modalities ranging from topical corticosteroids to systemic drugs targeted at the immune system. Light based therapies for psoriasis include photochemotherapy, UV therapy and laser therapy. These treatments are known for their relative long duration of treatment free remission (5,6). I consider four different laser or intense light systems, three of which have been previously described in the treatment of psoriasis, and investigate how certain variations in psoriasis affect their efficacy. The studied systems are the 577 nm Pulsed Dye Laser (PDL), 585 nm PDL, 595 nm PDL and an Intense Pulsed Light (IPL) system designed for skin rejuvenation. Figure 3 shows a 595 nm PDL system, the V-Beam by Candela. The laser itself is shown in the background, and the delivery system is placed on the skin. Similarly, figure 4 shows the Nordlys by Ellipse, an IPL system. The right side of the image shows the applicator, the hexagon crystal serves as a light guide and is placed on the skin.
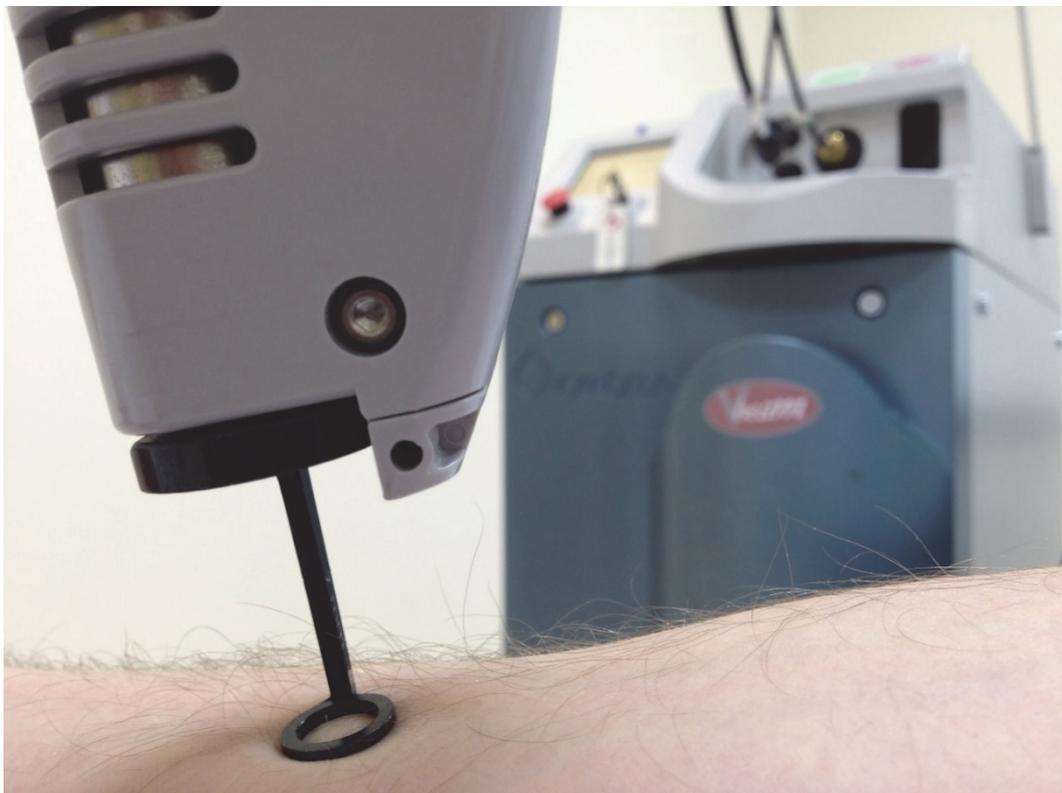
Figure 3: 595 nm PDL system (Candela V-Beam)

Figure 4: IPL system with 10 mm applicator (Ellipse Nordlys and PRS applicator)

The variations are changes in blood oxygenation, blood concentration in the skin and scattering in the epidermis.

The motivation for these investigations stems from discussions I had with clinicians who apply these techniques in their day-to-day provision of care for patients. By increasing our knowledge of these techniques, we can improve the quality of care that is provided, and perhaps extend the application of these techniques beyond their current scope.

Fluorescence detection has not seen widespread adaptation in dermatological practice. Therefore, the body of experience is rather limited. The analysis contained in the subsequent chapters can, to a degree, act as a substitute for the limited experience, elucidating some of the limitations of the approach. There is an ongoing discussion within the dermatological profession regarding the need for early detection: Most KSC develop slowly, and monitoring is a costly activity. I note that this is a question for the dismal science and not a medical issue. The scientific community has developed proper tools which would aid us in determining the optimal method of surveillance, assuming the dermatologists and GP's can provide us with the data of sufficient quality. The question can be formulated as a simple problem of decision-making under uncertainty, as described in the handbook by Hirschleifer and Riley (7). To my knowledge, such an analysis has not been performed, making the question whether or not it is desirable that

most patients being treated for skin cancer are likely going home with an untreated, not observed lesion, not something we need to concern ourselves with for this research. It does suggest that, given the low rate of technological innovation in medical dermatology, computational analysis as a substitute for clinical real life experience is a worthwhile endeavour.

Laser therapy for psoriasis, like fluorescence detection, is a technique which is applied more often in specialised clinics such as those located in academic medical centres, than in regional hospitals. The equipment used for the therapy requires substantial investment, and return on investment might be an issue in systems with national health care insurance / provision. Thus, experience again is limited, making computational modelling an interesting alternative to clinical experience or clinical studies. The limited interest of the dermatological community in laser therapy for psoriasis is to the detriment of their patients. Current treatments, such as methotrexate, show limited efficacy, short duration of remission and serious potential side effects. For example, prolonged use is associated with a marked increase in the risk for KSC (5,8,9). In addition to the relative small number of clinics being able or willing to provide patients with laser therapy, dermatologists usually restrict the application of this modality to patients in which a limited surface area is affected by the disease. Consequently, a large portion of the population is deprived from having access to this treatment modality. Given the relative long duration of treatment free remission, and the excessive costs of some systemic drugs this is an unsatisfying outcome for patient and society. The inconsistency of this traditional view is even more obvious when we consider that treating large areas of skin for cosmetic purposes is not considered to be an issue. This needs to change, and perhaps the insights formed in this work allows us to take another step towards the full body laser treatment of psoriasis.

One could extend the argument in favour of the use of analytical rather than clinical methods to a utopian worldview. Clinical and animal research involves subjecting sentient beings to potential harm. Research implies uncertainty and risk: some treatments will show to be ineffective. Others will cause severe adverse events. Complications can and do result in loss of life. Furthermore, practical limitations affect the depth of knowledge that is acquired. Clinical research requires treatment groups of sufficient size, implying that there is a bias towards the most common type of patient.

Ethically, from a welfare perspective, this is undesirable (10). Analytical methods do not suffer from these problems. In a world where the models are sufficiently accurate, the data on the relevant properties are known, and sufficient computing power is available, we could discover the complete therapeutic potential of an intervention for all possible types of patient without ever having to harm anyone. Regardless if the nature of the intervention is pharmacological, surgical or psychoanalytical. One could regard the use of deep learning algorithms for diagnostical purposes as a first step towards this development. Computers will find variables we as humans have missed. Alas, we are far from a world in which the scientific knowledge on the human physiology and the pathology of diseases is sufficient to design accurate complete models. Data on properties of human tissue is scarce and published results can vary wildly, a problem addressed by Welch et al. under the heading "Second task of tissue optics" (11). Computing power is a valuable resource, and there is much potential for analytical methods for research on medical treatments.

1.2 Hypotheses

To increase our knowledge of the laser treatment for psoriasis using PDL and IPL, as well as our knowledge on the fluorescence detection of KSC, I conduct computational studies simulating these treatments and adjusting relevant parameters as to better understand how these parameters influence the efficacy and accuracy of the studied techniques.

The aim of the research is to improve our understanding of the effect of variations in technique and skin on the efficacy and accuracy of dermatological treatments. As I have worked for several years next to clinicians who apply these techniques on a daily basis, I was fortunate to observe the real-life performance of these techniques. The limitations studied are not hypothetical; they are chosen because in actual application situations are encountered in which practitioners ask themselves and others these questions. Physicians seek to apply the optimal therapy, choosing that method which is best suited for the patient, wanting to use those settings which will result in the optimal result. Since each patient is unique, often the question arises if settings need to be adapted or not and which technology is best suited.

The work presented below seeks to flesh out those situations that are seldom in practice, but valuable in terms of the acquisition of knowledge and experience. This

previous experience is used as a foundation for the computational analysis, with the objective of generating results that in turn can be used to improve clinical practice.

I will address the following hypotheses in my research.

1. The combined use of protoporphyrin IX (PpIX) fluorescence and auto fluorescence in fluorescence detection of KSC results in a higher reported contrast in terms of fluorescence between healthy skin and skin containing a KSC than the contrast reported by PpIX fluorescence or auto fluorescence alone.

2. The higher reported contrast by the combined method of fluorescence detection is not affected by an increase in scattering in the skin.

3. The higher reported contrast by the combined method of fluorescence detection is not affected by an increase in epidermal melanin.

4. The higher reported contrast by the combined method of fluorescence detection is not affected by an increase in vascularisation of the KSC.

5. The higher reported contrast by the combined method of fluorescence detection is not affected by a decrease in width of the KSC.

6. The higher reported contrast by the combined method of fluorescence detection is not affected by a decrease in the thickness of the KSC.

7. The higher reported contrast by the combined method of fluorescence detection is not affected by the depth of the KSC.

8. The higher reported contrast by the combined method of fluorescence detection is not affected by a decrease in PpIX concentration in the KSC.

9. The higher reported contrast by the combined method of fluorescence detection is not affected by an increase in PpIX concentration in the surrounding tissue.

10. PDL and IPL therapy can induce Heat Shock Protein 72i (HSP72i), vasoconstriction, and/or thermal injury in separate areas of the psoriatic skin.

11. The ability of PDL or IPL therapy to induce HSP72i, vasoconstriction, and/or thermal injury in psoriatic skin is affected by differences in blood oxygenation.

12. The ability of PDL or IPL therapy to induce HSP72i, vasoconstriction, and/or thermal injury in psoriatic skin is affected by differences in blood concentration.

13. The ability of PDL or IPL therapy to induce HSP72i, vasoconstriction, and/or thermal injury in psoriatic skin is affected by differences in light scattering in the epidermis.

1.3   Methodological approach

The work presented in this research is based on the application of three research methodologies.

First, I conduct a critical review of the scientific literature that is relevant for the performed study. The information and knowledge acquired from the work of previous studies then is used in a systematic study using a computational model, which is the second research method applied. The motivations for applying computational analysis have been discussed in section 1.1. The third research method consists of the comparison of the result of the analysis with published and unpublished clinical data and experience as a coarse benchmark for external consistency.

1.4   Structure of the thesis

Chapter two is devoted to a discussion of the structure of the skin and the theories and techniques used in the current study. Chapter three discusses the study of the fluorescence detection of KSC, and how it is affected by changes in the optical properties of the tissue, the geometry of the target, and the distribution of the photosensitiser. These studies show that some of these variables, such as the concentration of melanin in the epidermis, the concentration of haemoglobin in the tumour, and the concentration of protoporphyrin IX in target and tissue, have a significant effect on the accuracy of the different methods of fluorescence detection. Other factors do influence the accuracy of fluorescence detection, but more as a boundary condition. Tumour thickness is a good example of this: Too small tumours cannot be detected because

there hardly is a signal to detect, while thick tumours are not distinguishable from smaller tumours as the extra tumour tissue is hidden from observation.

The fourth chapter focusses on the treatment of psoriasis using pulsed dye laser systems and IPL. Instead of using some physical measure such as target vessel destruction, heat shock protein induction is regarded as the primary driver of the beneficial effects, and the classic hyperthermic damage measure as a countervailing effect, forcing the user to make a trade-off between heat shock protein induction and tissue damage. A third measure is vasoconstriction, which is registered because of a potential use in establishing the size of the heat shock protein induction now that this outcome cannot be readily observed. This outcome measure is determined for four devices: 577 nm PDL, 585 nm PDL, 595 nm PDL and one IPL. Since psoriatic lesions show a large clinical variation, the effect of these variations on the four systems is investigated. It is shown the systems differ in depth at which they can induce an effect. Differences in blood oxygenation, scattering in the epidermis, and blood concentration in the lesion have a limited effect on the behaviour of the devices. The required energy for a given biological effect does change, so clinicians are advised to take these factors into account when deciding which settings they would like to use.

The final chapter presents a short overview of the results and discusses how these can be used to improve clinical practice. Finally, some future avenues for research are discussed.

2. Theoretical framework

2.1   Structure of the skin

The following discussion of the structure of the skin is based on the introductory chapter of the eighth edition of Rook's handbook of dermatology (12). The skin is the largest organ of our body, having an area exceeding 2 m^2 in a 70kg adult. It forms a barrier preventing water loss, acts as an important immunological defence, serves in the thermoregulation of the human body, is a neurosensory interface with the outside world, through the sub-cutaneous fat prevents and limits trauma by acting as a cushion. The skin is comprised of the epidermis (50 – 1000 µm), the dermis (500 – 5000 µm) and the subcutaneous fat. In addition, it contains various adnexa which play a role in the maintenance of the skin and e.g. thermoregulation. A schematic representation of the skin is shown in figure 5.
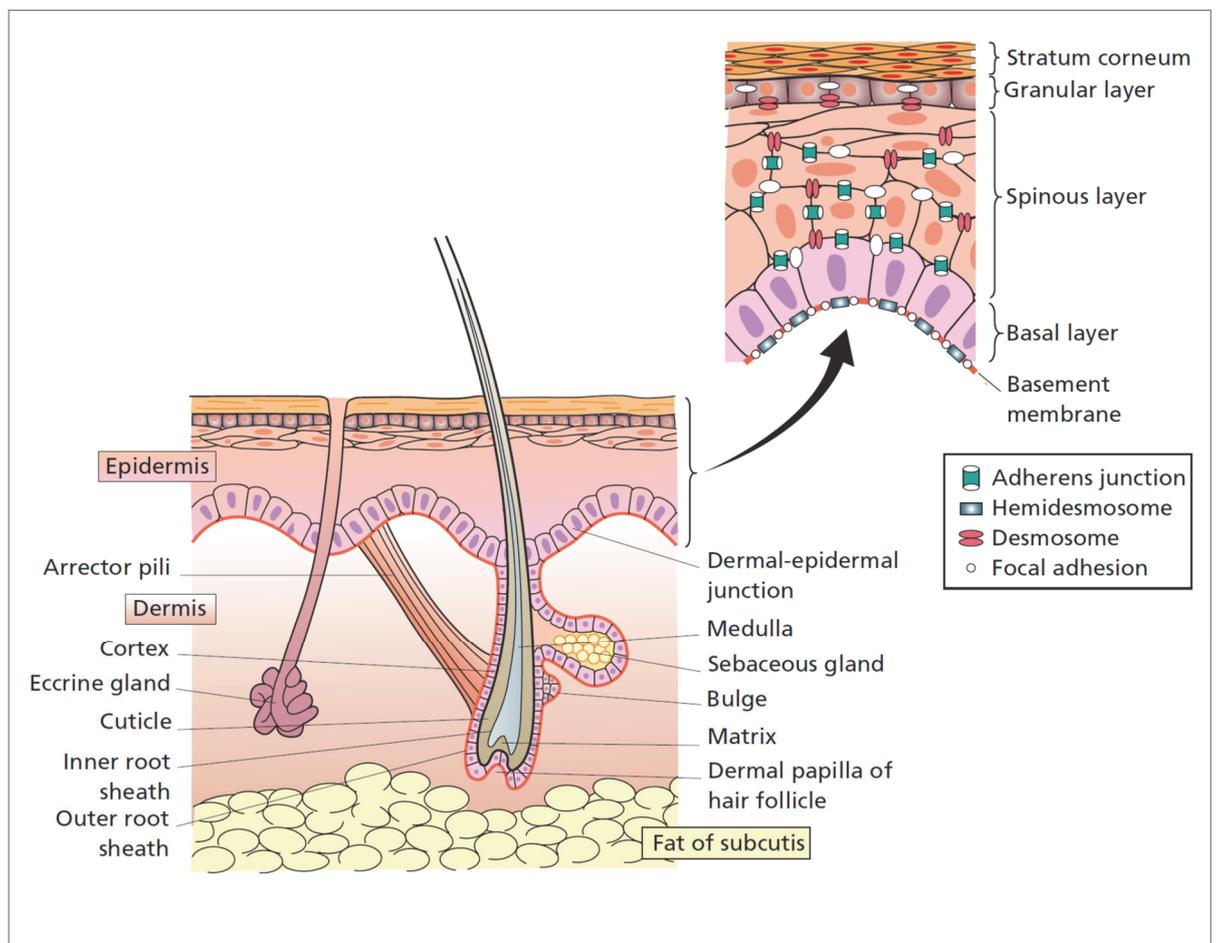
Figure 5: Structure of the skin (12)

The epidermis is the outermost part of the human skin and is mainly comprised of keratinocytes or corneocytes. The latter are cornified keratinocytes and envelop the skin, creating a very insoluble outer layer. The epidermis is continuously renewed: in healthy skin, it takes 30 days for the skin to completely renew. As can be seen in the abstract illustration of the epidermis as represented in figure 6, the structure of the epidermis is stratified, or layered. The lowest layer is a single line of basal cells and called the stratum Basale. Basal cells are rectangular cells and ordered side by side, much like the Phalanx of the Roman empire. The largest subset of basal cells is called transit-amplifying cells. When these cells divide one cell is moved into the next layer, the stratum spinosum. Once the transit-amplifying cells have reached eight divisions, they are released into the stratum spinosum as well. A limited subset of the basal cells though are stem cells: When they divide, new basal cells are created. In addition to the keratinocytes, there are also melanocytes and Langerhans cells present in the basal layer. The first are dendric cells responsible for the production and allocation of melanin. This natural pigment serves as an important protection against UV radiation, which can induce severe damage to human tissue. Melanin is of importance in light based therapies that use visible light, such as fluorescence detection and non-ablative laser therapy for psoriasis. Langerhans cells are also dendric cells, but act as anti-gen presenting cells: the envelop an anti-gen and transports it to the lymph nodes, which can elicit an immune response. Basal cells can develop into malignancies, which are called basal cell carcinomas (BCC). BCCs retain the palisading organisation of the keratinocytes and can be recognised in histopathology based on this property. BCCs tend not to metastise to other organs, although treatment is required as the BCC can damage other tissue through its unlimited progression. E.g. it can grow through the small channels contained in bones, thus reaching the brain or eyes.

The second layer of the epidermis is the stratum spinosum. Here the basal cells detached from the dermal membrane, are rounded and desmosomes are added. The most common form of skin cancer. Squamous cell carcinoma (SCC) originates from these squamous cells (13,14). It is this form of keratinocyte skin cancer that is capable of spreading to other organs. Although the probability of a SCC spreading to other parts of the body is generally held to be about 2%, the data acquired by Van der Leest in the Rotterdam study suggests that this is an significant underestimation (15–17).

The third layer is the stratum granulosum. Here the squamous cells are further flattened and lipids are produced which are important for the protective function of the cornified envelope. The grain-like keratinocytes also form a tight junction: the stratum granulosum acts as a secondary barrier, potentially enabling the shedding of the skin. In a mouse model, Yokouchi et al. found that the keratinocytes in the granular layer of the skin resemble Kelvin's tetrakaidekahedron, explaining the tight seal (18).

In palmoplantar skin there is an additional small layer, which due to its translucent nature is called the stratum lucidum.

The final layer of the epidermis is called the stratum corneum. Here the keratinocytes have lost their nucleus, are completely flattened, filled with filaments and contained in a layer of various types of fats. At that point they are no longer called keratinocytes, but corneocytes.
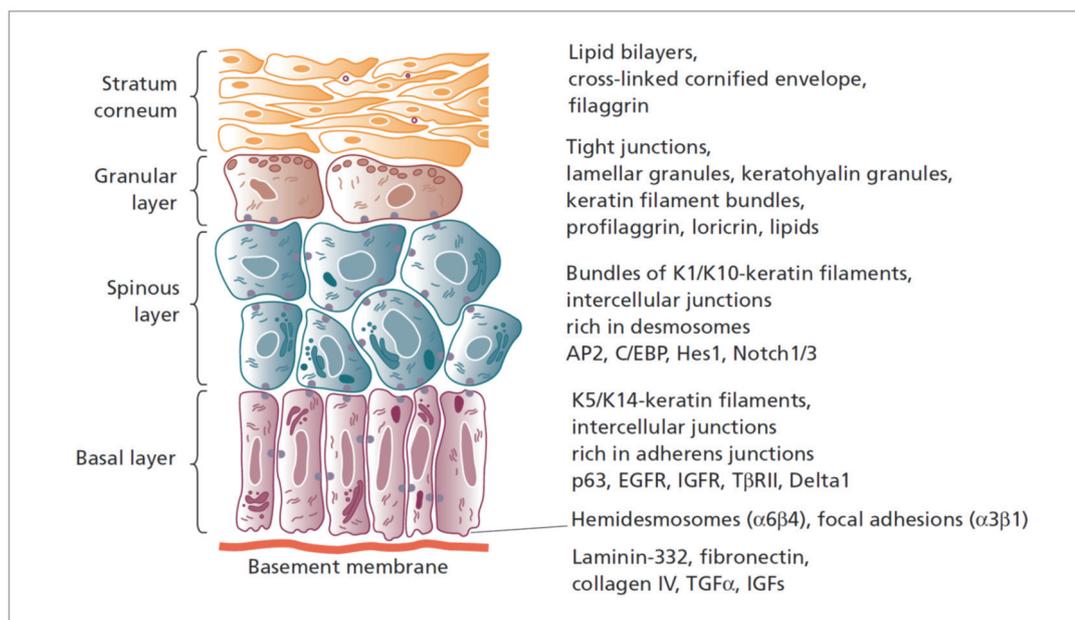
Figure 6: Differentiation of the epidermis (12).

The dermis and epidermis are separated by the basal membrane, which is permeable for a limited number of molecules. The dermis contains a large amount of water, thanks to the presence of molecules which are able to bind a large amount of water molecules. The structure of the dermis is not layered, like the epidermis, but more like a mesh created from collagen and, to a much lesser degree, elastin fibres. In addition to this mesh there are blood vessels, which provide oxygen and nutrients to the tissue and play

a central role in the thermoregulation of the body. Blood vessels are allocated in two planes, the superficial plexus and the reticular plexus. In particular, the first is an important target in vascular laser therapy, such as the treatment of acne or psoriasis. The lymphatic vessels and nodes drain the excess fluids and waste from the tissue, and are an integral part of the cutaneous immunology. The dermis contains several adnexa, such as the eccrine and apocrine sweat glands and the pilo-sebaceous unit. The latter provides the growth of hairs and the production and excretion of sebum. The hair root plays an important role in the regeneration of tissue, and contains a significant number of pluripotent cells.

The subcutaneous fat is located below the dermis and in non-obese humans contains 80% of the caloric reserves that are stored as fat.

2.2 Behaviour of light in tissue

2.2.1 Absorption

When light travels through a turbid medium, it is either scattered or absorbed. The probability that a photon is absorbed or scattered when traveling 1 meter through a given medium is called the absorption coefficient μ_a(m^{-1}) and scattering coefficient μ_a(m^{-1}) respectively.

The absorption coefficient of a medium is derived from the the molar extinction coefficient (MEC), or molar attenuation coefficient, of its constituent compounds. The MEC tells us the probability that a photon of a given wavelength is absorbed by one mole in a cm. Since I do not study the behaviour of individual compounds, but that of tissues which are comprised of a varying mixture of light absorbing compounds, it is more useful to work with the absorption coefficient of the medium. This is derived from the molar extinction coefficient (cm^{-1}M^{-1}), the molar mass (kgM^{-1}) and the concentration in the tissue (kgm^{-3}) of the light absorbing molecules.

$$\mu_a = \frac{MEC * concentration}{molar\ mass}$$

Equation 1: Calculation of absorption coefficient (cm^{-1})

An increase in a chromophore of fluorophore, such as melanin, haemoglobin, protoporphyrin IX, or flavin adenine nucleotide, results in an increased absorption of light in that medium.

The main light absorbing compounds in the skin are the two types of melanin, eumelanin and pheomelanin, and the two types of haemoglobin, oxyhaemoglobin and de-oxyhaemoglobin. Their MEC is shown in figures 7 and 8. Melanin plays an important role in the protection of the skin against the harmful effect of solar (and artificial) UVB and UVA radiation, and hence strongly absorbs those forms of "light". Longer wavelengths are more weakly absorbed. Haemoglobin is a particular strong absorber of blue light (400 – 450 nm), and a moderately absorber of green and yellow light (500 – 600 nm). Note that the curves for oxyhaemoglobin and de-oxyhaemoglobin generally lie close together, except for the double hump between 550 nm and 600 nm. As we shall see in the chapter on laser therapy for psoriasis, this difference is relevant for the efficacy of the various devices.
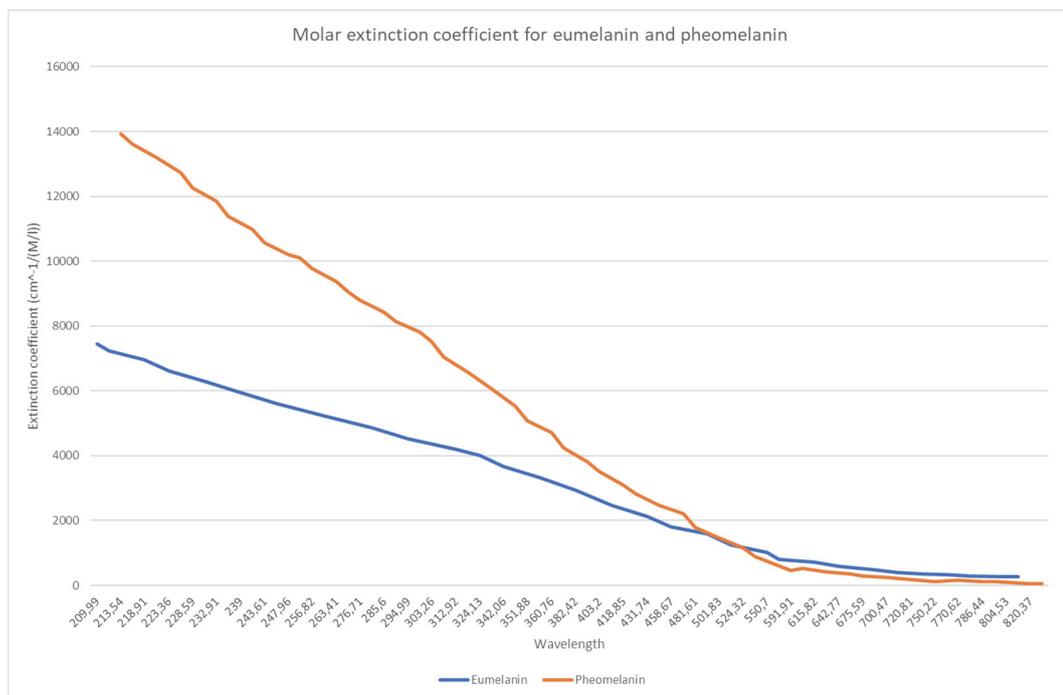
Figure 7: Extinction coefficient for Eumelanin and Pheomelanin (19)
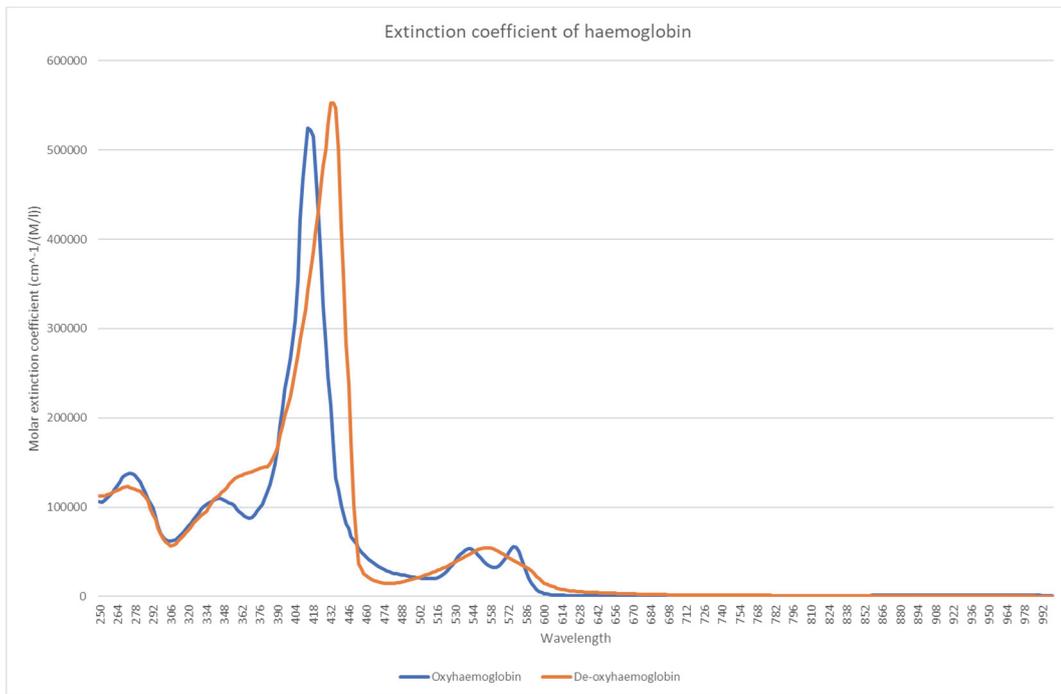
Figure 8: Molar extinction coefficient of Haemoglobin (20)

The effect of other light absorbing molecules contained in the skin are combined and treated as constituents of the "virgin" dermis or epidermis. Like haemoglobin and melanin, the remaining light absorbing compounds tend to absorb shorter wavelengths better than longer wavelengths. An example of this is illustrated in figure 9. Not illustrated is the absorption of light by water, which has a relative modest molar extinction coefficient over the range of visible light when compared to haemoglobin and melanin.
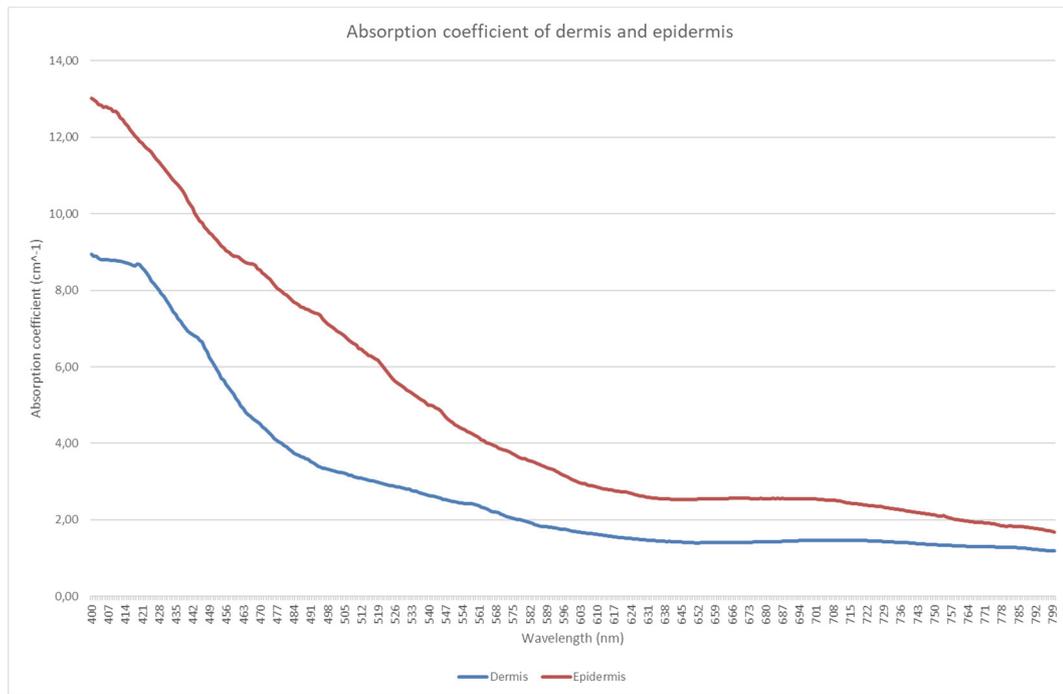
Figure 9: Absorption coefficient of dermis and epidermis (21)

Depending on the nature of the light source and the absorbing molecules light can cause various effects. These effects can occur simultaneously.

One class of events that can follow irradiation I have already mentioned are fluorescence and phosphorescence. Fluorescence and phosphorescence are used for the detection of skin cancer and can be used to investigate immunological mediated skin diseases (22). Phosphorescence and fluorescence differ in the lifetime of the exited state: Fluorescence results from the relaxation of the more unstable singlet state of exited molecules, whereas phosphorescence is produced when an exited triplet state of a molecule relaxes. The probability distribution of the wavelength of the emitted photons differ as well. Chapter three will discuss the use of fluorescence in the detection of the most common forms of skin cancer.

A second effect is heating of tissue. Energy lost by the absorbing molecules through vibrational relaxation causes an increase in heat. Thus, light can turn certain molecules, such as melanin, haemoglobin, or water, into heat sources. Selective heating of tissue is beneficial in the treatment of acne, psoriasis, atopic dermatitis and skin cancer to mention just a few (23–26).

A third class of effects which can be induced using light irradiation are photochemical. Examples are inter-molecular energy transfer, such as in photodynamic therapy (PDT) (27), intra-molecular energy transfer, dissociation, ionization such as in the production of plasma in the skin, and isomerisation, such as the isomerisation of urocanic acid in UV therapy (28).

2.2.2   Scattering

In order to be absorbed by a molecule or atom, the photon first needs to reach it. As the photon travels towards the molecule, it is affected by other molecules and atoms which results in scattering of the light particles. Scattering changes the direction in which light propagates. If inelastic scattering occurs, such as in Raman scattering, both direction and frequency of the light are changes. Raman scattering is used in Raman spectroscopy to detect basal cell carcinomas (29). Elastic scattering only changes the direction in which the photon travels. The two forms of scattering most relevant for my investigations are two forms of elastic scattering: Raleigh scattering and Mie. Raleigh scattering occurs when the molecule is much smaller than the wavelength of the light it interacts with. Oxygen and nitrogen molecules for example have a size of $60*10^{-12}$ m and $65*10^{-12}$ m respectively, much smaller than the wavelength of blue light, 400 nm. Raleigh scattering is different for shorter and longer wavelengths. Thanks to this effect, the sky usually is blue.   Mie scattering describes what happens when light interacts with a larger molecule. In those situations, there are multiple scattering events in the molecule, so that the difference in the treatment of different wavelengths cancels out. This is why clouds appear white. The scattering coefficient μ_s (m^{-1}) is used to describe the probability that a photon undergoes a scattering event when it travels 1 m through a medium. The skin is comprised of both relatively large and small molecules and structures, and thus exhibits both types of scattering.

2.2.3   Radiative transport

In a turbid medium like skin, the light-tissue interaction is determined by the scattering and absorption events. The next step then is to determine how light travels through a medium, or more precise, how the energy in terms of radiation is transported through the medium. For that purpose I shall use the Boltzmann Radiative Transport Equation (RTE) (11). The RTE is not a solution to Maxwell's equation, but rather a statistical

approximation of the transport of a photon particle in multiple scattering media. It states that the change in a beam of light L travelling in the direction s at point r, and travelling through a cylinder with infinite small area and infinite small length, is determined by the amount of light that is absorbed at that point, the amount of light that is scattered at that point, and the light that is scattered in from points in the medium.

$$\frac{dL(r,\hat{s})}{ds} = -(\mu_a + \mu_s)L(r,\hat{s}) + \mu_s \int_{4\pi} p(s,\hat{s}')L(r,\hat{s})\,d\omega'$$

Equation 2: Boltzmann Radiative Transport Equation

$p(s,\hat{s}')$ is the phase function and describes probability distribution of light being scattered in direction $\hat{s}'$ if it originates from direction s. For example, Raleigh scattering is more isotropic, i.e. the light is equally scattered in all directions, whereas Mie scattering is anisotropic with a forward momentum. More precise, anisotropy refers to the effect of a change in angle on the observed optical properties of the medium. The phase function has an angular and azimuthal component. The two components are independent of each-other. The azimuthal component depends on the index of refraction, and the angular component on the angle of the incoming light.

The phase function used in the studies presented below is the Henyey – Greensstein phase function, since it is considered to be appropriate for light transmission in tissue (30).

$$p(\cos\theta) = \frac{\mu_s}{\mu_a + \mu_s} \cdot \frac{1 - g^2}{(1 + g^2 - 2g\cos\theta)^{\frac{3}{2}}}$$

Equation 3: Henyey-Greenstein phase function for turbid media (31)

Here g is the anisotropy factor $g = \int_{4\pi} p(s,\hat{s}')\,(s,\hat{s}')d\omega$: the expected average cosine of the scattering angle. If it has a value of -1, all the light is backscattered and if it has a value of 1 all light is scattered forward. A anisotropy factor with value 0 could be isotropic, but also anisotropic scattering, e.g. if the probability of perfect forward scattering and perfect backscattering are equal. The value of g for skin differs with wavelength due to the inhomogeneous nature of skin and its mix of Raleigh and Mie scattering.

The code used in this research uses a different formulation of the Henyey-Greenstein phase function:

$$p(\theta) = \frac{\frac{1}{2}(1-g)^2}{(1-2g\cos\theta + g^2)^{\frac{3}{2}}}$$

Equation 4: Henyey-Greenstein phase function used in the code

The reason for this function rather than the one mentioned above is that in the hop-drop-and-spin algorithm in each drop only a fraction of the bundle of photons is deposited. This fraction is $\frac{\mu_a}{\mu_a + \mu_s}$, so that the fraction $\frac{\mu_s}{\mu_a + \mu_s}$ is scattered.

Alternatives to the Henyey-Greenstein phase function are the linear anisotropy phase function and its extension, the delta-Eddington approximation. However the Henyey-Greenstein phase function has become the accepted standard to represent photon transmission through turbid tissue. The alternative phase functions are not used in the thesis, and the interested reader is referred to the discussion by Willem Star in chapter 6.3.7. of the textbook by Welch and Van Gemert (32).

2.2.4 Lambert-Beer law

Since the transport of light through a medium depends on both absorption and scattering, it can add to the understanding of the behaviour of light by considering the effect of absorption and scattering independent from each other. For media where absorption is much stronger than scattering, the attenuation of light can be described using Lambert-Beer law. In situations when a collimated beam of light travels through a homogeneous, highly absorbing tissue in which there are very few scattering events scattering is of minor importance, and the phase function can be ignored. The Lambert-Beer law states that the attenuation of light in a medium is described by the function

$$E_{(z)} = E_0(1 - r_{sc})e^{-(\mu_a + \mu_s)z}$$

Equation 5: Lambert-Beer law from (11)

Where $E_{(z)}$ is the fluence rate at point z (Wm^{-2}), z (m) is the distance from the surface z, r_{sc} is Fresnel surface reflection of the collimated light striking the external surface, and E_0 is the collimated irradiance. r_{sc} relates to what happens when light crosses from one medium to another, a topic that is treated below.
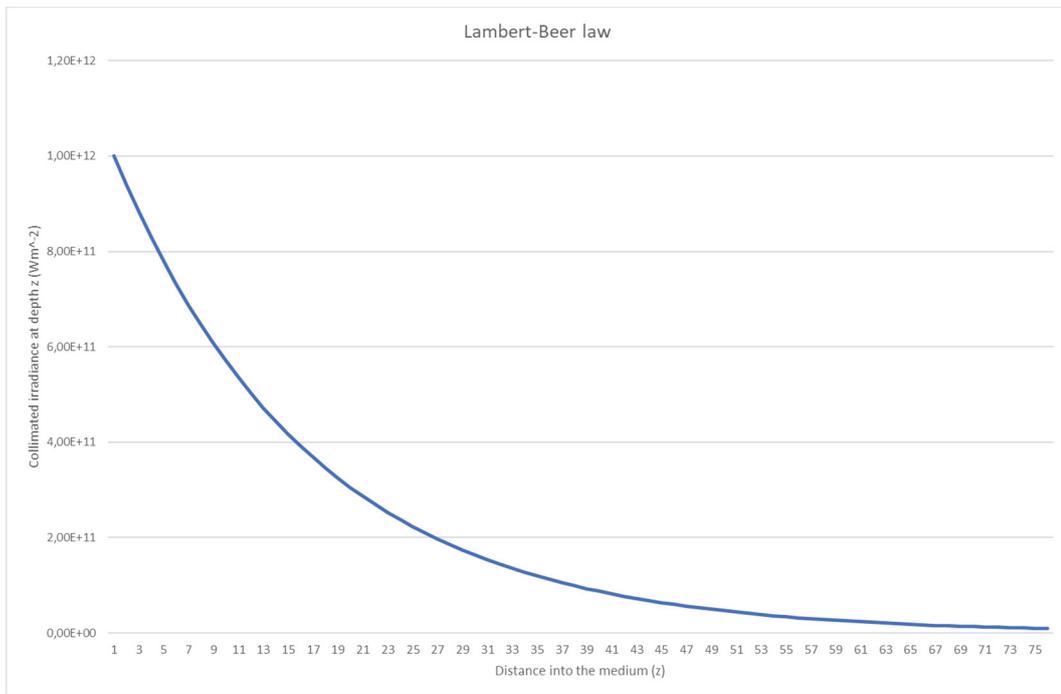
Figure 10: Plot of attenuation of light according to Lambert-Beer law.

The corresponding values for figure 10 are $\mu\_s=0$, $\mu\_a= 0.0625$, $r\_sc=0$ $E0=1E12$ W.m-2.

The Lambert-Beer law states that when absorption strongly dominates scattering, the attenuation follows an exponential decay curve.

2.2.5 Diffusion approximation

In some media scattering is much stronger than absorption. When scattering is equal or greater than absorption, the Boltzmann Radiative Transport Equation is appropriate. If scattering (strongly) dominates absorption, the diffusion approximation to the Boltzmann Radiative Transport Equation can be used. However, the diffusion approximation lacks the ability to include highly directional light sources at the boundary. In this thesis I apply a stochastic approach using the Monte Carlo method to solve for the photon distribution equivalent to the full solution of the Boltzmann Radiative Transport equation. This approach avoids the diffusion approximation and permits collimated and diffused boundary conditions easily without the use of a specialist phase function that would be required to model collimated beams in the diffusion approximation.

The diffusion approximation describes light as a diffusion process. The diffusion of light can roughly be imagined akin the diffusion of tea in a (still) cup. The propagation of light is determined by the gradient of photon density in the medium. This implies that photon

propagation has limited memory, only the local gradient is of relevance. So diffusion can be described as a Markov process, just like no-claim schemes in car insurance (33).

The diffusion approximation to the RTE is valid when the dimensions of the medium greatly exceed the pathlength of the light and when the number of scattering events a photon undergoes is sufficiently large.

In order to determine how many photons (or, if multiplied by hv, the amount of energy) are / is present at a certain location at a certain time, we thus need to determine the expected number of photons that originate from within the medium and have travelled to that location at that time. This is perhaps comparable to the calculation of expected utility in decision theory using Von Neuman-Morgenstern expected utility functions (34).

From this it follows that in diffusion theory we calculate the flux of light at a point $\phi(r)$ (Wm^{-2}) by solving the differential equation for the expected scattering from all directions, i.e. the solid angle integral. During laser therapy, some of the light that travels through a certain point r in direction s comes directly from the light source, whereas the rest is first scattered within the tissue. So, in order to simplify the analysis, the flux can be separated into the contribution from the columnated light source and the contribution from scattered photons.

Star discusses the diffusion theory in light transport in detail, to which interested readers are referred (35). He states that what sets transport theory apart from simple diffusion theory is the addition of the source term, and, from the Eddington approximation, simple expressions for the diffusion coefficient and the effective attenuation coefficient.

2.2.6   The transition of light from one medium to another

Before light travels through a medium, such as the skin, it generally needs to enter the medium. If the media have different indices of refraction, i.e. the speed of light differs in both media, reflection and refraction will occur. When light is reflected, it does not enter the medium, but is reflected away from the boundary under some angle.

The portion of light that is reflected can be determined using the Fresnel equations. In the formula θ_i is the angle under which the light hits the normal from the boundary and θ_t is the angle of refraction. η_t is the index of refraction of the medium to which the

light travels, and η_i is the index of refraction of the medium from which the light travels. The fraction of light being reflected differs for the type of polarized light.

$$r_\parallel = \frac{\eta_t \cos\theta_i - \eta_i \cos\theta_t}{\eta_t \cos\theta_i + \eta_i \cos\theta_t}$$

$$r_\perp = \frac{\eta_i \cos\theta_t - \eta_t \cos\theta_i}{\eta_i \cos\theta_i + \eta_t \cos\theta_t}$$

Equation 6: Fresnel equations

Where $r_\parallel$ describes the fraction of parallel polarized light that is being reflected and $r_\perp$ is the fraction of perpendicular polarized light being reflected.

When light enters a medium with a different index of refraction, the direction in which it travels is altered. The angle of refraction is the direction in which light travels if it is able to enter the medium. That is given by Snell's law.

$$\frac{\sin\theta_i}{\sin\theta_t} = \frac{\eta_t}{\eta_i}$$

Equation 7: Snell's law.

At a certain angle, the critical angle, light is unable to cross the boundary and is completely reflected. The angle in which reflected light travels is described by the law of reflection, $\theta_i = \theta_r$

2.2.7   Types of light sources

Light originates from a light source. This can be the sun, a laser, or a fluorescent molecule. One way in which the light sources investigated in this study differ is the direction in which the light is emitted. Most lasers emit a collimated beam of light. The emitted photons travel in parallel.

For the incident light source used in the Monte Carlo model, is modelled by an initial angle of incidence and a distribution function. This facilitates diffuse and highly collimated beams to be modelled easily. If the diffusion approximation were used,

collimated sources have to be approximated by a succession of buried light sources to represent the collimated nature of the beam (36).

Figure 11 shows the different types of light sources: The light produced by an IPL is divergent, the photons generally travel in the same direction, but some are directed away from the normal. Fluorescent molecules act as a point source, emitting light in all directions.
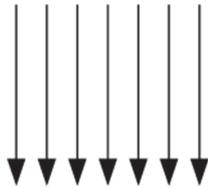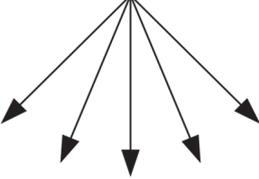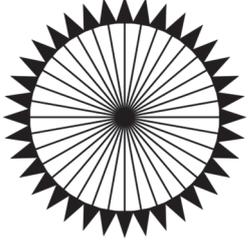
Collimated	Divergent	Point source
Laser	IPL	Fluorescence

Figure 11: Light sources

2.3   Solving the RTE in TODDY

For my study I will use the Two-Dimensional Laser-Tissue Model with Dynamic Boundary Conditions (TODDY) software package.(37) It has been used, amongst others, for the study of laser therapy for vascular lesions (38,39), PDT using a light source embedded in the skin (40), and optimisation of IPL therapy for hair removal in skin of varying colour (41). It is comprised of a Monte Carlo simulation for the solution of the RTE, and can solve Pennes' bioheat equation using the alternate direction implicit (ADI) finite difference method, and calculates the values of the Arrhenius damage integral.

2.3.1   Methods to solve the RTE

The Monte Carlo method is used for solving integral functions and can be used to solve the RTE in turbid media (42,43). The difference with other approaches for solving or

approximating the RTE such as the discrete ordinate method and the finite element method is that the Monte Carlo method is based on statistical convergence of a random walk, rather than a direct solution to a set of differential equations. The variation on the Monte Carlo simulation used in this research follows a bundle of photons as they travel through the skin. The Monte Carlo approach is suitable in situations where solving the equation directly is either impossible or requires a disproportionate amount of resources. The journey of the bundle of photons is separated into various individual steps, and each time the value for the random variables is selected using a random scheme based on the probability density function of the variable. The results of the calculations are added, which if the calculation is performed a sufficient number of times, results in the value for the integral of the function.

Various random elements of photon transport need to be taken into account. Random events are modelled by drawing a random number from a uniform distribution over (0,1) and associating certain values of the variable with a range of (0,1). In the case of path length there is a one-on-one correspondence between the distance that the photon travels and the result from the random number generator. So the random events present in simulation light-tissue interactions are the path length, the direction in which the photon travels and the balance of absorption and scattering at an interaction event.

Although the reflection event at an internal boundary can be modelled as a random event, in the software package used in this research it results in the photon energy being separated in two independent bundles. The size of the bundles depends on the Fresnel equation for reflection. For example, if $R = r^2 = 15\%$, then 15% of the remaining energy of the photon bundle is reflected and traced until the energy falls below the threshold. This is followed by the tracing of the photon bundle that had remained at the boundary and continues in the direction as determined by Snell's law.

Depending on the type of light source, the initial direction of the photon is given. If the light source is a laser, the direction is given by the orientation of the laser. In fluorescence though, the initial launch of a photon can occur in any direction. In isotropic fluorescence, the direction of the initial launch is randomly chosen from a equiprobable distribution of all angles.

Once the initial direction is known, the distance the photon travels, the path length, is determined. The path length is randomly drawn from an exponential probability density function based on the total attenuation coefficient. Now that we know direction and distance, we can establish the new location. It is important that one checks if no boundaries are crossed: The direction and path length are calculated under the implicit assumption that the medium in which the photon travels for that step is homogeneous.

If the photon indeed could cross a boundary a new calculation must be performed and the photon is relaunched from the boundary, either into the new medium or back into the old medium, depending on the outcome of the randomization.

Once the location to which the packet of photons has travelled is determined, a fraction of the photons contained in the packet is deposited at the location. The fraction is equal to $\frac{\mu_a}{\mu_t}$. The remaining bundle of photons is relaunched.

The direction for the subsequent step is determined based on the phase function, the anisotropy factor g and a random number. This is followed by the determination of the path length, a check if a boundary is crossed, and the deposition of photons. This sequence is repeated until the fraction of photons remaining in the bundle falls below a certain predetermined threshold. Then a new photon is launched from the light source. The sequence is illustrated in Figure 12.

Location 0: r^2 of the photons are reflected

Energy transmitted is $(1-r^2)$

Location 1: $(1-r^2)$ mu_a/mu_t of the energy is deposited. Rest undergoes a scattering event

Location 2: $(1-r^2)$ $(mu_s * mu_a)/mu_t$ of the energy is deposited.
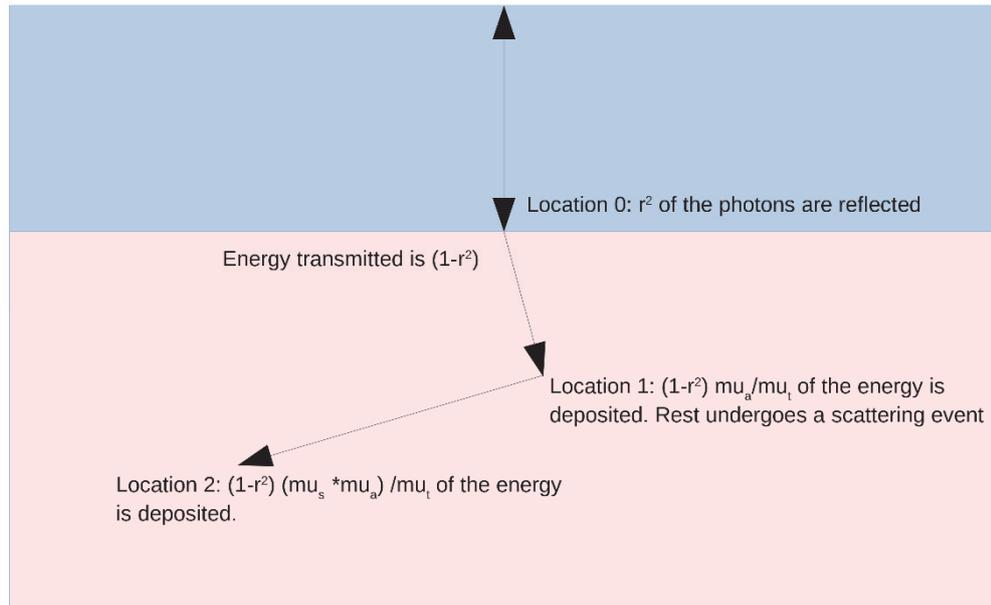
Figure 12: Illustration of a random walk of a bundle of photons in the Monte Carlo method.

A collimated bundle of light is directed at the surface of the skin. At the skin – air boundary, some of the light is reflected. The rest is refracted and moves one path length in certain direction. There, a fraction of energy, determined by the ration of the absorption coefficient and the total attenuation coefficient, is deposited. The remaining bundle undergoes as random scattering event. The path length is determined following a random event as well. This establishes the second location for the bundle to travel to, at which another fraction of the energy is deposited. This sequence is repeated until the remaining energy drops below a certain pre-determined threshold.

The Monte Carlo has some attractive strengths, but is not without its weaknesses either. It is able to solve the RTE for a wide range of geometries. The code can be easily adapted for various phase functions and it is not sensitive to relative sizes of the scattering and absorption coefficients. But it does require sufficient numbers of photons for convergence, something that cannot be checked in advance. Also, it is relatively computationally intensive.

2.3.2   Geometry

The TODDY package is based on a 2D layered representation of tissue on a Cartesian mesh. Each layer has its individual optical properties such as scattering coefficient,

absorption coefficient, concentrations of those chromophores and fluorophores that are modelled individually and anisotropy factor. The width of the layers is given by the width of the tissue, but the length can be set for each layer individually. Some limitations exist, e.g. the target cannot extend beyond the lower dermis. All layers have base attenuation and scattering coefficients which represent the optical properties for the tissue without its main chromophores such as melanin for the epidermis and haemoglobin for the dermis. For example, the absorption coefficient of the epidermis is calculated as a linear combination of the absorption coefficient of pure epidermis (i.e. without any melanin) and the absorption coefficient of melanin. These values are derived from the work by Jacques (44).

Figure 13: Geometry in TODDY

The light source is located at the bottom of the graphical representation shown in figure 13. The light source can be mono-chromatic as well as consist of a broad-band source. After launch, the photons are scattered according to the Henyey-Greenstein phase function and values for the anisotropy factor, g, are taken from published work. The light source can be of equal width as the tissue, or smaller. In a previous version of TODDY a light source was embedded in the tissue (40), but the current version requires the light to enter the skin from the air.

The first layer represents the epidermis. The absorption and scattering in the epidermis is represented by a base absorption function and a base scattering function as published by Jacques (44). The additional absorption by melanin is added to the attenuation coefficient. Town has studied the effect of melanin concentration in the epidermis on the optimal pulse profile for laser hair removal using a previous version of TODDY (41). The basal layer is not represented directly, but rather the concentration of melanin is represented as a percentage in the epidermal layer using the formula for absorption by epidermal melanin from Jacques (44). In addition to melanin, the version of TODDY used in this work allows for the introduction of one additional chromophore. Here this is used to study the effect of an increase in PpIX in the epidermis, but the program allows for any chromophore to be modelled. The absorption from this chromophore is calculated from actual biological and physical properties: A table of the molar extinction coefficient ($cm^{-1}.M^{-1}$) for the various wavelengths is added by the user and together with the concentration of the chromophore present in the skin ($mg.l^{-1}$) and the molar weight of the chromophore ($gr.M^{-1}$) used to calculate the additional attenuation from the chromophore (cm^{-1}).

The second layer is the dermis. As in the epidermis, absorption and scattering of the bloodless dermis is modelled using a function from Jacques . To this I add absorption by haemoglobin and two additional chromophores or fluorophores. In the current work the option to add chromophores was used to model absorption by PpIX and Flavin. Attenuation by haemoglobin, PpIX and Flavin was calculated from the molar extinction coefficient, concentration and molar weight. Blood oxygenation is incorporated in the values for the molar extinction coefficient table for the whole dermis. The used values are calculated using a linear concentration of the values for deoxygenated haemoglobin and oxygenated haemoglobin. The dermis is separated into an upper dermis, which is

located above the target area, and a lower dermis, which surrounds the target area and continues below it.

The third layer, or more precisely area, is the target. Individual optical properties can be defined, so that it can represent a tumour, hair follicle, blood vessel, or the papillary dermis. The location of the target is limited to the dermis. The distribution of the chromophores within the different layers is assumed to be homogenous.

The boundaries in the model are defined as crossing from the air to the epidermis or vice versa, crossing from the edge of the epidermis or dermis into the adjacent, not explicitly modelled tissue, crossing from the epidermis into the dermis or vice versa, and crossing from the dermis into the target and vice versa. When a photon crosses a boundary, it is relaunched at the boundary for the share of the remainder of the path length relative to the original path length.

After each path length, some of the energy is stored at that location. The share of energy stored, or share of photons stored, is dependent on the share of the absorption coefficient in the total attenuation $\frac{\mu_a}{\mu_t}$. For fluorescence, the share of photons absorbed by the fluorophores is stored separately and is the basis for the subsequent fluorescence calculations $\frac{\mu_a\,(fluorophore)}{\mu_a}$.

In the simulation of the photothermal treatment, there is one Monte Carlo simulation which produces the distribution of photons in the tissue. The results are stored for the absorption of all light absorbing molecules, and in addition separately for the two chromophores / fluorophores. For the simulation of the fluorescence detection, this data is used to determine the location and number of photons that need to be launched. The initial launch of a photon from a fluorophore is performed using an isotropic scattering function. Thereafter the same algorithm as that for the initial photons is used, with the absorption from the two fluorophores being stored in a separate matrix as to allow the determination of the distribution of the fluorescence signals.

The final output of the calculation thus consists of five matrices containing total absorption of the initial irradiation, absorption for the first chromophore / fluorophore, absorption for the second chromophore / fluorophore, absorption of the fluorescence from the first fluorophore by any and all suitable chromophores, and absorption of the

fluorescence from the first fluorophore by any and all suitable chromophores. Additionally, the distribution of backscattered light and emitted fluorescence from both fluorophores measured at the skin surface is printed in a separate file. The total absorption matrix is used in the calculation of the heat diffusion, which is discussed below.

2.3.3 Limitations of the photon distribution calculations

The TODDY package has attractive features for the research conducted in this thesis.

- The results can be validated using skin surface temperature measurements and surface back-scatter measurements (41),
- The diffusion calculations are in accordance with the analytical solution by Morse and Feshbach (45,46)
- It is capable of modelling photothermal treatments for vascular conditions and hair removal
- It can study both mono-chromatic and polychromatic light sources
- It can model mono-chromatic and polychromatic fluorescence
- It can calculate heat diffusion and biological effects
- allows for the application of individual molecules using concentrations and molar extinction coefficients
- It allows for different anisotropy values for the light source and the tissue
- It can simulate photodynamic therapy using embedded light sources (40)
- And thanks to parallelisation is able to utilize the full computing capability of the available workstation (46).

There are some limitations though. The optical properties of the skin are assumed to be constant, which e.g. in photodynamic therapy is an unrealistic assumption because of photobleaching (47). I note that previous simulations of photodynamic therapy did not account for that, suggesting that they underestimate the efficacy of PDT (48,49). The target area consists of a single continuous rectangle located in the dermis. Therefore I cannot study the effect of laser therapy on a collection of individual capillaries and other blood vessels (50), or study the detection of actinic keratosis and other squamous cell carcinomas located in the epidermis. Nor can I accurately represent the variation in blood oxygenation in normal skin, as shown by Schwarz et al. (51). By representing the

skin as a collection of layers, the effect of the rete ridges is understated. The 2D presentation puts further limits on the complexity of the skin that can be studied: A complete model of the skin requires the representation of hair follicles, sebaceous glands, eccrine glands and lymphatic tissues to mention just a few.

Finally, the Monte Carlo method is potentially wasteful in its search for convergence. That is, the limit factor for complete convergence, that is convergence in all areas within the tissue, are those points in the tissue that have the smallest positive probability of absorbing a photon, i.e. where local convergence is hardest to achieve. Without additional measures, a calculation can reach a point where most photons added to the simulation will not result in a change in local convergence of the area in which they are deposited. E.g. the absorption near the surface of the skin is several magnitudes larger than at the edge of the lower dermis. So, for each 1000 photons added, say 1 or 2 might improve the accuracy of the calculation in terms of complete convergence. This is of particular relevance to the fluorescence study, as either poor local convergence at the deeper areas of the tissue during the irradiation phase of the simulation, or an insufficient number of photons being fired from those deeper, less irradiated areas, could result unacceptable statistical uncertainty in the fluorescence transport calculation.

2.4   Thermal diffusion and heat driven biological effects

In the study of the photothermal treatment of psoriasis the energy introduced by the laser or IPL results is predominantly by the blood vessels as well as the melanin in the epidermis and converted into heat. Thus, the blood vessels, melanin, and other chromophores in the skin act as a local heat source. This heat subsequently is diffused into the rest of the tissue and the skin surface. The temporary increase in heat can drive various biological effects, such as vasoconstriction, the induction of heat shock proteins, or create thermal injury. These effects are modelled using the Arrhenius damage integral, which requires the temperature and duration of heating as input variables. The TODDY package uses the Alternate Direction Implicit algorithm for a Finite Difference Mesh to solve the heat equations and the Arrhenius damage integral to determine the size of the biological effects.

2.4.1 Heat diffusion in biological tissue

The selective absorption of light by structures in the skin can result in considerable heating. Per volume of tissue, one can calculate the increase in temperature per Joule that is absorbed from the laser. This depends on the specific heat of the tissue, c (J.kg^{-1}.K^{-1}) and the density of the tissue ρ (kg.m^{-3}).

From the second law of thermodynamics follows that the increase in temperature of the tissue, or heat, will tend to diffuse to other parts of the tissue that are cooler. Since biological and physical effects in laser therapy depend on a sufficient and prolonged increase in temperature, heat diffusion needs to be taken into account. Note though that an increase in temperature is not the exclusive outcome of heating of tissue. In addition to the sensible energy storage, there also is the potential for an increase in latent energy, e.g. through phase change. In my research, I explicitly avoid phase change, and therefore will limit the discussion to sensible energy storage.

The most basic representation of heat diffusion in human tissue follows the work of Pennes (52).
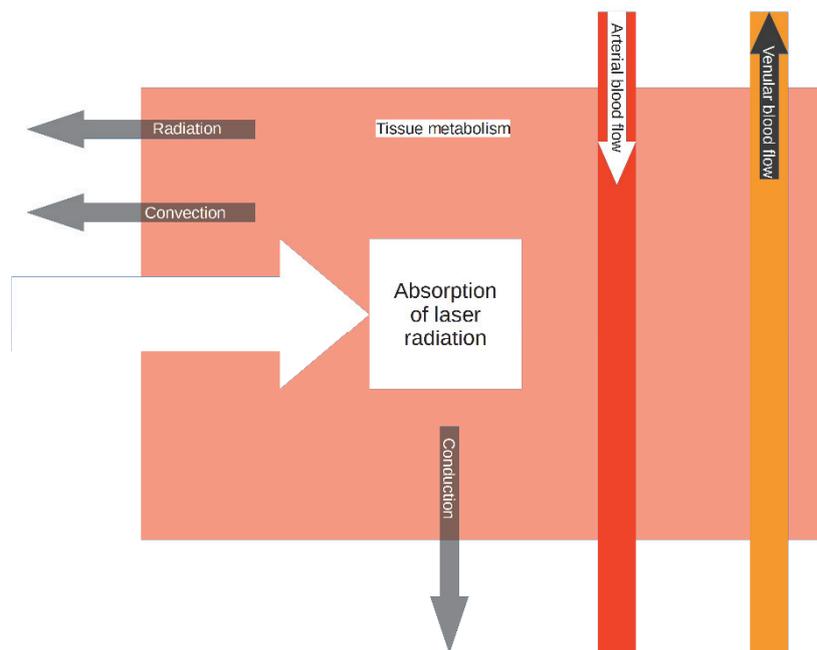
Figure 14: Bioheat in laser therapy.

Figure 14 presents a simple model of bioheat in laser therapy. The black arrows present heat being removed from the tissue, and the white arrows represent heat being

introduced into the tissue. Heat sources are the metabolism from the cells in the tissue, blood flow in the arteries, and the tissue absorbing the energy from the laser. This heat is dissipated through conduction into adjacent tissue, removed by the blood flow in the venules, radiative heat transfer, and convection of air or water on the skin (potentially including a phase change).

The transfer of heat depends on the gradient of heat: The larger the difference in temperature, then, other things equal, the stronger the diffusion is. Diffusion can take place in three forms:

First, the increase in temperature can cause an electronic excitation of the molecule. The resulting relaxation to the ground state produces radiation in the infrared spectrum, removing energy from the system, i.e. cooling the tissue. From the Stefan-Boltzmann law it follows that for the modest heating in tissue, this effect is very small in the context of laser therapy for skin conditions.

Second, the decrease in temperature can occur by a displacement of a fluid or vapour, i.e. convection. If the convection occurs under pressure, it is called forced convection, otherwise it is called free convection. The latter occurs when the heating results in a decrease in density of the fluid. Then under influence of the gravitational field, the heated mass is displaced, resulting in an increase in cooling. In the current study, the heat at the tissue surface is removed through free convection.

Third, the energy can be transferred from one area of a medium to another due to the increase in collisions between molecules. The molecules in the warmer tissue have a higher vibrational state and transfer this energy to molecules with which they collide. If the adjacent molecules have lower vibrational energy, the energy is transferred. Thus, the heat is conducted to cooler regions of the tissue. It is this time-varying diffusion process that occurs within the tissue during the photothermal studies presented in this book.

Following laser irradiation, the heat is diffused within the tissue through conduction. This process can be described using the thermal diffusion equation as derived from Fourier's law of conduction.

$$\rho c \frac{\partial T}{\partial t} = k\nabla^2 T$$

Equation 8: Thermal diffusion equation (53). *During laser irradiation additional heat can be added using a source term Q, which is not shown in the current equation.*

For two-dimensional Cartesian coordinate systems such as the one in the TODDY package, it can be written as

$$\frac{\rho c}{k} \frac{\partial T}{\partial t} = \frac{\partial^2 T}{\partial x^2} + \frac{\partial^2 T}{\partial y^2}$$

Equation 9: Thermal diffusion equation in a 2-dimensional Cartesian mesh.

Here ρ is the density of the tissue in kg.m³, c is the specific heat of the tissue in J.kg⁻¹.K⁻¹ and k is the thermal conductivity of the tissue in W.m⁻¹.K⁻¹. Heat is conducted perpendicular to the heat gradient. The larger the difference in temperature, the stronger the diffusion of heat. Tissue that has a large heat capacity absorbs more energy per degree increase in temperature than tissue with low heat capacity. Material with a small thermal conductivity, such as keratin in sheep wool, transfers less heat than material with a high thermal conductivity such as water.

In biological tissue, such as skin, it is assumed that, except for the blood in the arteries and venules, there is no change in the location of the tissue. This is different at the skin surface. Air, water and carbon gels undergo more than just conduction, there is also a reallocation of mass. This can occur as a result of the heating itself, or as a result of an external pressure that is being applied onto the liquid or vapour. If there is no external force it is said that the convection is free. As the temperature of the liquid or vapour increases, its density decreases. Under the influence of the gravitational field, the heated liquid or vapour is relocated to an area in which the density of the surrounding vapour or liquid is equal to that of the heated mass. At the original site, the heated liquid or vapour is replaced by cooler liquid or vapour, which has a higher density. This affects the temperature gradient at the boundary. Under forced convection the liquid or vapour is forced over the surface, creating a steady supply of the cooling agent.

The heat removed trough convection is given by a convective Boundary Condition:

$$\dot{Q} = hA(T_s - T_\infty)$$

Equation 10: Convective boundary equation

Here $\dot{Q}$ is the flow of heat in W, h is the heat transfer coefficient W.m^{-2}.K^{-1}, A is the area of the boundary m^2, T_s is the substrate surface temperature in K and T_∞ is the bulk fluid temperature in K.

2.4.2 Computational model for heat diffusion in tissue

In laser therapy, the heated tissue acts as a heat source: the absorbed energy is converted into heat and from there diffuses to the rest of tissue. Not all heat sources and forms of diffusion described in Pennes' bioheat equation are studied in the model applied in this research. First, since at 5 ms the duration of a laser pulse is short compared to the thermal regulation by the arteries and venules, the effect of blood flow is ignored. Second, since the increase in heat studied in the subsequent chapters does not result in any area of the tissue reaching a temperature of more than 100 °C, radiative heat transfer is ignored because the size of that effect too is minimal.

The thermal diffusion equation can be computationally solved using the finite difference method. In this method, a rectangular mesh is superimposed on the domain, with the mesh spacing chosen to give good resolution of each layer's mean free path. The temperature at time t is calculated for each node (x,y). To achieve this, the partial differentials in the equation for thermal diffusion (equation 9) are replaced by the forward, backward and central differences of a Taylor series expansion. This gives us a set of algebraic equations that, given the initial and boundary conditions, can be solved.

$$\frac{\partial^2 T}{\partial x^2} = \frac{T_{x-h}^n - 2.T_x^n + T_{x+h}^n}{h^2} + o(h^2)$$

$$\frac{\partial^2 T}{\partial y^2} = \frac{T_{y-h}^n - 2.T_y^n + T_{y+h}^n}{h^2} + o(h^2)$$

$$\frac{\partial T}{\partial t} = \frac{T_{i,j}^{n+1} - T_{i,j}^n}{\Delta t} + o(\Delta t)$$

Equation 11: Numerical approximation of the first and second derivative of the temperature terms

The set of difference equations can be solved explicitly, implicitly, or through a combination of both. The explicit algorithm defines the temperature at node $N_{x,y}^{t+1}$ as a function of the temperature of the adjacent nodes and the thermal diffusion:

$$\frac{h^2}{\alpha \Delta t} T_{x,y}^{t+1} = T_{x-h,y}^t + T_{x+h,y}^t + T_{x,y-h}^t + T_{x,y+h}^t - \left(4 - \frac{h^2}{\alpha \Delta t}\right) T_{x,y}^t + \frac{h^2 Q^t}{k}$$

The problem with the direct method is that there are restrictions on Δt. In two dimensions, it must be within $0 < \Delta t \leq \frac{h^2}{4\alpha}$. A fine mesh thus requires a small Δt, otherwise the algorithm becomes unstable. This increases the required number of computations for a given problem.

A way to avoid the potential instability is by using the simple implicit method. It uses the backward difference approximation to discretise the temporal derivative of the temperature. In the implicit method the temperature at node $N_{x,y}^{t+1}$ is implicitly calculated by defining the known value $T_{x,y}^t$ in terms of the unknown values $T_{x-h,y}^{t+1}, T_{x+h,y}^{t+1}, T_{x,y-h}^{t+1}, T_{x,y+h}^{t+1}, T_{x,y}^{t+1}$:

$$-\frac{h^2}{\alpha \Delta t} T_{x,y}^t = T_{x-h,y}^{t+1} + T_{x+h,y}^{t+1} + T_{x,y-h}^{t+1} + T_{x,y+h}^{t+1} - \left(4 + \frac{h^2}{\alpha \Delta t}\right) T_{x,y}^{t+1} + \frac{h^2 Q^{t+1}}{k}$$

The implicit functions then are solved simultaneously, making the simple implicit method an unconditionally stable algorithm.

In TODDY the method used to solve the difference equations is the Alternate Direction Implicit (ADI) method. The ADI is a combination of the explicit method and the implicit method for solving the set of finite difference equations used to represent the thermal diffusion. The advantage of the ADI over the explicit and implicit method is that it is unconditionally stable, which the explicit method is not, and that it is computationally efficient, which the implicit method is not. What is particular about the ADI is that the algorithm switches between the explicit and implicit methods in-between time steps. It may start with using the explicit method for the nodes in the x axis and using the implicit method for the y axis for a time step $\frac{1}{2}\Delta t$, and then applies the implicit method for the nodes on the x axis and the explicit method for the nodes on the y axis for the second half of the time step. Its computational efficiency comes from the ability to formulate the problem in the matrix form A.X=Y, where X and Y are vectors and A is a tridiagonal matrix. Formulated this way, the problem can be solved using matrix inversion, which

reduces the required computational resources, while thanks to the use of the implicit method retaining the unconditional stability.

2.5 Biological effects of laser therapy

Photothermal laser therapy is aimed at inducing a certain effect in the tissue by inducing a specific and prolonged heating of some part of the tissue. In the research presented below, heat shock protein induction, vasoconstriction, and hyper-thermic tissue damage are used as outcome variables for laser therapy. There is a multitude of effects that photothermal treatments can induce in tissue (54). These can be direct, i.e. the effect is visible directly following the application of the laser such as ablation or the formation of vacuoles, and can be indirect, resulting in clinically observable changes after days or weeks such as inflammation.

Some of the effects from laser therapy can be described using first order kinetics. The effects studied in this work belong to that group. Biological effects from photothermal treatments are assumed to be irreversible. Thomsen and Pearce stress that the kind of reactions that are described by the first order rate processes are not phase change: Energy is consumed both by inducing the change and, if possible, in undoing the change (54). The classical work on the effects of hyperthermia on skin is the result of research conducted in the second world war and published in a series of papers. Two authors who made significant contributions to the project were Henriques and Moritz (55–57). They defined hyper thermic tissue damage as the result of a combination of heat and time, and expressed thermal damage using a simple first order expression $\Omega = \int_0^\tau A e^{\frac{-E_a}{RT(t)}} dt$. Here Omega is the damage measure, A is the frequency factor (s^{-1}), τ is total heating time (s), E_A is an activation energy barrier required for a change in the configuration of the molecule (JM^{-1}), R is the universal gas constant 8.3143 J.M^{-1}.K^{-1} and T is the temperature (K).

This measure can be reformulated into Arrhenius' equation for the survival of cell cultures. The Arrhenius integral signified the fraction of cells that are in the native, undamaged, state at a time τ, $\Omega(\tau) = \ln \frac{C(0)}{C(\tau)}$. This approach can be applied to quantify the effects of heat on tissue, assuming the appropriate frequency factor and activation

energy are known. In that case, the damage integral can be expressed as $\Omega(\tau) =$
$\ln\frac{C(0)}{C(\tau)} = \int_0^\tau Ae^{\frac{-E_a}{RT(t)}}dt.$

Equation 12: Arrhenius damage integral

A few things can be derived from the damage equation. First, for a fixed temperature, thermal damage is linear with respect to time, and for a fixed duration of heating, damage is exponential with regard to temperature. Henriques and Moritz already noted that for temperatures near 55 C°, an increase in temperature of 1° would result in a doubling of damage. Second, using the damage equation, one can establish the minimum temperature required to start the reaction regardless of the duration of heating, $T_{critcal} = \frac{E_a}{R \ln A}$. Studying laser pulses which are unable to achieve at least heating to the critical level do not have to be studied, since the desired effect cannot be achieved.

Calculating one or more first order kinetics is not difficult to incorporate into the model discussed above, as long as the time steps in the heat diffusion calculation are sufficiently small. That is, since damage is exponential to temperature, calculating damage from a linear combination of temperatures might under or overestimate the actual damage. In the Toddy software used in this study, the value of the Arrhenius damage integral is calculated and printed for each cell in the matrix.

2.6   Application of the software

When using the software, the first step is to formulate the problem for the radiative transport stage (Figure 15).

Figure 15: Menu for the formulation of the radiative transport problem

Here one defines the number of bundles of photons to be launched, the dimensions of the layers, the anisotropy factor, the concentration of melanin, the concentration and molecular weight of one chromophore and two fluorophores, a multiplication factor for the scattering function, the used wavelength or file for the broad-band light source, as well as the incident angle and the anisotropy factor.

Before the execution of the calculations, the user can specify a value or file for the mono-spectral or broad-band fluorescence.

After the Monte Carlo simulation is completed, the variables for the thermal and biological effect calculations can be specified.
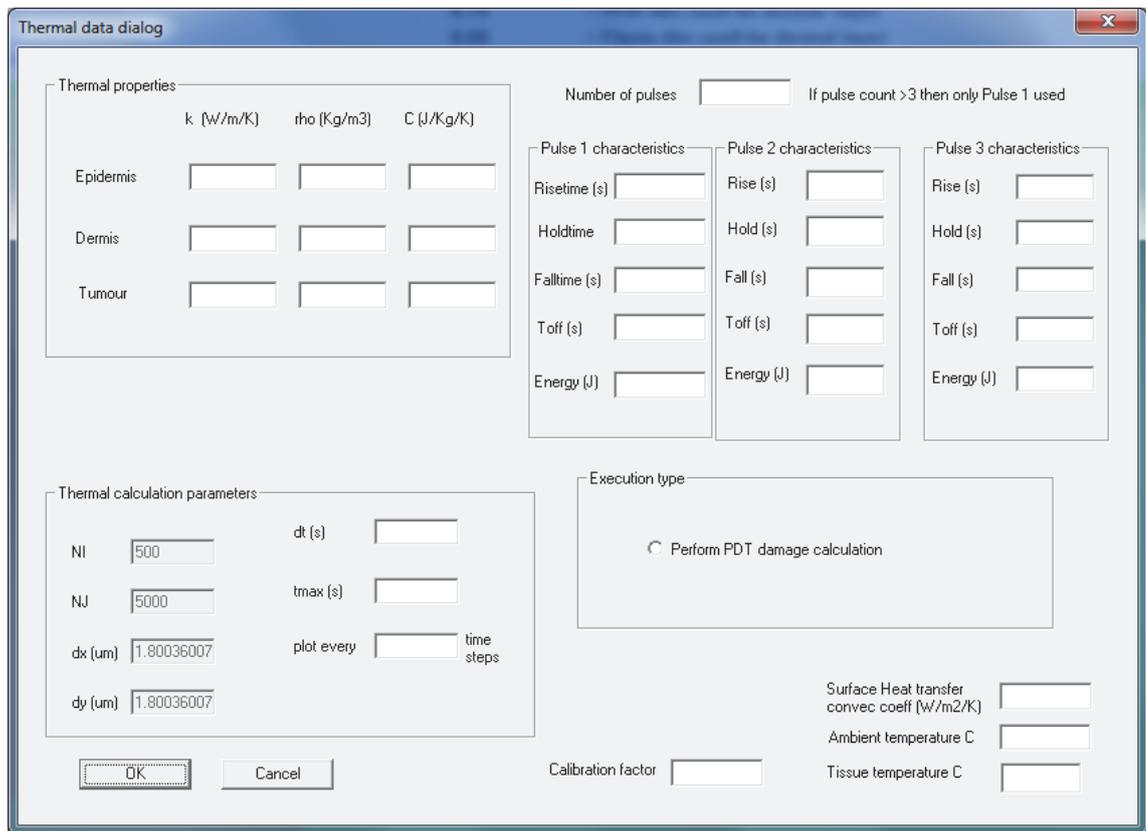
Figure 16: Thermal calculation variables

As is shown in figure 16, the user can enter the thermal conductivity of the different layers, as well as the heat capacity and the density. The program allows for the specification of pulse train profiles, including a rise time, hold time and fall time. Up to three pulses can be individually modelled, a larger number of micro-pulses is a sequence of identical micro-pulses. Temperature of tissue and ambient temperature, as well as the heat transfer coefficient are required, as is the size of the time step in the finite difference method calculation using the ADI and the total time. The software package is capable of the simulation of PDT treatments; if these calculations are to be performed this option needs to be selected separately.

The output of the calculations is a table describing the percentage of backscatter, fluorescence from the first fluorophore at the tissue surface, and fluorescence from the second fluorophore at the tissue surface. In addition, five matrices are saved. These describe:

1: The distribution of photon bundles emitted by the light-source and subsequently absorbed by any chromophore or fluorophore;

2: The distribution of photon bundles emitted by the light-source and subsequently absorbed by the first fluorophore;

3: The distribution of photon bundles emitted by the light-source and subsequently absorbed by the second chromophore;

4: The distribution of photon bundles emitted by the first fluorophore and subsequently absorbed by any chromophore or fluorophore;

5: The distribution of photon bundles emitted by the first fluorophore and subsequently absorbed by any chromophore or fluorophore.

Figure 17: Data logger dialogue

Using the menu shown in figure 17, the user can define 12 points at which the change in temperature over time can be logged and printed in a separate file. Skin surface and the area with the largest amount of heat are always recorded, and 10 other locations can be specified.
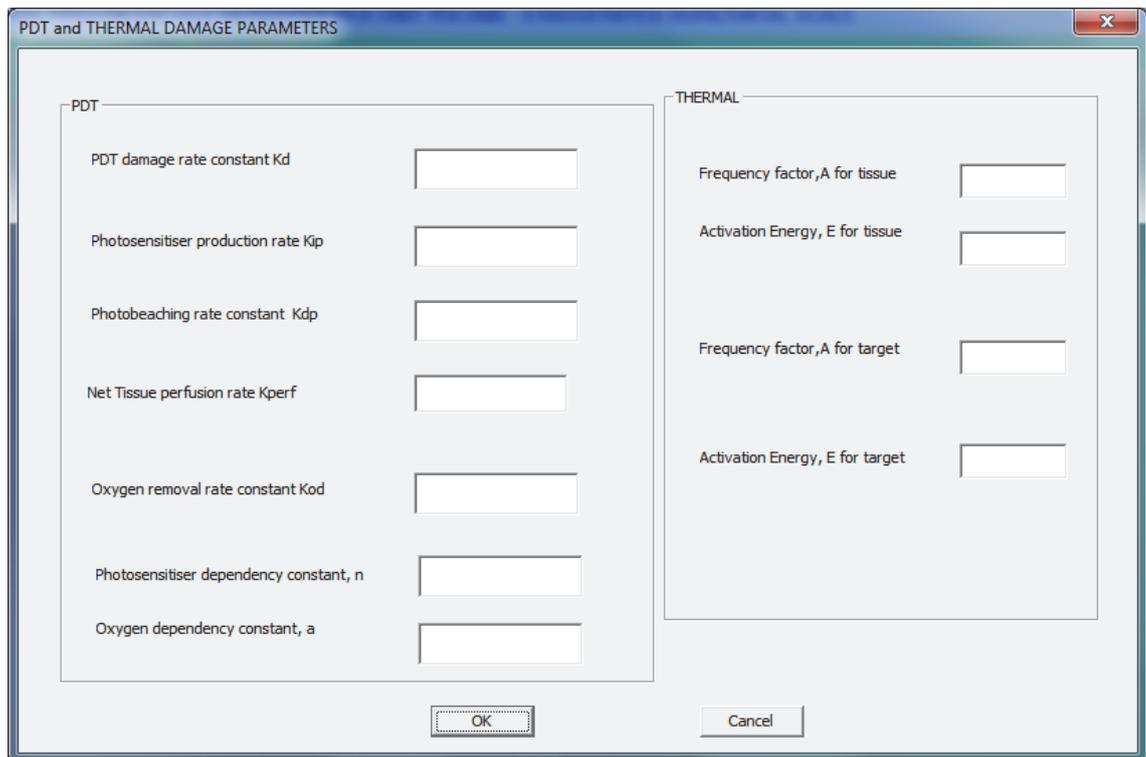
Figure 18: PDT and biological effects

In situations in which PDT is modelled, the user is required to specify the constants for the rate equations in PDT. The frequency factor and activation energy for the studied biological measure can be specified for the target area and for the dermis and epidermis. This is done in the menu shown in figure 18.

The results of the calculation are printed in a table containing the temperature of the tissue at the chosen time-steps and chosen locations in the tissue. The cumulative biological effect is printed in a table, giving the value of the Arrhenius damage integral for each point in the tissue.

The files produced in the calculations were loaded into Libreoffice Calc and Microsoft Excel for further calculations such as the contrast in measured fluorescence, absorption of photons in the tissue, and the distribution of the heat and damage in the tissue.

3. Fluorescence detection of keratinocyte skin cancers: Effects of tissue variance on reported contrast in fluorescence.

3.1 Introduction

Keratinocyte skin cancer (KSC), also known as non-melanoma skin cancer (58,59) is a malignancy arising from the keratinocytes of the skin. KSCs are classified according to the cells from which they originate, such as basal cell carcinoma (BCC) and squamous carcinoma (SCC). KSC is the most common form of skin cancer and its incidence is rising (13,14,60–66). Although mortality and metastasis are less common compared to malignant melanoma, there is a risk of metastasis in SCC and BCC. Moreover if untreated BCC can cause severe disfigurement, or disability when it invades organs such as the eyes or the brain (67).

Current treatments consist of surgical excision, laser therapy, pharmacological therapy using 5-fluoruracil or imiquimod, brachytherapy, cryotherapy, or photodynamic therapy (PDT). These modalities differ in terms of one-year efficacy and the ability to prevent new lesions in the area surrounding the treated KSC. Ablative laser therapy and fractionated PDT for example result in high clearance rates compared to pharmacological interventions. Additionally the number of new lesions occurring within the area treated with ablative laser therapy was less than in a control area treated with 5-fluoruracil (4,26,68).

The main cause of KSC in the general population is UV-induced changes in the genetic code of keratinocyte cells. Certain genes that are tumour promoting, the so-called oncogenes, are activated, whereas genes that are responsible, amongst others, for limiting cell proliferation or inducing cell death, the tumour suppressor genes, are deactivated. Since the influence of UV radiation generally affects larger areas of the skin, it his hardly surprising that KSC is far from a once in a lifetime event. On the contrary, patients who have had at least two BCCs, assuming they do not suffer fatal events, are guaranteed to witness the development of consecutive BCCs (69). KSC is starting to become regarded as a disease that affects larger areas of the skin, i.e. the field, and that treatments should be aimed at the field rather than the occurring lesions. (70–78).

I am inclined to state that currently there are two important barriers to the formulation of an effective and efficient treatment strategy to cope with the skin cancer epidemic.

The first concerns the efficacy treatment modalities have on the field. Some generalizations can be drawn: The effect of surgery is limited to the area that is being treated. Likewise, cryotherapy cannot exert an effect on the surrounding tissue. Modalities that can be applied to a larger area either have a limited effect on the field, e.g. 5-fluoruracil (4), or have not been studied in sufficient detail regarding the emergence of new lesions in the treated field, such as is the case with PDT. One modality that has shown to result in a significant decrease in the number of new lesions, Er:YAG ablative laser therapy, is associated with a less favourable risk profile and side effects (3,26). Furthermore, if a lesion has progressed beyond a certain point, quite a few therapeutic options are withdrawn from the menu. At that point surgical excision, either using Mohs' micrographic surgery or not, is the only alternative.

The second limitation concerns the demarcation of the area that needs to be treated. Field treatments are no different than other treatment modalities in their propensity to cause discomfort and adverse events. As such, unnecessary treatment ought to be avoided. Yet if one underestimates the field required for treatment, the whole endeavour loses some of its value compared to lesion based treatment strategies. The field treatment approach versus the lesion removal approach fits the more general prevention versus wait and see distinction in medicine.

Not all systems of reimbursement or local traditions among dermatologists could allow a physician to follow a strategy based on field treatment, requiring him or her instead to treat each lesion as it emerges. In those scenarios both the total costs of treatment for KSC as well as the health of the population might benefit from a method for the early detection of skin cancers. This is due to the fact that the larger a lesion is, the higher the total costs of treatment, the higher the probability of adverse events and complications, and the higher the change of an incomplete removal of the tumour become (79–82).

I argue that both the field treatment approach and the lesion based strategy would benefit from the use of fluorescence detection (FD) methods for KSC. FD is based on the idea that KSC are susceptible to the preferential accumulation of photosensitisers. As noted in the previous chapter, when a photon is absorbed by a molecule, and results in an electronically exited state, the return of the molecule to the ground state might

involve the release of visible light. So, by increasing the likelihood of a photochemical reaction in the tumour, one also increases the likelihood of fluorescence.

3.2   Fluorescence detection of keratinocyte skin cancers

Fluorescence detection, and its parent, photodynamic therapy, are far from new. The photodynamic effect describes the situation in which an effect on an organism is the resultant of the application of a photosensitizing compound in combination with irradiation by a light source which emits light that is capable of being absorbed by the photosensitiser. Oscar Raab was the first to discover this effect (83). During his studies in München on the effect of acridine orange on paramecium, he noted that some of the organisms had died whereas others had not. More precise, those Petri dishes that where located in the vicinity of a window had perished, whereas those that resided in more dark areas of the laboratory had survived. Neither acridine orange nor sunlight is harmful to paramecium, so it had to be the combination of the two that evoked the (detrimental) effect. The relationship with fluorescence was immediately appreciated, and in 1904 Raab's supervisor, Von Tappeiner, equated fluorescent compounds with photodynamic compounds (84).

Fluorescence had been described 50 years earlier, and the introduction of Woods' lamp allowed for the application of fluorescence in the medical clinic. Stübel reported on the use of fluorescence for diagnostic purposes (85). The research on the application of photodynamic therapy resulted in the discovery that the application of hematoporphyrin, a photosensitiser, resulted in a preferential uptake in malignant tissue (86). While conducting research with hematoporphyrin for the treatment of malignancies, Policard noted the presence of a brick like red fluorescence emerging from tumours when the sensitised tissue was illuminated with a Woods' lamp (87). At the time, Policard ascribed this effect to the presence of an inflammation, and not the porphyria in the tumour. Auler and Banzer were the first to purposely apply hematoporphyrin for the localisation of malignant tissue (88). This research was extended by Figge et al. using an animal model with transplanted tumours (89). Fluorescence detection and photodynamic diagnosis was initially applied in the detection of tumours of the bronchi, notably by Profio and Doiron (90). Although few organs are as accessible as the skin, neither photodynamic therapy or fluorescence detection received much attention from the dermatologic community. Even though the

first application of PDT for malignancies of the skin dates back to 1903, when Von Tappeiner and Jesionek used 5% eosin as a photosensitiser (91), it was only after the discovery of 5-aminolevulinic acid (5-ALA) as a pro-drug for protoporphyrin IX (PpX), and its successful application in photodynamic therapy for KSC by Kennedy et al. (92), that both PDT and fluorescence detection for KSC started to gain interest. In the haem cycle, 5-ALA is a precursor to PpIX, and in particular in malignant tissue 5-ALA is a rate limiting step. After the exogeneous administration of 5-ALA, the conversion of PpIX to haem is the new rate limiting step due to a lack of ferrochelatase (93–95). Since in non-malignant tissue, with its lower metabolism, 5-ALA isn't as much a rate limiting step, the application of 5-ALA is biased towards tissue with a high metabolism, such as malignancies (96). The application of 5-ALA in PDT resulted in a less prolonged duration of photoxicity and could be applied topically, which greatly improved the safety and tolerability of photodynamic therapy. Wilson et al. showed that lack of specificity of the photosensitiser can be a problem (97), which three years earlier had been demonstrated by Van der Putten and Van Gemert using Kubelka-Munk theory (98). Benefitting from the interest in photodynamic therapy, fluorescence detection received more interest and both mono-spectral and multispectral approaches have been pursued (2,99–110). The studies mentioned above all used either an exogenous photosensitiser, that is an externally administered photosensitiser not normally present in the organism (e.g. indocyanine green), or a precursor of an endogenous photosensitiser, that is a photosensitiser that is normally present in the organism, but the concentration or location of which is altered by administering a compound that is part of the cycle of the photosensitiser (e.g. 5-ALA). As in the classical application of the Woods' lamp, one can also use auto-fluorophores (e.g. Flavin) to locate and demarcate KSC. This approach was used by amongst others Na et al., Brancaleon et al., and Leslie (111–113).

Methods utilising fluorescence characteristics of fluorophores in tissue can be categorised according to three axis (114). First, the nature and type of the photosensitiser. It can be endogenous, that is naturally present in the tissue, such as PpIX contained in bacteria such as P.acnes, or the auto-fluorophores in the skin. Alternatively, it can be an exogeneous photosensitiser which is not naturally present in the tissue but must be introduced externally. Examples are mTOR or hematoporphyrin derivative. Or one can apply a precursor of a naturally occurring photosensitiser such as

5-ALA. An important property of an efficient photosensitiser is that it is selective for the tumour, e.g. because a preferential uptake. This is the case for 5-ALA. Although not a photosensitiser itself, it is synthesised inside mammalian cells to form PpIX, which is a photosensitiser. Both 5-ALA and PpIX are part of the haem cycle in mammalian cells. 5-ALA is, eventually, synthesised into PpIX, which in turn forms haem, which regulates the synthesis of 5-ALA, thus forming a cycle. By introducing additional 5-ALA, the feedback form haem is rendered ineffective. This results in an increase in PpIX. At that point, the synthesis of PpIX into haem by ferrochelatase becomes the rate limiting step. The rate of synthesis of 5-ALA into PpIX is higher in more proliferative tissue than in normal tissue. As a consequence, the concentration of PpIX in the malignant or otherwise hyperproliferative tissue will for some time be much higher than in the surrounding healthy tissue. Hence the administration of 5-ALA results in a selective photosensitization of KSC. It is this selectivity that allows us to image the tumour using FD or treat it using PDT.

The second axis concerns the instrument with which the fluorescence is measured. An analogue measure, such as direct observation by the eye, a point measurement using a fiberglass coupled to an optometer, or a chip such as CMOS or CCD. These differ in accuracy, quantifiability, and field of view. Multispectral imaging is not available when one observes with the naked eye, but can be achieved with point measurements or electronic sensors. Similarly, fluorescence lifetime measurement and imaging is only possible with suitable sensors.

The third axis concerns the light source. As noted above the first investigations used a Woods' lamp, but lasers, flash lamps, and LED's can be applied.

The exact configuration influences the practicability, cost and accuracy: Using a Woods' lamp in clinical practice to evaluate infections is cheap and quick, but the measurements themselves cannot be stored and if an endogenous fluorophore is lacking, observing the tissue is not possible. The use of hematoporphyrin requires the admission of the patient due to prolonged phototoxicity, and devices capable of fluorescence lifetime imaging and hyperspectral imaging require substantial investment of capital. For a complete discussion of all the different potential applications and techniques for fluorescence

detection I refer the reader to the reviews by Richards-Kortum and Sevick-Muraca, as well as that by Wagnieres et al. (114,115).

The feasibility of fluorescence detection in clinical practice was further enhanced with the development of cheaper and more accurate photo sensors. Although nowadays most smartphones are equipped with two small and capable CCD chips, in the 1990's most used their mobile phone to call and perhaps send the occasional text message. Abels et al. studied the in vivo kinetics of 5-ALA induced PpIX by measuring fluorescence (116). Unfortunately, the study was conducted in a transplant model using a Syrian hamster, an approach which was shown by Van der Veen to be less suitable for the study of PDT in humans (117).

Together with my colleagues I published about a particular FD system before (2,109), and the research presented below is inspired by my experience acquired during the execution of that clinical research. The fluorescence detection system, the DyaDerm Expert, is developed to measure PpIX fluorescence following the application of liposomal encapsulated 5-ALA. Liposomes are very small spheres, in this case having a diameter of 50 nm, with a double layer of phospholipids. Figures 19 and 20 show a schematic representation of the cross-section of a liposome. In figure 19 the outer layer is formed by pairs of phospholipids. The lipophilic tails are directed towards each other and thus form a compartment in which lipophilic substances can be dissolved and transported. The head are directed both towards the exterior and the interior of the sphere. Water trapped inside the sphere serves as a medium for water soluble compounds.
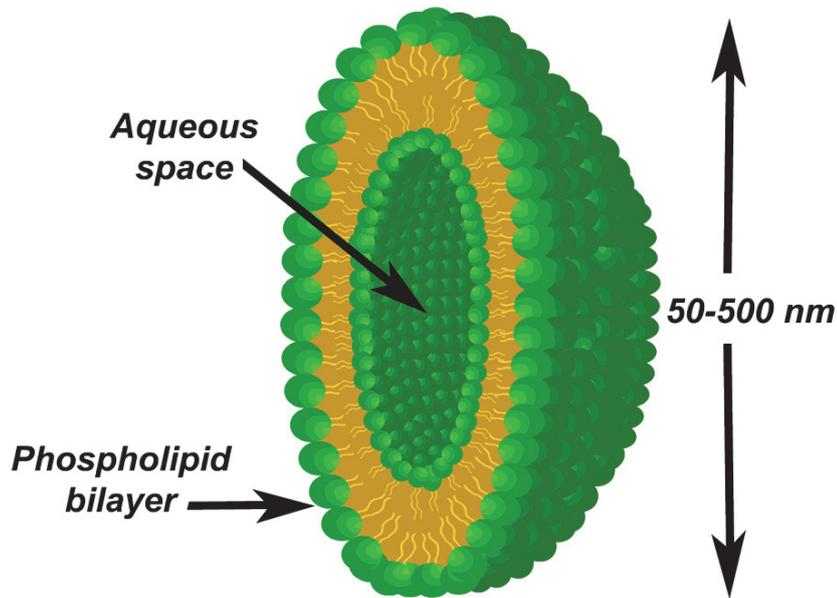
Figure 19: 3D representation of a bi-layer phospholipid liposome.
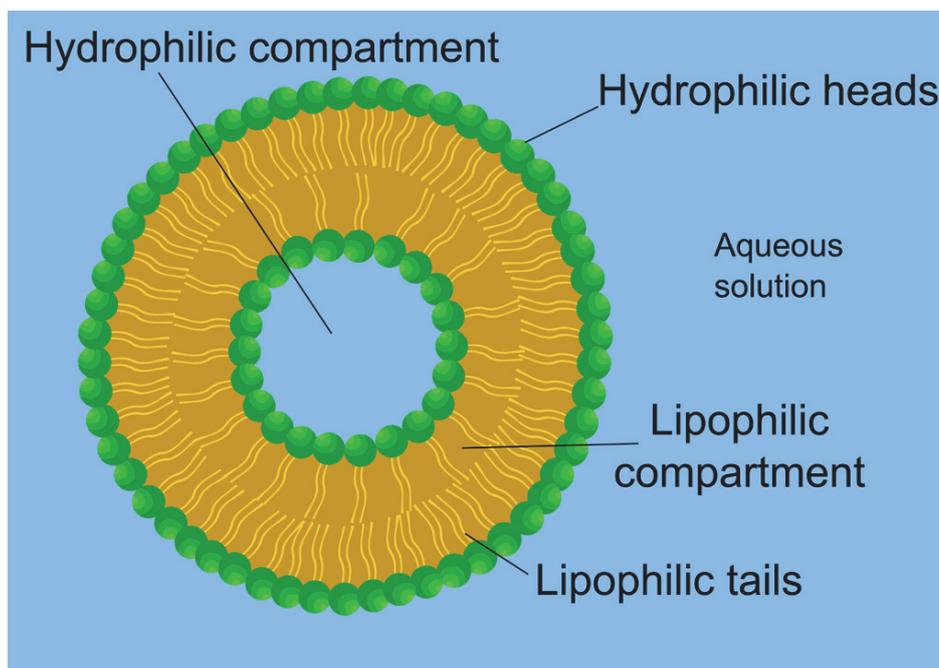
Figure 20: Cross section of a bi-layer phospholipid liposome. Note the lipid ring suitable for the storage of lipophilic compounds, and the aqueous core capable of storing hydrophilic compounds.

Through liposomal encapsulation, the selectivity of the applied 5-ALA is enhanced. Liposomes are more sensitive to disturbances in the epidermal barrier function, as is the case in KSC as well as in inflammations (118). This can be seen in figures 21 and 22. They show the results of a fluorescence detection measurement using the combined method discussed below. The 16% methyl-aminolevulinic acid in crème applied to the left side of the scalp. Here there is a less specific and prolonged fluorescence, indicated by the

green and yellow coloured areas. On the right side a liposomal solution containing 0.5% aminolevulinic acid was applied. Due to the strong intensity of the fluorescence from the MAL a dark cloth had to be used to make the fluorescence from the liposomal solution visible.
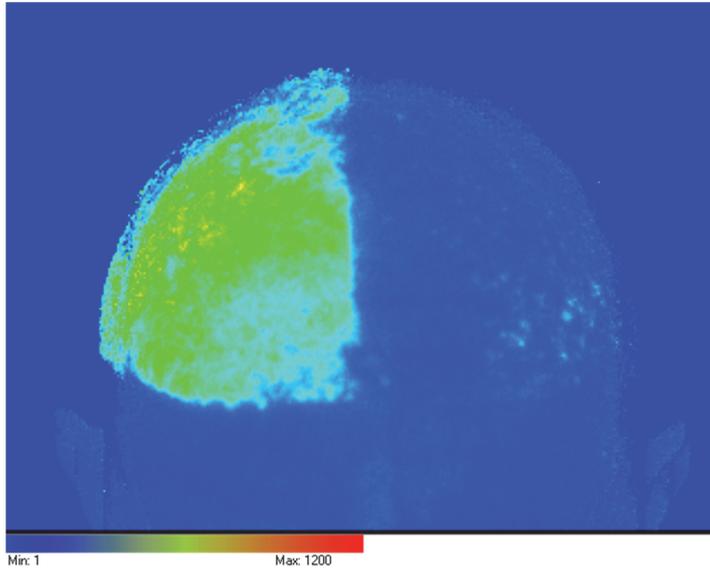
Figure 21: Combined method fluorescence image of 16% methyl-aminolaevulinic acid (MAL) (left) and 0.05% liposomal encapsulated 5-ALA (right) 3 hours after application to the scalp.

Note the none-specific fluorescence invoked by the MAL.

Figure 22: Same as in figure 21, with the MAL side covered.

The liposomal encapsulated 5-ALA is applied during three hours. The liposomes are contained in a spray, which is applied every 5 minutes. As a consequence, the investigated skin cannot be covered during the application, and the patient is required

to stay in the clinical environment. After application, any residual spray is removed using water and a mild detergent. Fluorescence measurements are taking using 409 nm LED's as a light source. These LEDs produce pulsed light with a frequency of 1 Hertz and a pulse length of 100 microseconds. Fluorescence is measured using a CCD camera. The auto fluorescence and PpIX fluorescence signals are separated by using the RGB channels of the chip. Green is used for auto fluorescence and Red is used for PpIX fluorescence. The device is able to present the PpIX fluorescence image, auto fluorescence image, and a combined image in which the PpIX fluorescence is normalized using the auto fluorescence. The three methods are shown in figure 23. The left panel shows PpIX fluorescence, the middle panel the auto fluorescence and the right panel the combined fluorescence measure.

$$Combined\ measure = \frac{PpIX\ fluorescence\ intensity}{Auto-fluorescence\ intensity}$$

For healthy skin, the range of combined measure fluorescence varies between 0.6 and 0.8. A location is deemed of interest if the amount of fluorescence exceeds 1, and 1.5 is regarded as being strongly suggestive of the presence of tissue with an increased metabolism.

PpIX fluorescence of KSC   Auto fluorescence of KSC   Combined   measure
                                                                 fluorescence of KSC

Figure 23: PpIX fluorescence, auto fluorescence, and combined fluorescence of KSC using the DyaDerm Expert system

The evaluation of areas with a reported increase in fluorescence is performed manually. Not all lesions that show an increase of fluorescence are malignant (2). Sebaceous hyperplasia for example, a marker for cumulative UV exposure, results in an increase in PpIX fluorescence and a high combined measure fluorescence. The lesions show a high degree of symmetry, and no decrease in auto fluorescence, which enables an

experienced operator to appreciate their benign nature. Machine learning could be applied to automate the evaluation, but currently no such system is available on the market.

In the clinical study, it was found that the modern, auto fluorescence corrected PpIX fluorescence detection method, was superior to the classical PpIX fluorescence detection method. Yet even the combined method failed to detect all lesions. When applying these techniques one of the first questions to arise is whether lesion size is a limitation. Early detection implies the desire to detect lesions as soon as possible. Yet each lesion starts with just a very small number of cells, which eventually through the increase in cell division and the absence of tumour supressing mechanisms grows sufficiently to be observed by the naked eye.

PpIX-fluorescence   Auto fluorescence   Combined   fluorescence
                                                                          measure
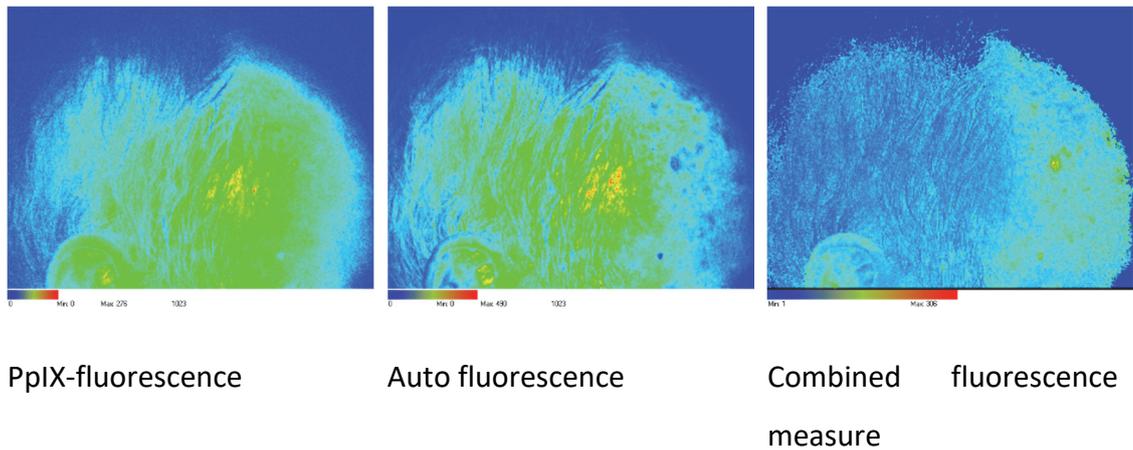
Figure 24: Fluorescence detection of various actinic keratosis.

Colour image of sBCC	PpIX fluorescence
Auto fluorescence	Combined fluorescence
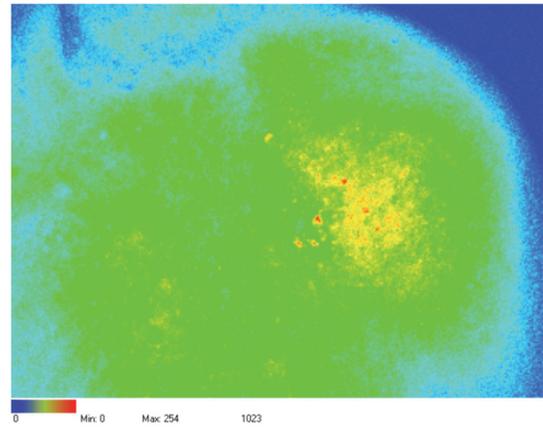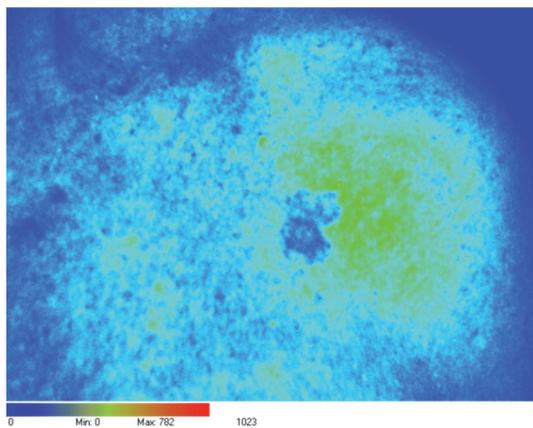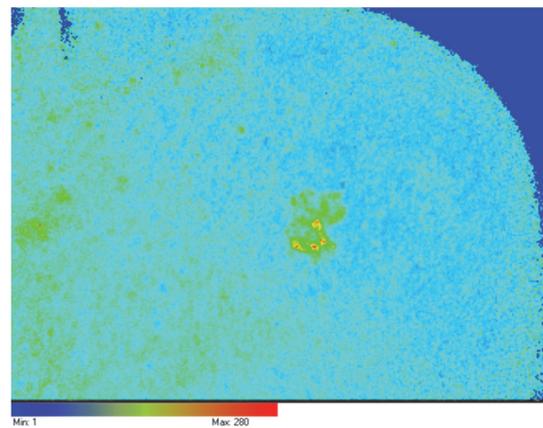
Figure 25: Fluorescence detection of sBCC.

The fluorescence detection images presented in figures 24 and 25 show how a KSC is presented to the user. Note that the PpIX fluorescence does not clearly show the lesion. There is some increase in blood concentration visible, but this might not completely explain the decrease in auto fluorescence. The combined method not only clearly demarcates the complete target, but is able to identify hotspots within the malignant tissue.

Recent work on the fluorescence detection of metastatic colorectal cancer in liver tissue applied a similar approach (119). An animal model of metastatic colorectal in liver was injected with indocyanine green and fluorescein. Subsequently, the researchers illuminated the tissue and imaged both the fluorescence from fluorescein and from indocyanine green. They noted that malignant tissue showed a lower ratio of fluorescein fluorescence over indocyanine green fluorescence compared to healthy tissue.

Clinicians working with the combined fluorescence detection system noted that it performs less when the skin of the patient contains more pigment, when the patient has a suppressed functioning of the epidermal barrier function which increases the uptake of 5-ALA in the healthy skin (shown in figure 26), and when the amount of 5-ALA applied to the investigated area was lower than expected.

PpIX-fluorescence   Auto fluorescence   Combined fluorescence measure
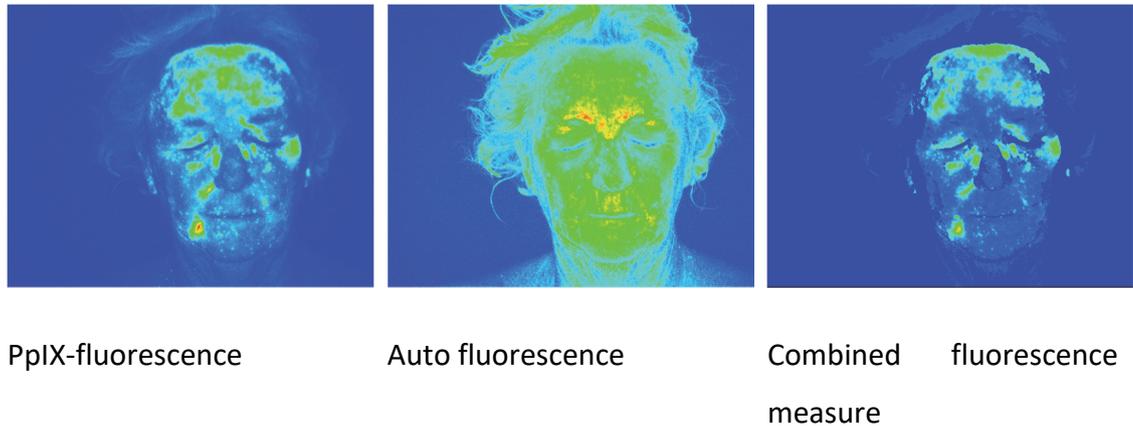
Figure 26: Non-specific PpIX-fluorescence caused by the use of an exfoliating topical cream, which compromises the epidermal barrier function.

KSC, in particular squamous cell carcinoma, can have a very aggressive character. In very rare cases the lesions occur within no more than two weeks and after histo-pathological analysis these lesions tend to be located further from the skin surface than other KSC. Both prevalence and the risk of metastasis is generally underestimated in squamous cell carcinomas (17). In personal communications, clinicians noted that these lesions had not been detected using fluorescence detection, even when such an examination had been performed just prior to the clinical presentation of the invasive squamous cell carcinoma. This suggests that target depth is a significant factor for the accuracy of fluorescence detection systems. Thus, even though fluorescence detection systems have been reported to have quite high sensitivity and specificity, these techniques too have their limitations.

Therefore here, using computational methods, I investigate the effect of some of the variations encountered in clinical practice on the accuracy of three types of fluorescence detection. The advantage of the computational approach lies in its ability to strictly prescribe the tissue properties, allowing for stepwise increase or decrease of the relevant variables, i.e. a parametric sweep. The study is divided in three sections.

I consider the effect of the most important chromophores in the skin, melanin and haemoglobin, as well as the effect of an increase in scattering on the accuracy of the three FD methods.

I adjust the tumour dimensions and location and establish the relative performance of the three methods.

I vary the concentration of the photosensitiser in the target and tissue and investigate how this affects the three methods.

My study is not the first one to study fluorescence detection, nor the first to apply computational methods for this purpose. Saarnak has studied the effect of blood concentration in tissue, depth and thickness of the target, auto-fluorophore concentration, fluorophore concentration for situations comparable to the one depicted here (120), and as far back as 1984 Van der Putten and Van Gemert studied the effect of varying concentrations of photosensitiser in the target and the surrounding tissue, albeit using Kabulka-Munk theory instead of the Monte Carlo method employed here (98). Welch et al. studied the propagation of fluorescent light using the Monte Carlo method (121). Amongst others, they noted that (optical) depth of the target has a significant effect on the measured fluorescence, as more and more of the fluorescence signal originates from non-targeted tissue, and more and more of the fluorescence emitted by the target travels to other directions than the surface. Drezek et al. described lower auto fluorescence in neoplastic tissue of the cervix (122). Valentine et al. studied PDT and photo-bleaching, i.e. the decrease in PpIX fluorescence over time during the PDT treatment (48,123). Liu similarly studied dosimetry in PDT using fluorescence measurements (124,125).

3.3   Materials and methods

This study investigates the effect of variations in the skin on the contrast in fluorescence reported by three types of fluorescence detection.

The first method is based on 5-ALA induced PpIX fluorescence following irradiation with 409 nm light. The topical application of 5-ALA results in a temporary preferential build-up of PpIX in the tumour. Irradiating cells containing PpIX results in the creation of reaction oxygen species, an effect utilized in photodynamic therapy (PDT). If the excited PpIX molecule does not interact with another molecule, it reverts to the ground state

and the remaining energy is converted into light. I am only concerned about the creation of this fluorescence and its measurement. The duration of illumination in fluorescence detection is very short compared to PDT protocols, allowing us to ignore effects of photobleaching, i.e. the decrease in PpIX concentration due to the PDT. So, PpIX fluorescence is based on the idea that the fluorescence signal of malignant tissue can be increased versus that of healthy tissue by applying appropriate amounts of 5-ALA. I say appropriate because saturating the skin with 5-ALA will result in an increase in PpIX in healthy tissue as well, a situation I address in my calculations. The investigations by Smits and Kleinpenning are an example of this method (102–106). The second method is based on the measurement of fluorescence from auto-fluorophores, or more specific, the lack thereof. Na, Stender and Wulf, as well as Brancaleon et al. and Lycette and Leslie (109–111) have reported that KSC show relative low intensity of auto fluorescence compared to healthy tissue. I use Flavin Adenine Dinucleotide as a model for this source of fluorescence. PpIX takes no part in this type of fluorescence detection. The third method is more of a post-measurement algorithm, using a auto fluorescence signal to improve the accuracy of the PpIX fluorescence signal (2,97–99,107).

I apply the Monte Carlo method to solve the radiative transfer equation in a simulation of the light-tissue interaction. The tissue is represented using the well-known layered approach (31). The model consists of three areas with their individual optical properties. Those are the epidermis, the dermis and the target. Neither epidermis nor dermis are separated according to their distinct parts, such as the stratum corneum, stratum lucidum, stratum granulosum, stratum squamous, or stratum basale in the case of the epidermis. Furthermore, the shape of the target area is restricted to rectangular geometries.

These three methods are used to detect a 5000x400 μm target area located 100 μm from the skin surface. The skin is represented as a combination of layers. The tissue as a whole has a width of 25000 μm and a height of 3600 μm. The first layer is 25000 μm wide and 70 μm in height. It represents the epidermis and contains melanin, FAD, PpIX and other non-specified chromophores such as water. The second layer is 3530 μm in height and 25000 μm wide and represents the dermis. It contains PpIX, FAD, haemoglobin and other non-specified chromophores such as water. The target area is contained within the dermis and contains PpIX, FAD, haemoglobin and other non-

specified chromophores such as water. Pigment was set to represent fair skin (126). Haemoglobin concentration in skin was set to 543 micrograms per litre in healthy skin and 1500 micrograms per litre in the target area (127). PpIX concentration was set to 1.3 microgram per litre (127). Blood oxygenation was set to 90%. The data provided by Scott Prahl (20) was used for the molar extinction coefficients of haemoglobin and is shown in figure 27 and 28. I used the absorption and fluorescence profiles of Flavin Adenine Dinucleotide for the flavin calculations. Only part of the curve is shown. Flavin for example has much higher attenuation in the ultra-violet spectrum. In the studied fluorescence detection procedure, UV light is neither emitted or absorb, and therefor that part of the spectrum has been omitted. For the visible part of the electromagnetic spectrum, the MEC is generally higher for PpIX than for Flavin, except for a short range between approximately 440 nm and 485. With regard to the light source I note that the MEC for PpIX is at its peak for the presented range and significantly exceeds that of Flavin.
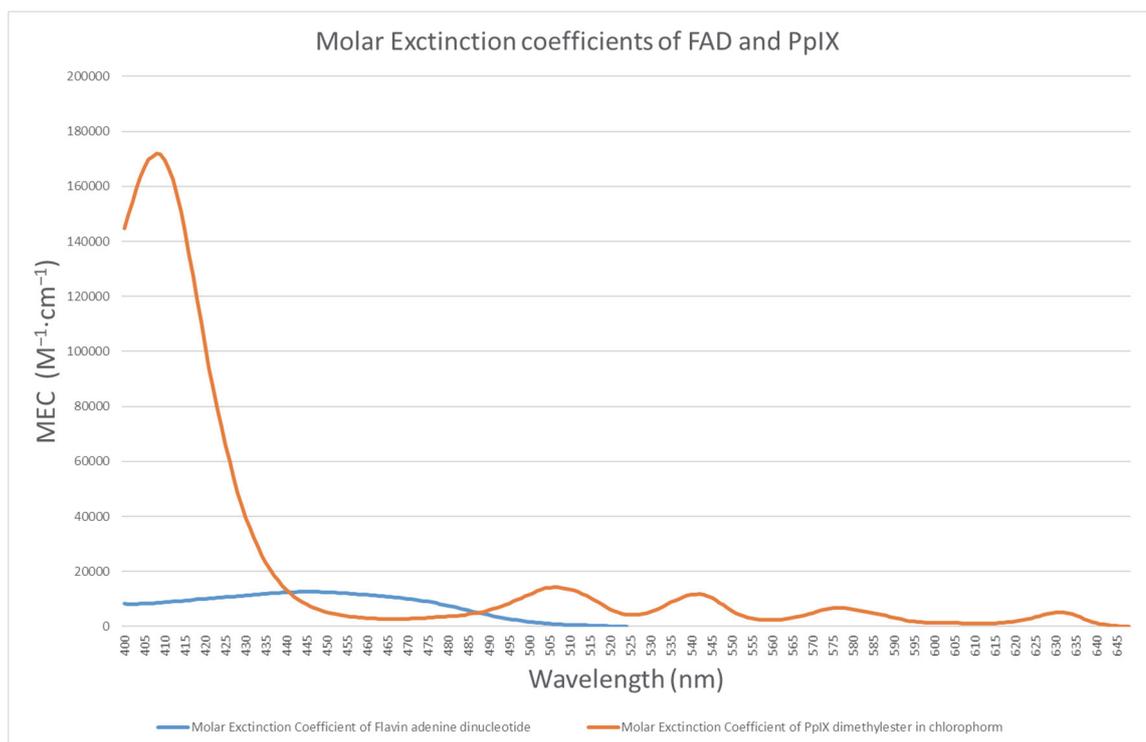
Figure 27: Molar extinction coefficient of FAD and PpIX.

Source for FAD: (128). Source for PpIX (129). I note that the data for PpIX is for a dimethyl ester of PpIX in chloroform, which differs from PpIX in water.
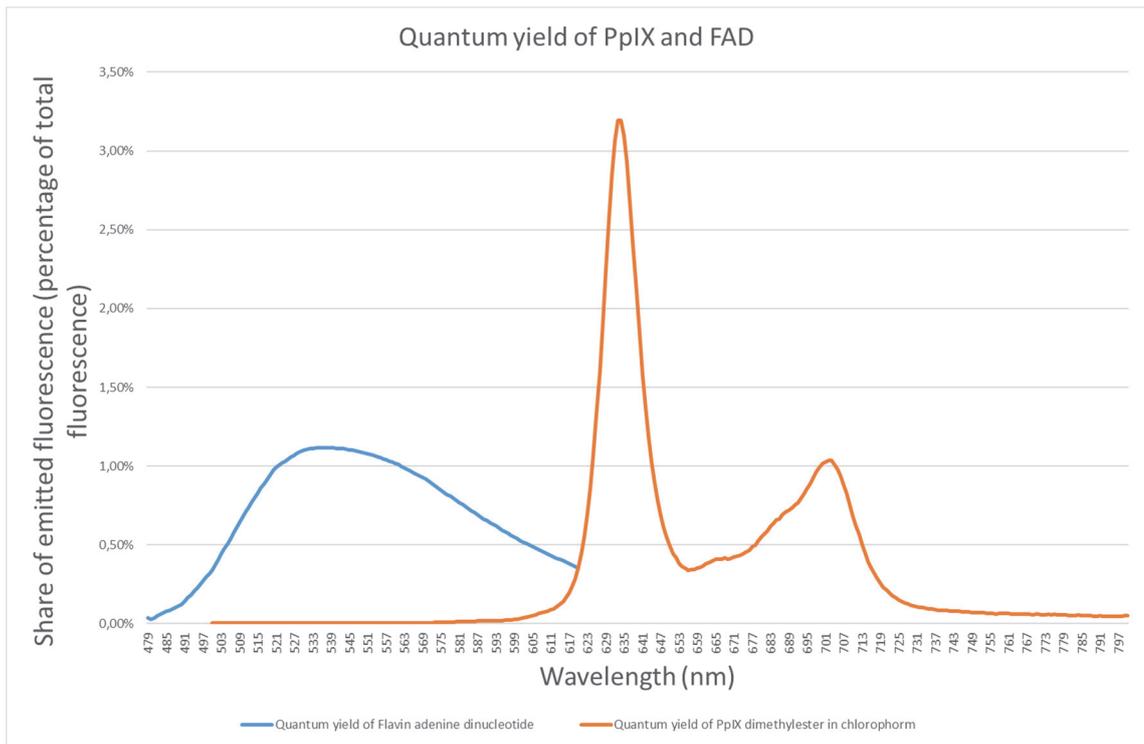
Figure 28: Distribution of emitted fluorescence by FAD (130) and PpXI: (129)

Out of considerations of efficiency I chose not use the actual quantum yields for FAD (128) and PpIX (110). The quantum yield is the fraction of absorbed photons that is emitted as fluorescence and indicates the efficiency of the fluorescence process.

$$\Phi = \frac{number\ of\ photons\ emitted\ as\ fluorescence\ or\ phosphorescence}{number\ of\ photons\ absorbed\ by\ the\ fluorophore}$$

Instead I used the ratio of quantum yields to 1:2.3 for PpIX and FAD respectively. The actual quantum yields are two orders of magnitude lower. By using larger numbers for quantum yields I was able to achieve convergence for the fluorescence simulations at lower number of initial photons than had otherwise been required. Due to the demands in computing power, I also used a single wavelength for FAD and PpIX rather than the distributions shown in figure 27. FAD fluorescence was represented by 550 nm and PpIX fluorescence by 636 nm.

Since in my experiments FAD serves as a proxy for auto fluorescence in general, I determined the concentration of FAD by calculating the fluorescence ratio between PpIX and auto-fluorophores, and setting the concentration such that the resultant PpIX over FAD ratio was near 0.75.

Using the previously described Monte-Carlo simulation method, light is modelled to be emitted by a slightly divergent light source, represented by a anisotropy factor for the Henyey-Greenstein phase function of 0.9. The light has a wavelength of 409nm and enters the skin from air. Light absorbed by PpIX or FAD was registered separately and used for the fluorescence calculations. Beam width was set to 20000 µm, so that the transition from illuminated skin to non-illuminated skin was registered in the simulations.

The model diverges from reality in respect to the homogeneity of the epidermis in normal skin and malignant skin. The latter is thicker than normal skin (127). Furthermore, the target tissue was always contained in the dermis. The epidermis was assumed to be completely healthy. Again, this is not in accordance with the nature of KSC, which generally start in the epidermis. As such, the model can be regarded as representing a variation of the nodular basal cell carcinoma.

In my model, I take the invasive basal cell carcinoma (iBCC) as the basic case. In order to prevent a border solution for one variable to dominate the others, I apply a most modest case. None of the variables in the standard case approaches the boundaries of the values for these variables in the real world. The epidermal thickness e.g. is 70 µm. Epidermis in cancerous tissues can be 30 µm or even 1000 µm. Likewise, I use a 1.5% blood volume content for the target tissue and 0.5% blood volume for the normal skin. Melanin content of the epidermis is a bit low with 1.3%, but since these cancers occur predominantly in fair skinned individuals this is not an extreme departure from reality. The iBCC is of average size, with a width of 5 mm and a depth of 0.4mm. It is located just beneath the epidermis. PpIX content in the skin is 1.3 mg/l, which is an average value according to Middelburg (127).

The reason why I choose these default settings is that I want to be sure that I get some insights from experiments. Should I choose a value which I know to significantly influence the accuracy of the fluorescence detection, this choice would dominate the variables in which I am actually interested: Setting the epidermal thickness to 1000 µm is likely to interfere with the study on the effect of target width for example.

I defined two areas of interest in order to evaluate the contrast registered by the different techniques. The first is the area directly over the target, the second is an area

located at the edge of the beam serving as a control tissue. The control tissue measurement was taken over an area of 2500 μm to prevent contamination of the measurements in the control area by scattered light emitted from the target area. The three fluorescence detection techniques are evaluated by their ability to detect the presence of target based on the difference in fluorescence registered above the target area and registered above the control area. The PpIX fluorescence detection technique and the combined measure fluorescence technique are ranked per the ratio of the registered fluorescence emitted from the two areas. In the case of the auto fluorescence detection technique I report the contrast in negative terms, because the auto fluorescence signal emitted above the target will be lower than that above the control tissue. This change in representation makes it easier for the reader to interpret and compare the results.

The computational experiments can be grouped according to the nature of the variations studied. The first group concerns the influence of chromophores and scattering coefficients on the contrast reported by the three fluorescence detection techniques. The second group of calculations concerns variations in the dimensions and location of the target tissue. Finally, the third group involves variations in the concentration of PpIX.

3.4   Results

3.4.1   Section I: Scattering and absorbing compounds of the skin

The following section presents the results from the computational experiments on variations in scattering and absorption in the skin. A discussion of the results is contained in section 3.5.2.

The effect of scattering on the accuracy of FD

From previous research it is known that keratinocyte skin cancers differ markedly from normal skin (127). Especially the epidermis is larger in comparison to unaffected skin. The difference though is not such that there is a non-overlapping distribution. I do not look at the effects of an increase in the thickness of the epidermis directly. The reason is that by increasing epidermal thickness, I'd be changing two variables simultaneously. First, the epidermis holds melanin, so increasing epidermal thickness would also increase melanin, a variation I discuss below. Second, increasing the epidermis would also relocate the target to an area more distant to the surface of the skin. This too is a

variation I investigate below. Instead I chose to investigate the effect of an increase or decrease of scattering within the skin on the accuracy of the fluorescence detection techniques. Accuracy here is represented as a change in the reported contrast between the fluorescence detected above the control tissue and the fluorescence detected above target tissue.

I used a specially developed version of the Toddy software in which the scattering coefficients can be adjusted using adjusting a constant with which the actual scattering coefficient is multiplied. The value of this coefficient was varied from 0.5 up to 2.1 in steps of 0.4. This range is well in excess of the variation in scattering as reported by e.g. Salomatina et al. (21). Actual variation in scattering would be closer to 0.75 to 1.25 times the average value for the scattering coefficient. Nonetheless the broader range is used to acquire a better understanding of the effect of changes in the scattering coefficient, even if some of the results will be clinically less relevant.

The scattering coefficients of all three types of tissue, epidermis, target tissue, dermis, were varied simultaneously. Figure 29 shows the effect of a change in the scattering coefficient on the accuracy of the three investigated methods. The reported contrast in fluorescence between the healthy, uninvolved skin and the tumour is shown on the vertical axis. The correction factor used in the calculations is shown on the horizontal axis. The combined fluorescence detection method reported higher levels of contrast than the auto-fluorescence detection method and the PpIX fluorescence detection method. Changing the scattering coefficient had little effect on the reported contrast. As scattering increased, and the penetration of the light into the tissue decreased, the contrast reported by the auto-fluorescence detection method decreased. Both an increase and a decrease in scattering negatively impacted the combined fluorescence detection method. The PpIX fluorescence detection method performed better when scattering increased.
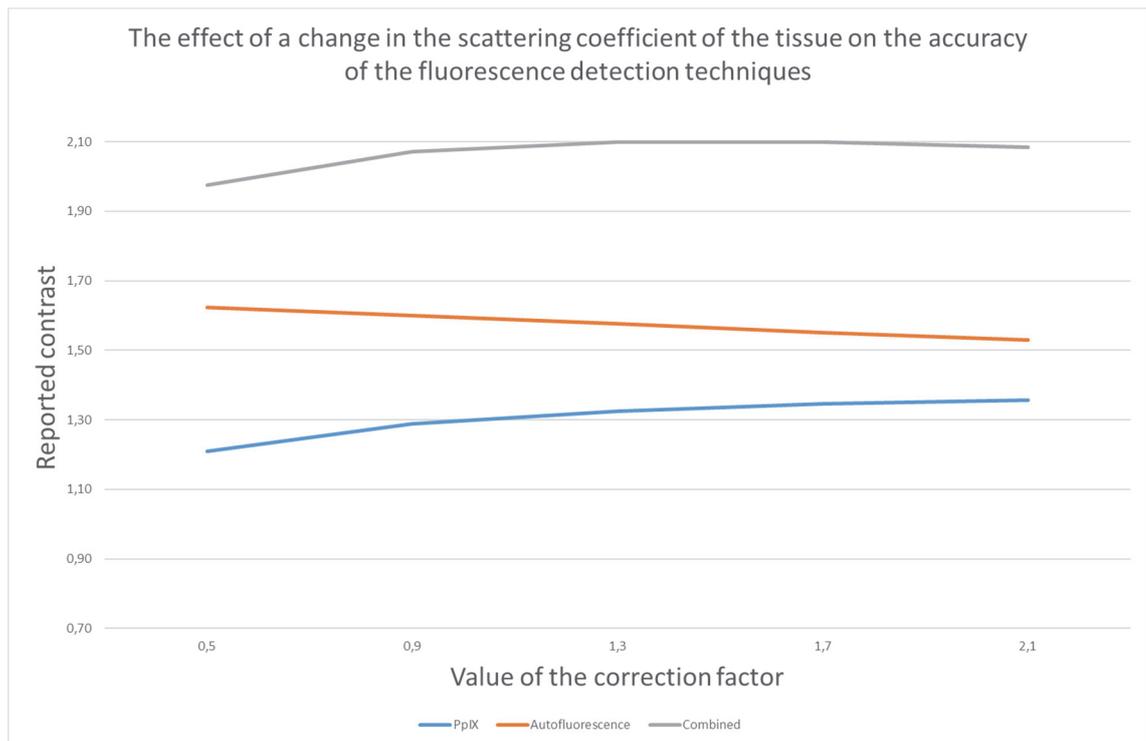
Figure 29: The effect of a change in the scattering coefficient using a correction factor on the accuracy of the studied fluorescence detection techniques.

The effect of a change in scattering was limited, but clearly did influence the three techniques to some degree. I note that each technique was affected in different way. The auto fluorescence method performed better with less scattering. This is probably due to more light being absorbed deeper into the dermis and thus creating a more intense background signal from which the interfering effect of the increase in chromophore in the target tissue can be observed. The PpIX fluorescence detection method on the other hand performs better as scattering increases. It is a well-known result from the literature on light tissue interactions in photothermal treatments that scattering increases the energy available at the more superficial areas of the tissue (129). This would increase the number of photons available to excite a PpIX molecule in the target area, and thus increase the amount of fluorescence. Because the combined method depends on both the PpIX fluorescence detection method and the auto fluorescence detection method, it is negatively affected by either an increase or decrease in scattering. Nonetheless the combined fluorescence method dominated the PpIX fluorescence detection technique and the auto fluorescence detection technique in terms of reported contrast.

The results show that scattering influences the accuracy of the three fluorescence detection techniques, but in my model it does not result in a failure to detect the target tissue. It does though influence the accuracy of the delineation in the auto fluorescence detection method.

The effect of melanin concentration on the accuracy of FD

One of the prime causes of skin cancer is UV radiation induced DNA damage. The human body protects itself from the harmful effect of sole or UV radiation by producing melanin in the skin. The problem is that UV exposure is necessary for the production of vitamin D. So, depending on the season and the geographic location there is an optimal concentration of pigment in the skin. This optimal concentration balances the benefits from solar UV radiation, i.e. vitamin D production, against the harm incurred from the exposure in terms of skin cancer risk. Melanin though does not just absorb UV light, but also absorbs light from the visible spectrum, most notably blue light and to a lesser degree green light and yellow light. This is evident from the colour of tanned skin: it is brown.

This poses a potential problem for fluorescence detection, since the illumination is performed using blue light. Furthermore, the auto fluorescence method and the combined fluorescence method depend on green light emitted from the skin by the autofluorophores.

Therefore, I investigated the effect of an increase or decrease in the concentration of melanin in the epidermis on the accuracy of the three fluorescence detection methods. Melanin concentration was increased in steps of 1%, starting at 0% and continuing up to 10% pigment in the skin. This corresponds to Fitzpatrick skin type I up to and including III (41). The change in melanin concentration results in a corresponding change in the absorption coefficient for the epidermis. The results are presented in Figure 30.
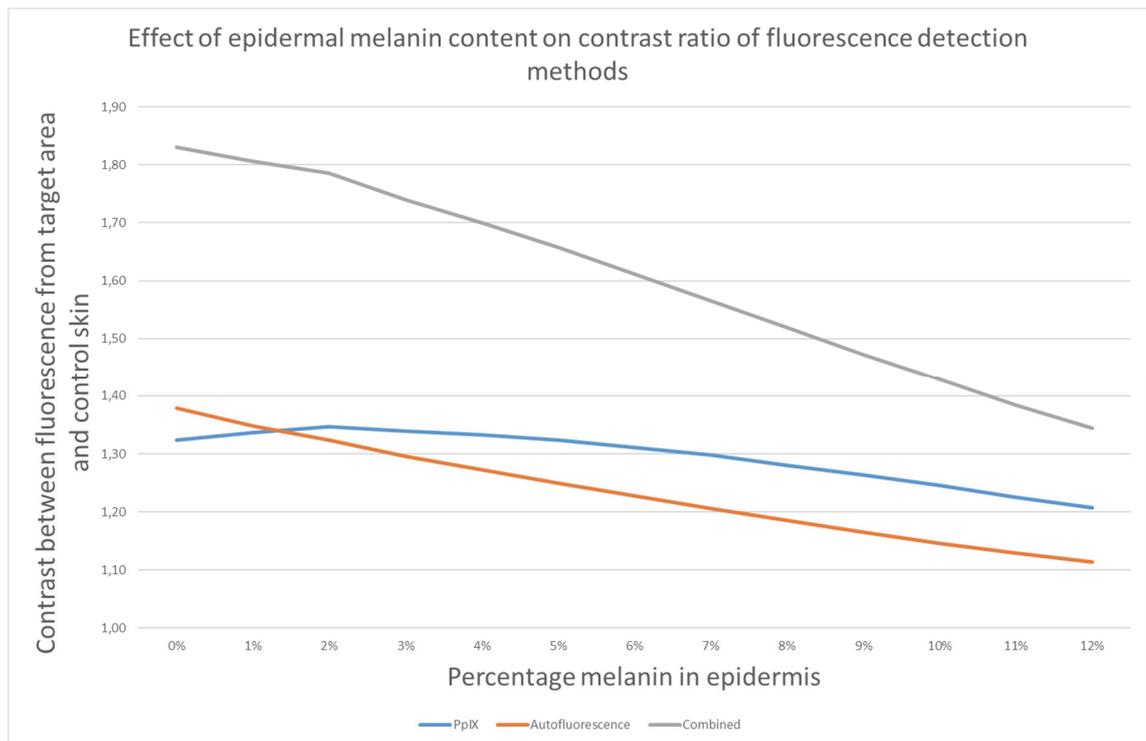
Figure 30: Effect of melanin concentration in epidermis on accuracy of fluorescence detection methods.

As expected, an increase in melanin has a detrimental effect on the accuracy of fluorescence detection, irrespective of the method applied. The trend suggests that there is a concentration of melanin in the epidermis at which all three methods are unable to detect the target area. One rather surprising observation is that for a very small and perhaps clinically irrelevant range the PpIX fluorescence detection method actually benefits from an increase in pigmentation. An explanation for this observation is that at these extremely low levels of pigmentation a larger share of PpIX fluorescence originates from below the tumour. The increase in background noise makes it harder to distinguish the signal from the PpIX in the tumour.

The effect of blood content in tumour on the accuracy of FD

Keratinocyte skin cancer is more generally known as "red skin cancer", in contrast to the malignant melanoma which is called the black skin cancer. This difference in colour is generally due to the increase in vascularisation in combination with the absence of an increase in pigment, although some forms of keratinocyte skin cancers do present themselves with an increase in pigmentation such as the pigmented basal cell carcinoma. The increase in vascularisation is a necessary condition for the presence of a keratinocyte skin cancer, as otherwise the increased metabolism and proliferation could not be sustained due to lack of nutrients and oxygen. Moreover, more aggressive KSC's

are associated with higher blood volume content (130,131). This is why the target area is represented as having a threefold higher haemoglobin content than the surrounding tissue.

Blood is a potent absorber of the light used in the illumination of the target. Although not as intense, the auto fluorescence signal is absorbed as well. Therefore, in the experiment I study the effect of an increase in blood concentration on the accuracy of the fluorescence detection methods.
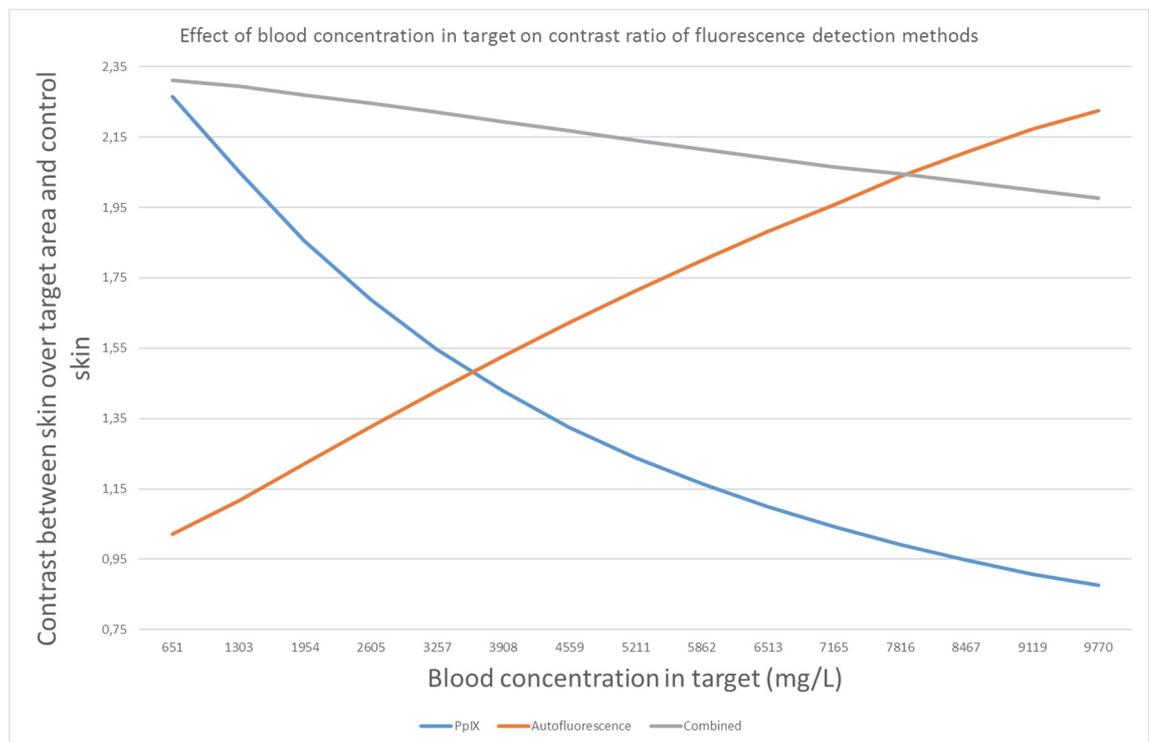
Figure 31: Change in contrast between fluorescence over target and fluorescence over control.

For PpIX and Combined: higher is better. For FAD: Lower is better.

Figure 31 presents the effect of an increase in the blood volume on the contrast reported by the three methods of fluorescence detection. The vertical axis indicates the contrast in fluorescence between the normal skin and the target skin. I.e. a value of 2 indicates that the fluorescence measured above the target is twice that measured over the healthy skin. In those situations, we can identify the location of the tumour, or better said classify that area as an area of interest. The blue curve shows that PpIX fluorescence is negative impacted by an increase in blood volume since the reported contrast decreases with an increase in blood volume.

The results presented above show that an increase in blood concentration affects each of the three fluorescence detection techniques differently. The PpIX fluorescence detection technique is negatively affected by the increase in blood concentration. The fraction of energy absorbed by PpIX molecules in the target decreases, resulting in less contrast between the fluorescence emitted by the target, or observable in the skin over the target area, compared to the fluorescence observed over the control skin. The auto fluorescence based technique benefits from the additional absorption of the background auto fluorescence signal by the target area. Both the PpIX based technique and the auto fluorescence based technique show a non-linear relationship between blood concentration and reported contrast. In the combined method, negative impact of blood concentration in target on the PpIX fluorescence detection method is somewhat compensated by the increase in accuracy of the auto fluorescence based method. So even though the increase in blood concentration does negatively impact the accuracy of the combined fluorescence detection technique, the relationship becomes linear. The combined method again is more accurate than the other two fluorescence detection techniques studied.

The tested values exceed what can be expected in practice. For BCCs, the increase in microvessel width, area fraction and length density of the blood vessels is respectively a factor 2.4, 4.9 and 5.9 compared to the normal skin. So, a physician would not expect to be confronted with a tumour with an increase in blood volume of a factor 15. Similarly, a tumour with a blood concentration indistinguishable from the normal skin is quite unlikely (we cannot ignore the situation in which a tumour is at the very initial stages of development). Nonetheless these extreme cases shed some additional light on the effect of the increase of blood concentration on the performance of the fluorescence detection methods.

3.4.2   Section II: Target dimensions

When diagnosing a keratinocyte skin cancer, and in particular a basal cell carcinoma, the dimensions of the target of particular interest because therapeutic interventions differ in efficacy with regard to deeper located malignant tissue. Low fluence photodynamic therapy, i.e. photodynamic therapy using 37.5 J/cm^2, for example is less effective in nodular basal cell carcinomas and larger superficial basal cell carcinomas (132,133). The

following section will discuss the effect of target width, target thickness and target depth on the contrast reported by the three fluorescence detection techniques. The discussion of the results is relegated to section 3.5.3.

The effect of tumour width on the accuracy of FD

Target width was increased from 500 µm to 4000 µm in 500 µm steps.
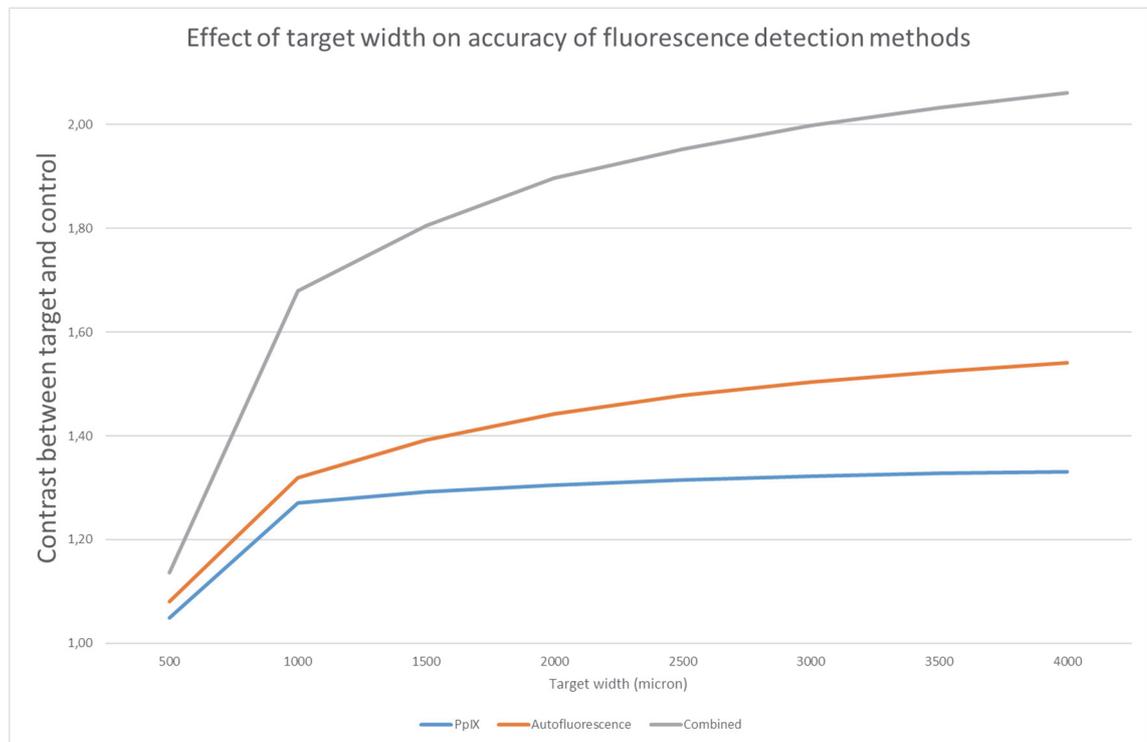
Figure 32: Effect of target width on contrast reported by fluorescence detection techniques.

The results of the experiment on the effect of target width show that all three methods are similarly affected. Figure 32 is a graphical representation of the effect of an increase in target width on the contrast reported by the three fluorescence detection methods. Very small targets are hard to distinguish from the surrounding skin, since the ratio is close to one. The amount of fluorescence measured at the centreline of the target decreases as the target with decreases. This is due to some of the fluorescence signal emitted by the target area being scattered away from the centre line. This result is comparable to the observation in computational analysis of optical-thermal treatments for e.g. port wine stains that a small diameter laser results in less propagation of the energy into the tissue (11). A small target emitting fluorescence is like a small diameter laser beam. Once the target is sufficiently large, the reported contrast remains constant for the PpIX fluorescence detection method and slightly increases for the auto fluorescence and combined methods.

The effect of tumour thickness on the accuracy of FD

In this experiment, I transform the superficial like KSC into a nodular KSC. The tumour thickness is varied between 10 μm and 500 μm.
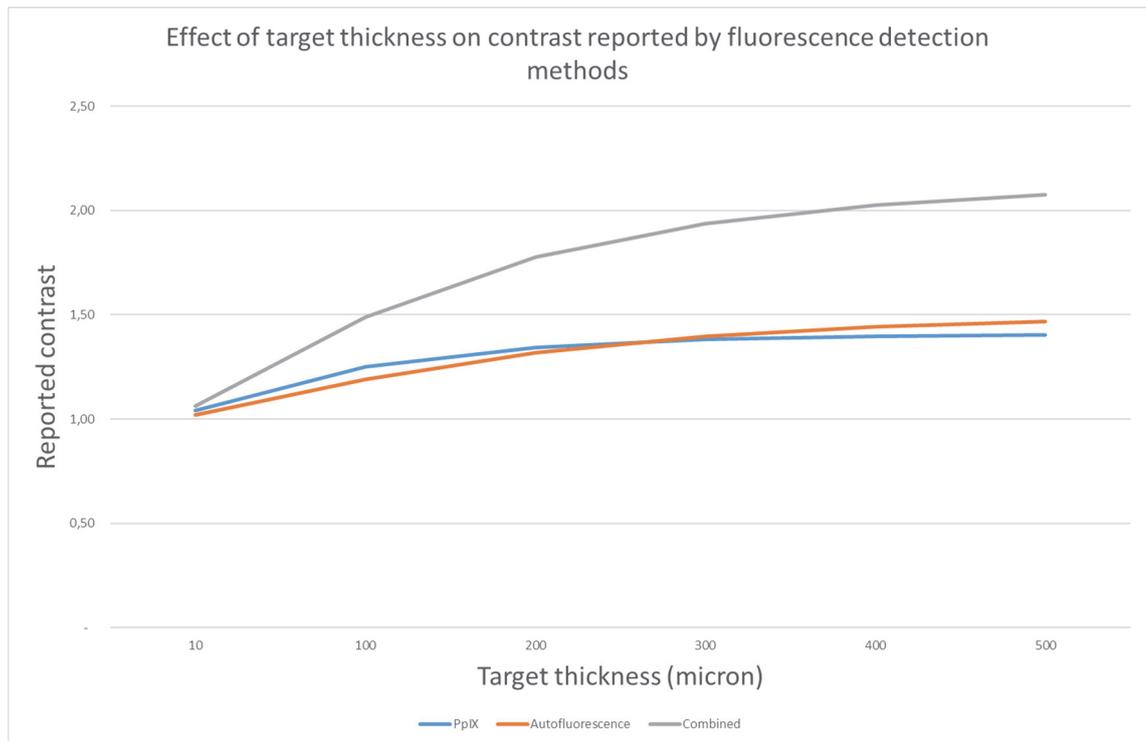
Figure 33: Effect of target thickness (in μm) on contrast between fluorescence from control skin and skin over the target area.

The story figure 33 tells us is not to dissimilar to what we have seen in figure 32: For very small / thin targets, the methods report no or very small levels of contrast. As a consequence, those targets are likely to be missed, regardless of the applied method. At the boundary, the amount of fluorescence emitted by the target is so low that it is indistinguishable from the normal skin. The amount of PpIX fluorescence emitted or the amount of auto fluorescence absorbed increases as the target increases in size. The relationship between reported contrast and target thickness is comparable for all three methods. As the volume of the target increases, so thus the reported contrast. But with each marginal increase in volume, there is an incrementally decreasing increase in the reported contrast. This is seen by the "tapering off" of the function. At some point the PpIX curve runs horizontally: Any further increase in thickness of the target will not result in an increase in the reported contrast. I note that the saturation point is reached in smaller sized target for PpIX fluorescence than for auto fluorescence.

I conclude that fluorescence detection systems are not particularly affected by the subtype of BCCs. Both nodular and superficial variants of BCC can be easily detected, assuming they have grown sufficiently to contain a sufficient concentration of PpIX and chromophores, and assuming that the precursor has been able to completely saturate the target tissue. The results of De Haas et al. (134) though suggests that this is not necessarily the case in all tumours.

Experiment 6: The effect of tumour depth on the accuracy of FD

In the final experiment of this section I look at the effect of target depth on the accuracy of the three fluorescence detection techniques. The relevance of this experiment lies in the fact that aggressive tumours tend to originate from deeper areas of the skin, in particular with solid organ transplant recipients (135). The more sensitive a technique is to deeper located targets, the more valuable it is in skin cancer screening for this patient population. Organ transplant recipients run a significant higher risk of developing a fatal form of keratinocyte skin cancer, especially if they are treated with a calcineurin inhibitor (136).
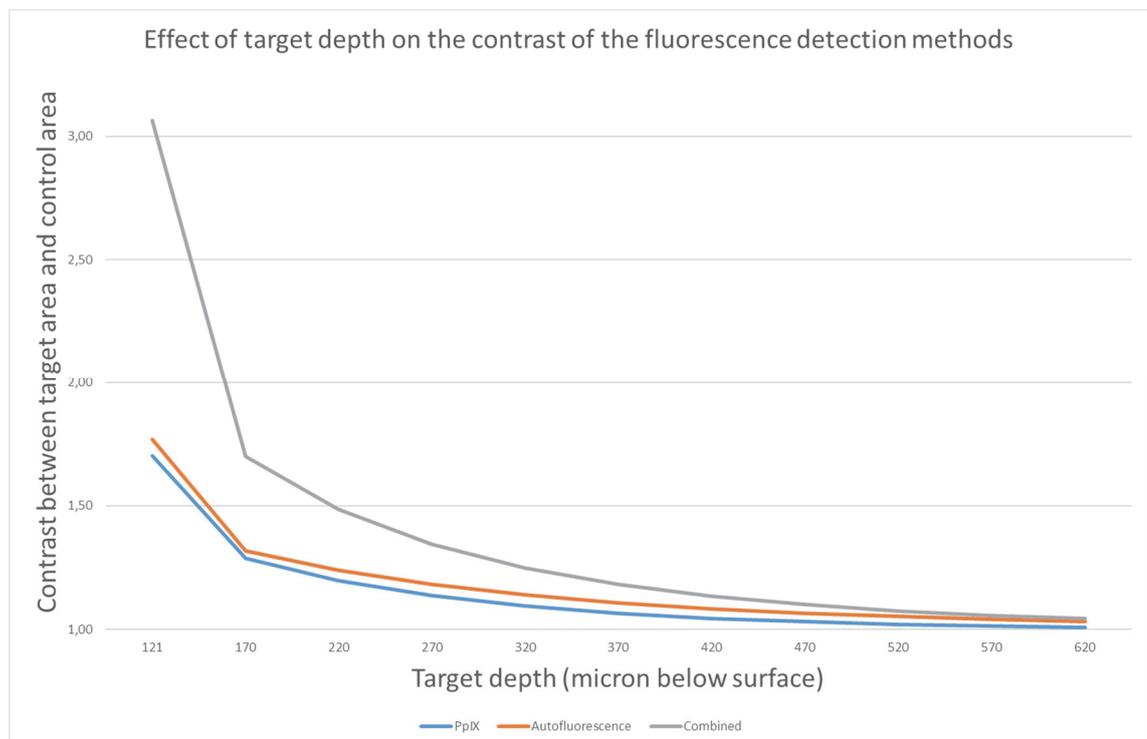
Figure 34: Effect of target depth on contrast reported by fluorescence detection techniques.

The results shown in figure 34 clearly show that all three methods are significantly influenced by the depth at which the target is located. Very superficial targets are associated with higher levels of contrast, in particular for the combined method. Targets

located at very deep areas of the dermis are not susceptible to fluorescence detection. Furthermore, the relationship between observed contrast and target depth is quadratic. The obvious explanation for this is absorption of the 409 nm light used to illuminate the skin. This indicates that fluorescence detection systems will not be able to detect at least some of the more aggressive tumours, insofar these develop from within the deeper layers of the skin. This, though, is of relative little practical concern, because the pace at which such lesions develop is so high that they would completely develop well within the timeframe between to check-ups.

3.4.3 Section III: Fluorophore distribution

The final section of my investigations into the field of fluorescence detection is concerned with the effect of the distribution of the photosensitiser. Section 3.5.4 contains the discussion of the presented results.

The effect of photosensitiser in target on the accuracy of FD

In this experiment, I increase the concentration of PpIX in the target while keeping the concentration in the surrounding tissue constant.
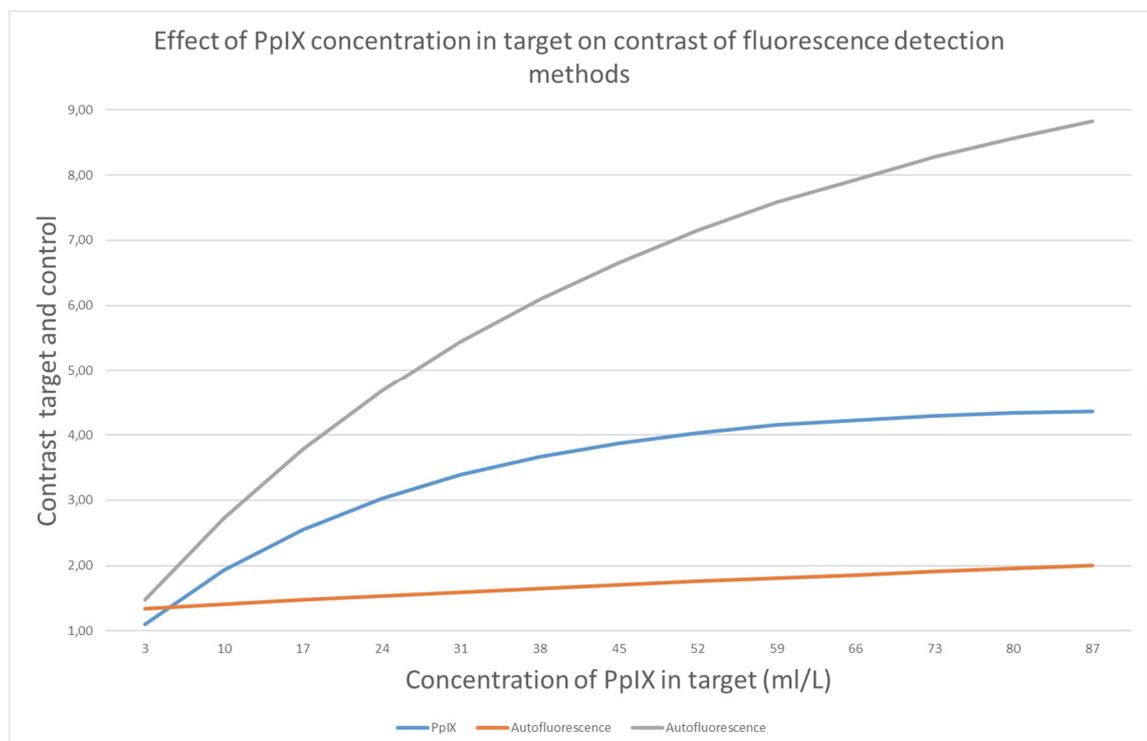
Figure 35: Effect of increase in PpIX in target on contrast between target and control reported by the fluorescence detection techniques.

Page 73

Note that as PpIX concentration increases, there is less absorption in the deeper regions of the target. Figure 35 illustrates this by the decreasing marginal contrast with a marginal increase in PpIX concentration in the target. Both the combined method and the PpIX method start to taper off and in the case of PpIX run horizontally at the maximum value studied. This is caused by more absorption of the photons at the superficial areas of the target tissue.

The results show that all three methods benefit from an increase in the selectivity of the photosensitiser. As can be expected, the improvement in the reported contrast is most notable in the PpIX fluorescence detection method and the combined fluorescence detection method. The experiments did suffer from a relative low number of calculations used, but there was a sufficient number to achieve convergence.

At higher concentrations of PpIX in the target, light penetration in the target is limited. Should one seek to determine the thickness of a tumour using fluorescence, it would be wise to apply a moderate amount of photosensitiser or prodrug. Ackerman has previously discussed this "inner cell effect" in the context of fluorescence detection of KSCs (110), and it is in essence equal to the plea by Dougherty and Potter (137). An increase in the light attenuation of a photosensitiser is not necessarily a good thing, as it has a detrimental effect on the penetration of light (and thus the photodynamic effect) into the tumour. One can consider this as an example of having too much of a good thing: Selectivity of the photosensitiser is preferred, but at some point those molecules closest to the light source absorb so much light that too little energy remains for the deeper located molecules to induce a sufficiently large PDT effect or fluorescence. The next experiment touches on the related problem of having a non-selective highly absorbing photosensitiser in the surrounding tissue, a question previously investigated by Wilson et al. (97).
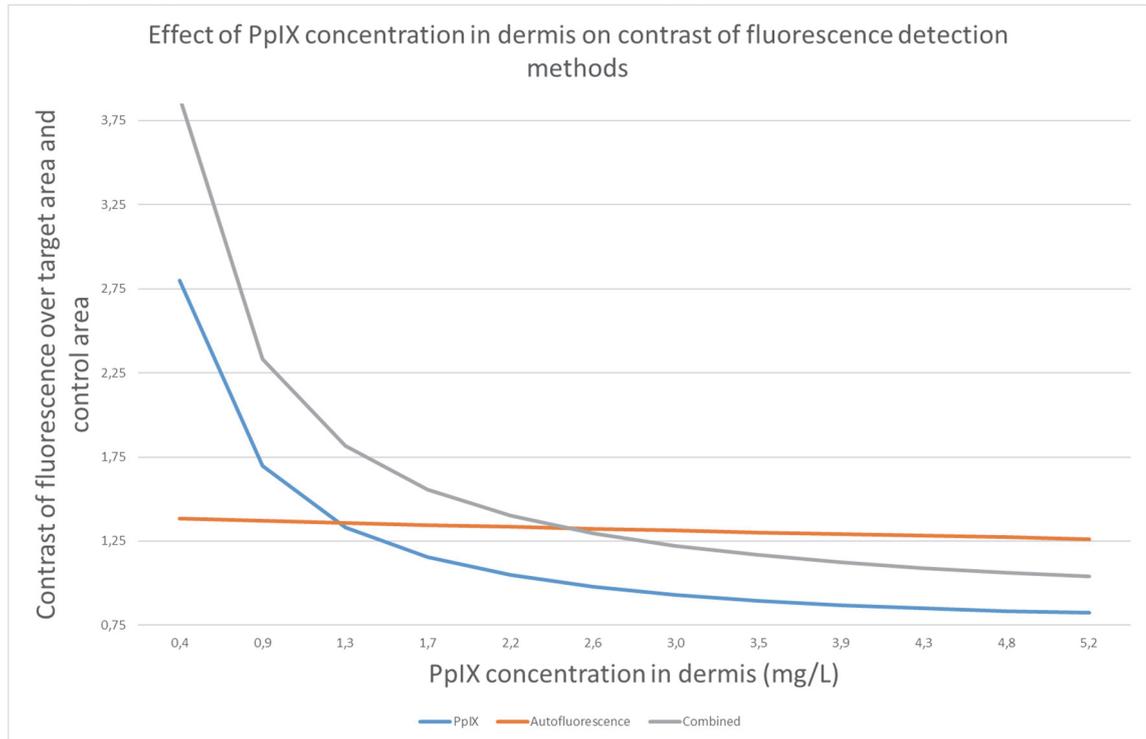
Figure 36: Effect of increase in PpIX concentration in surrounding tissue on contrast reported by fluorescence detection methods

The results of the experiments, as shown in Figure 36, confirm the findings by Wilson, Patterson and Burns (97) for tissue in which scattering dominates absorption. The initial reported levels of contrast drop quickly as the selectivity of the photosensitiser is lost. There is a steep decrease in the reported contrast, and at some point the target tissue cannot be distinguished from the surrounding tissue. PpIX fluorescence detection and the combined method are quite sensitive to a lack of specificity of the photosensitiser. This scenario actually is the only one in which for a considerable range auto fluorescence dominates the two other methods. The range of PpIX concentration in the surrounding tissue did not exceed that in the target area. Nonetheless the contrast reported by the PpIX fluorescence detection method was negative, i.e. there was more fluorescence emitted by the healthy tissue than was emitted by the malignant tissue. Figure 21 shows the clinical presentation of the phenomenon.

3.5 Discussion

3.5.1 General considerations

3.5.1.1 *Advantage of computational analysis using parametric sweep*

I analysed the reported contrast by three methods of fluorescence detection in eight different scenarios, each of which aimed at determining the effect of a change in one parameter on the reported contrast. My investigations are motivated by clinical experience. During conversations with experienced clinicians who use the fluorescence detection method to locate areas which are susceptible of having a keratinocyte skin cancer, became apparent that certain physiological properties of some keratinocyte skin cancers resulted in a markedly different image than other keratinocyte skin cancers. In addition, fluorescence detection was difficult or near impossible in patients who either had applied keratolytic agents or had a relatively high concentration of melanin. In order to overcome the difficulties that result from these influencing factors, the participating clinicians used the information of all three methods of fluorescence detection supported by the investigated system. The outcome of the deliberations was that there was a clinical need to understand how certain physiological characteristics affect the reported contrast of the three fluorescence detection techniques.

The classical method for conducting scientific research in clinical practice, the randomised comparative double-blind study, is relatively un-suited for this task. One cannot engineer his or her patients, so large numbers of patients are required to satisfy the statistical requirements of a negative outcome. Furthermore, a large amount of quite sophisticated histopathological analyses would have to be conducted in order to establish the concentration and distribution of the various fluorophores and chromophores in the skin. Computational analysis allows for the careful design of experiments, as well as the determination of the relevant variables both during and after the illumination. Of course, this level of detail comes at a cost. The quality of the analyses is as good as the data that is used in the computational model. Unfortunately, there are significant limitations on the availability of data. Therefore, my investigations are aimed at establishing relationships rather than absolute values.

3.5.2 Effect of scattering and absorbing compounds

The investigations on the effect of change in scattering and chromophore concentration on the reported contrast by the three fluorescence detection techniques showed that

generally the combined fluorescence technique reported a higher contrast than the other two techniques.

Epidermal scattering

An increase in scattering decreases the penetration of the light. In the Monte Carlo simulation, an increase in μ_s results in an increase of the total attenuation coefficient $\mu_t = \mu_s + \mu_a$ and thus a decrease in mean free path length $\frac{1}{\mu_t}$. As a consequence, the density of simulated interactions in the tissue is shifted towards the surface. This implies two things in my model. First, since the auto fluorescence method basically depends on the auto fluorescence of the skin acting as a background for the more strongly absorbing target tissue, as scattering increases this background signal becomes weaker and the auto fluorescence method becomes less effective. Second, because the PpIX fluorescence detection method depends on the strength of the fluorescence emitted by the target tissue, the upward shift in the interactions increases the number of photons absorbed by PpIX molecules, and therefore results in an increase in the PpIX fluorescence signal.

The combined method depends on both the PpIX fluorescence detection method and the auto fluorescence detection method. Depending on the strength of the effects of an increase in scattering on both base fluorescence detection methods, the combined method either suffers or gains.

Melanin concentration in epidermis

One of the most notable differences of the skin in humans is its colour, which is caused by a variation in the melanin content of the skin. Following the famed dermatologist Thomas Fitzpatrick, the skin of the patient is usually said to fall within one of six classes (138). Recently Town has determined the melanin content of the skin for each of these skin types (41).

Melanin influences the fluorescence detection through an increase in the absorption of light, in particular with regard to the shorter wavelengths such as blue and UV sources (139). Thus, the epidermal melanin shields the target area from the light source and blocks the fluorescent light from leaving the skin. In my experiment this effect is more pronounced for the incoming signal than the return (fluorescent) signals due to the

shape of the function describing the values for the molar extinction coefficient over wavelength.
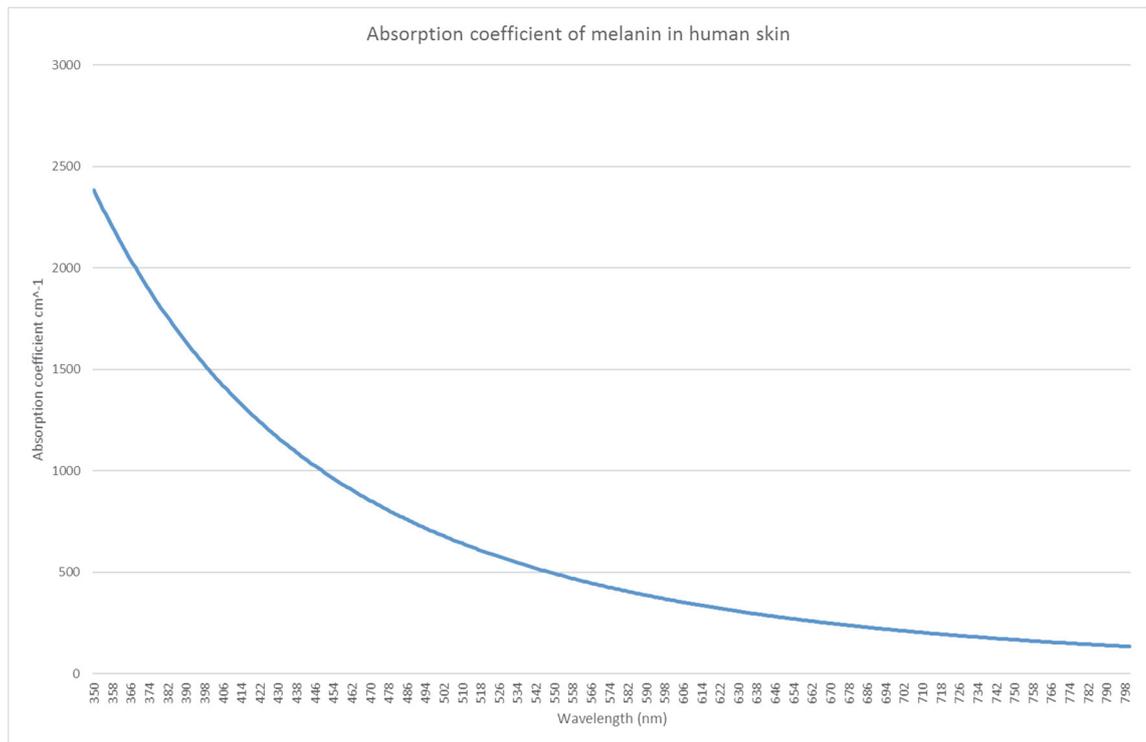
Figure 37: Absorption coefficient of melanin in human skin, (19)*.*

My results show that the fluorescence detection methods are quite sensitive to epidermal pigmentation. Two aspects of my results are noteworthy.

First, the auto fluorescence method is more sensitive to increases in pigmentation than the PpIX mono-spectral method. This observation can be understood by looking at the absorption spectrum of melanin and the differences in the light emitted in the auto fluorescence method and the PpIX fluorescence method (figure 37). The absorption curve of melanin is decreasing with wavelength. The shortest wavelengths used in my experiments is 409 nm, emitted by the light source. The light emitted by the auto-fluorophores has been modelled having a wavelength of 530 nm. PpIX emitted fluorescence has a comparably long wavelength at 636 nm. This is one part that explains why the auto fluorescence method is relatively more sensitive to the increase in pigmentation: A larger proportion of its signal is being absorbed on its way towards the surface of the skin in comparison to the PpIX fluorescence. The second aspect is similar to what I observed in the scattering experiments: The auto fluorescence depends on the fluorescence signal emitted from the deeper layers of the tissue. An increase in

pigmentation implies that less energy is available in those deeper regions to produce the auto fluorescence.

Blood concentration in target

The results of my experiments show that the accuracy of the PpIX based detection methods decrease with increasing blood concentration in the target. Likewise, the accuracy of the auto fluorescence based method increases with blood concentration. Given the fact that the spectral range of the source as well as the fluorescence signals are well within the absorption spectrum of haemoglobin and oxyhaemoglobin, this can hardly be seen as surprising. I did note that the way the various techniques are influenced by the blood concentration differs markedly.

The contrast of the PpIX fluorescence detection decreases exponentially with an increase in blood concentration. Similarly, the accuracy of the auto fluorescence detection method increases in a concave manner. This can be explained by the absorption of all three involved types of light by the blood. The PpIX suffers from the additional absorption since less fluorescence is produced in the target and less fluorescence reaches the surface of the skin. Conversely the auto fluorescence method gains from the additional absorption in the target, as its fundamental method of action is based on the relative low intensity of the auto fluorescence signal over the target. Both absorption by the fluorophores and the emission of the fluorescence from the skin are negatively affected.

The combined method was negatively impacted by the increase in blood, but not nearly as dramatically as the PpIX mono-spectral method. The relationship between contrast measured with the combined method and the increase in blood concentration in the target could be described by a linear function. This method was effective for all tested values for blood concentration. I also checked for a corner solution, in which blood concentration was chosen to be equal to that of a blood vessel. Even then the combined method would have met the threshold of a contrast of at least 1.25. I decided not to present this result, as those concentrations are (even more) biologically impossible and thus are of limited interest to my investigation.

Gambichler et al. found that the use of the combined fluorescence detection method underestimated the area of keratinocyte skin cancers if a threshold of 1.4 was used

(140). This result has likely been influenced by the concentration of blood in the tumour. It has been reported in the literature that keratinocyte skin cancers are associated with lower levels of auto fluorescence (111,112). Rather than being an effect of lower concentrations of auto-fluorophores, these clinical results might be better explained by the increase in blood concentration in tumours. It is this increase in vascularization that gives the keratinocyte skin cancers their characteristic red colour, leading to the moniker "red skin cancer" (130,131).

The increase in blood concentration limited the penetration of photons into the deeper parts of the tumour. Highly vascularised tumours will only present fluorescence from their more superficial parts. This would imply that for such tumours, increasing the thickness of the tumour would not alter the fluorescence. As we will see below, in general longer tumours present more fluorescence, but this will only be true for moderately vascularised tumours.
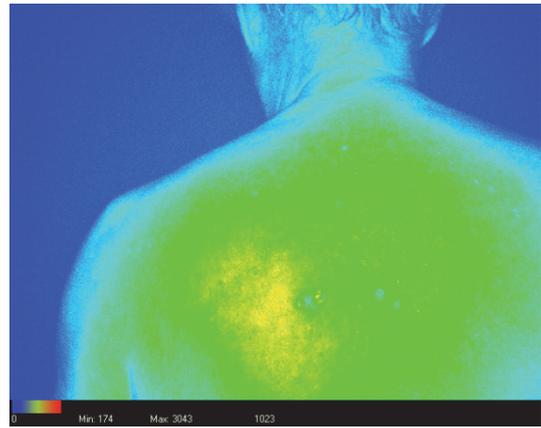
Colour image	PpIX fluorescence
Auto fluorescence	Combined method
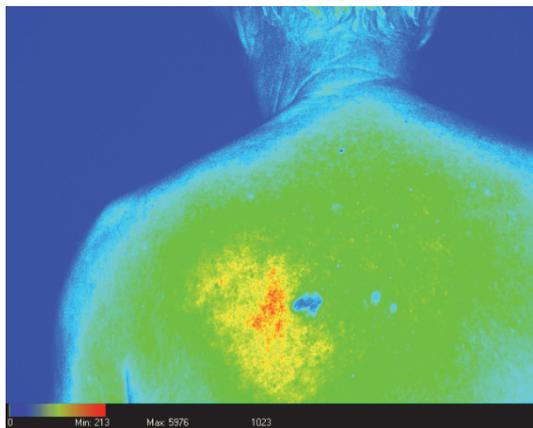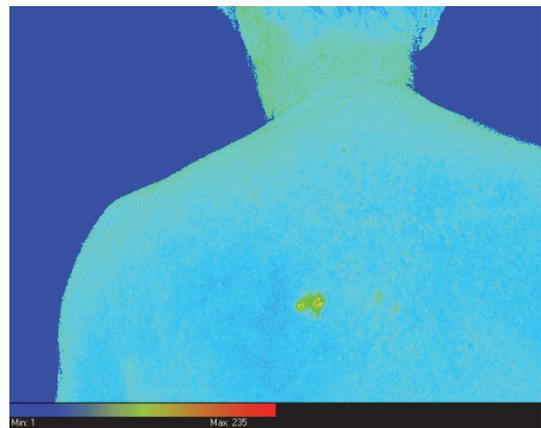
Figure 38: Example of difference in outcome of fluorescence detection methods in a highly vascular lesion.

As can be seen from the images in figure 38 above, my results fit well with the clinical experience. The lesion, a superficial squamous cell carcinoma / Morbus Bowen, shows less PpIX fluorescence than the surrounding skin as well as less auto fluorescence than the surrounding skin. But when analysed using the combined method, it is clearly demarcated from the healthy tissue.

The distribution of the fluorescence signal of the tissue surface of the PpIX fluorescence shows that at higher levels of blood concentration in target scattering at the edge of the target results in an increase of fluorescence at the border. In highly vascularised targets one would expect to observe a halo kind of phenomenon, with the area of higher fluorescence forming a kind of ring around the target area. In their analysis of the data acquired in the study by Arits et al. (132), Roozeboom et al. noted that low fluence photodynamic therapy was less effective in superficial basal cell carcinomas that had an

area exceeding 60 mm² (133). As noted before, more aggressive basal cell carcinomas are associated with more vascularisation. The combination of low levels of fluence and a high degree of vascularisation thus can explain the result noted by Roozeboom et al. (133). I have raised additional concerns against the two mentioned studies in (141). Recently some of the authors confirmed in a retrospective study that indeed fractionated PDT, which applies a three-fold higher light dose than the low fluence protocol, achieves much higher cure rates (68).

3.5.3 Dimensions of target area

The dimensions of the target are of interest since the main purpose of fluorescence detection system is the localisation of tumours that are difficult to observe with the naked eye, potentially aided by palpation. Large tumours tend to stand out due to the reddish appearance of the lesions, not seldom accompanied by scaling or crusting. Small tumours lack such prominent features, which in combination with that asymptomatic nature, explains why they are difficult to detect at their earliest stages. The results of the experiments show that the three different methods differ in their sensitivity to an increase in target tissue, with the combined method clearly dominating the primary methods of fluorescence detection.

Target width

The results of the target width calculations show that all three methods experience a decrease in accuracy when the tumour becomes very small. Once the target is sufficiently large, there is not much change in the relative performance of the three methods. This is due to some of the light being scattered in a not-perfectly forward direction. The light fans out to the sides, causing the observer to detect a mixture of the fluorescence signal from the target and the directly adjacent tissue. In larger targets, the boundaries are sufficiently separated to allow a signal to form that contains mainly fluorescence from the target tissue. As the target decreases in size, this region of the "true" fluorescence from the target signal disappears, resulting in a limited ability of the fluorescence detection systems to locate the target.

I did not note an effect in very wide KSC. This suggests that the decrease in efficacy of PDT when treating larger sBCC reported by Roozeboom et al. is not actually due to the width of the target, but due to changes that are more prominent in the centre of the

lesion, such as thickness or vascularisation, both of which do negatively influence the reported contrast (133).

Target thickness

The results of the experiments on the effect of target thickness of the accuracy show that there is a large effect for very small targets. Again, the relative size of the signal emitted by the target versus the background noise emitted by the healthy tissue is causing a more mixed signal, limiting the ability to detect the target. As the target increases in size, the strength of the signal emitted by the target increases and the contrast is readily observed. At some point though, adding more fluorescent or absorbing tissue does not improve the contrast. This happens in the case of PpIX. When the incident light is unable to reach the added PpIX molecules, a phenomenon comparable to the inner cell effect as described by Ackerman can be observed (110). In the case of the auto fluorescence this point is reached when the complete auto fluorescence signal emerging from below the target area has been absorbed within the target area. Adding more chromophores cannot result in an improvement in shading. In this respect, I note that although PpIX is more sensitive to an increase in the target tissue, it also reaches the saturation point sooner than the auto fluorescence detection does.

Moreover, for larger targets, the sensitivity of a change in the detected contrast to the increase in target tissue is rather small, suggesting that this technique might be poorly suited to determine the thickness of a tumour. That is unfortunate, because that information is very useful to clinicians. Superficial targets can be treated with non-invasive or minimally invasive treatment methods, such as PDT, ablative laser therapy, cryotherapy or topical chemotherapy. More invasive tumours, such as the nodular BCC, on the other hand are best treated using surgical excision. So being able to determine if a tumour belongs to the superficial class or the nodular class without having to perform a biopsy would improve the quality of care for the patient. Fortunately, there diagnosis can be performed using other optical techniques such as dermatoscopy. It does confirm the position of the existing fluorescence detection system as a method to detect areas of interest, and not as a method for determining a diagnosis. Perhaps the results could be improved upon by conducting a second measurement using a light source with a longer or shorter wavelength. As shown in figure 40, the molar extinction coefficient for

oxygenated blood is quite high at 409. Since the absorption coefficients for PpIX, FAD, and haemoglobin are lower for longer or shorter wavelengths, the depth at which the light would be absorbed is slightly shifted downwards. In particular 365 nm UVA seems an interesting candidate, as it is part of the spectrum emitted by Woods' lamp, a device regarded as being part of the default equipment used in dermatological practice and, as seen in figure 40, has a more favourable ratio of PpIX absorption compared to haemoglobin absorption. It is possible that the saturation point for 365 nm FD is reached in larger targets. Comparing the 365 nm FD combined measure and the 409 nm FD combined measure would then be indicative of the type of the target and could even be used to non-invasively map out the target.
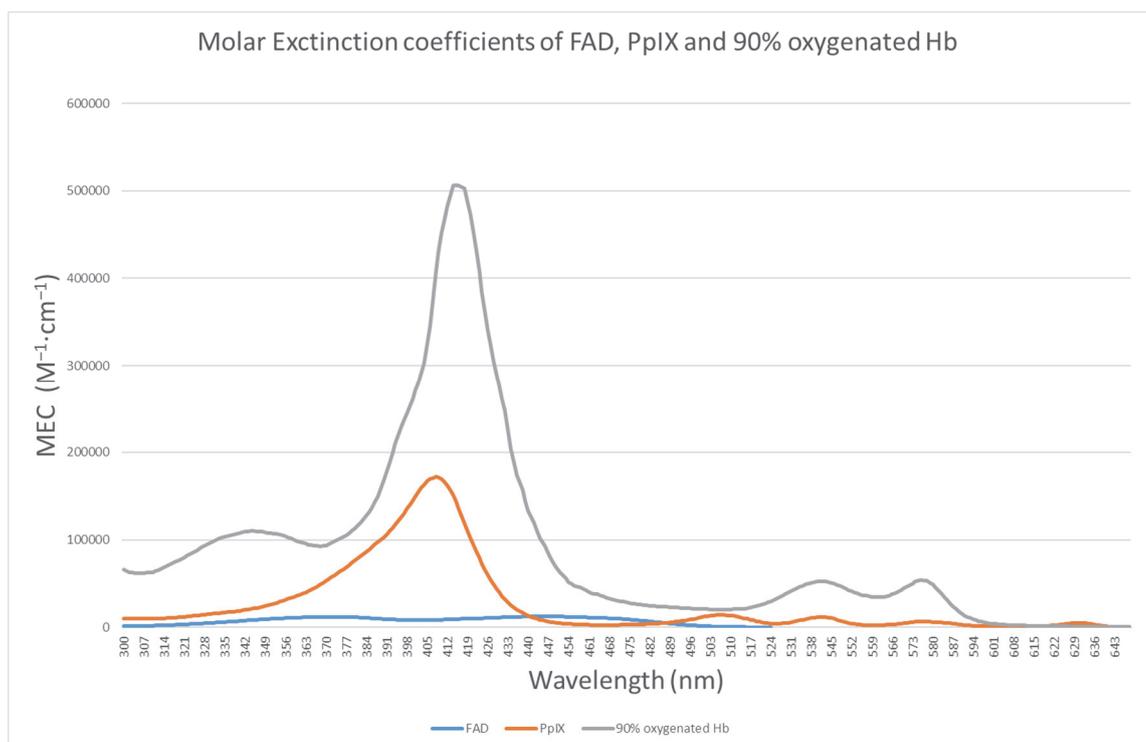
Figure 39: Molar extinction coefficients of FAD, PpIX and 90% oxygenated Hb for 300 nm to 650 nm.

Note that the applied light source emits at the peak of the absorption curves, whereas 365 nm results in a significant decrease in absorption by PpIX and Hb.

I studied tumour depth on the accuracy of the fluorescence detection methods. My results show that all three methods are vulnerable to an increase in tumour depth, or conversely perform better when tumour is close to the surface. As a consequence, these methods of fluorescence detection cannot be relied upon to distinguish superficial and invasive tumours. Similarly, they cannot be completely relied upon to inspect a previous excision for remaining cancerous tissue. At least, we need to understand that the sensitivity is lower than in the untreated lesion.

One rather unorthodox way to interpret these results is to look at the effect of keratolytic agents on the accuracy of fluorescence detection. Smits et al. and Kleinpenning et al. note that there is more fluorescence when the epidermis is thinner (105–108). They focus on the effect this has on the pharmacological aspect of the method, that is a preferential accumulation of 5-ALA and thus PpIX in areas with a weaker epidermal barrier function. This will indeed affect the concentration of PpIX and thus result in a disturbance of the accuracy of the PpIX dependent fluorescence detection methods, such as the mono-spectral method and the combined method. But a thinner epidermis also implies less distance between the target and the surface. I have shown that this can have a dramatic effect, in particular for superficial targets. The gradient of the contrast curve at the lower boundary of the target depth is quite steep. I used a rather thick epidermis of 120 μm. In a separate calculation, not shown in the figures, I determined the contrast for an epidermis of 1 μm and total distance to the target of 31 μm. The contrast for the PpIX mono-spectral method at that extreme scenario is 1.84, while the ratio for the auto fluorescence method is 1.72. The careful reader can already guess what this implies for the combined method: A contrast ratio of 3.18. I do not favour that approach, as the epidermis influences the method in four ways: It increases the concentration of PpIX in the target and the surrounding skin, it removes melanin which is a relatively highly absorbing agent, it removes a layer which tends to have a bit higher scattering coefficient, and it decreases the distance to the target. These effects cannot be separated. Still this effect has been noted in clinical practice and is represented in figure 26 above. E.g. in a patient which failed to report the use of a keratolytic agent such as retinoid acid or salicylic acid.

Tyrell et al. used photobleaching, i.e. the decrease in PpIX fluorescence during MAL-PDT, as a measure for clinical efficacy and noted that illumination should continue well after complete photobleaching was achieved (47,142). Valentine et al. reported that the penetration of PDT in the treatment of superficial BCC was dependent on the level of fluence applied (123). The results achieved with PDT for superficial BCCs could be dramatically increased when switching from the low-fluence protocol using 37.5J/cm^2 to a dose of 75 – 150 J/cm^2. The fractioned approach as described by Van der Veen and De Haas (117,143), which uses 100 J/cm^2 instead of the 37.5 J/cm^2 used in the low fluence protocol, has indeed proven to be very effective in the treatment of the KSC, showing much higher cure rates than reported by the low fluence variant (68,132). The results of the geometry section fit the observation by Tyrrell et al.: The number of PpIX molecules in the tissue decrease as some are lost during the PDT treatment. Even though the excitation of the PpIX molecule, and the transfer of the energy by the triplet PpIX molecule to the triplet oxygen molecule does not consume the PpIX molecule, reactions of the resulting singlet oxygen decrease the available PpIX. The decrease in PpIX starts from the most superficial parts of the enriched tissue. As the treatment progresses, more and more of the fluorescence will originate from deeper parts of the tissue. The target depth results show that, therefore, the intensity of the fluorescence signals will decrease even when there remains a fairly large volume of enriched tissue.

3.5.4   Distribution of fluorophores

The final section of our experiments concerned the distribution of PpIX in target and surrounding tissue. This relates to the specificity of a photosensitiser. A sensitizer with a low specificity will illuminate the surrounding tissue as well as the target. This negatively impacts the fluorescence detection. Conversely, a photosensitiser with a high sensitivity results in a stronger fluorescence signal from the target. The ideal photosensitiser thus has both high sensitivity and specificity. Unfortunately, in practice you usually can't get one with the other. I isolated the sensitivity and specificity in the last two experiments.

PpIX concentration in target

The results show that all three methods of fluorescence detection benefit from an increase in photosensitiser concentration. The PpIX method benefits from the increase in the PpIX fluorescence signal, the auto fluorescence method benefits from an increase

in shading, and the combined method is aided by both these effects. The advantage was more pronounced in the PpIX fluorescence detection method and the combined fluorescence detection method, with the latter dominating the other two methods over the complete range.

Dougherty and Potter warned against the use of a highly absorbing photosensitiser in PDT (137). It would limit penetration of the light and thereby limit the efficacy of the treatment. In FD, this is not of much concern. Unless a multi-excitation variation is developed, the shading effect is of little concern. It doesn't matter how much of the target area participates in the fluorescence signal, as long as the contrast between target and surrounding tissue is sufficient for detection. In that sense, FD could benefit from a more light-absorbing sensitizer, assuming the specificity is not changed.

In their study on fluorescence detection of cancerous tissue, Auler and Bantzer noted that not all tumours resulted in an increase in fluorescence following the administration of hematoporphyrin (88). A disturbance in the haem cycle thus could affect the uptake of 5-ALA or the accumulation of PpIX, which would lower the probability of detection.

PpIX concentration in tissue

Increasing the concentration of PpIX in the surrounding tissue has a pronounced effect on the PpIX and combined methods of fluorescence detection, and a limited effect on the auto fluorescence detection method. The increase in PpIX in the dermis results in a decrease in the energy absorbed by the target area. Given that the light used to evoke the fluorescence has a wavelength that is near the peak of the absorption spectrum of PpIX, an increase in PpIX in the dermis has a strong effect on the number of photons available in the target area. Additionally, the fluorescence signals themselves are absorbed by the added PpIX, but this effect is small compared to the first.

Van der Putten and Van Gemert in 1986 described fluorescence detection using hematoporphyrin derivative. They analysed multiple wavelengths using Kubelka-Munk theory. Under the assumptions used in those calculations, changing the excitation wavelength from 400 nm to 500 nm did not result in an increase in depth at which the tumour could be located using fluorescence measurements. The explanation the authors offered was that the photosensitiser in the skin over the target absorbed much of the excitation light, making the shift to 500 nm insignificant. (97)

The results from our experiment are in agreement with this result insofar that as the concentration of the photosensitiser in the dermis / skin increased, the fluorescence detection methods that rely on the PpIX fluorescence from the target started to fail.

Our findings support the use of photosensitisers and prodrugs which have a high specificity and sensitivity for tissue with a higher metabolic rate, such as the liposomal encapsulated 5-ALA used in our previous research.

3.6   Limitations of current work

The approach used in this work has notable limitations.

The geometry lacks realism. The skin is represented by two layers, ignoring the actual heterogeneity of the epidermis and the dermis. Auto fluorescence was modelled using Flavin Adenine Dinucleotide, rather than the actual mix of fluorophores in the skin. The fluorescence emission was reduced to a single wavelength. Optical parameters where simplified and not adjusted according to studied wavelength; e.g. the anisotropy factor of the excitation wavelength was also applied in the simulation for the FAD and PpIX fluorescence.

I performed partial analysis, and not a full parametric sweep, thus ignoring certain interactions between the studied variables. I do not believe that the effect of e.g. target depth and concentration of PpIX in the target would result in a fundamental different relationship between one of either variable and the performance of the studied fluorescence detection methods, and therefore regard this limitation of minor significance.

The target was assumed to be situated exclusively in the dermis, rather than having a notable component in the epidermis. This creates a bias against the fluorescence detection systems, as more superficial targets are easier to locate.

Since this study was intended to increase the understanding of the effect certain biological variations on the accuracy of a real-world fluorescence detection system, I did not investigate potential improvements of that system. As noted in the discussion, the system might perform better if a combination of 409 nm and 365 nm light is used in essentially a combination of fluorescence detection measurements.

3.7   Summary and conclusion

Fluorescence detection of KSC can aid in the early detection of lesions. Since early treatment is associated with higher cure rates and fewer complications, as well as a higher degree of patient comfort and lower cost per treatment, the application of such systems might be beneficial in the management of the skin cancer epidemic (82). This is in particular true for patients who undergo a solid organ transplant: the calcineurin inhibitors prescribed in order to prevent the rejection of the organ are associated with a sharp increase in the incidence of fatal squamous cell carcinomas (136). Even though the fluorescence detection procedure is both intensive in terms of required time investment of the patient and the physician, the benefits of early detection and treatment could well outweigh the costs.

Currently, there is one fluorescence detection system in active use in dermatological clinics. This system is based on the detection of PpIX fluorescence and normalisation of that signal using fluorescence from auto fluorophores such as flavin. The measurements thus can be separated in three components: PpIX fluorescence, auto fluorescence, and the combined measure based on the two raw fluorescence measurements. Clinical research has shown that the latter outperforms the first in terms of sensitivity and specificity, particular when a low concentration of liposomal encapsulated 5-ALA is used as a prodrug. Based on reports by clinicians using these systems, there is a need to determine the effect of certain variations in the healthy human skin and the tumour.

For that purpose I have used a Monte-Carlo simulation of fluorescence detection of KSC to perform a parametric study, and determine of certain parameters affect the ability of the fluorescence detection methods to determine the location of the target based on the contrast in fluorescence emitted of the target area and the surrounding healthy tissue.

The studied parameters are divided in three groups. First, I studied parameters that are given at the outset of the fluorescence detection and pertain to the optical properties of the target and the skin. These were scattering of light in the skin, the concentration of haemoglobin in the target, and the concentration of melanin in the epidermis. The concentration of blood in the target in particular had a significant effect on the accuracy of the three methods. The contrast reported by the PpIX fluorescence detection method

decreased as the concentration of blood in the target increased, making the method less suited for highly vascularized targets. The auto fluorescence detection method in contradiction benefited from the additional shading caused by the blood in the target. The combined method did experience a negative effect from the increase in blood concentration, but the effect was mitigated by beneficial effect on the auto fluorescence method. Scattering had a limited effect, suggesting that this is of lesser concern in practice and not something one would want to take into account in inclusion criteria for fluorescence detection. Epidermal melanin on the other hand could frustrate a fluorescence detection, hampering all three methods to such a degree that they were unable to detect the target.

The second group was concerned with variations in the location and shape of the target. Target width was determined to be of limited importance. Very small targets are hidden from observation even when using advanced techniques such as the fluorescence detection system studied here. The combined method outperformed the other two methods, but its performance in small targets was lacklustre compared to the situations of relatively more developed targets. The results on target thickness showed that there is a saturation effect, at which increasing the volume of the target does not result in more accurate readings, this also suggests that the fluorescence detection system is not suited to distinguish between nodular and superficial KSC. Perhaps adding a second excitation light source, such as a 365 nm LED, could elicit more information from the target. The distance between the target and tissue surface had a significant influence on the reported contrast. Very superficial targets resulted in quite high fluorescence, and targets located in deeper regions of the skin could not be detected using either of the three tested systems. The latter result has some clinical relevance, as in particular squamous cell carcinoma's can develop de-novo in the deeper regions of the skin. Most invasive SCCs though originate from superficial SCCs which can be detected using the fluorescence detection systems.

The third group looked at the concentration of PpIX in the target and in the skin. PpIX in target resulted in an increase in accuracy of the PpIX fluorescence detection method and the combined fluorescence detection method. Increasing the concentration of PpIX in the healthy tissue though had a pronounced and negative effect on the fluorescence detection methods. Even when the concentration of PpIX in the target exceeded that of

the concentration in the healthy tissue, the contrast reported by the PpIX fluorescence detection method in particular was worryingly low.

Based on the findings in my study, I would classify the parameters according to the type of effect they have on the fluorescence detection method. Some are to be regarded as introducing a limit to fluorescence detection in general, such as target width, thickness, PpIX concentration in tissue, and melanin in epidermis. As long as one stays away from certain values, all three methods perform sufficiently. For example, unless the target becomes really small, volume of the target is of limited influence. These form the limitations of the system, and should be avoided or managed using additional measures, if needed.

Others parameters affect the performance of the fluorescence detection methods over a range, such as blood concentration in the target, target depth, or PpIX concentration in the target. This information is needed for a better understanding and evaluation of the results. Being aware of the nature of the effect of blood concentration, target depth or photosensitiser concentration allows one to be more proficient at performing the investigation. Target depth can be estimated using a dermatoscope; deeper targets will show more scattering / a fuzzier image. Blood concentration is readily observable through the colour of the lesion. Concentration of photosensitiser is a bit more difficult to establish; an operator would have to enquire about the amount of applied prodrug and the possibility of unintended photobleaching.

Future research can extend the current analysis by applying models that more realistically represent the geometry of the skin and the target. Multi-wavelength excitation could be added, as well as the use of broadband fluorescence.

4. Laser and IPL therapy for psoriasis – Heat Shock versus Hyperthermia

4.1 Introduction

Although laser therapy in dermatology generally is applied in the context of cosmetic and plastic surgical interventions, there are some medically curative oriented applications for the technology. Usually the lasers have not been developed with that application in mind, but rather are the result of clinicians recognising the potential of the technology for the treatment of diseases. As a consequence, manufacturers tend not to invest significant amounts in research aimed at showing the safety and efficacy of the treatment. I shall not address the various factors which contribute to this outcome, but rather address an interesting application of laser therapy in the context of medical dermatology: the treatment of psoriasis. Due to the introduction of a new class of drugs, the so-called biologicals, the pressure the treatment of this disease exerts on the provision of public health care insurance has become a significant threat to the durability of that kind of Social Security. Laser therapy has been shown to be effective in the treatment of various inflammatory skin conditions, including psoriasis (144). The efficacy and safety of laser therapy has been shown in a series of somewhat modest clinical studies, few of which are comparative in nature (145–148). Other studies measured the actual physical effects of the treatment on the skin (24,149–151) most of the scientific and clinical potential has remained untouched. In this chapter I present an explanation for the efficacy of laser therapy which adds to the current paradigm and study the comparative performance of pulsed dye laser (PDL) systems and an intense pulsed light (IPL) therapy according to the presented explanation. I start with a short and limited discussion of psoriasis. Then I discuss a here hitherto neglected stage in the pathogenesis of psoriasis. This stage is used as an apex for the explanation of the efficacy and long treatment free duration of remission of laser therapy. This is followed by the description of the performed calculations and the presentation of the results. Finally, I discuss how the results fit the proposed theory as well as some relevant publications from the dermatological scientific literature.

4.1.1 Clinical presentation, pathogenesis and treatment of psoriasis

Psoriasis is a common skin condition clinically characterized by the emergence of erythematous-squamous plaques which are either locally present or are more distributed over the whole body. Figure 40 shows clinical presentations of three types of psoriasis, although in practice both level of erythema and presence of scaling varies considerably within subtypes. The most common form, psoriasis vulgaris, affects 80% of patients. In addition to the excessive scaling, the lesions can cause considerable itching. As such, psoriasis has a significant impact on the quality of the lives of those affected. The lesions are usually symmetrically distributed over the body. The scalp, chest, back and extremities are commonly involved. Lesions may resemble coins, as is the case in nummular psoriasis, or palm sized lesions in the case of geographic psoriasis. Other variants include guttate psoriasis, which is generally attributed to a staphylococcus infection, and pustular psoriasis which, as the name suggests, is characterised by accompanying pustules (152,153). It was reported in 2016 that 2.8% of the population in the UK suffers from this chronic skin condition (154).

Nummular psoriasis   Geographic psoriasis   Pustular psoriasis

Figure 40: Clinical presentation of psoriasis.

Note the presence of scaling in the examples of nummular and geographic psoriasis in contrast to the example of pustular psoriasis. Reprinted with permission from (155)

The pharmacological therapies for psoriasis range from topical ointments containing compounds such as corticosteroids, tar, and calcineurin inhibitors, to systemic therapies such as retinoids, calcineurin inhibitors, folic acid analogues, fumaric esters, and interleukin-17 (IL-17), tumour necrosis factor alpha (TNF-α) or other cytokine blocking "biologics". These modalities vary in efficacy and safety. Prolonged use of methotrexate for example results in a significant increase in the risk for cutaneous carcinomas (8). Calcineurin inhibitors too are a known carcinogenic, possible responsible for the relative large percentage of organ transplant recipients passing away due to invasive keratinocyte skin cancers (136).

Another mainstay of the dermatological management of psoriasis involves physical modalities such as UV radiation therapy. Here the affected skin is frequently irradiated with UV light, either as mono-therapy or combined with light sensitising drugs such as psoralens in the case of PUVA or tar in the case of Goeckerman therapy. The treatments can be performed in the hospital or at home (155).

The history of UV therapy has not been without its misgivings though. Following the notion in the nineteen hundreds that sunlight and fresh air was good for the physical well-being of the individual, the emergence of the skin cancer epidemic has taught us that moderation is required even in good things (60,63,64). In particular prolonged and intense PUVA therapy has been shown to introduce an increase in the risk for skin malignancies (156).

Currently the dominant form of light therapy involves narrow-band 311 nm UVB therapy, which exerts an immunosuppressive effect on the skin in part through the isomerisation of urocanic acid (28) and apoptosis of T-cells (157,158). In contrast to other UV sources, narrow-band UVB does not seem to increase the synthetisation of epidermal TNF-α (159). Narrow-band UV therapy results in lower cumulative doses for a given therapeutic effect, nonetheless when deciding to apply the technique the expected benefits need to be weighed against the potential risks (160,161). Currently there are no studies that show an increase in skin cancer incidence in patients treated with narrow-band UVB (162,163), but the quality and quantity of studies leaves something to be desired for (164).

Both pharmacological and UV based interventions for psoriasis are limited in the sense that the resulting clearance of lesions generally is short lived. Duration of (treatment free) remission generally ranges from a few weeks up to a year (5,165). The treatment of psoriasis can come at a hefty price, in particular with the emergence of a new class of drugs, the biologicals, which require continuous treatment and cost between € 10.000,- and € 18.000,- per patient per year (166). In addition, the long term safety of these interventions is unknown, as is the actual impact of the suppression of the immune system on the daily life of the patient. The combination of impact on quality of life, the large incidence, and the potential excessive and continuous costs stresses the need for effective, safe and affordable treatments which can induce prolonged duration of treatment free remission. Thus, the optimal treatment for psoriasis is not known at the moment.

In my opinion intense light emitting devices, such as lasers and flash lamp pulsed systems, have the potential to be such a treatment. Pulsed Dye Laser therapy and Excimer Laser therapy have been shown to be effective in the treatment of psoriasis, achieving a duration of remission that differs significantly from non-radiation based interventions (5,6,24,144–147,149,151,167–169). The efficacy of lasers operating closer to the IR spectrum has not been proven, but here an optimisation of the treatment parameters and the application of fractional system make any generalisations premature (170). Unfortunately, the reported achievements have not been adopted by the wider dermatological community or the academic centres (171–173), and thus remain the exclusive domain of highly skilled and innovative dermatologists. As a result, there is a paucity of literature on the treatment of psoriasis.

The medical community is in good company, as the clinical physicists also seem not to have paid much attention to the study of laser therapy for psoriasis. This is surprising, since the geometry of the psoriasis lesions suggests that it is well suited for laser therapy: the typical psoriasis vessels are aligned perpendicular to the skin surface, which allows more of the laser light to be absorbed within the target (174–178). The rete ridges that are typical for psoriasis on the other hand could cause the tissue light interactions to show some less straightforward behaviour, as the interface of the epidermis and dermis will present itself at a much larger angle, increasing the number of reflection

events within the skin, in addition to the presence of scaly areas which locally would induce more scattering (179).

4.2 Histological-pathological and immunological properties of psoriatic lesions

Psoriasis can be characterised as a condition of increased proliferation and lack of maturation of the sensory nerves, papillary vasculature and keratinocytes of the skin, with a strong involvement of the immune system. In this section I discuss some changes that are present in psoriatic lesions compared to healthy skin.
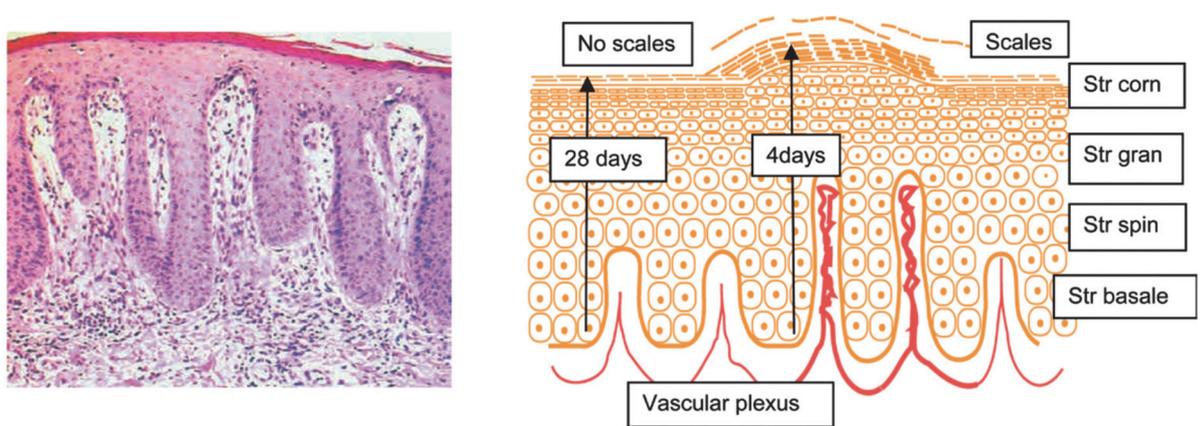
Figure 41: Changes in the histology of a psoriatic lesion

The size of the epidermis usually ranges from 30 μm at the top of the rete ridges to 1000 μm. Reprinted with permission from De Leeuw (181).

One of the most striking features of psoriasis is the downward elongation of the epidermis. This is observable in the left part of figure 41: the "teeth" sinking into the dermis are the so-called rete-ridges. As a result of the hyperkeratinisation there is a tremendous increase in thickness. In areas such as the back and chest the epidermis normally has a thickness of 70 to 100 μm, in psoriasis it ranges from 30 μm above the capillaries up to 1000 μm between the capillaries (179). It is this reduction in thickness above the capillaries that, in part, is responsible for the (incorrectly) (58) named Auspitz sign. The rate at which the skin renews itself increases to once every eight days. The hyperproliferation comes at a cost in terms of maturation and as a consequence there is little adhesion, causing the characteristic scaling.

Psoriasis lesions usually present as pink or reddish lesions, indicating a change in the vasculature. Although no new blood vessels are formed, the existing ones are elongated and have relatively thin vessel walls. There are gaps in the endothelium lining, which is not common for the arterioles. They somewhat resemble lymphatic vessels, which do not occur at the dermal plexus. Noteworthy is that these differences are not limited to the plaques, but are also visible in the clinically normal skin. The blood vessels in psoriasis are elongated and feature prominent tortuous loops at the top (174–176,178,180–182). As we will see below, there is a marked increase in the neuropeptides that affect the cutaneous vasculature. This results in angiogenesis, which according to Heidenreich et al. is the main driver of psoriasis (183). Hendriks et al. reported a strong correlation between blood perfusion in psoriasis lesions and drivers of psoriasis such as IL-17 (184).

There is a proliferation of dermal nerve fibres, which reach into the epidermis and its surface. In contradiction to healthy controls, protein product gene 9.5 positive fibres are present in the epidermis. The Schwann's cells are poorly differentiated and axons are protruding through the nerve fibre. The nerves produce neuropeptides such as calcitonin-gene related peptide (CGRP), substance P (SP), Vascular Endothelial Growth Factor (VEGF), and vascular intestine protein (VIP) to mention a few. The concentration of these neuropeptides in markedly increased in psoriatic lesions. The psoriatic skin also presents an increased number of receptors for these neuropeptides in comparison to controls. Morphology suggests that proliferation of Schwann Cells (SC) was so rapid that normal orientation in relation to other SC and epidermis is lost (185–197). An increase in neuropeptides can upregulate the immune response, e.g. through the activation of T-lymphocyte helper 17 (Th-17) cells (198). Myelation might also be hindered by a lack of maturation of Schwann cells, given that myelation is quite slow in skin to start with (193). An increase in nerve growth factor (NGF) precedes the development of new psoriatic lesions, which is relevant as NGF results in an increase in the proliferation of the superficial cutaneous nerves and decrease in maturation. Both the vascular and nervous hyperplasia precede the hyperplasia of the keratinocytes.

4.2.1 Immunological changes in psoriatic lesions

Except for the hyper-keratinization, the histological abnormalities mentioned above are present in lesional and non-lesional skin. Even the sebaceous glands are abnormal (199). In a psoriatic lesion the changes though are not limited to abnormalities in the cell-cycle such as the hyper-proliferation and maturation of the keratinocytes, even though this had been the dominant paradigm for many years (200). The adaptive immune system is a major driver of psoriasis, in particular an IL-17 producing Th-17. Blocking that stage of the immune system results in a full clearance of psoriasis in a large percentage of patients (201–203). This insight explained the prolonged treatment free remission following PUVA therapy, as it resulted in a marked reduction of T-cells (204), whereas treatments that require continuous treatment like Ixekizumab, methotrexate, and cyclosporine merely suppress the T-cell activity and proliferation (152).

For my research the distribution of T-cell subtype is of relevance. The T-helper cells that are CD4 positive reside in the dermis, whereas the T-effector cells that are CD8 positive migrate to the epidermis or remain in the dermis depending on the expression of integrin CD103. The T-helper are involved in the T-lymphocyte signalling process: When presented with an anti-gen, they produce cytokines and chemokines which invoke a further response from the immune system. Th-17 and Th-1 cells are activated by the secretion of IL-12 and IL-23 by the antigen presenting cells (APC) called dermal dendritic cells for example. This IL-23/IL-17 axis has become a central focus in the pharmacological treatment of psoriasis. Notable is that IL-17 is not elevated in serum of psoriasis patients; it is a pure local phenomenon (152).

4.2.2 Cutaneous sensory neurons in psoriasis

Although the immunological based explanation for the pathogenesis is a significant step forward in our understanding of this condition, it fails to provide the complete answer. This becomes obvious when one looks at the complex relationship between the cutaneous sensory nerves and psoriasis. Psoriasis lesions respond to events that exclusively involve the cutaneous nerves. Weddel made it clear that he saw a prominent role for the cutaneous nerves in the pathogenesis (192). Unfortunately for dermatology, he pursued a career in the research on leprosy, eventually becoming one of the prominent scientist in the field.

Referring to the claim by Weddel et al. (192) that the nerve supply related to the development of psoriatic lesions, Dewing (205) shared the observation by one of his patients suffering from psoriasis that the accidental dissection of nerve during a procedure to remove the medial meniscus cleared the psoriasis lesion, with the lesion returning as the nerve regenerated. Dewing wondered if nerve blocks could be a therapeutic option. Perlman (206) responded in an affirmative manner. He had a similar experience: A patient had experienced a complete remission of a lesion following a procedure in which an anaesthetic was applied. After consulting the anaesthesiologist, it turned out to be novocain crystals dissolved in spinal fluid. Based on this information Perlman started to intra-lesional applications of the in-dermatology commonly used-anaesthetic 1% lidocaine. And behold, it resulted in a clearance of lesions. Not with all patients, but a proof of concept was certainly provided.

These experiences did not evoke much of a response from the dermatologic field for quite some time. From the mid-eighties until the early 2000 a group forming around Eugene M. Farber focussed on the role of the neuropeptides in the pathogenesis of psoriasis. Although he had studied psoriasis for decades (207), it wasn't until the eighties that he started to consider the role of neuropeptides (191). His group eventually made a number of contributions, focussing on the role of NGF and other neuropeptides in psoriasis (186,208–210) and the role in the emergence of psoriasis (185,211). They discovered that an increase in NGF precedes the formation of the rete ridges, and confirmed reported the lack of psoriasis in patients suffering from leprosy, a condition in which there is a decreased density and function of cutaneous and in that sense the mirror image of psoriasis. Wahba et al. (212) had noted the absence of psoriasis in lepers

as well, and wondered if psoriasis would somehow provide protection against leprosy. Kumar et al. (211) suggested the inverse relationship, i.e. that psoriasis required good functioning nerves and thus lepers being protected against psoriasis. The induction of a psoriasis lesion in lepers is not impossible, as has been reported by Wahba, Dorfman and Sheskin (213).

There are additional case reports that describe the clearing of psoriasis and other inflammatory conditions of the skin following injury to a nerve or the coexistence of a condition that (locally) inhibits the functioning of the cutaneous nerves such as polio (190,214).

This research is further supported by the successful treatment of psoriasis using compounds that activate the transient receptor potential vanilloid 1 (TRPV1) such as capsaicin (215,216). Capsaicin is used for the treatment of itch, or pruritus. Its mechanism of action is depletion of the c-fibre nerves thus inhibiting subsequent signalling. The application of capsaicin is far from comfortable, the receptor is activated by temperatures above 42 degrees Celsius and the cream invokes a similar sensation. A limitation of capsaicin is that the lesions re-emerge once therapy is discontinued, and it could not achieve complete clearance in all patients. This suggests that some of the nerves contributing to the psoriatic lesions lack a TRPV1 receptor. The complimentary situation is the effect of stress on psoriasis, as well as the effect of psychotherapy on psoriasis severity (217). Animal models too have shown a dose-dependent effect of denervation of psoriasis severity, as well as the emergence of psoriasis like lesions following the administration of VEGF (218,219).

A further consideration is the correspondence between the shape of the psoriasis lesions and the distribution of the cutaneous C-terminal nociceptor units. Schmelz et al. and Schmidt et al. (187,188,220) mapped the innervation territories of the skin, which, as is shown in figure 42, are remarkably similar in shape and size compared to nummular psoriatic lesions.
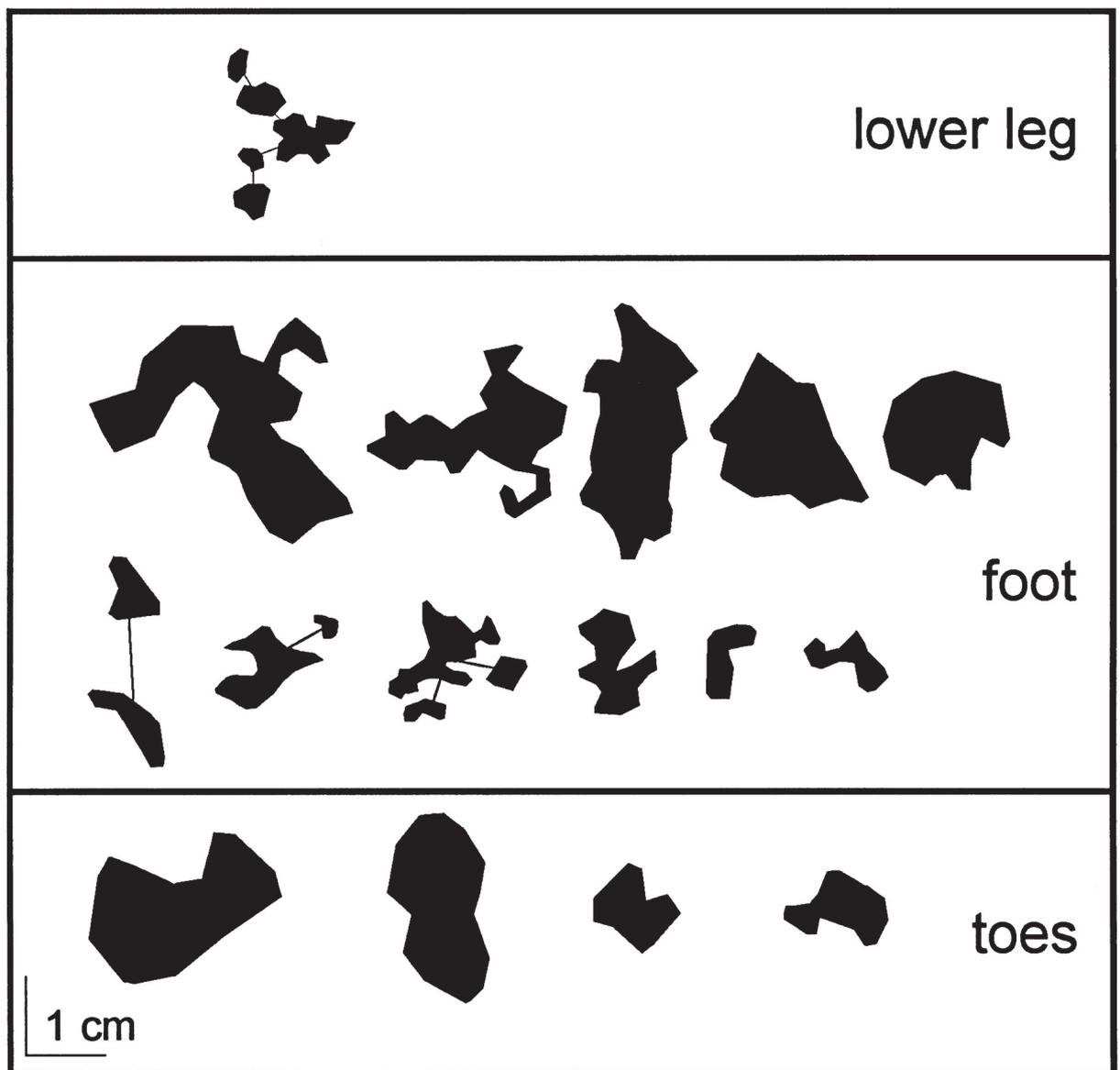
Figure 42: Shapes and areas of innervation territories of 16 sympathetic efferents in 3 different regions of the leg.

Complex territories innervated by the same parent C axon are connected by lines. Reprinted with permission from Schmelz et al. (190).

From the discussed literature follows that the abnormality in the cutaneous innervation typical for the skin of psoriasis patients is not just a bystander, but rather the scaffolding on which psoriatic lesions are formed. There is a dose dependent effect of nerve blocking on the severity of psoriatic lesions. Yet, patients in which the neurological functioning of the skin is perturbed, either due to pathology or due to adverse events in surgical Interventions, are not regarded to be immunologically compromised. A general anti-inflammatory effect of nerve blocking has been reported in the literature, although the quality of that study was insufficient to draw any real conclusions (221,222). The

peripheral nervous system is able to influence the immunological system of the skin and the two act as an integrated system (223–230). For example CGRP can induce a Th2 type response (231). This interaction between the nervous system and the immunological system could serve as the basis for a logical chain of events which starts with the activation of the deficient neurological system by an external event and results in a persistent dysregulation of the local cutaneous immunology in combination with the angiogenesis and hyper-keratinization. Although it is possible that the chain of causality starts with the immunology before the participation of the cutaneous neurology and angiogenesis, this is less plausible as it fails to account for the marked increase of NRG at the location of the emerging rete ridges as well as the increase in vasculature that precedes the increase in lymphocytes. The experience with therapies such as cyclosporine A and biological therapies based on the IL-17 / IL-23 axis does suggest that the immunology influences both angiogenesis and acanthosis, either through its effect on the peripheral nervous system or through a direct effect on the keratinocytes and dermal vasculature.

4.3 The effects of heat shock on immunology and regeneration

The mechanism of action of laser therapy in psoriasis is poorly understood, but it is unlikely to be driven by the pure surgical effect of the laser on the vasculature. Hern et al. showed that the effect on the capillaries alone was not sufficient to explain the observed effect of laser therapy on psoriasis (149). Rather, an indirect effect on the immunology seemed to be driving the process. As can be seen from figure 43, they noted that 585 nm PDL laser therapy resulted in a spectacular decrease in CD4+ cells, which play an important role in inducing and sustaining an immunological response by releasing cytokines such as IL-17. This was accompanied by a lesser but clearly present decrease in the CD8+ T-cells, which actually act upon the targeted cells.

A "fanning out" effect has been observed in the treatment of psoriasis and atopic dermatitis (24,25,146), indicating a non-surgical mode-of-action for the therapeutic effect of laser therapy on psoriasis. A clear anti-inflammatory effect can be observed long after the capillaries have been restored (144,151).
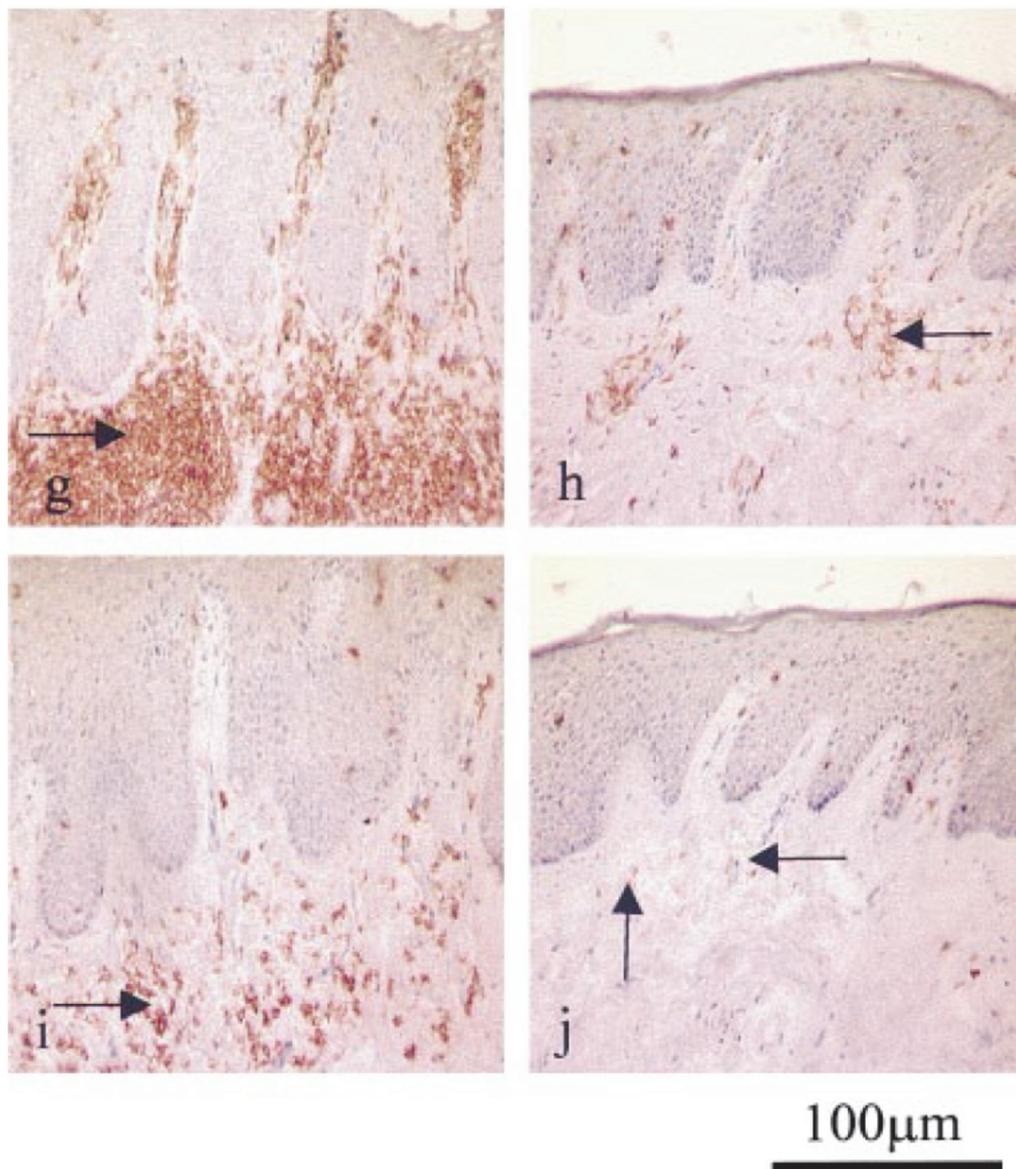
Figure 43: Effect of 585 nm PDL therapy in psoriasis on T-helper cells (g,h) and T-effector cells (i,j).

As the name suggest, photothermal laser therapy is based on the (selective) heating of tissue. The (selective) introduction of heat can have a detrimental effect on the survival of cells and tissue, resulting in severe burn wounds (55,57). One of the clinical applications of this effect is the treatment of malignancies of the prostate. By heating the tissue sufficiently, i.e. given a certain temperature profile heating is attained for a duration sufficient to induce the desired effect, the cells either implement programmed cell death (apoptosis) or undergo uncontrolled cell death (necrosis). Sub-lethal levels of thermal damage can induce effects as well. One mechanism that comes into play here is the induction or release of heat shock proteins (HSPs), a class of stress proteins. These HSPs can have an pro-inflammatory effect (232), harden the cells against further

stressful events (233), assist in the restoration of neurons (234–236),or have an anti-inflammatory effect in particular if heat shock precedes an inflammation (237).

It should come as no surprise that photothermal laser therapy can induce dermal HSPs (238–242). I note that the location of the induction of the HSPs follows the location of the targeted chromophore. When the target is water or pigment, HSPs induction could be quite prominent in the epidermis and dermis. With haemoglobin on the other hand the primary target will be the dermis, since the epidermis does not contain haemoglobin. The above suggests that photothermal therapy of inflammatory conditions could have at least three effects: A lethal heating of cells resulting in apoptosis or necrosis, a pro-inflammatory effect due to the release of pro-inflammatory HSPs, and an anti-inflammatory effect based on the induction of anti-inflammatory HSPs. I regard the first two effects as being detrimental to the efficacy of the therapy and the latter having a beneficial effect. Nijhuis showed in chapter 6 of his thesis that HSP70 downregulation promotes apoptosis in cell lines (243), thus supporting the assumption used in the remainder of this chapter that HSP72i exerts an anti-inflammatory effect.

The destruction-protection paradox resulting from the induction of apoptosis as well as the creation of HSPs has been discussed previously by Rylander (244,245) in the context of the treatment of malignancies of the prostate using diode lasers in combination with chemotherapy. The problem faced in that context is that treating the tumour by irradiation will inevitably induce the production of protective heat shock proteins at the boundary. Unless there is a discontinuity in the stress response of space, a protective shell is formed which will be more resilient to chemotherapy than it was before the radiation based therapy. In this context we face the inverse problem. At lower levels of thermal stress, the anti-inflammatory effects will dominate. But as the levels of stress increase, lethal doses of heat will occur as well.

In this chapter I will address the following questions:

1. What are the characteristics of the pro-inflammatory vs. anti-inflammatory trade-off with increasing energy per pulse for PDL therapy in psoriatic lesions?

2. How is the trade-off affected by a switch between 577 nm PDL, 585 nm PDL, 595 nm PDL, or a commercially available IPL?

3. How is the trade-off affected by changing the blood oxygenation, vascularisation of the target tissue, and scattering in the epidermis?

4. How does a reduction of superficial haemoglobin concentration following vasoconstriction relate to the trade-off?

These questions will be addressed by computational analysis using the 2D Monte Carlo simulation software described in chapter 2. Although I am unable to engage the complete problem, as temporal, technological, and financial constraints put limits on what can be reasonably achieved within the context of the kind of research I am conducting in this work, I seek to answer some questions that are relevant for dermatologic practice.

After the calculations for a general case in which the psoriatic capillaries contain blood conforming to a common degree of oxygenation of 90%, I investigate the influence of a change in the oxygenation of the blood in the capillaries to an oxygenation of 50% (246). As psoriatic skin can be quite scaly, I also look at the effect of an increase in the scattering of the epidermis (179). Finally, I make use of the opportunity to investigate the potential of pharmacologically manipulating the psoriatic skin in order to further increase the size of the blood vessels, i.e. the blood volume in the target area. One such compound with known neuromodulating properties, capsaicin, has already been shown to be beneficial in psoriasis (216,247,248). These four geometries are subjected to three different types of pulsed dye lasers (PDL): the 577 nm PDL, the 585 nm PDL, and the 595 nm PDL, as well as an IPL device that like the PDL devices is aimed at the treatment of superficial vascular abnormalities. The latter two PDL devices have been used in the study of

photothermal laser therapy for psoriasis and were shown to be effective (24,145–147,169).

4.4 Materials and methods

4.4.1 Geometry

The structure of the psoriatic skin has been described in detail by a number of studies. The psoriatic skin differs from the skin of healthy individuals by a hyperproliferation and limited maturation of the keratinocytes, the nerves, and the blood vessels (175,179,192). The epidermis is more voluminous and the rete ridges are more accentuated. The thickness ranges from 30 to more than 1000 μm, whereas the normal epidermis has a thickness closer to 70 and 100 μm (179,249). The blood vessels are more numerous, in addition the capillaries are elongated and tortuous at the top, the vessels have a thinner vessel wall and contain gaps in the endothelial lining. The epidermal thickness is minimal just above the capillaries. As a consequence the psoriatic skin can be made to bleed by minimally scratching the surface, the Auspitz sign (176,177,250) The diameter of the blood vessels does not seem to differ from those in healthy individuals, but the smaller walls imply an increase in the lumen (251). The oxygenation in psoriatic plaques is very low compared to that in healthy skin, reaching as low as 30% (246). The nerves are more numerous as well, reaching into the epidermis, and there is poor differentiation of axons and Schwann cells (192). The sebaceous glands lack maturation as well (199). The neuronal, keratinocyte and vascular hyperproliferation with limited maturation is striking.

I apply a variation on the simple sandwich or layered model as developed by Anderson and Parrish (252). The model consists of an epidermal layer and a dermal layer. Within the dermal layer a rectangular area is defined as the target area. Each of these three layers has its own optical properties, but otherwise is optically homogeneous. The psoriatic lesion is modelled using a thin epidermis and an area with a blood content of 50% (250). The thin epidermis ignores the more intricate behaviour caused by the rete ridges and is likely to affect the results. Further research will have to extend beyond my explicit assumption and the results should be interpreted with this simplification in mind. The thin epidermis is based on the observation that in psoriatic lesions the skin is quite thin above the capillaries, as is evident by the well-known but incorrectly named Auspitz sign (58,152). A situation in which the thin epidermis assumption is more

accurate than it can naturally be expected is when patients are instructed to treat the lesions with a preparation containing a high percentage of salicylic acid, or when scaling has been removed physically through tape stripping.

Figure 44: Geometry of psoriasis lesion used in study.

Layer	Dimension (µm)	Reference
Epidermis	30	(249,250)
Distance between epidermis and target / Upper dermis	30	(250)
Diameter of target	9000	(51,250,251)
Thickness of target	300	(176,177,250)

Table 1: Physical properties of geometries

4.4.2   Radiative transport equation

The optical properties for the various layers and geometries are described in the table below.

4.4.2.1   Scattering and absorption

Although melanin and haemoglobin are the principal chromophores in the skin that absorb light in the range of 500 – 800 nm, and thus are of most interest for my study, the skin absorbs and scatters light even in absence of melanin of haemoglobin. The software package uses the function from Jacques (31) to determine the absorption and scattering coefficients for the bulk skin for a given wavelength. In order to determine the appropriate values for light absorption and scattering, this value is adjusted in accordance with melanin content or blood content and blood oxygenation through a linear combination of the absorption coefficient for those chromophores. The values for the absorption by blood is calculated using the values provided by Prahl (20). These values differ for the various calculations since either the used wavelength(s) change, or the concentration of the chromophore chances. Table 2 provides an example of the used values for the calculations on the 595 nm PDL with 90% oxygenated blood.

Example given for 595nm	Epidermis	Dermis	Blood (90% oxygenation)
Absorption coefficient (cm^{-1})	5.38 (126)	2.33 (126)	(20,253)
Scattering coefficient (cm^{-1})	64.85 (126)	64.5 (126)	900 (254)
Anisotropy factor g for the H-G phase function	0.77 (126)	0.715 (126)	0.995 (254)

Table 2: Example of optical properties used in experiments

4.4.2.2   Blood oxygenation

Type	Percentage Oxy-haemoglobin	Percentage deoxy-haemoglobin	Reference
50%	50	50	(51,246)
90%	90	10	(51,246)

Table 3: Blood oxygenation used in experiments

4.4.2.3   Tissue width

I performed a series of experiments in order to establish the minimal tissue width required for my experiments. That way the maximum resolution (cells per cm^2 of simulated tissue) was achieved. The limiting factor is scattering, since photons that leave the boundary cannot return. Although the code does account for this effect by allowing a photon to backscatter when it is about to cross the boundary, I prefer to keep the

relevant scattering events, i.e. those that will result in the heating of tissue, within the domain of the actual Monte Carlo simulation.

Monochromatic Monte Carlo simulations were performed for 409 nm and 950 nm. Since the maximum and minimum value for absorption and scattering coefficients in the range from 409 nm to 950 nm are located at the boundary values, tissue that is of sufficient width to account for those cases will be able to deal with the intermediate values as well.

The simulation was performed on a 10 cm wide tissue, containing a 70 µm thick epidermis and a single blood vessel of 30x300 µm located at 270 µm below the surface of the skin. The dermis continued for 200 µm after the blood vessel. Scattering, anisotropy and absorption coefficients where used as noted above. A light source emitting a top hat profile was applied in the middle of the tissue, illuminating a strip of 100 µm.

The results showed that 95% of photons where absorbed within 1000 µm adjacent to the laser beam. From this I concluded that the width of the tissue had to exceed that of the laser beam by 1000 µm. Therefore, I decided to simulate a 7 mm laser pulse on a 9mm wide tissue. A slab of normal dermal tissue continued for 500 µm beyond the capillary layer.

4.4.3 Applied light systems

Pulse dye lasers are presumed to emit light with a wavelength as specified in the name, i.e. 577 nm, 585 nm or 595 nm. The beam is slightly diffuse with an anisotropy value of 0.9 at the source.

The studied IPL applicator is intended for rejuvenating treatments, in which the microvasculature and pigmentation are prime targets. The spectral profile is shown in figure 45. It is more attenuated at the shorter wavelengths. Thanks to the combination of a cut-off filter and a IR filter, it lacks the NIR tail commonly present in IPL devices. In addition to rejuvenation, it is used in and approved for inflammatory conditions such as acne and rosacea, suggesting that it is suitable for other inflammatory conditions with a similar presentation such as psoriasis and atopic dermatitis.
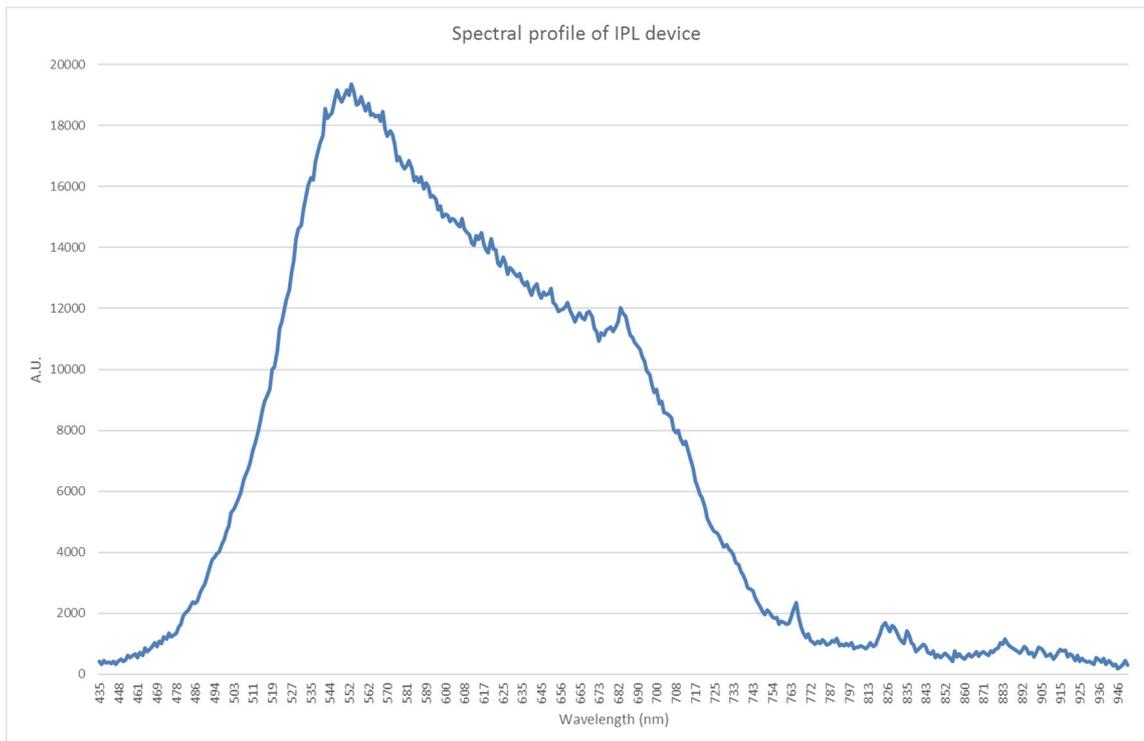
Figure 45: Spectral profile of double filter applicator. Horizontal axis represents wavelength (nm). The vertical axis is an arbitrary unit.

Calculating the absorbed energy distribution for each wavelength with sufficient photons to achieve convergence over the whole tissue width would require an excessive amount of computing power, whereas the contribution of the wavelength with the lowest number of photons would be quite modest as they represent a small share of the total energy output. Therefore, the spectral output for the lower and higher ranges where combined and introduced as a larger value for a single wavelength, resulting in the spectral curve presented in figure 46 below.
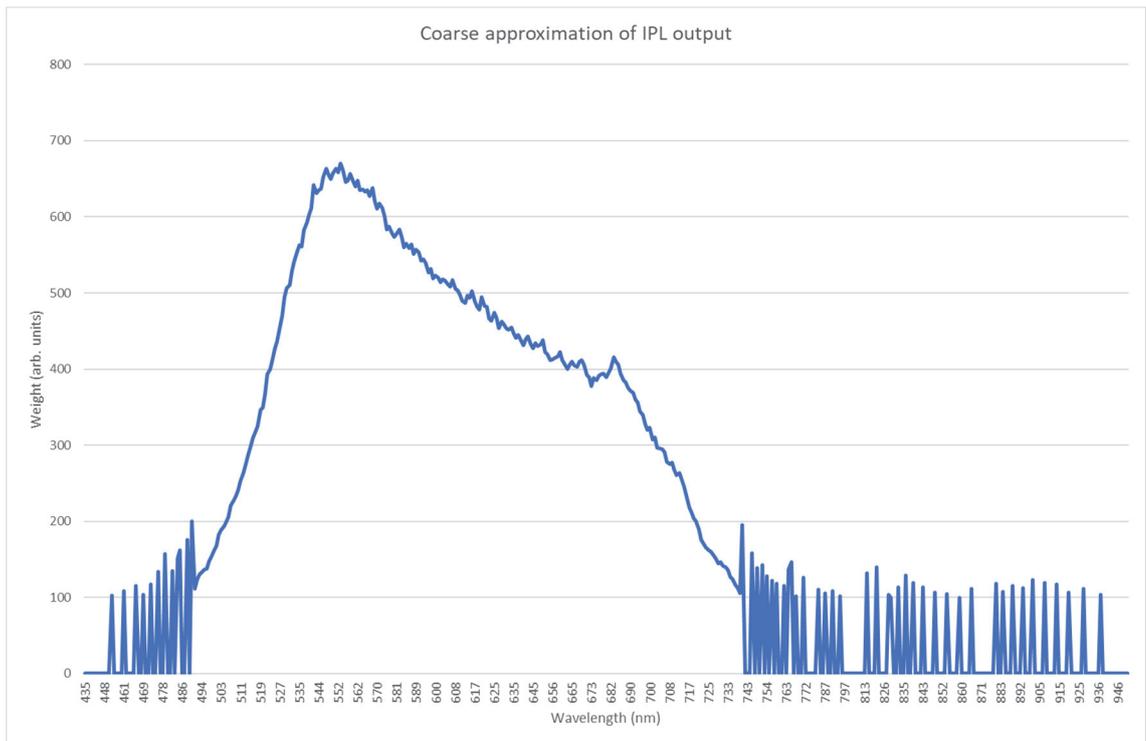
Figure 46: IPL profile used for calculations. Based on data from Town (255)

Since IPL systems produce divergent light, and the software package did not allow for the use of a separate value for g for each wavelength, I applied g=0.75 for anisotropy in the phase function of the light source.

4.4.4 Variables used for the calculation of the diffusion of heat following laser irradiation

The thermal properties of tissue used in this study are mentioned in the table below.

(256,257)	thermal conductivity coefficient k $(Wm^{-1}K^{-1})$	Tissue density ρ (kgm^{-3})	Specific heat c $(Jkg^{-1}K^{-1})$
Epidermis	0.21	1200	3600
Epidermis (HSE)	0.24	1210	3500
Dermis	0.36	1100	3200
Target area	0.47	1080	3520
Target area (dilated vessels)	0.51	1073	3627

Table 4: Thermal properties of tissue

For each configuration of device and tissue I calculated the energy needed to heat at least one area within the tissue to a temperature of 48 degrees Celsius (°C). That is the critical temperature for HSP induction. This determined the minimum energy. The upper limit of the applied energy was calculated by determining which energy would induce a temperature of 100 °C. Four additional pulses were simulated, with the applied energy being linearly distributed between the calculated maximum and minimum energy.

This approach for the determination of the maximum temperature was also used by Pfefer (50). My motivation for using this approach is that above 100 °C water undergoes a phase change, an event the current software package did not account for.

With regard to pulse duration a pulse of 1.5 ms was used. This value is close to what some actual 585 nm and 595 nm PDLs claim to produce although, the actual pulse train

profile differs significantly from any reasonable interpretation of that phrase. (255,258,259)

Although the software is capable of doing so, I did not apply actual pulse train profiles. Neither did I use the exact value of the thermal relaxation time for a 30 μm vessel (260,261). That predicts a pulse width of 1.41 ms for the 30 μm vessels assumed to be present in a normal psoriatic lesion, and a pulse width of 1.88 ms for the larger 60 μm dilated vessels. The thermal relaxation time, that is a theoretical optimal pulse width which maximises the selectivity of the photothermal treatment in terms of the thermal properties of the target tissue, is determined by $d^2/16\alpha$ where d is the target diameter in mm and α is the thermal diffusivity of the target (cm^{2}s^{-1}x10^3). I used the values mentioned for blood by Duck (256): 1.19 cm^{2}s^{-1}x10^3.

At this time, I find the discussion on the optimal pulse width or the actual pulse profile of lesser concern, as I do not model the actual vessels and thus the refinement introduced by realistic pulses and optimal pulse width would be lost in the generalised treatment of the vascular field. I hope that these details will be included in future work using a fully three-dimensional Monte Carlo code, which in addition to the thermal diffusion between the small vessels, can also represent the actual vessel bed as determined by Qin et al. (250) and Schwarz et al. (51).

For readability, I will present the maximum temperature rather than all time-temperature plots. Biological effects are the result of a certain temperature being attained for a certain time. The higher the temperature, the shorter the duration of heating required to induce the effect. This relationship is convex. Thus, determining the maximum temperature, or the temperature at time t, is of limited value. The determination of the biological effects is more suited for the representation of the effects of the irradiation.

4.4.5 Biological effect computations

The biological effects of the laser therapy are calculated using the well-known Arrhenius damage integral. These calculations were performed in tandem when solving the heat diffusion equation.

The aim was to compare the ability of the four systems to induce the activation and release of HSP72i in blood vessels. In order to prevent an increase in inflammation, it is important to limit the actual damage to the tissue. As a measure for that kind of overtreatment I use the Arrhenius damage integral for hyperthermic damage to skin based on the seminal work by Henriques and Moritz during the second world war (55–57), using the recalculation by Diller and Klutke (262) for temperatures exceeding 50 °C. Additionally I use the measure by Brown et al (263) for the effect of hyperthermia on the microvasculature. The idea behind using the measure is the practical potential of methods like laser Doppler flowmetry to indicate if one has surpassed a certain threshold which would indicate a predetermined level of HSP induction. What this level of HSP induction should be would have to be established by further clinical research. Also, there are reasons to assume that this measure is not universally applicable. An earlier study did not show a significant change in blood flow following UV therapy (264). On the other hand, the use of techniques such as laser speckle contrast imaging to determine the progression of the treatment of psoriasis has received new interest, and could easily be extended to the laser therapy case (184,265,266). Such an approach then could be combined with IR measurements at skin surface, allowing an estimation for a maximum and minimum therapeutic threshold.

Rather than presenting the absolute values of the Arrhenius damage integral, the size of the vasoconstrictive effect is presented as the percentage of cells or the percentage of the tissue that has undergone the effect. Thus, a value of 100% for HSP induction implies that further stimulation will not induce additional HSP72i induction. Similarly, 100% for the vasoconstriction measure implies that complete blanching in that particular volume has been achieved. For the hyperthermic tissue damage, the values for the Arrhenius damage integral are translated to the typology of Henriques and Moritz. I.e. a value of 1 implies persistent erythema and oedema, a value of 2 implies focal necrosis, and a value of 3 implies complete loss of the epidermis. This representation is intended to help the reader to interpret the extent of the damage. The used representation was not intended for the study of local damage, but nonetheless is informative about the severity of the effect. The settings used for the calculation of the biological effects are given in Table 5.

	Frequency factor	Activation energy (J/mole)	Reference
Microvascular damage	1,98E+106	6,67E+05	(263)
Hyperthermia induced tissue damage	1.3E95	6.04E5	(262)
HSP72i	6.9E282	1.74E6	(240)

Table 5: Values for the Arrhenius damage integral used in this study.

4.4.6   Studied scenarios

I study four different variations that are common is psoriatic lesions. The first is the oxygenation. As noted above, Dwyer and Parish reported that blood oxygenation levels in psoriasis can be much lower than the normal 90% (51,246). Thus, I study two different configurations, or cases, based on the level of oxygenation. The first case describes 50% oxygenated blood, whereas the second describes 90% oxygenated blood. I've used 50% oxygenation rather than the minimum of 30% as reported by Dwyer and Parish since as can be seen in figure 5 of their paper the minimum in most of the presented lesion was 50% oxygenation, with a small range at the centre of the lesion having 30% oxygenation (246).

Another difference in psoriasis is the increase blood concentration in the lesions due to the changes in micro-vascularization (250). The application of certain compounds can temporarily increase blood concentration in tissue by inducing vasodilatation (247). In the third case I model the effect of a further increase in blood concentration to see if this could further enhance the efficacy of the laser treatment. Here I apply 90% oxygenation as it is reasonable to expect that the temporary increase in blood concentration will not be matched by an increase in oxygen consumption. Scaling is prominent in psoriasis, which results in an increase in scattering. Thus, in the fourth case, I look at the effect of a significant increase in scattering. I use 90% oxygenated blood in order to isolate the effect of the increase in scattering compared to the treatment of healthy skin. For the situation of psoriasis, though, this is less realistic

4.5   Results

In this section, I present the results of my calculations. The section is divided according to the studied devices, with each tissue type being independently discussed when necessary and in conjunction with the others where possible.

The biological effects in terms of heat shock protein induction, tissue damage due to hyperthermia, and effect on microvascular are presented. Energy levels used in the calculation are based on preliminary calculations determining the virtual energy level required to heat some area withing the tissue to 100 degrees Celsius. This threshold was chosen since higher temperature levels would have to take phase change and multiple changes to the optical properties of the tissue into account, which the used software package was not capable of. Vasoconstriction is only shown for the target area. The

presented data is based on an average for a 1 µm column under the laser beam. The measure applied here for vasoconstriction and HSP72i induction is the fraction of cells showing the discussed biologic effect. So, a value of 1 indicates that the maximum effect has been reached. With regard to the tissue damage due to hyperthermia I present the data based on the typology developed by Henriques and Moritz in their papers on the study of thermal injury. i.e. cells are divided according to the "degree" of skin burn they incurred. The latter approach was developed for the study of human skin as a whole, whereas I use it to classify a small area of tissue within the skin. Therefore, the reader is asked to interpret the measure as a global measure of hyperthermic damage, and e.g. not as an indication that a small area of tissue has developed necrosis and blistering.

577 nm Pulsed Dye Laser

Haemoglobin, and in particular oxyhaemoglobin, has a relative high affinity for 577 nm. As a consequence, the 577 nm PDL has the least penetration into the tissue of all studied devices. Switching from 90% oxygenated blood to 50% oxygenated blood slightly increases the penetration into the tissue, and as a consequence, the depth at which HSP72i is induced. This is illustrated in figure 47.

Figure 47: Effect of a change in the properties of the psoriatic lesion on the induction of HSP72i by 577 nm PDL therapy. The x-axis represents the depth into the tissue from the surface. Values are given for the centre of the lesion. Data is shown form the surface up to 400 micron, as this was the maximum depth at which any effect was visible. The y-axis shows the fraction of total HSP72i induction that is caused at that particular location on the x-axis. The curves show the medium and maximum energy for each variation of the psoriatic lesion. Red represents 90% oxygenation, orange 50% oxygenation, green the dilated vessels, and blue the highly scattering epidermis. The dotted curves represent the medium energy settings used for each situation. The values are shown in the legend. The continuous curves represent the maximum energy value, i.e. that value for each situation which would increase the temperature in the tissue to 100 degrees Celsius. This representation is consistent with the figures on the induction of HSP72i that follow for the other devices.

An increase in scattering from the epidermis had a small effect on the depth at which the HSP72i was induced, but did result in a significant increase in the amount of energy required (3.83 J versus 4.30 J, an increase of 12%). The most prominent effect was seen in the dilated vessels scenario: Both the depth at which HSP72i could be induced as well as the amount of energy required to heat the tissue to 100 degrees Celsius were considerably lower than in the other three scenarios. Depth of HSP72i induction decreased by 7% (highly scattering epidermis) to 16% (50% oxygenation), and required energy was reduced by 13% (90% oxygenation) to 22% (highly scattering epidermis).

In terms of effect size, at maximum energy levels the 577 nm PDL was able to induce at least 67% HSP72i induction in 35% (dilated vessels) up to 46% of the psoriatic lesion.

At maximum settings, the 577 nm PDL caused severe and permanent damage to the skin (third degree burn). This is a direct consequence of the chosen methodology: Heating the skin up to 100 degrees Celsius is bound to cause this kind of damage. The most

excessive damage was present at the superficial areas of the target tissue, although at the direct boundary only recoverable, second degree, damage was present. Note that with increasing depth the severity of the damage decreases to the second degree. Also the changes in the tissue properties only influenced the effects in the deeper affected areas: For the first 100 micron into the tissue, all four maximum energy curves overlap. At medium settings, none of the scenarios showed hyperthermic tissue damage. The ranking of volume of tissue affected is equal to that of the HSP72i induction: The smallest volume was noticeable for the dilated vessels scenario, and the largest volume for the 50% oxygenation scenario. This is shown in figure 48.
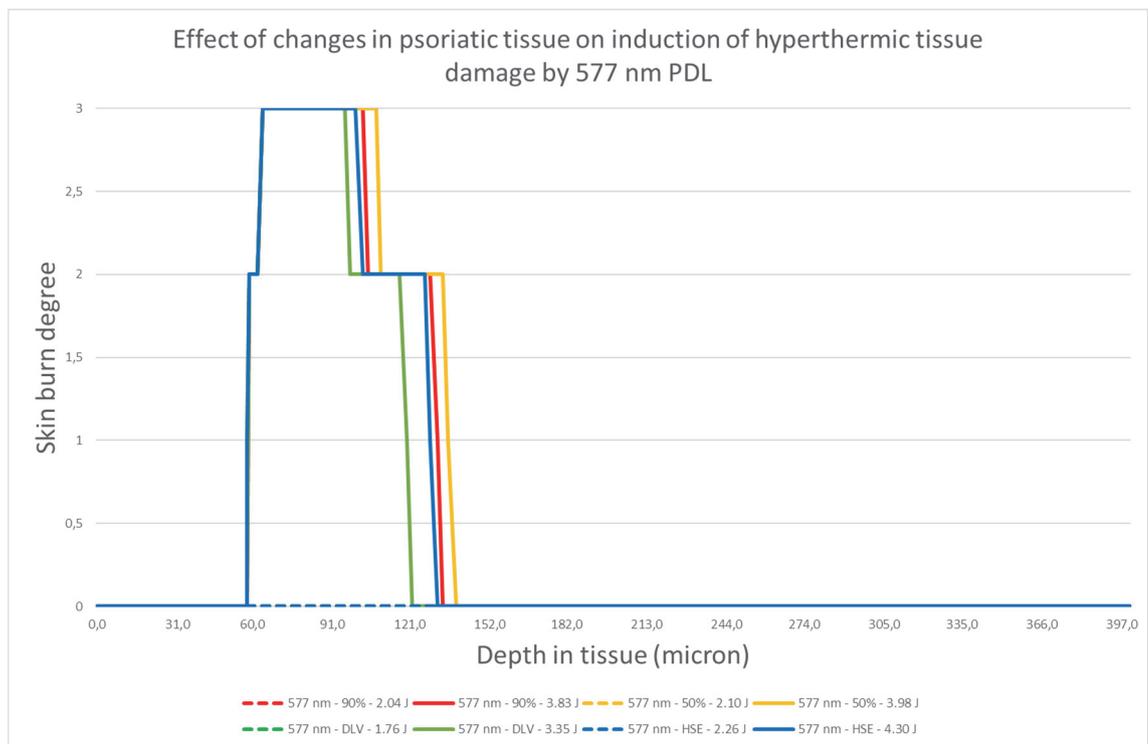
Figure 48: Effect of a change in the properties of the psoriatic lesion on tissue damage to hyperthermia by 577 nm PDL therapy. The x-axis represents the depth into the tissue from the surface. Values are given for the centre of the lesion. Data is shown form the surface up to 400 microns, as this was the maximum depth at which any effect was visible. The y-axis shows the "degree" of skin burn that is caused at that particular location on the x-axis. The curves show the medium and maximum energy for each variation of the psoriatic lesion. Red represents 90% oxygenation, orange 50% oxygenation, green the dilated vessels, and blue the highly scattering epidermis. The dotted curves represent the medium energy settings used for each situation. The values are shown in the legend. The continuous curves represent the maximum energy value, i.e. that value for each situation which would increase the temperature in the tissue to 100 degrees Celsius. This representation is consistent with the figures on tissue damage that follow for the other devices.

By comparing figure 47 and 48 one can start to appreciate a trade-off: A larger effect in terms of HSP72i induction in the target tissue can be achieved by increasing the energy levels. This is not without its negative consequences, as doing so causes significant

damage to the tissue, which could mitigate the anti-inflammatory effect one intends to induce.

The effect of laser therapy on constriction of the microvasculature is similar to that if tissue damage: The effect starts slightly below the surface of the target tissue, as the build-up of heat is countered at the interface due to the conduction of heat into the colder surrounding dermis. This is seen in figure 49.
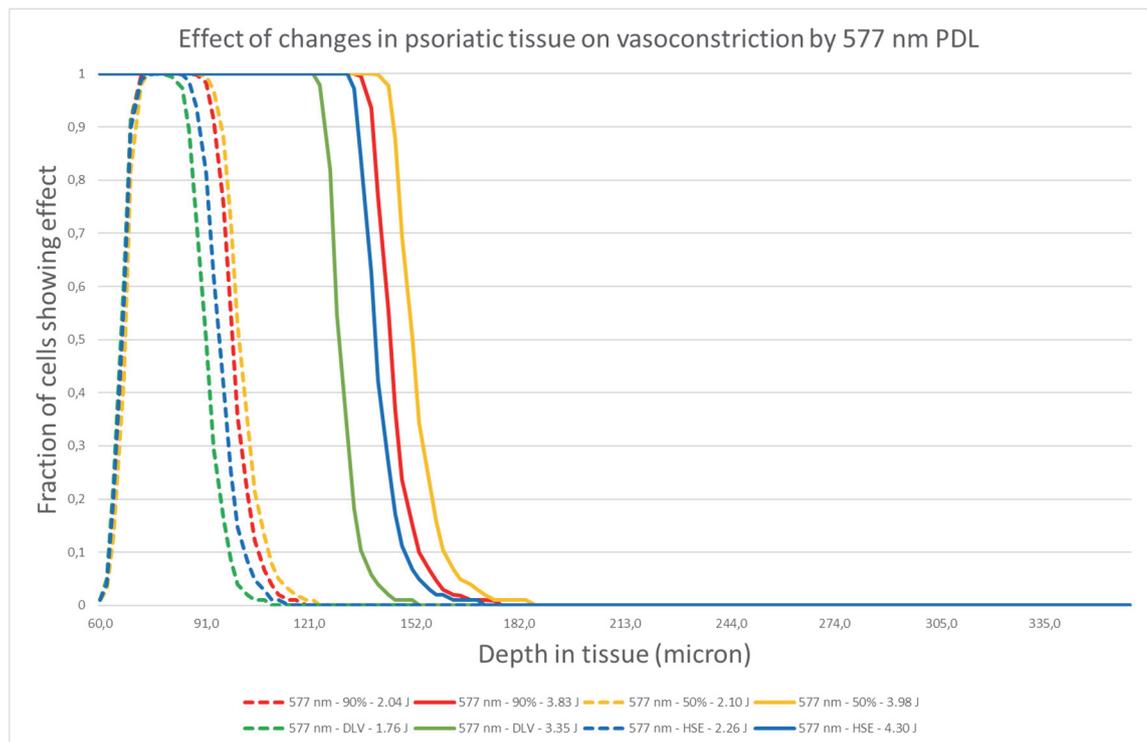
Figure 49: Effect of a change in the properties of the psoriatic lesion on constriction of the microvasculature by 577 nm PDL therapy. The x-axis represents the depth into the tissue from the surface. Note that data is only shown for the target tissue, i.e. starting from 60 microns below the surface of the skin. Values are given for the centre of the lesion. The y-axis shows the fraction of total HSP72i induction that is caused at that particular location on the x-axis. The curves show the medium and maximum energy for each variation of the psoriatic lesion. Red represents 90% oxygenation, orange 50% oxygenation, green the dilated vessels, and blue the highly scattering epidermis. The dotted curves represent the medium energy settings used for each situation. The values are shown in the legend. The continuous curves represent the maximum energy value, i.e. that value for each situation which would increase the temperature in the tissue to 100 degrees Celsius. This representation is consistent with the figures on constriction of the microvasculature that follow for the other devices.

An important finding is that vasoconstriction is non-zero for the (non-damaging) medium energy levels. Depending on the duration of the vasoconstriction this effect could be used in a multiple pulses treatment strategy.

Similar to the findings on HSP72i induction and tissue damage, the change in tissue properties was most prominent for the 50% oxygenation scenario and the dilated

vessels scenario, with the first showing a positive effect on treatment effect and the latter having a negative impact on treatment effect.

The HSP72i induction versus tissue damage trade-off is further illustrated in table 6.

Effect size for 577 nm PDL	90% oxygenation	50% oxygenation	Dilated vessels	Highly scattering epidermis
Fraction of target tissue with at least 66% HSP72i induction	43%	46%	35%	42%
Fraction of target tissue with third degree damage	13%	15%	11%	13%
Ratio of HSP72i induction versus third degree damage induction	3,24	3,11	3,21	3,31

Table 6: HSP72i induction versus tissue damage for 577 nm PDL.

Although the dilated vessels scenario had the lowest score in terms of efficacy, the 50% oxygenation scenario, which had the highest efficacy in terms of penetration, showed the lowest efficiency, i.e. number of cells showing third degree damage relative to cells showing HSP72i induction.

The area above the target showed little to no damage, as is seen in table 7.

Epidermal and upper dermal damage for 577 nm PDL	90% oxygenation	50% oxygenation	Dilated vessels	Highly scattering epidermis
First degree	0%	1%	0%	1%
Second degree	1%	1%	1%	1%
Third degree	0%	0%	0%	0%

Table 7: Damage to skin above target tissue for 577 nm PDL.

585 nm Pulsed Dye Laser

The difference in the molar extinction coefficient for oxygenated and de-oxygenated blood is relative small for 585 nm compared to those for 577 nm and 595 nm. As a consequence, one wouldn't expect that the shift from 90% oxygenated blood to 50% oxygenated blood would have a large effect on the efficacy of the treatment. Haemoglobin does have less affinity for 585 nm compared to 577 nm. This results in

more penetration of light into the deeper parts of the target tissue. The effect is evident in figure 50.
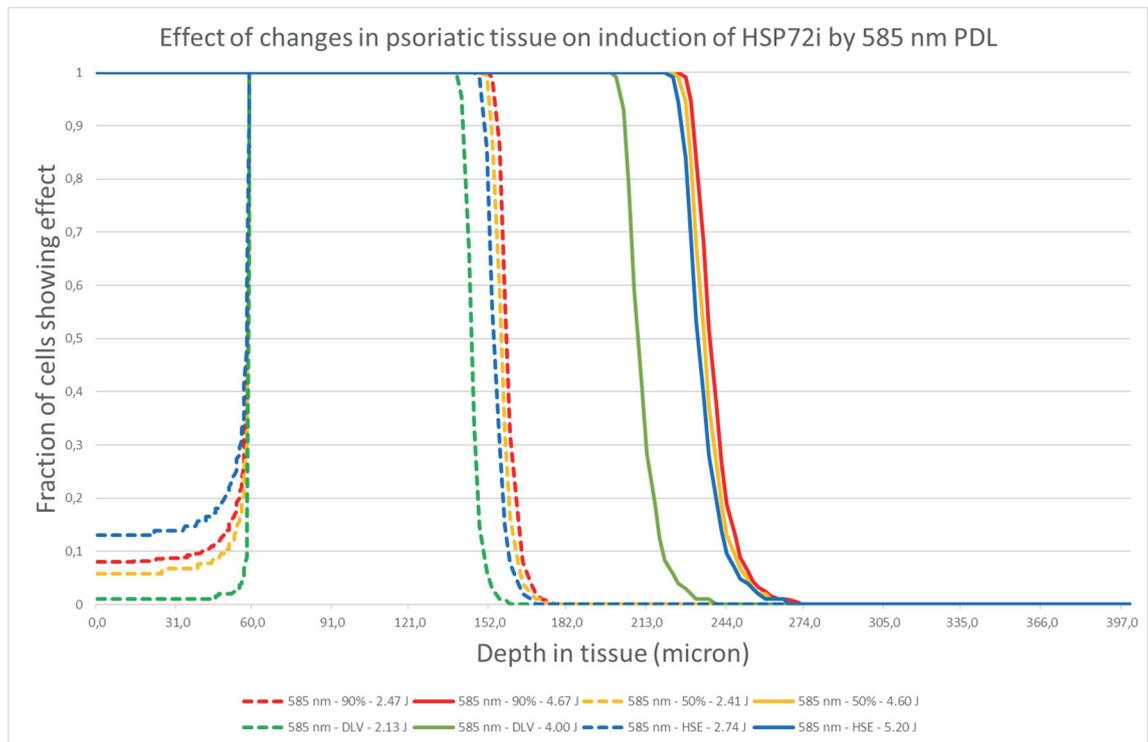
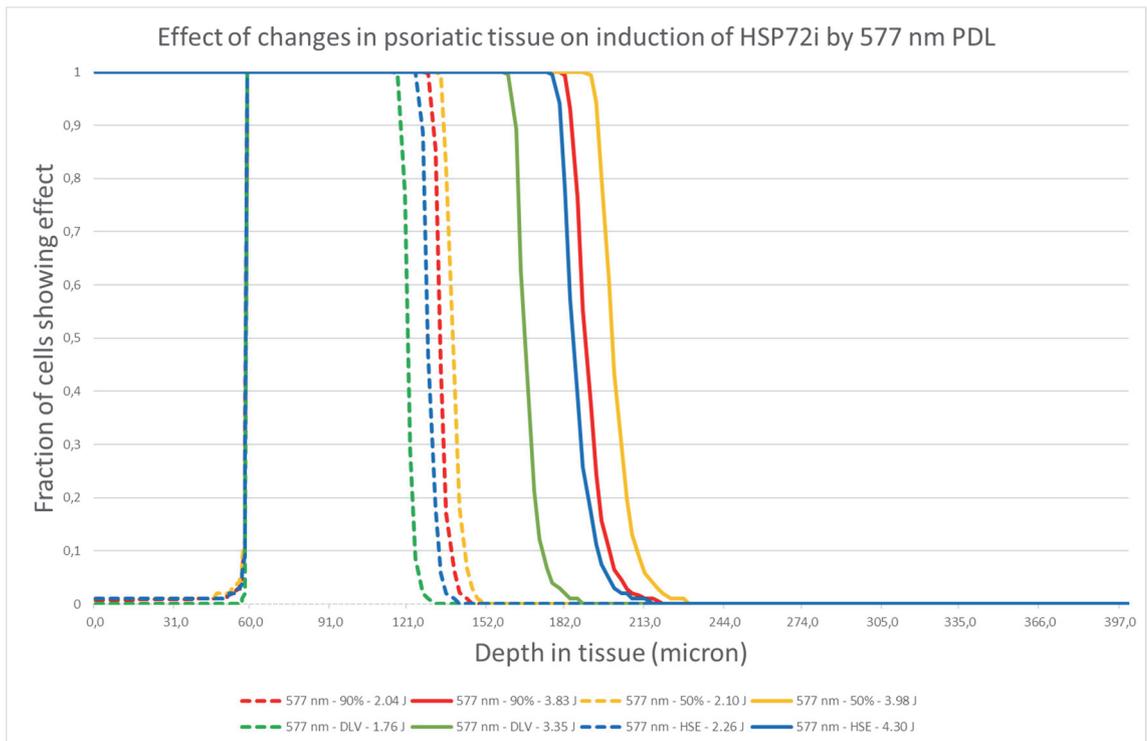*Figure 50: Effect of a change in the properties of the psoriatic lesion on the induction of HSP72i by 585 nm PDL therapy.*

Maximum depth for the strongest pulses now is 235 microns below the tissue surface for the 90% oxygenation scenario versus 208 microns below the tissue surface for the dilated vessels scenario, an increase compared to the 577 nm PDL. The dilated vessels scenario showed the biggest effect on the depth of HSP72i induction: As was the case with the 577 nm, there is a noticeable decrease in the depth at which HSP72i is induced at maximum energy levels.

Unfortunately, there is no free lunch: The increase in total volume of HSP27i releasing tissue is joined by a larger volume of tissue being damaged due to the build-up of heat. As figure 51 shows, this effect now extends beyond the target tissue, in particular for the highly scattering epidermis scenario.

Figure 51: Effect of a change in the properties of the psoriatic lesion on tissue damage to hyperthermia by 585 nm PDL therapy.

The effect of a change in composition of the psoriatic tissue on the capacity of the 585 nm PDL to induce vasoconstriction in the target tissue is limited, as shown in figure 52.

Figure 52: Effect of a change in the properties of the psoriatic lesion on constriction of the microvasculature by 585 nm PDL therapy.

As in the case of the 577 nm PDL, the moderate energy levels are capable of inducing vasoconstriction without tissue damage.

Table 8 presents the efficiency of the 585 nm PDL. Although the efficacy of the 577 nm PDL in terms of depth of achieved effect is clearly inferior to the 585 nm PDL, their efficiency in terms of damage per HSP72i is quite comparable, with a minor increase in efficiency for the 585 nm PDL. The dilated vessels scenario stands out, as it has the lowest efficacy. The other three scenarios show comparable results in terms of efficacy, with the 90% oxygenation case scoring higher in terms of efficiency.

Effect size for 585 nm PDL	90% oxygenation	50% oxygenation	Dilated vessels	Highly scattering epidermis
Fraction of target tissue with at least 66% HSP72i induction	59%	58%	50%	57%
Fraction of target tissue with third degree damage	17%	17%	15%	17%
Ratio of HSP72i induction versus third degree damage induction	3,41	3,36	3,32	3,32

Table 8: HSP72i induction versus tissue damage for 585 nm PDL.

The 585 nm PDL, like the 577 nm PDL, shows a favourable safety profile, although patient comfort might be a bit less given the increase in first degree skin burn damage in the skin above the target area (table 9).

Epidermal and upper dermal damage for 585 nm PDL	90% oxygenation	50% oxygenation	Dilated vessels	Highly scattering epidermis
First degree	12%	11%	1%	52%
Second degree	2%	2%	1%	4%
Third degree	0%	0%	0%	0%

Table 9: Damage to skin above target tissue for 585 nm PDL.

595 nm Pulsed Dye Laser

The molar extinction coefficient of haemoglobin and oxy-haemoglobin for 595 nm is considerably less than that for 585 nm or 577 nm. In addition, attenuation is higher in de-oxygenated blood compared to oxygenated blood. As a consequence, the 595 nm PDL has the highest penetration of all studied systems. This becomes evident from figures 53, 54 and 55.
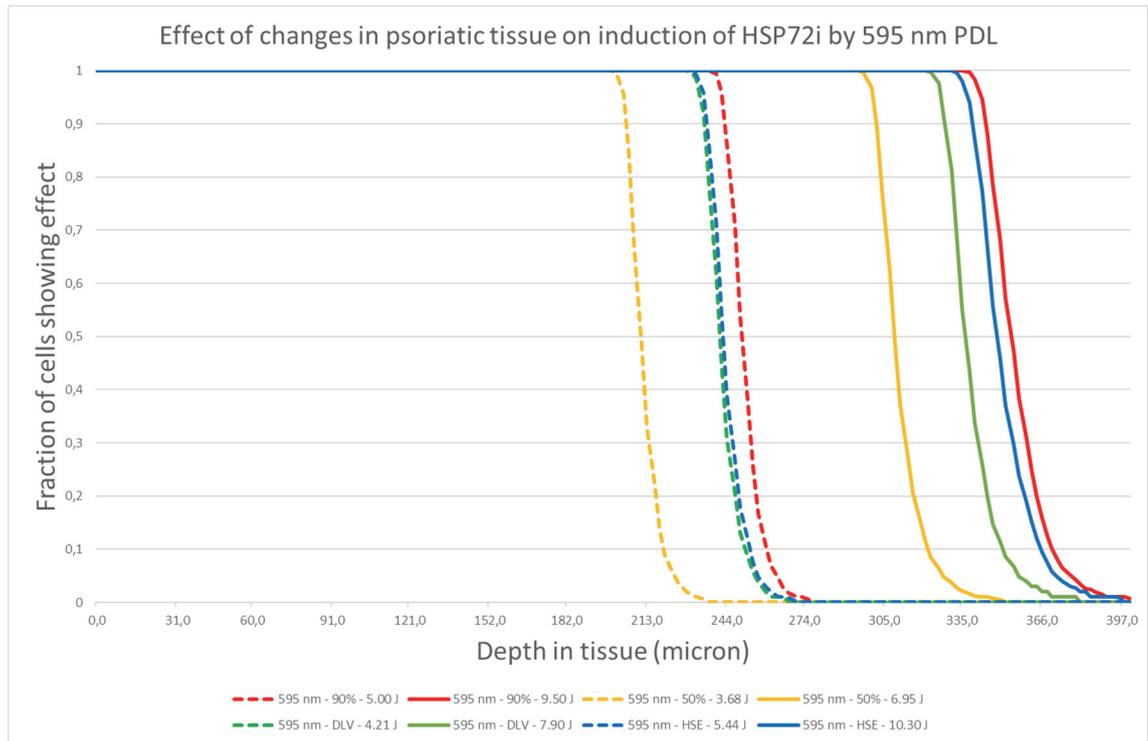
Figure 53: Effect of a change in the properties of the psoriatic lesion on the induction of HSP72i by 595 nm PDL therapy.

In Figure 53 we see that even the moderate settings are able to induce HSP72i well beyond what is possible with the 577 nm PDL irrespective of the scenario studied. Noteworthy is that this time the dilated vessels scenario is not the poorest performer. Here that distinction goes to the 50% oxygenation. Blood composition is more relevant to the 595 nm than the actual amount of blood, a clinically significant finding. Not the least since blood oxygenation is more difficult to assess with the naked eye than blood volume.
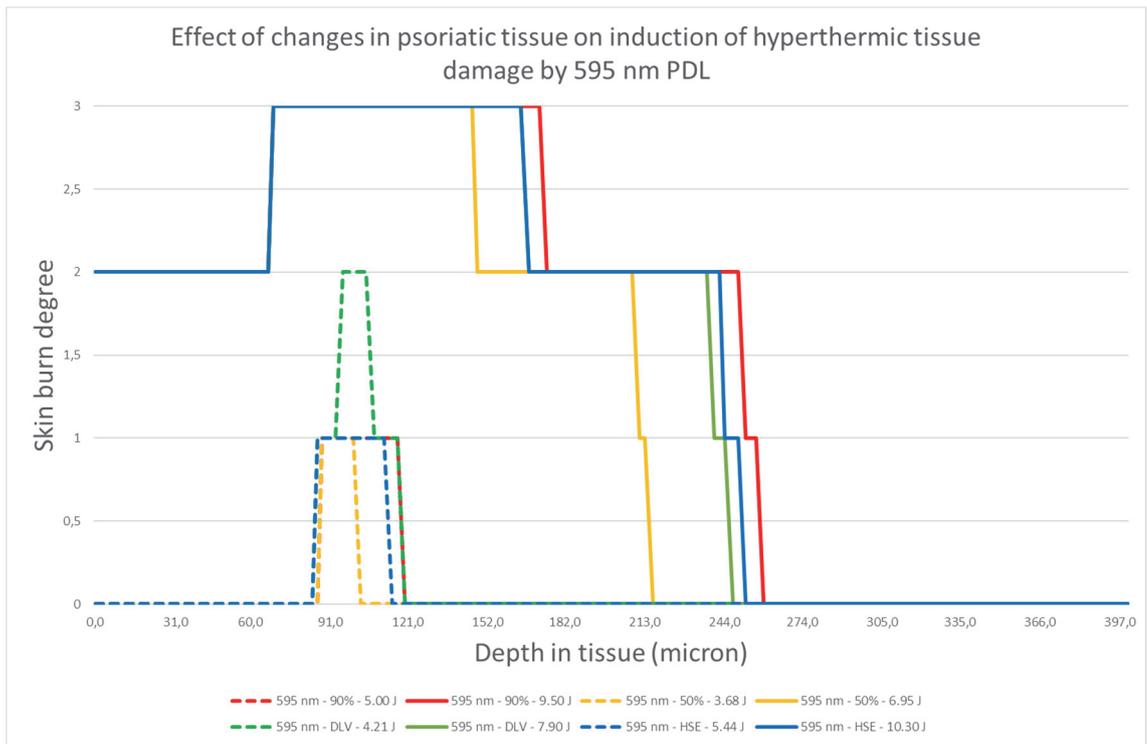
Figure 54: Effect of a change in the properties of the psoriatic lesion on tissue damage to hyperthermia by 595 nm PDL therapy.

Unfortunately, the increase in efficacy is accompanied by an increase in damage. Still, even though the moderate settings not just outperform the maximum settings in terms of depth of HSP72i induction, they do so while causing considerably less damage to the tissue.
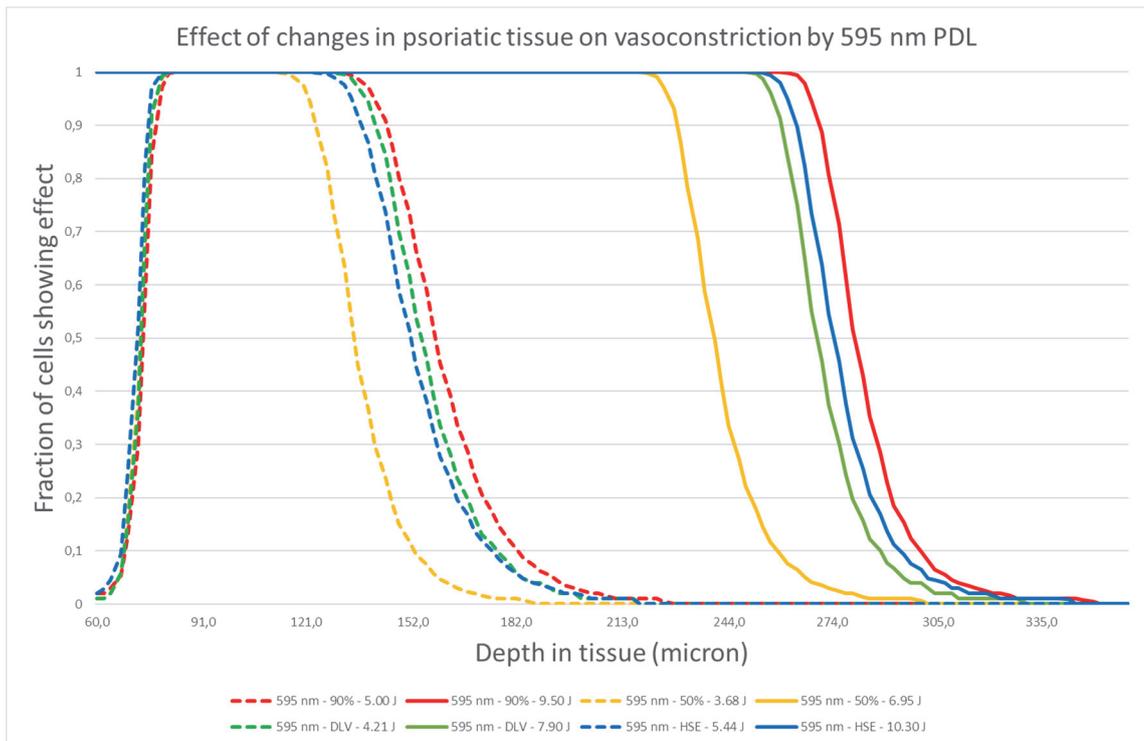
Figure 55: Effect of a change in the properties of the psoriatic lesion on constriction of the microvasculature by 595 nm PDL therapy.

At maximum setting, the 595 nm PDL should be able to induce complete blanching of the target tissue. Whether or not this effect would be obscured by potentially occurring purpura resulting from rupture blood vessels cannot be determined by the analysis conducted in this work. It does suggest that the 595 nm PDL, ignoring the potential limitations arising from the pulse train profile applied by the commercially available machines, could be suited for a stacked pulses approach.

The efficiency, safety and comfort of the 595 nm, as shown in tables 10 and 11, generally is lower than that of the 585 nm and 577 nm PDL, with an exception for the 50% oxygenation.

Effect size for 595 nm PDL	90% oxygenation	50% oxygenation	Dilated vessels	Highly scattering epidermis
Fraction of target tissue with at least 66% HSP72i induction	97%	82%	91%	95%
Fraction of target tissue with third degree damage	35%	26%	32%	32%
Ratio of HSP72i induction versus third degree damage induction	2,80	3,15	2,83	2,95

Table 10: HSP72i induction versus tissue damage for 595 nm PDL.

Epidermal and upper dermal damage for 595 nm PDL	90% oxygenation	50% oxygenation	Dilated vessels	Highly scattering epidermis
First degree	0%	0%	0%	0%
Second degree	100%	100%	100%	100%
Third degree	0%	0%	0%	0%

Table 11: Damage to skin above target tissue for 595 nm PDL.

Intense Pulsed Light

IPL devices differ from laser devices in that they are a broad-band light source. This makes it relatively more difficult to interpret the expected behaviour, in particular when producers fail to publish the spectral output curves. Still, applicators which perform better in the treatment of superficial enlarged red blood vessels like in the case of spider veins than e.g. in the treatment of unwanted hair can be expected to behave more akin to a PDL than to a 1064 nm Neodymium doped Yttrium Aluminium Garnet (Nd:YAG) laser or 755 nm Alexandrite laser. The studied IPL showed behaviour comparable to that of a 585 nm PDL, and in lesser degree of a 595 nm PDL. It did require significantly higher energy levels to achieve the same physical effect, e.g. heating some part of the tissue to 100 degrees Celsius. Although falling short of the 595 nm PDL in terms of depth at which HSP72i could be induced, the IPL showed more penetration than the 585 nm PDL (figure 56). An increase in total blood content in de tissue had a detrimental effect on maximum

depth of effect, whereas an increase in scattering in the epidermis showed the greatest depth at which HSP72i could be induced.
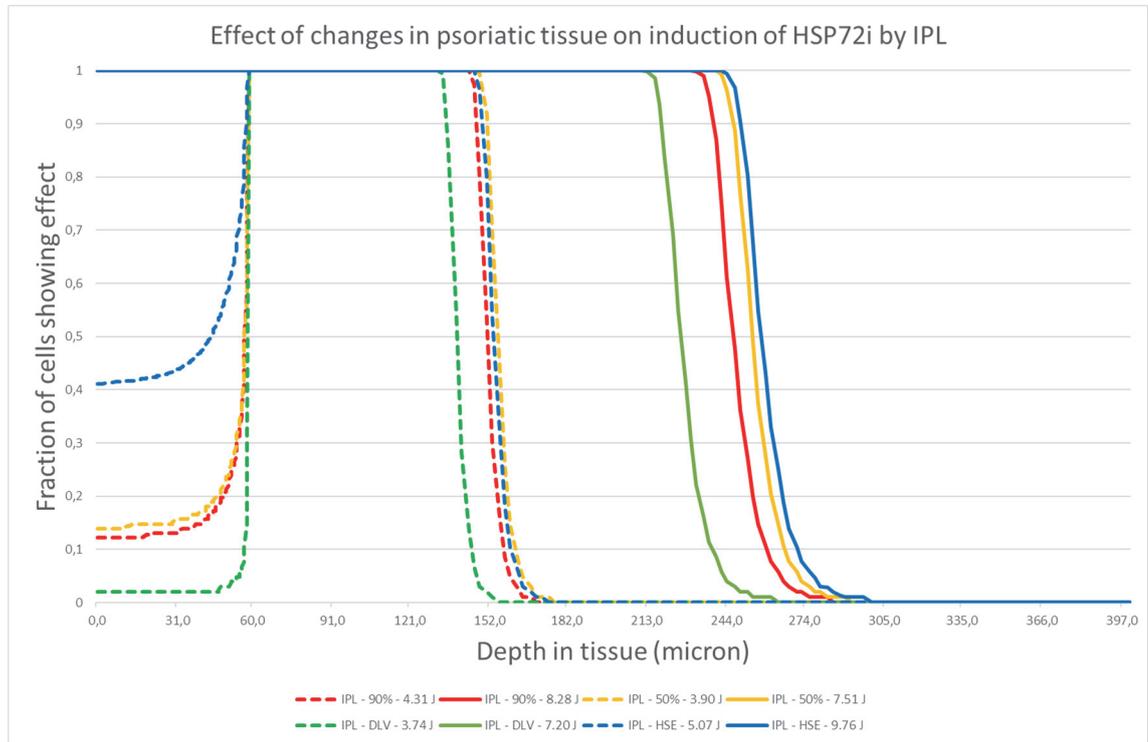
Figure 56: Effect of a change in the properties of the psoriatic lesion on the induction of HSP72i by IPL therapy.

The IPL showed less favourable results than the 585 nm PDL in terms of patient comfort and safety, as shown in figure 57 and table 13. Surprisingly, the IPL seems to greatly benefit from an increase in total blood content: There a significant amount of HSP72i induction can be achieved with, in comparison to the other devices, quite limited damage.
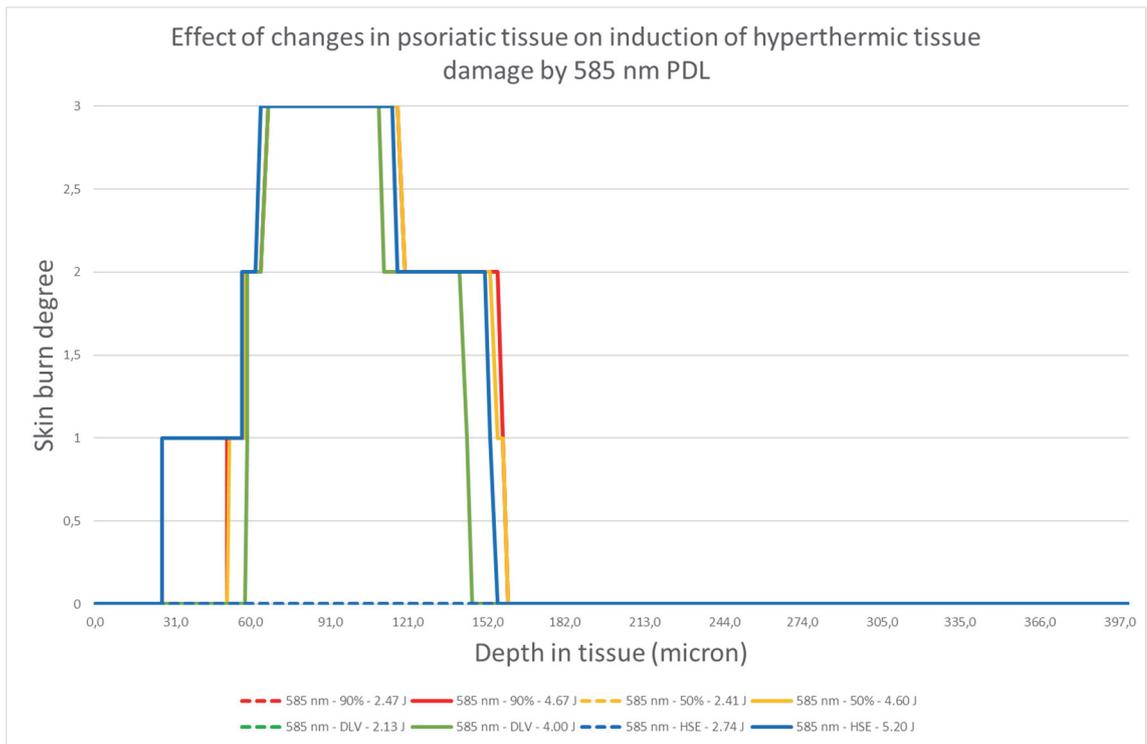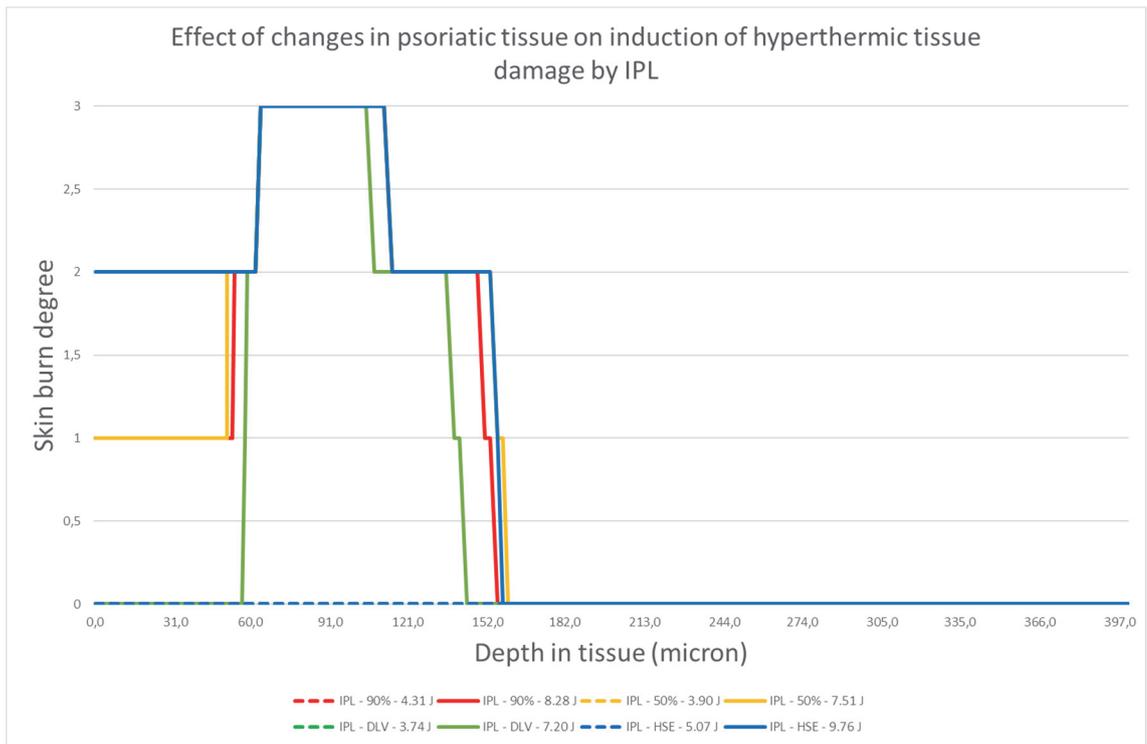
Figure 57: Effect of a change in the properties of the psoriatic lesion on tissue damage to hyperthermia by IPL therapy.

The vasoconstriction effect noted for the PDL system is also present in the treatment with the IPL. The shape of the curves is not too dissimilar to those of the 585 nm PDL.
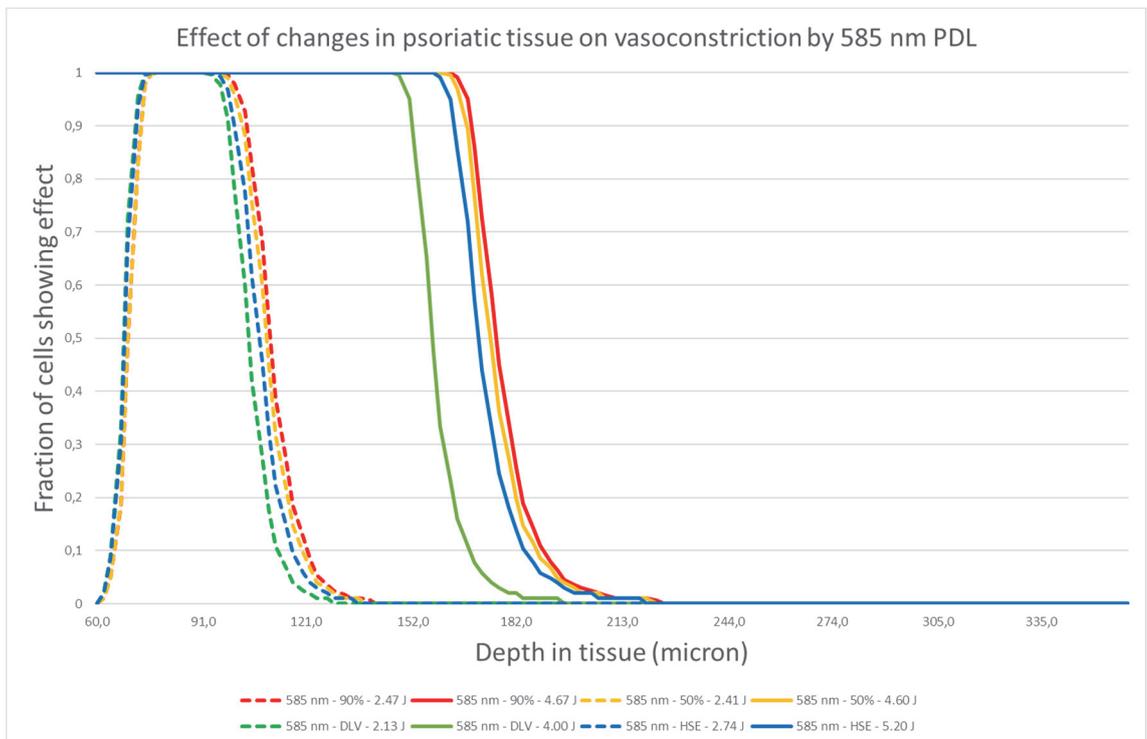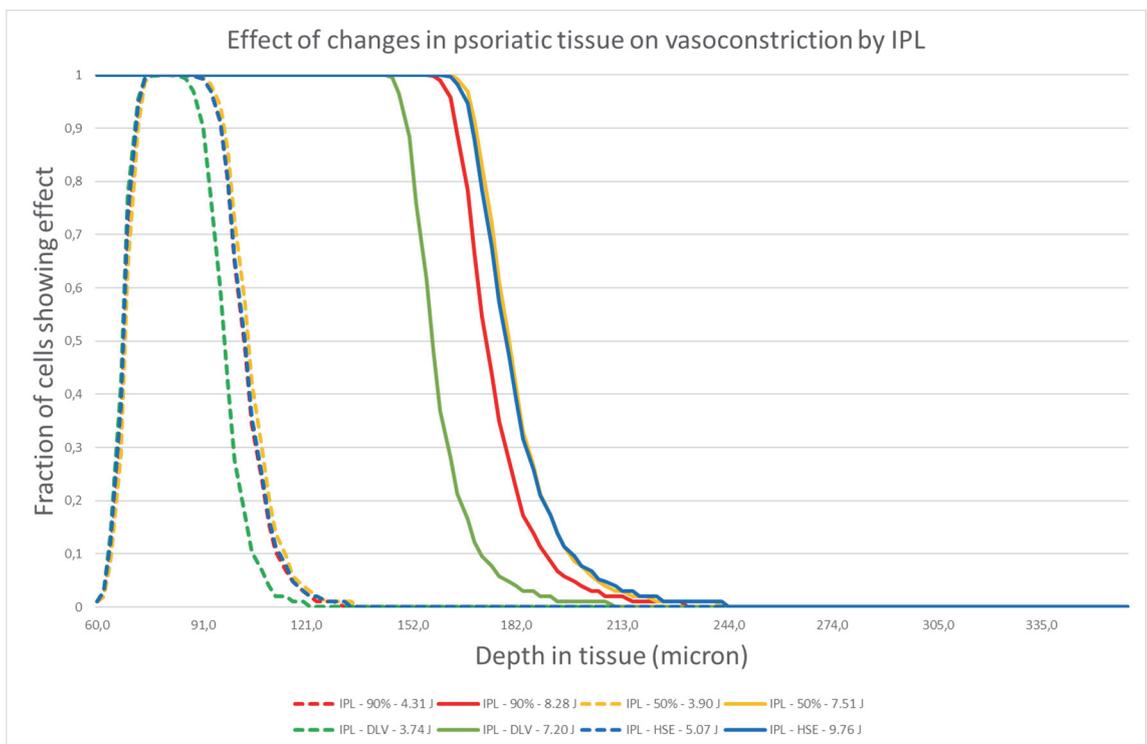

Figure 58: Effect of a change in the properties of the psoriatic lesion on constriction of the microvasculature by 595 nm PDL therapy.

Page 131

In terms of efficiency (table 12) the IPL seems to score top marks, dominating the PDL systems in terms of HSP72i induction per unit of third-degree tissue damage. This is surprising, since the technology is generally regarded as being inferior to "true" laser systems as a consequence of the lower degree of selectivity. Patient comfort might have something to be desired for though, at least in comparison to 585 nm PDL. Techniques such as dynamic cooling, in which cooling is postponed until some milliseconds after the application of the laser pulse, could become relevant here.

Effect size for 595 nm PDL	90% oxygenation	50% oxygenation	Dilated vessels	Highly scattering epidermis
Fraction of target tissue with at least 66% HSP72i induction	61%	64%	55%	65%
Fraction of target tissue with third degree damage	17%	17%	14%	17%
Ratio of HSP72i induction versus third degree damage induction	3,71	3,86	3,89	3,95

Table 12: HSP72i induction versus tissue damage for IPL.

Epidermal and upper dermal damage	90% oxygenation	50% oxygenation	Dilated vessels	Highly scattering epidermis
First degree	90%	86%	1%	0%
Second degree	10%	14%	1%	100%
Third degree	0%	0%	0%	0%

Table 13: Damage to skin above target tissue for IPL.

Required energy levels

As noted in the beginning of this section, the results are based on the calibration according to the achieved temperature in the target area. As a consequence, the difference in energy required to actually achieve the increase in temperature is somewhat obscured. Figure 59 shows the amount of energy used for the calculations.

The software package used for these experiments contains a calibration factor which allows it to be validated against thermographic measurements of the skin surface. I did not have access to data describing these values for psoriatic lesions treated with the different systems. As a consequence, we cannot provide real world values, and the reader is reminded that these values are intended to allow one to compare the relative values and thus understand the relative performance or characteristics of the investigated light sources.
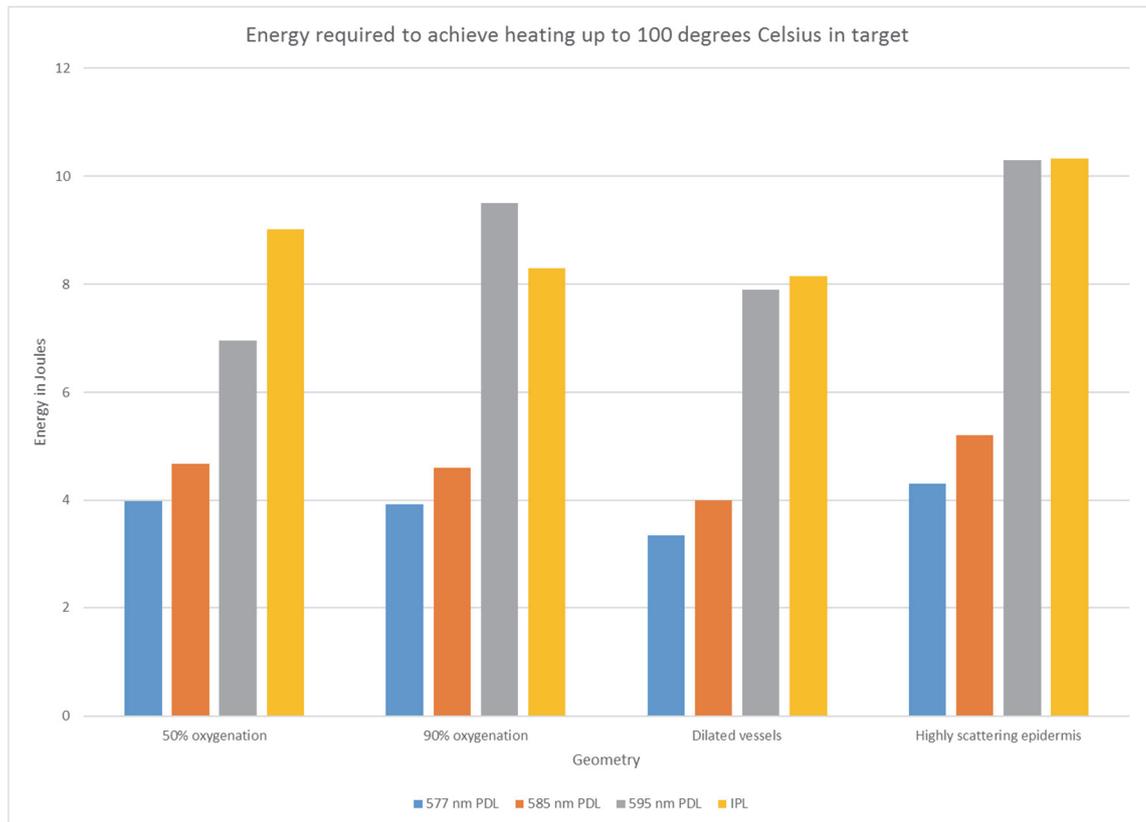
Figure 59: Energy levels required for 100 °C in target areas.

The 577 nm PDL and 585 nm PDL are similar in terms of required energy. The 595 nm PDL on the other hand requires between 75% and 140% more energy than the 577 nm PDL in the same geometry in order to achieve, or rather be limited, by the 100 °C threshold. I note that like the 595 nm PDL the IPL required significantly larger energy levels than the 577 nm PDL and 585 nm PDL for a given increase in temperature, even though in terms of induced effect the IPL is much more similar to the latter than it is to the prior.

4.6   Discussion

Efficiency vs. Effectiveness

We have seen from the results that the different devices show clear differences in terms of efficacy (what is the maximum depth at which an effect can be induced) and efficiency (how much undesired damage does the treatment cause for a given beneficial effect). E.g. the 595 nm PDL showed the highest degree of efficacy, as it could induce HSP72i throughout the psoriatic lesion. Its performance in terms of efficiency though left something to be desired for. Within the set of scenarios studied for the 595 nm PDL, the 50% oxygenation case stood out: There the efficiency greatly improved, albeit to the detriment of the efficacy. The difference between the 50% oxygenation and the other scenarios is the absorption coefficient for the blood: De-oxygenated blood has a stronger affinity for 595 nm than oxygenated blood has. Here the efficiency of the 595 nm PDL was not too dissimilar to that of the 577 nm PDL, for which both studied variants of haemoglobin have an even stronger preference. Yet the efficacy of the 595 nm in the 50% oxygenation scenario was nearly double that of the 577 nm. This illustrates that more selectivity is not always desired. Just like is the case in fluorescence detection, here a balance must be struck between penetration of the light and selective absorption of that light by the target tissue. If you have insufficient selectivity, the volume of tissue that is unintentionally damaged is too large. When there is too much selectivity, too much targeted tissue remains untreated.

I note that in the current study efficiency is only studied for the maximum energy values. For each device there exists an energy level for which there is a strictly positive amount of HSP72i induction without any third-degree skin damage. For those situations, the used efficiency measure would break down, and one would have to resort to a related measure such as a second-degree skin damage. Additionally, an efficiency measure not reported here, but which potentially could be pursued in future work, would be the maximum volume of HSP72i induction and vasoconstriction without third degree skin damage in any part of the tissue. This measure would be of particular interest for the use of stacked pulses, as discussed below.

IPL for the treatment of psoriasis

It is worthwhile to further investigate the application of IPL devices in the treatment of psoriasis, since other interventions either lack efficacy, cannot achieve treatment free duration of remission, are associated with severe adverse effects and complications, and may burden society with an unsustainable cost of treatment. Even when laser or IPL therapy might not be optimal for a given patient, they would be suited as a supporting therapy in addition to treatment with e.g. systemic or biological pharmaceutical modalities, since the latter are regularly unable to achieve complete clearance. Laser treatments are limited in their practicability because of the small area that can be treated per pulse, requiring a relatively large amount of specialised labour that needs to be committed for a treatment. IPL devices are relatively cost-effective and are associated with applicators that allow for the treatment of quite large areas per pulse compared to the PDL devices. (Vascular) laser therapy could be relatively better equipped to treat psoriasis than the pharmacological modalities or UV based therapies. The emitted photons are too weak to induce DNA damage, laser therapy will not damage the kidneys or liver, are not associated with atrophy of the skin (rather the opposite), and do not cause gastro-intestinal discomfort. Patients do not have to change their lifestyle for sake of the therapy, allowing for the enjoyment of the occasional alcoholic refreshment. Moreover, the fact that blood perfusion in psoriatic lesions is associated with the immunological drivers of the disease creates a natural selectivity other therapies lack (184,265). It implies that dermal HSPs are particularly induced in those locations where they are most required: the dermis below the psoriatic lesions, close to the CD4+ and CD4+CD8+FOX3+ T-cells.

Due to the technology of IPL devices, they can be constructed as to offer the clinician more flexibility in the application. E.g. applicators can differ in area of the light source, shape of the optical band, and the temporal profile of the light emission. The latter in particular is a potential advantage of IPL devices compared to PDL devices. Although I chose not to analyse the pulse train profile in this study, I do note that some laser devices are not capable of producing anything but sub- millisecond pulses. IPL devices on the other hand are generally better equipped to deliver longer pulses, to the range of 5 ms per pulse. Longer pulses might result in a downward shift of the HSP production, as more heat from the superficial regions of the target is being diffused towards the surface

during the pulse. Longer pulses do require higher energy levels to attain a given degree of heating, increasing the risk of hyperthermal damage to the epidermis.

In the current study I used a relative low percentage of melanin. The results presented in this work should be verified for different levels of pigmentation, as well as for various additional factors such as the use of cooling techniques and pulse trains profiles.

Therapeutic effect versus damage

In my study, I noted a consistent trade-off between expected efficacy, that is the total HSP72i production as well as the location of that production, and the expected adverse effects, that is the degree of tissue damage which might invoke a Koebner phenomenon or even result in skin burn. This is a departure from earlier approaches in laser therapy, which focus on achieving a certain histological effect such as the destruction of a hair follicle or the coagulation of a blood vessel. The approach presented here seeks a maximum net biological effect which is the resultant of a positive and a negative effect. This is not to say I am the first to depart from the maximum damage paradigm: the application of what is called long pulsed dye laser for rosacea by Nymann et al. (270) precedes the approach presented in this thesis. Rylander et al. took the effect of heat shock approach as a countervailing power for photothermal therapy for malignancies into account (245). But neither sought an optimum between two effects: Nymann et al. wanted to avoid damage, but did not relate the lower settings to some measure of efficacy, whereas Rylander et al. still maximized the damage function. In this study thermal injury and heat shock are different sides of the same coin, requiring a balancing act.

Future research will have to identify the drivers of the pro- and anti-inflammatory effect of laser therapy, as well as the associated kinetics, and hopefully will provide us with either sensors or an associated clinical response which allows us to determine if we have achieved maximum net effect or not. The presented results could be used to optimize and generalize the HSP approach so one could achieve more HSP72i induction for the same degree of thermal damage, or induce less damage for a given amount of HSP72i. Furthermore, given the noted efficacy of PDL therapy for inflammatory conditions in general, as reported by Erceg et al. (144), the HSP72i versus thermal injury paradigm

could be used to improve the treatment of much more inflammatory conditions than is currently the case.

HSPs are a family of molecules that play a central role in the response of cells to various stressors. The name heat shock protein is a bit of a misnomer and reflects the fact that they were first discovered as a response to thermal injury in Drospholia (271). Although HSPs are the primary response of tissue to heat, research has shown that HSPs can be induced by non-thermal events as well, including UV irradiation (272–275). Heat shock proteins are differentiated according to their molecular weight. They are highly conserved in cells and can be either constituent or induced by stressors.

The literature on heat-shock proteins has shown that some of the proteins can induce an anti-inflammatory effect (276,277), as well as a regenerative effect on the malformed cutaneous innervation (233,235,236,278–280). As I noted before, the latter is a hallmark of psoriasis lesions (189,191,192,208,209,281,282). HSPs have been identified as an important player in the differentiation of neural cells (283), which would correct limited maturation of the neurons in the psoriatic skin as reported by Weddel et al. (192).

Lasers are not unique in their ability to induce HSPs, further supporting the notion that it is the induction of HSP that drives the efficacy of laser therapy. On the contrary, the mainstay of phototherapy in dermatology, UV therapy, as well as the more novel photodynamic therapy are capable of producing dermal HS, or at least with a decrease in pro-inflammatory cytokines such as IL-17 and neuropeptides associated with the onset of psoriasis lesions such as SP and CGRP (151,238,240–242,272,275,284–289). It also explains why laser therapy is more effective in inflammatory conditions such as acne or eczema. (25,144–146,290).

Of particular relevance is the observation by Bovenschen et al. that regulatory T-cells produce IL-17 in psoriasis, in effect behaving as a T-helper cell (277). This could explain the chronic nature of psoriasis. HSP70 also exerts an effect on these regulatory T-cells (276). Since laser therapy can induce perivascular HSP70 (239,242,285,291), it might not just create an anti-inflammatory effect, but at the same time prevent the role reversal of the CD4+CD8+Fox3+ T-cells in psoriasis.

In practice, it has been observed that the 595 nm PDL treatment for psoriasis is more effective when it is combined with a potent corticosteroid, such as clobetasol-17-proprionate (145). As I have noted above, laser therapy achieves its success by decreasing the supply of T-cells. The demand for an immunological response, to frame the interaction in the terminology of the dismal science, on the other hand will not decrease by laser therapy alone. Corticosteroids do, and that might explain the presumed efficacy of a combination therapy. So even though Bovenschen et al. and Erceg et al. showed that the 585 nm PDL is superior to quite potent topical corticosteroids and vitamin D analogues (147,169), one might find that the combination is superior to PDL monotherapy. Obviously, this question cannot be answered through computation and requires an appropriately designed randomized double blind study.

An addition to the observation by Hern et al that a purely surgical effect on the vascular bed is unlikely to explain the observed effects (149), can be derived from a study on the efficacy of the 1064 nm Nd:YAG (170). The contrast in absorption between blood vessels and the surrounding tissue of the light emitted by the Nd:YAG laser is much lower than that of either of the studied PDL devices, resulting in a deeper penetration of the light and of the therapeutic effect. The notion that biological rather than surgical effects are responsible for the efficacy of laser therapy in psoriasis is also supported by the findings by Higgins et al. (292). They found that increasing the UV dose did not result in a more effective treatment, faster onset of remission, or longer duration of remission.

As noted above, there are some striking similarities between UV therapy and selective photothermolysis based laser therapy. The results of studies on the use of sub erythematous doses of UV light in psoriasis suggest that a similar trade-off is present in UV therapy (293). That is, using lower doses of UV light results in delayed clearing of the lesions, but at a lower total cumulative dose. The latter implies a lower risk for skin cancer. Increasing the intensity of a UV session would increase both the depth and amount of HSP72i induction, but also the induction of the mutagenic cyclobutane pyrimidine dimer in the epidermis and dermis (148,294), which results in the apoptosis of keratinocytes (295). The idea of a therapeutic effect – detrimental effect trade-off is further supported by the observations by Gu et al. who suggest that oxidative stress should be avoided, in particular when reaching the end of the schedule and thus the relative higher doses of radiation(296). This would strengthen the case for large area

laser or IPL therapy for psoriasis, as it isn't carcinogenic in contradiction to most systemic pharmacotherapeutics or UV therapy.

Another striking similarity of light based therapies when compared to pharmacological interventions is the duration of remission. Both UV therapy and laser therapy can achieve comparable long durations of remission (5,6,165). The effect of HSP72i on the regeneration of the innervation of the skin could be a potential explanation for this difference in effect.

Noteworthy is that in the study by Zelickson et al. the regrowth in a partially treated psoriatic lesion emerged from the boundaries of the remaining parts of the lesions, and not homogenous, indicating a biological process which requires the conditions typically present in the psoriatic lesions (24). Narrow-band UVB results in decrease in peripheral blood mononuclear cells, indicating another supra-regional effect (297).

Unfortunately, temporary worsening in disease severity during laser treatment has not been systematically analysed or reported, but from experience, personal communications and the sparse mentions in the literature we know that Koebner in laser therapy of (neuro)inflammatory conditions is possible (298–300). As noted in the introduction, HSPs can evoke an immunological response as well (301,302), allowing the possibility of a worsening of the condition even at sub-lethal intensities. Kakeda et al. showed a marked increase in HSP90 in psoriatic lesions, both in the dermis and the epidermis (303). Senderup et al. further showed that a HSP90 blocker was able to reduce the severity of psoriasis in a graft model (304). Wu et al. note that HSP90 can increase the levels of IL-17 (305). Lehner et al. on the other hand notes that some HSP70 proteins are capable of activating the immune system, mentioning a potential role in vaccination strategies (306). This suggests that HSP90 is likely to cause a pro-inflammatory response, especially in tissue such as the epidermis of psoriasis patients.

Figure 60: Pro-inflammatory and anti-inflammatory effects of 595 nm PDL in psoriasis

Figure 60 illustrates my point. Here we see psoriatic lesions before and after 595 nm PDL treatment. De red-brown spots in the post-treatment are post-inflammatory hyperpigmentation, a tell-tale sign of inflammation. It indicates that with this patient, the settings were too aggressive. What I note though is that the area around the spots has cleared, indicating the beneficial effect of HSP72i. So here we see both pro-inflammatory HSPs and anti-inflammatory HSPs having their effect on the lesions.

The HSP in epidermis paradox is solved by observing that these HSPs do not pass through the dermal barrier. Therefore, they are separated from both the CD4+ cells and CD4+CD8+Fox3+ cells responsible for the therapeutic effect, ignoring the question whether the epidermal HSPs actually are inducible by nature or rather constitutive.

The notion that both UV therapy and laser therapy can, through the induction of HSPs, result in an anti-inflammatory or a pro-inflammatory response explains the paradoxical observation by De Leeuw et al. that the combination of 585 nm PDL and 311 nm UVB was less effective than each treatment on its own (146). From the results above, we know that both 585 nm PDL and 311 nm UVB therapy have a more pronounced effect at the superficial regions of the target area and the overlying dermis and epidermis. If UVB therapy has progressed sufficiently to induce erythema, implying that most of the HSP72i induction at the superficial areas had already been achieved, one would expect only a marginal benefit of a subsequent application of the PDL in terms of HSP72i induction, and a strong increase in terms of tissue damage as some level of damage had already been induced. The 595 nm PDL would suffer less from this effect, as it has a more pronounced effect at the deeper regions of the skin, yet one would expect optimal settings to prescribe lower energy levels.

Vasoconstriction as a measure of actual effect

One measure which has up to this point avoided discussion is the effect of the lasers on the constriction of the vasculature of the lesion. The reason why I am interested in this measure is a practical one. A practitioner would be interested in determining the effect of laser therapy in a non-invasive and cost-effective manner, allowing for the real-time adjustment of treatment parameters as to achieve an optimal result given the limitations of the available technology. To become an expert in the application of lasers for the treatment of skin conditions, one must learn to "read" the skin. That is, one judges the concentration and distribution of melanin by looking at the skin tone. The depth of the target is estimated by looking at the colour and sharpness of the presentation. And the thickness of the skin affects safety and efficacy. This and much more is considered when the initial setting is determined. After the first pulse, the skin response is observed, which to the trained eye gives an indication how close the settings are to the optimum for the patient. Developing these skills generally requires many years of training and a lot of practical experience. Yet in technical terms this can be simplified to the application of a straightforward algorithm following a repetitive measurement by an optical sensor. We can measure colour and temperature before, during and after the pulse. The question then is can we emulate the decision process of the experienced clinician using relatively cost effective technological solutions? The issue of costs and ease of use are binding constraints in this sense. There are quite interesting and promising technologies available on the market, such as ultra-high frequency ultrasound, laser speckle contrast imaging, and multiphoton tomography. The application of deep learning algorithms could be of benefit as well: Recently it was shown that image recognition techniques perform as well as board certified dermatologists when it comes to the recognition of melanoma skin cancers (307) . Unfortunately, the costs associated with the acquisition of these devices exceeds tens of thousands of euros, and not all of them are suited for an instantaneous or quasi-instantaneous measurement during treatment.

Less advanced techniques such as colourimetry and laser Doppler flowmetry are better suited in terms of practicality and affordability, but require the therapy to induce a sufficiently large effect on the blood flow to be measurable. The results in a study suggest that this indeed is the case. The distribution of the energy and the subsequent

heating of the target issue indicate that vasoconstriction will first occur at the top of the target tissue and continue deeper into the target tissue as energy levels increase. One would expect the lesion to show a certain amount of blanching: the vasoconstriction will remove the most superficial amounts of blood, thereby creating a "milk-like" appearance of the remaining lesion. This of course is nothing more than an increase in the amount of light back scattered towards the observer. Further computational studies could create colour tables for various geometries prior to and after successful laser therapy, indicating the feasibility of that approach and potentially creating the justification for a clinical study.

Perhaps more interestingly, the vasoconstriction offer more insight into the logic behind the stacking of sub-purpura pulses in the PDL treatment of e.g. photoaging or telangiectasia (270,308,309). The vasoconstrictive effect is located at the top of the target area. If one would apply a second pulse in sufficiently short succession to the first, the effect of the second pulse would be exerted at a further distance from the skin surface than the first. As such, stacking would allow for the induction of higher concentrations of HSP at deeper levels of the target area. Yet a second pulse could also create significant additional damage if the tissue hasn't cooled sufficiently yet. The latter can be avoided by spacing the pulses such that the temperature of the tissue has returned to its initial values. The question then is if the time required for sufficient cooling is longer or shorter than the duration of the vasoconstriction. The answer to the question is interesting for the IPL. In a one pulse setting, it is inferior to the 595 nm PDL and could be on par with the results of the 585 nm PDL. The main difference between the 585 nm PDL and IPL is that the latter results in more pronounced heating of the dermis and epidermis at a certain heating of the target tissue, as well as a slightly deeper effect into the target area. Nonetheless, the IPL seems to be able to achieve a higher degree of efficiency in terms of induced heat shock protein per tissue damage for the currently studied scenario.

4.7   Limitations

The presented study suffers from significant limitations, which I will discuss here.

1. The sandwich model ignores the shape of the rete ridges. Since in psoriasis there is a significant increase in size of the rete ridges, we might be unaware of additional effects in terms of scattering, reflection, or heat diffusion.

2. The computational software is based on a two-dimensional code. This again might underestimate certain effects, in particular depths (310). Bashford however shows that the two dimensional and three dimensional Monte-Carlo codes both are able to derive the same benchmark diffusion problem given by the analytical expression in chapter 12 of the classical work by Morse and Feshbach (45,46). This result is shown in figure 61 below.
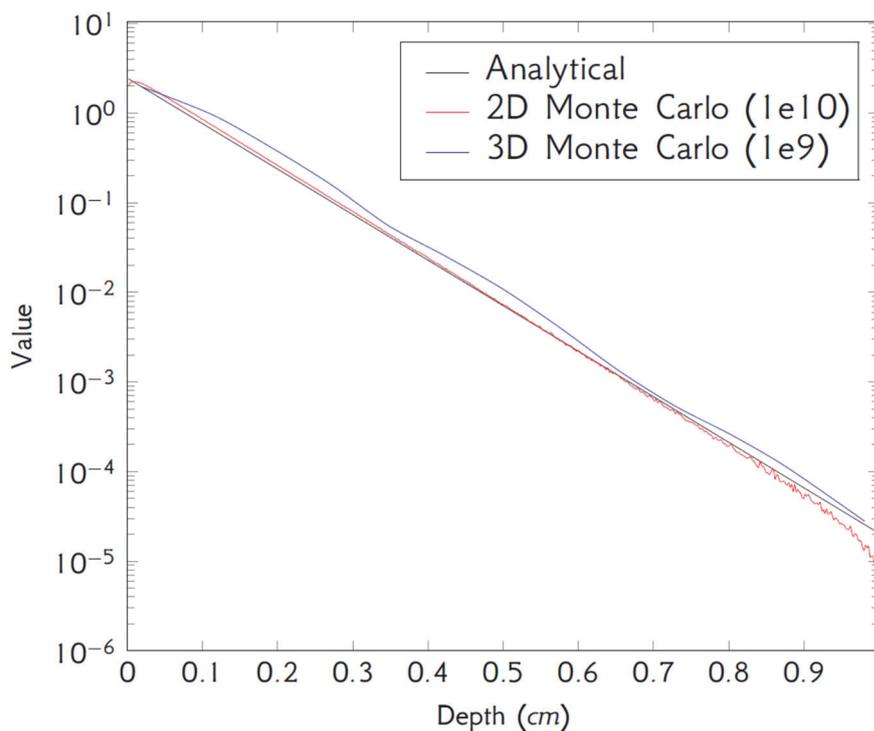
Figure 61: Graph to show 2D and 3D Monte Carlo against the analytical solution for g=0.8.

3. The target area was treated as a homogenous slab, whereas in reality it is more akin to a mesh of blood-vessels. The noted existence of a relationship between

light source, energy, HSP72i, vasoconstriction, and thermal energy is unlikely to be affected by this lack of realism.

4. Various important variables were kept constant, including haemoglobin concentration, blood oxygenation within the skin, pigmentation in the epidermis, size of the epidermis, cooling during or after pulse, thermal conductivity of tissue, heat capacity of tissue, pulse train profiles. Although this limitation does not invalidate the results presented here, it does show that there is scope for further research using the approach presented in this chapter.

5. Heating to a maximum of 100 °C was used as a threshold. The motivation for this threshold was that at that temperature there is a phase change for water (even though water vapour will form at lower temperatures as well). A phase change has dramatic effects on the optical and thermal parameters, draws energy from the system without an increase in temperature, can result in the formation of vacuoles, all of which was not accounted for in the used software. The 100 °C threshold is not an accurate representative of the occurrence of a phase change in the tissue, as the 100 °C is the resultant of heat increase in the capillaries which is diffused to the surrounding skin. At 100 °C for tissue, the temperature in the capillaries will have exceeded the temperature associated with the phase change.

6. The code allows for calibration using skin surface temperature data, which has been performed by Town (41). Unfortunately, this data was not available for psoriatic lesions, let alone when using the devices studied here. Therefore, I decided to use a standard value applicable to IPL treatments in healthy skin. As a consequence, we can compare the results between the devices, but the

absolute values should not be regarded as representative for real world situations.

These limitations could be addressed in future research. Other avenues which might be worth exploring include a comparison of 311 nm UVB induced HSP induction, the use of pre-treatment cooling to increase HSP induction depth, or the analysis of newer IPL devices and laser systems such as the 1064 nm Nd:YAG or its frequency doubled variant the 532 KTP.

4.8   Concluding remarks

I used computational analytical methods to study the production of HSP72i, thermal injury, and vasoconstriction in psoriatic lesions during and following treatment using 577 nm PDL, 585 nm PDL, 595 nm PDL, and IPL. In addition, I adjusted the geometry of the lesions in terms of blood oxygenation, blood volume content in target, and scattering of the epidermis.

All devices could produce HSP72i prior to the induction of thermal damage to the tissue. The devices differ in the depth at which they could induce HSP72i without heating the target area above 100 °C. The 577 nm PDL achieved the most superficial effects, followed by the IPL device and the 585 nm PDL devices. The differences between these devices are limited though. The 595 nm PDL could induce HSP72i all the way through the target tissue and showed the largest potential. In terms of induced heat shock protein for a given degree of severe damage to the tissue, the IPL showed the most favourable results, in particular for tissue with a higher blood content.

The 577 nm PDL is no longer used in dermatologic practice. The results presented here show that of all devices, the 577 nm PDL had the least favourable HSP72i induction profile. IPL devices have not been studied for psoriasis vulgaris, even though as a platform they have clear advantages over PDL systems. The fact that the applicator and device used in the calculations above showed results comparable to the 585 nm PDL in terms of induced effects, albeit at slightly less favourable safety profile and at higher energy levels, should encourage research into the broader application of these systems in standard dermatological practice. IPL systems can be equipped with multiple applicators, which generally have a much larger spot size. Consequently, fewer pulses

are required and a treatment can be completed within a shorter timeframe. This contributes to the economic efficiency of the therapy. The fact that generally a user of a laser or IPL system is more likely to be a beautician or paramedic than a MD illustrates the cost efficacy of such devices, and argues against the idea that laser therapy is expensive compared to alternative treatment modalities.

Changes in blood oxygenation resulted in a minor shift in required energy levels for a given level of heating. Increasing the blood volume in the target resulted in less penetration and lower required energy levels. An increase in the scattering of the epidermis had a detrimental effect on the efficacy of the devices.

As energy levels increased, a larger part of the target area exhibited vasoconstriction, suggesting that either laser Doppler blood flow measurements or colorimeter measurements can be used to rate the effect of laser therapy on the induction of HSP72i, although further research is required.

Future research can extend the approach applied in this study and validate its results either through calibration using real life patients or comparison with similar calculations in a three-dimensional Monte Carlo code.

5. Summary and Conclusions

The previous chapters have confirmed earlier results that computational analysis can be used to find clinically relevant relationships between tissue properties and light based technologies applied in dermatology. The results are consistent with the clinical experience noted in the literature and accrued through practical experience at a specialised independent treatment centre for dermatology. Thus, they add to the knowledge on the limitations on the techniques. The insights derived from the investigations can be directly translated to clinical practice. The outcome of the study allow for the formulation of testable hypotheses for the validation of the results with clinical data.

Chapter three investigated the detection of areas of the skin which, based on the emitted fluorescence, are suspected of containing keratinocyte skin cancers. Three methods of fluorescence detection have been analysed:

- Auto fluorescence detection, which is based on a difference in the measured fluorescence emitted by the endogenous fluorophores of the skin.

- PpIX fluorescence detection, which is based on a difference in the measured fluorescence emitted by PpIX. In tissue with a higher rate of metabolism, PpIX can be temporarily increased by the application of 5-ALA.

- Combined fluorescence detection, which uses both the PpIX fluorescence and auto fluorescence. The latter is used to normalize the signal from the first.

The contrast in fluorescence measured over the tumour bearing skin and measured of healthy control skin was used as a metric for the accuracy of the fluorescence detection techniques. The study was aimed at determining the effect of certain variations in the skin on the relative performance of the three methods. This was done by means of a parametric sweep: The value of the variable of interest was systematically increased or decreased in a number of calculations. The independent variables studied were scattering in the skin, melanin content in the epidermis, blood concentration in the target area, width, height and depth of the tumour, the concentration of PpIX in the tumour and the concentration of PpIX in the surrounding tissue. The computational

analysis produced some clear results, which seem to be in accordance with the results reported in the literature and known through clinical experience.

The fourth chapter was devoted to the treatment of psoriasis using pulsed dye laser or IPL therapy. Three different PDL systems and one IPL systems were compared in terms of their ability to induce certain biological effects: the induction of heat shock protein 72i, the creation of hyperthermal tissue damage, and causing vasoconstriction of the microvasculature. HSP72i induction was regarded as beneficial for the healing process, hyperthermic tissue damage was regard as being detrimental to the therapy, and vasoconstriction of the microvasculature was recorded as a potential clinical feedback mechanism.

Psoriatic lesions differ in terms of blood oxygenation, blood concentration and the presence of scales. Thus, each situation was presented by a separate geometry. In each geometry and for each device, a series of pulses was modelled. The applied energy was determined by the amount of energy that was required to induce heating up to 100 °C and that was required to induce some production of HSP72i in the skin, with four additional pulses linearly distributed between the two border conditions.

The investigations showed that all four systems are able to induce HSP72i, and that the depth at which HSP72i can be induced correlates with the amount of energy applied. Unfortunately, as the applied energy levels increased, so did the degree of hyperthermic damage, suggesting that some trade-off needs to be made in terms of optimal parameters. The different geometries resulted in different maximum and minimum energy levels. The 595 nm PDL was able to induce HSP72i at the deepest level, and 577 nm PDL resulted in the most superficial effect. The IPL and 585 nm PDL showed comparable results. Vasoconstriction correlated with the depth of effect.

The results from the study can be directly applied to clinical practice. Moreover, the calculations produced some falsifiable predictions which can be tested in future clinical research.

5.1 The position of computational analysis in medical research

I reiterate the plea of the first chapter that computational analysis of therapeutic interventions for skin conditions are to be preferred over clinical studies and animal studies. For the purpose of this argument, medical research is defined as a method to determine the equation of therapeutic and patient related independent variables such as type of skin condition, body weight, skin colour, used drug, applied schedule, etc. into the dependent outcome variables such as improvement of the health status of the patient, the occurrence of side effects, changes in the quality of life, etc. After the research is completed, the researcher can more accurately predict the probability of a set of outcomes given the set of patient and therapeutic characteristics. The claim then is built on the following observations and consideration:

- Clinical research is more resource intensive than computational analysis. Here a comparison can be made with the Monte Carlo method: All relevant properties, or potentially relevant properties of the patient and the treatment are being mapped into an outcome space. The probability distribution of this function is at the outset unknown. As more and more patients are treated, and the outcome of the treatment is being recorded, the relationship between the various independent variables and the dependent outcome variables becomes more and more obvious. At some point in time treating more patients will not change the shape of the probability function. The reader probably has noted that this process is not that different from what is happening when one performs a Monte Carlo simulation. Just as the Monte Carlo method demands relatively many computational resources, the clinical method requires relatively many patients. Recruiting, treating and following patients is no small feat. Note that just like the Monte Carlo method, clinical trials too can suffer from limited local convergence even if global convergence has been achieved.

- Another advantage of computational analysis compared to clinical research is the degree of freedom the researcher has in engineering and designing the problem. In clinical research the investigator can only analyse those combinations of variables which are present within the patient population. It may well be possible that even if one would treat all patients in the world, certain combinations of interest would not present themselves. In computational

analysis, any combination of variables can be studied irrespective of the degree of realism. And even if patients exist that show the desired combination of independent variables, the researcher must be able to actually recruit these patients.

- The liberty computational analysis gives to a researcher is not constrained to the formulation of the problem. One can investigate situations which without a doubt would be extremely harmful to the health of the patient, without ever hurting a sentient being. The risk profile for innovative applications and protocols therefore is especially encouraging. I have applied computational analysis for laser treatments and fluorescence detection. Complications in laser therapy include the formation of severe burn wounds which, if the laser therapy is applied over very large area of the skin, could even induce shock and sepsis. Fluorescence detection involves the detection of types of skin cancer which have the potential to spread throughout the body and cause mortality in the patient. So, the endeavour I have undertaken here, which included situations in which targets could not be detected, would have potentially caused the demise of at least one patient. Or, regarding laser therapy, would have resulted in one or more patients suffering from severe burn wounds which very well could have resulted in the formation of disfiguring and potentially painful permanent scars. It is not without reason that clinical research is subjected to prior ethical approval.

- If one further broadens one's perspective, and takes into account the application of computational analysis in the development and optimisation of pharmacological treatments, it becomes even more evident that at its core computational analysis as a method for medical research on the safety and efficacy of therapeutic interventions, all the accuracy and safety of diagnostic interventions, are to be preferred over the classical clinical prospective randomised double blind study. What would the world look like if we could accurately test all potential pharmaceutical compounds on all types of patients for all existing conditions without ever having to actually administer the drugs to a test subject?

Yet if computational analysis has significant advantages over clinical research, why is it that the latter still is the staple of medical scientific research? What limits the broader application of computational analysis compared to fields such as engineering? Although this goes beyond the scope of the study, one could suspect that this is related to what Welch, van Gemert and Star call the second task of tissue optics (11): that area of optics which is dedicated to the acquisition and collection of all relevant properties of tissue and biologic processes. This, the fundamental science, seems to have been overlooked. Data on topics such as the concentrations for all compounds present in the skin is not effortlessly accessible, and might be completely absent. If we do not know the structure, contents and behaviour of the skin, limits are imposed on the use of computational analysis.

 The treatment of the effects of HSP72i is an illustration of this: The underlying assumption of the use of the HSP72i metric is that these proteins start a chain of effects which contributes to the suppression of the immune system, e.g. by binding to a suitable receptor on the CD4+CD8+FOXP3+ T-cells (276,277), in combination with a restoration or repair of the perturbed cutaneous innervation (236,281). But the exact steps and their diffusion and rate equations have not been addressed explicitly. The hyperthermic tissue damage is even coarser, being based on changes in the epidermis and dermis following prolonged heating, without addressing things like apoptosis, protein denaturation or any of the other underlying effects explicitly.

5.2   Fluorescence detection of non-melanoma skin cancers

In chapter 3 the limits of fluorescence detection techniques have been explored. The combined fluorescence detection method reported a higher contrast in emitted fluorescence between healthy skin and tumour bearing skin that reported by the PpIX fluorescence detection method or the auto-fluorescence detection method in all but a few clinically less relevant situations. With increasing tumour vascularisation, there is some level of vascularisation at which auto-fluorescence will start to dominate the combined fluorescence detection method. At that point the level of contrast reported by the combined method is sufficient to warrant a closer inspection of the area, so that this effect does not have clinical implications. The same is not true for an increase in the fluorescence in the surrounding tissue. The auto-fluorescence detection method will dominate the combined fluorescence detection method at modest levels of enrichment,

and the combined method can reach lower levels of reported contrast which could result in a false negative. With regard to the hypotheses formulated in chapter one, our conclusion is that for most situations the statement would be true, except for cases of a very highly vascularised tumour and in situations in which the photosensitiser shows limited selectivity. In the latter case, there is a risk of a missed lesion: Fluorescence detection using the combined method should not be performed in situations where the operator notes elevated PpIX fluorescence in normal or control skin.

Hypothesis 1: The combined use of PpIX fluorescence and auto fluorescence in fluorescence detection of KSC results in a higher reported contrast in terms of fluorescence between healthy skin and skin containing a KSC than the contrast reported by PpIX fluorescence or auto fluorescence alone.

Conclusion 1: The combined method reported a higher contrast in terms of fluorescence for the tumour bearing skin than the control skin, although this is not true for all configurations.

Hypothesis 2: The higher reported contrast by the combined method of fluorescence detection is not affected by an increase in scattering in the skin.

Conclusion 2: The combined method reported a higher contrast in fluorescence measured over the tumour bearing skin than the other two methods. The effect of scattering on the reported contrast was small.

Hypothesis 3: The higher reported contrast by the combined method of fluorescence detection is not affected by an increase in epidermal melanin.

Conclusion 3: The increase in melanin generally had a negative impact on the reported contrast of all methods of fluorescence detection. For the range investigated the combined fluorescence detection method reported higher levels of contrast than the other two methods, but the trend was negative for all three methods. Fluorescence detection on people with skin of colour is contra-indicated.

Hypothesis 4: The higher reported contrast by the combined method of fluorescence detection is not affected by an increase in vascularisation of the KSC.

Conclusion 4: The combined method reported higher levels of contrast of the lower and mid ranges of vascularisation. The increase in vascularisation had a less pronounced effect on the contrast reported by the combined method than that reported by the PpIX fluorescence method and auto fluorescence method. The latter reported a higher contrast than that reported by the combined method by highly vascularized tumour bearing skin. The reported level of fluorescence was sufficient for clinical practice. The PpIX fluorescence method was very sensitive to an increase in vascularisation. It failed to report the presence of the tumour for clinically plausible levels of vascularisation, which is consistent with the results reported in the literature.

Hypothesis 5: The higher reported contrast by the combined method of fluorescence detection is not affected by a decrease in width of the KSC.

Conclusion 5: The combined method reported higher levels of contrast over the whole range of investigated target widths. All methods are sensitive to the width of the tumour: Very small tumours are associated with lower levels of reported contrast and could be missed during a detection procedure.

Hypothesis 6: The higher reported contrast by the combined method of fluorescence detection is not affected by a decrease in the thickness of the KSC.

Conclusion 6: The combined method reported higher levels of contrast over the whole range of investigated target lengths. Generally, there was in increase in reported contrast with increase in thickness for all three methods. There was a decrease in increase in reported contrast with increase in target thickness. For very thin targets, all three methods are likely to result in underreporting.

Hypothesis 7: The higher reported contrast by the combined method of fluorescence detection is not affected by the depth of the KSC.

Conclusion 7: The combined method reported higher levels of contrast over the whole range of target depths. Reported contrast was exponentially decreasing over target depth for all three methods. There exists a depth at which targets cannot be detected using fluorescence detection.

Hypothesis 8: The higher reported contrast by the combined method of fluorescence detection is not affected by a decrease in PpIX concentration in the KSC.

Conclusion 8: An increase in photosensitiser in the tumour results in an increase in the reported contrast by all three methods. The contrast reported by the combined method was higher than that reported by the PpIX fluorescence detection method and auto fluorescence detection method for the whole range of investigated photosensitiser concentrations. The combined method and auto-fluorescence method reported clinically relevant levels of contrast at lower concentrations of photosensitiser.

Hypothesis 9: The higher reported contrast by the combined method of fluorescence detection is not affected by an increase in PpIX concentration in the surrounding tissue.

Conclusion 9: The combined fluorescence detection method and the PpIX fluorescence detection method showed a quadratic decrease in reported contrast with an increase in photosensitiser concentration on surrounding tissue. The levels of contrast reported by these methods fell below clinically necessary levels of contrast, which would have resulted in undetected lesions. The auto fluorescence detection method was only slightly sensitive to the increase in photosensitiser in the surrounding tissue and reported higher levels of contrast exceeded that of the other two methods for higher levels of photosensitiser in skin.

The work described in this thesis hold some lessons for clinical practice. PpIX fluorescence detection is quite sensitive to some frequently observed variations in skin composition.

- Fluorescence detection is contra-indicated in patients with a Fitzpatrick skin type of three or more (41).
- Contrast in fluorescence is underreported for very narrow targets. Very small lesions showing even a marginally elevated level of fluorescence might deserve closer (dermatoscopic) inspection.
- Similarly, fluorescence contrast is underreported for very thin targets.

- Fluorescence detection based on PpIX, including the combined method, are quite sensitive to a low selectivity of the photosensitiser. In those situations, larger targets can still be detected using the auto fluorescence method, but the PpIX fluorescence and combined method fluorescence deserve scrutiny. Application of peelings or keratolytic agents is strongly contra-indicated.

- Lesions located deeper in the skin are more likely to be hidden from inspection. The use of fluorescence detection as a method to determine if a surgical procedure such as a shave or ablative laser therapy was successful is not recommended.

- Vascularisation negatively impacts PpIX fluorescence detection. Because large and aggressive KSC are associated with an increase in vasculature (127), the use of PpIX fluorescence detection rather than auto-fluorescence or the combined method is not recommended.

The relevance of the insights developed in this study are confirmed by a critical appraisal of a previous clinical trial on the use of PpIX fluorescence for the diagnosis of KSC. Kleinpenning and colleagues investigated the use of a PpIX fluorescence detection system for the diagnosis of KSC. That is, the lesions were already located using palpation and visual inspection, and the purpose of the investigation was to differentiate between benign lesions and malignant lesions, with the additional objective to differentiate the degree of progression of the lesion. The procedure consisted of the prior application of an ointment containing 5% or 10% salicylic acid. This reduces the size of the epidermis and increases the permeability of the skin for compounds such as 5-ALA. On the day of the investigation, a cream containing 20% 5-ALA was applied to the skin. This concentration is the same as that used in PDT, and can be regarded as sufficient to saturate the skin for more than 24 hours (311). Incubation time was set at three hours, following which PpIX fluorescence detection measurements were performed. The light source was a Xenon flashlamp combined with a pass filter over 370-440 nm and images were recorded using a 12 bit CCD sensor placed behind a 455 long pass filter. The researchers did apply a form of normalisation by using a fluorescence reference standard which was placed on the skin and correcting for shading using a previous measurement on a white sheet of paper. This approach was shown to be able to detect both invasive and superficial variants of SCC. The researchers ascribed the noted

variation in the fluorescence to epidermal thickness, i.e. in situations in which the target was located further from the surface. (104)

Note that the application of the 20% 5-ALA in a cream is likely to result in a more pronounced increase in PpIX concentration in the surrounding skin, which would be exacerbated by the use of the salicylic acid. Even though some normalization techniques were applied, these would not resolve the PpIX in dermis issue. Moreover, the progression of an actinic keratosis into an invasive squamous cell carcinoma would have been accompanied by an increase in vascularisation. These effects have not been observed in the study by Kleinpenning et al. So even though Kleinpenning did conclude that fluorescence diagnosis with ALA-induced porphyrins (FDAP) could be used to distinguish those KSC which have a higher propensity to progress into an invasive state, their results could have been further improved with vascularisation and PpIX in dermis had been taken into account, as well as the application of the combined method rather than the PpIX fluorescence detection method.

5.3 Laser and IPL therapy for psoriasis

The fourth chapter is dedicated to the investigation of a novel explanation for the method of action of laser therapy in psoriasis. Rather than focusing on the direct effect of laser therapy on the blood vessels, three separate effects are being studied: the induction of HSP72i, the creation of hyperthermic tissue damage, and the presence of vasoconstriction of the microvasculature. The first represents the beneficial effect of laser therapy on psoriasis. Although the diffusion of heat shock proteins and the rate coefficients describing the restorative and immunosuppressive effects are not explicitly dealt with, it does inform us about the geometric distribution of the effect. The second measure, hyperthermic tissue damage, represents the harmful effect of laser therapy on psoriasis and can be seen as a surrogate for the Koebner phenomenon. The third measure, vasoconstriction, informs us about the potential of a clinical feedback which can be used in practice to assess the size of the effect that has been induced.

Hypothesis 10: PDL and IPL therapy can induce HSP72i, vasoconstriction, and/or thermal injury in separate areas of the psoriatic skin.

Conclusion 10: All systems are indeed capable of inducing HSP72i, inducing hyperthermic tissue damage and evoking a further constructive response in the tissue.

Hypothesis 11: The ability of PDL or IPL therapy to induce HSP72i, vasoconstriction, and/or thermal injury in psoriatic skin is affected by differences in blood oxygenation.

Hypothesis 12: The ability of PDL or IPL therapy to induce HSP72i, vasoconstriction, and/or thermal injury in psoriatic skin is affected by differences in blood concentration.

Hypothesis 13: The ability of PDL or IPL therapy to induce HSP72i, vasoconstriction, and/or thermal injury in psoriatic skin is affected by differences in light scattering in the epidermis.

Conclusion 11 – 13: the studied variations did affect the maximum depth at which a certain effect could be evoked, but the size of the difference was rather modest compared to the differences between the devices. In contradiction, the required amount of energy for a given level of heating differed notably among the various studied configurations. The result that a similar effect of laser therapy can be achieved for a range of configurations, but that the appropriate energy level will vary significantly had not been initially expected. Laser therapy can be successfully applied in a wide range of lesions, but the operator needs to be aware of the relationship between the appropriate energy levels and the presentation of the lesion.

The results presented in chapter four support the notion that laser therapy in psoriasis involves a balancing act between the beneficial, anti-inflammatory, effects and the detrimental, pro-inflammatory, effects. The actual (inter)actions and involved in these two effects are likely to be more complex of nature than is shown by the simple model used here. Nonetheless, the relationship between optimal fluence and lesion composition is likely to hold. The relationship between difference in depth of effect that can be achieved and the used device is likely to hold in more accurate models or clinical investigations.

The investigations included one particular IPL, or better said, applicator. The reader should be aware that there is a large variation in IPL devices and applicators, and the results described here do not necessarily carry over to other systems: Additional analyses are required in order to establish the comparative behaviour of different devices. Unfortunately, information about the shape of the spectral profile of IPLs is scarce. An industry standard completely describing the shape of the curve, e.g. through

a Fourier transformation, would be welcome. Until that time, operators and patients are exposed to an unnecessary risk.

Other inflammatory conditions, such as acne, eczema / atopic dermatitis and rosacea, are also known to respond to PDL therapy (25,144,270,298). Since these conditions also show signs of a neuro-inflammatory foundation, it is possible that here too the actual healing effect is due to the induction of HSP72i, rather than a direct physical effect on the blood vessels (312).

The results from the 595 nm PDL and its response to a change in oxygenation and to an increase in blood concentration deserve separate mention. As Dwyer et al showed, there is considerable variation in blood oxygenation in a psoriatic lesion (246). Similarly, Hendriks et al showed considerable differences in blood concentration in the centre of the lesion and the periphery (184,265). This suggests that optimal settings for the 595 nm PDL are likely to differ in the centre and the periphery. Current protocols do not take this circumstance into account.

I modelled the situation in which the blood volume content of psoriatic skin was further elevated. That geometry resulted in a considerable decrease in the required energy levels. This improves the safety profile, although it did decrease the maximum depth at which an effect could be evoked. Blood concentration in the papillary dermis is not a given. Physicians can and regularly do employ techniques to increase blood flow, e.g. in patients suffering from rosacea. This can be achieved by the application of warm air or methods of thermal diffusion into the skin using conduction. The use of topical agents such as niacin has been described in the literature as well (247). Pre-treatment manipulation or engineering of tissue thus could potentially improve the efficacy and safety of laser therapy for inflammatory conditions. In situations in which there is significant heating of the surrounding tissue, such as in the IPL case, this technique might be beneficial. Another situation in which a decrease in energy would be preferred even if it implies a slight loss of depth effect is the treatment of patients with skin of colour.

The vasoconstriction results show that depth of effect correlates with the achieved vasoconstriction. This too allows us to improve the treatment, since measurements using either laser Doppler flowmetry or colourimetry, would give a more accurate and

reproducible indicator of relative change following treatment. Under- or overtreatment could be established immediately, rather than four or eight weeks after the treatment.

5.4   Contribution to knowledge

The contributions to knowledge of the presented research are as follows:

- It is the first use of a computational model for the simulation of fluorescence detection or laser therapy for psoriasis using biological values for haemoglobin, PpIX and Flavin as input variables.

- It is the first computational study on fluorescence detection of KSC using low concentration 5-ALA induced PpIX and the DyaDerm Expert fluorescence detection system, and in particular the effect of

  o Melanin concentration in the epidermis

  o Blood concentration in the target

  o Scattering of light in the skin

  o Tumour width

  o Tumour thickness

  o Tumour depth

  o PpIX concentration in the tumour

  o PpIX concentration in the surrounding dermis

  on the contrast in fluorescence over the target and the unaffected skin reported by the PpIX fluorescence detection method, the auto fluorescence detection method and the combined fluorescence detection method.

- It is the first computational study on the treatment of psoriasis using laser or IPL therapy.

- It is the first study to build on the notion that the effect of laser and IPL on psoriasis is driven by the induction of an anti-inflammatory or pro-inflammatory response to a range of pulses inducing various levels of sub-lethal thermal injury.

- It is the first to study the distribution of the anti-inflammatory and pro-inflammatory effects of 577 nm PDL, 585 nm PDL, 595 nm PDL, and IPL therapy in psoriasis.

- It is the first to study the effect of changes in blood oxygenation, blood concentration in the lesion and scattering of light in the epidermis on the

distribution of anti-inflammatory and pro-inflammatory effects of said laser devices and IPL.

- The first to study the distribution of vasoconstriction in the psoriatic lesion following the application of sub-lethal pulses using the studied laser and IPL devices.

Furthermore, I have contributed to the further extension of the capabilities of the used software package in terms of the simulation of fluorescence and, through a large number of preliminary experiments and validation of those results against clinical and published data, participated in verification of the code.

5.5   Avenues for further research

As noted above, the results of this work can be directly translated to recommendations for clinical practice. As a result, we can formulate new questions that can be addressed in clinical research. Additionally, other treatments could benefit from computational analysis aimed at certain questions that have emerged from clinical practice.

In terms of validation of the results of the analysis, it would be interesting to compare the induction of HSP72i following the application of two of the studied systems. The relevant parameters can be measured using laser Doppler flowmetry, colourimetry, heat diffusion during laser treatment would be measured using a high-speed thermal imaging camera, and the size of the epidermis, HSP72i induction and size of the papillary dermis can be established by subsequent histo-pathological analysis. The results of that investigation would be fed back into the model, further increasing its accuracy.

The analysis of fluorescence detection can be extended to different light sources such as broad-band UV lamps, different photosensitisers, the registration of fluorescence lifetime instead of the current steady state analysis, and measurement during PDT. The latter has been studied by Valentine et al. (48), but potentially these results could be improved upon by recalculating the energy distribution during PDT as to account for the change in the optical parameters. The application of a UV-A light source such as Wood's lamp would result in a different distribution of the absorbed photons, since the absorption and scattering coefficients for the different chromophores in the skin differs significantly. The molar absorption coefficient for oxy-haemoglobin is 88484 $cm^{-1}M^{-1}$ for 366 nm and 466840 $cm^{-1}M^{-1}$ for 410 nm, which implies that much less energy is lost to

blood for that particular UV-A wavelength compared to the analysed light source. A similar change in the penetration of light into the tissue

The laser therapy studies can be extended to different IPL applicators or lasers such as the Nd:YAG, as well as larger surface areas or pulse profiles. The applicator used in this study has a cross section of 10 mm, which is quite rare for IPL devices. Commonly they have rectangular applicators with dimensions in the range of 50 mm x 10 mm. This is likely to influence the thermal diffusion stage of the analysis.

An approach which has been used in the optimization of laser therapy for Port Wine Stains is index matching, e.g. by the topical application of glycerol. In the current model there was a difference in the index of refraction for the epidermis and the dermis. An extension of the current investigation thus could include changes in the index of refraction.

Finally the analysis might be improved by the use of more granular representations of the tissue than used in this analysis, such as performed by Pfefer et al. (50). The effect of a laser pulse on a blood vessel depends, amongst others, on the size of the blood vessel. Such details have not been taken into account in the sandwich model used here. New imaging techniques such as Raster Scan Optoacoustic Mesoscopy could offer interesting possibilities, as it is capable of not only determining the size and location of the blood vessels, but also can measure the blood oxygenation.

6. References

1.   Stokes GG. On the change of refrangibility of light. Philos Trans R Soc London. 1852;142:463–562.

2.   de Leeuw J, van der Beek N, Neugebauer WD, Bjerring P, Neumann HAM. Fluorescence detection and diagnosis of non-melanoma skin cancer at an early stage. Lasers Surg Med. 2009 Feb;41(2):96–103.

3.   Ostertag JU, Quaedvlieg PJF, van der Geer S, Nelemans P, Christianen MEMC, Neumann MHAM, et al. A clinical comparison and long-term follow-up of topical 5-fluorouracil versus laser resurfacing in the treatment of widespread actinic keratoses. Lasers Surg Med. 2006 Sep;38(8):731–9.

4.   Pomerantz H, Hogan D, Eilers D, Swetter SM, Chen SC, Jacob SE, et al. Long-term Efficacy of Topical Fluorouracil Cream, 5%, for Treating Actinic Keratosis: A Randomized Clinical Trial. JAMA dermatology. 2015 May 7;

5.   Koo J, Lebwohl M. Duration of remission of psoriasis therapies. J Am Acad Dermatol. 1999 Jul;41(1):51–9.

6.   Taibjee SM, Cheung S-T, Laube S, Lanigan SW. Controlled study of excimer and pulsed dye lasers in the treatment of psoriasis. Br J Dermatol. 2005 Nov;153(5):960–6.

7.   Hirshleifer J, Riley J. The analytics of uncertainty and information. Journal of Economic Literature. Cambridge University Press; 1992.

8.   Stern RS, Laird N. The carcinogenic risk of treatments for severe psoriasis. Photochemotherapy Follow-up Study. Cancer. 1994 Jun;73(11):2759–64.

9.   Schmitt J, Rosumeck S, Thomaschewski G, Sporbeck B, Haufe E, Nast A. Efficacy and safety of systemic treatments for moderate-to-severe psoriasis: meta-analysis of randomized controlled trials. Br J Dermatol. 2014 Feb;170(2):274–303.

10.   Kaplow L, Shavell S. Fairness versus Welfare. Harvard University Press; 2009. 576 p.

11. Welch AJ, Van Gemert MJC, Star WM. Definitions and Overview of Tissue Optics. In: Welch AJ, Van Gemert MJC, editors. Optical-Thermal Response of Laser-Irradiated Tissue. 2nd ed. Springer Science & Business Media; 2011. p. 27–64.

12. McGrath JA, Uitto J. Anatomy and Organization of Human Skin. In: Rook's Textbook of Dermatology. Wiley-Blackwell; 2010. p. 1–53.

13. Brand D, Ackerman AB. Squamous cell carcinoma, not basal cell carcinoma, is the most common cancer in humans. J Am Acad Dermatol. 2000 Mar;42(3):523–6.

14. Ackerman AB, Mones JM. Solar (actinic) keratosis is squamous cell carcinoma. Br J Dermatol. 2006 Jul;155(1):9–22.

15. Diepgen TL, Mahler V. The epidemiology of skin cancer. Br J Dermatol. 2002;146(s61):1–6.

16. Weinberg AS, Ogle CA, Shim EK. Metastatic cutaneous squamous cell carcinoma: an update. Dermatologic Surg. 2007;33(8):885–99.

17. van der Leest R. Multiple Cutaneous (pre)-Malignancies. 2015;

18. Yokouchi M, Atsugi T, Logtestijn M van, Tanaka RJ, Kajimura M, Suematsu M, et al. Epidermal cell turnover across tight junctions based on Kelvin's tetrakaidecahedron cell shape. Horsley V, editor. Elife. 2016;5:e19593.

19. Jacques SL. Melanosome absorption coefficient [Internet]. 1998 [cited 2016 Dec 20]. Available from: http://omlc.org/spectra/melanin/mua.html

20. Prahl S. Optical Absorption of Hemoglobin [Internet]. 1999. Available from: http://omlc.org/spectra/hemoglobin/

21. Salomatina E, Jiang B, Novak J, Yaroslavsky AN. Optical properties of normal and cancerous human skin in the visible and near-infrared spectral range. J Biomed Opt. Jan;11(6):64026.

22. Neumann HAM. Relevance of fluorescence techniques in immunological mediated skin disease. Universiteit van Amsterdam; 1983.

23. Rai R, Natarajan K. Laser and light based treatments of acne. Indian J Dermatol Venereol Leprol. 2013 Jan;79(3):300–9.

24. Zelickson BD, Mehregan DA, Wendelschfer-Crabb G, Ruppman D, Cook A, O'Connell P, et al. Clinical and histologic evaluation of psoriatic plaques treated with a flashlamp pulsed dye laser. J Am Acad Dermatol. 1996 Jul;35(1):64–8.

25. Syed S, Weibel L, Kennedy H, Harper JI. A pilot study showing pulsed-dye laser treatment improves localized areas of chronic atopic dermatitis. Clin Exp Dermatol. 2008 May;33(3):243–8.

26. Ostertag JU, Quaedvlieg PJF, Neumann MHAM, Krekels GA. Recurrence rates and long-term follow-up after laser resurfacing as a treatment for widespread actinic keratoses on the face and scalp. Dermatol Surg. 2006 Feb;32(2):261–7.

27. Hongcharu W, Taylor CR, Chang Y, Aghassi D, Suthamjariya K, Anderson RR. Topical ALA-photodynamic therapy for the treatment of acne vulgaris. J Invest Dermatol. 2000 Aug;115(2):183–92.

28. Gilmour JW, Vestey JP, George S, Norval M. Effect of phototherapy and urocanic acid isomers on natural killer cell function. J Invest Dermatol. 1993 Aug;101(2):169–74.

29. Nijssen A, Maquelin K, Santos LF, Caspers PJ, Bakker Schut TC, den Hollander JC, et al. Discriminating basal cell carcinoma from perilesional skin using high wave-number Raman spectroscopy. J Biomed Opt. 2007 Jan;12(3):34004.

30. Henyey LG, Greenstein JL. Diffuse radiation in the galaxy. Astrophys J. 1941;93:70–83.

31. Van Gemert MJC, Jacques SL, Sterenborg H, Star WM. Skin optics. IEEE Trans Biomed Eng. 1989;36(12):1146–54.

32. Welch AJ, Van Gemert MJC, editors. Optical-Thermal Response of Laser-Irradiated Tissue. 2nd ed. Springer Science & Business Media; 2011. 972 p.

33. Lemaire J. Bonus-malus systems in automobile insurance. Vol. 19. Springer science & business media; 2012.

34. von Neumann J, Morgenstern O. The Theory of Games and Economic Behavior. 1947;

35. Star WM. Diffusion Theory of Light Transport. In: Welch AJ, van Gemert MJC, editors. Optical-Thermal Response of Laser-Irradiated Tissue. Dordrecht: Springer Netherlands; 2011. p. 145–201.

36. Donne KE, Marotin A, Al-Hussany A. Dual Reciprocity Boundary Element Modelling of Collimated Light Fluence Distribution in Normal and Cancerous Prostate Tissue during Photodynamic Therapy. WIT Trans Biomed Heal. 2013;17.

37. Daniel G, Donne K, Song L. Computer Modelling of Photodynamic Therapy. In: IPEM Annual Scientific meeting. York; 2004.

38. Kiernan MN. An analysis of the optimal laser parameters necessary for the treatments of vascular lesions. 1997.

39. Daniel G. Optical and thermal transport modelling of laser-tissue interaction. 2002.

40. Liew YS. An Investigation into Embedded Photodynamic Therapy. Swansea, Wales, UK.; 2005. 187 p.

41. Town G. Quality Assurance in the Democratisation of Light-Based Therapies. PhD thesis. Swansea, Wales, UK.: University of Wales Trinity Saint David; 2014.

42. Wilson BC, Adam G. A Monte Carlo model for the absorption and flux distributions of light in tissue. Med Phys. 1983 Jan;10(6):824–30.

43. Keijzer M, Pickering JW, van Gemert MJ. Laser beam diameter for port wine stain treatment. Lasers Surg Med. 1991;11(6):601–5.

44. Jacques SL. Skin optics [Internet]. 1998. Available from: http://omlc.org/news/jan98/skinoptics.html

45. Morse PM, Feshbach H. Methods of theoretical physics. New York: McGraw-Hill; 1953.

46. Bashford T. Parallelisation techniques for the numerical solution of radiative and

thermal transport in tissue photonics. PhD thesis. University of Wales Trinity Saint David; 2016.

47.   Tyrrell J, Campbell S, Curnow A. Protoporphyrin IX photobleaching during the light irradiation phase of standard dermatological methyl-aminolevulinate photodynamic therapy. Photodiagnosis Photodyn Ther. 2010;7(4):232–8.

48.   Valentine RM, Ibbotson SH, Wood K, Brown CTA, Moseley H. Modelling fluorescence in clinical photodynamic therapy. Photochem Photobiol Sci. 2013 Jan;12(1):203–13.

49.   Liu B, Farrell TJ, Patterson MS. Comparison of noninvasive photodynamic therapy dosimetry methods using a dynamic model of ALA-PDT of human skin. Phys Med Biol. 2012;57(3):825.

50.   Pfefer TJ, Barton JK, Smithies DJ, Milner TE, Nelson JS, van Gemert MJ, et al. Modeling laser treatment of port wine stains with a computer-reconstructed biopsy. Lasers Surg Med. 1999 Jan;24(2):151–66.

51.   Schwarz M, Buehler A, Aguirre J, Ntziachristos V. Three-dimensional multispectral optoacoustic mesoscopy reveals melanin and blood oxygenation in human skin in vivo. J Biophotonics. 2015 Nov 4;

52.   Pennes HH. Analysis of Tissue and Arterial Blood Temperatures in the Resting Human Forearm. J Appl Physiol. 1948;1(2):93–122.

53.   Diller KR. Laser Generated Heat Transfer. In: Welch AJ, van Gemert MJC, editors. Optical-Thermal Response of Laser-Irradiated Tissue. 2nd ed. Springer; 2011. p. 353–97.

54.   Thomsen S, Pearce JA. Thermal Damage and Rate Processes in Biologic Tissues BT - Optical-Thermal Response of Laser-Irradiated Tissue. In: Welch AJ, van Gemert MJC, editors. Dordrecht: Springer Netherlands; 2011. p. 487–549.

55.   Henriques FC, Moritz AR. Studies of Thermal Injury: I. The Conduction of Heat to and through Skin and the Temperatures Attained Therein. A Theoretical and an Experimental Investigation. Am J Pathol. 1947 Jul;23(4):530–49.

56. Moritz AR, Henriques FC. Studies of Thermal Injury: II. The Relative Importance of Time and Surface Temperature in the Causation of Cutaneous Burns. Am J Pathol. 1947 Sep;23(5):695–720.

57. Moritz AR. Studies of Thermal Injury: III. The Pathology and Pathogenesis of Cutaneous Burns. An Experimental Study. Am J Pathol. 1947 Nov;23(6):915–41.

58. Hulmani M, Kudur M. Misnomers in dermatology: time to change and update. Indian J Dermatol Venereol Leprol. 2013 Jan;79(4):479–91.

59. Ruocco V, Ruocco E, Brunetti G, Schwartz RA. Non-melanoma skin cancer: an overindulged circumlocution articulating keratinocytic cancer. Int J Dermatol. 2014 Mar;53(3):e228-9.

60. Flohil SC, de Vries E, Neumann HAM, Coebergh J-WW, Nijsten T. Incidence, prevalence and future trends of primary basal cell carcinoma in the Netherlands. Acta Derm Venereol. 2011 Jan;91(1):24–30.

61. Flohil SC, van der Leest RJT, Dowlatshahi EA, Hofman A, de Vries E, Nijsten T. Prevalence of actinic keratosis and its risk factors in the general population: the Rotterdam Study. J Invest Dermatol. 2013 Aug;133(8):1971–8.

62. Flohil SC, Seubring I, van Rossum MM, Coebergh J-WW, de Vries E, Nijsten T. Trends in Basal cell carcinoma incidence rates: a 37-year Dutch observational study. J Invest Dermatol. 2013 Apr;133(4):913–8.

63. Memon AA, Tomenson JA, Bothwell J, Friedmann PS. Prevalence of solar damage and actinic keratosis in a Merseyside population. Br J Dermatol. 2000 Jun;142(6):1154–9.

64. Roberts DL. Incidence of non-melanoma skin cancer in West Glamorgan, South Wales. Br J Dermatol. 1990 Mar;122(3):399–403.

65. Asgari MM, Moffet HH, Ray GT, Quesenberry CP. Trends in Basal Cell Carcinoma Incidence and Identification of High-Risk Subgroups, 1998-2012. JAMA dermatology. 2015 Sep;151(9):976–81.

66. Rogers HW, Weinstock MA, Feldman SR, Coldiron BM. Incidence Estimate of

Nonmelanoma Skin Cancer (Keratinocyte Carcinomas) in the U.S. Population, 2012. JAMA dermatology. 2015 Oct;151(10):1081–6.

67.   Nouri K. Skin cancer. McGraw-Hill Professional; 2007.

68.   Kessels J, Hendriks J, Nelemans P, Mosterd K, Kelleners-Smeets N. Two-fold illumination in topical 5-aminolevulinic acid (ALA)-mediated photodynamic therapy (PDT) for superficial basal cell carcinoma (sBCC): A retrospective case series and cohort study. J Am Acad Dermatol. 2016 May;74(5):899–906.

69.   Wehner MR, Linos E, Parvataneni R, Stuart SE, Boscardin WJ, Chren M-M. Timing of Subsequent New Tumors in Patients Who Present With Basal Cell Carcinoma or Cutaneous Squamous Cell Carcinoma. JAMA dermatology. 2015 Jan 14;

70.   Vatve M, Ortonne J-P, Birch-Machin MA, Gupta G. Management of field change in actinic keratosis. Br J Dermatol. 2007 Dec;157 Suppl:21–4.

71.   Morton CA, Szeimies R-M, Sidoroff A, Braathen LR. European guidelines for topical photodynamic therapy part 2: emerging indications--field cancerization, photorejuvenation and inflammatory/infective dermatoses. J Eur Acad Dermatol Venereol. 2013 Jun;27(6):672–9.

72.   Prens SP, de Vries K, Neumann HAM, Prens EP. Non-ablative fractional resurfacing in combination with topical tretinoin cream as a field treatment modality for multiple actinic keratosis: a pilot study and a review of other field treatment modalities. J Dermatolog Treat. 2013 Jun;24(3):227–31.

73.   Gilaberte Y. The lesion, or the field, that is the question. Br J Dermatol. 2016 Oct;175(4):668–9.

74.   Stockfleth E. The paradigm shift in treating actinic keratosis: a comprehensive strategy. J Drugs Dermatol. 2012 Dec;11(12):1462–7.

75.   Togsverd-Bo K, Haak CS, Thaysen-Petersen D, Wulf HC, Anderson RR, Hædersdal M, et al. Intensified photodynamic therapy of actinic keratoses with fractional CO2 laser: a randomized clinical trial. Br J Dermatol. 2012;166(6):1262–9.

76.   Wiegell SR, Fabricius S, Gniadecka M, Stender IM, Berne B, Kroon S, et al.

Daylight-mediated photodynamic therapy of moderate to thick actinic keratoses of the face and scalp: a randomized multicentre study. Br J Dermatol. 2012 Jun;166(6):1327–32.

77.   de Vries K, Prens EP. Laser treatment and its implications for photodamaged skin and actinic keratosis. Curr Probl Dermatol. 2015 Jan;46:129–35.

78.   Togsverd-Bo K, Lei U, Erlendsson AM, Taudorf EH, Philipsen PA, Wulf HC, et al. Combination of ablative fractional laser and daylight-mediated photodynamic therapy for actinic keratosis in organ transplant recipients - a randomized controlled trial. Br J Dermatol. 2015 Mar;172(2):467–74.

79.   Joseph AK, Mark TL, Mueller C. The period prevalence and costs of treating nonmelanoma skin cancers in patients over 65 years of age covered by medicare. Dermatol Surg. 2001 Nov;27(11):955–9.

80.   John Chen G, Yelverton CB, Polisetty SS, Housman TS, Williford PM, Teuschler H V, et al. Treatment patterns and cost of nonmelanoma skin cancer management. Dermatol Surg. 2006 Oct;32(10):1266–71.

81.   van der Geer S, Reijers HA, van Tuijl HFJM, de Vries H, Krekels GAM. Need for a new skin cancer management strategy. Arch Dermatol. 2010 Mar;146(3):332–6.

82.   Chirikov V V, Stuart B, Zuckerman IH, Christy MR. Physician specialty cost differences of treating nonmelanoma skin cancer. Ann Plast Surg. 2015 Jan;74(1):93–9.

83.   Raab O. Ueber die Wirkung fluorescirender Stoffe auf Infusorien. 1900.

84.   Von Tappeiner H, Jodlbauer A. Uber die wirkung der photodynamischen (fluorescierenden) stoffe auf protozoen und enzyme. Dtsch Arch Klin Med. 1904;80:427–87.

85.   Stübel H. Die fluoreszenz tierischer gewebe in ultraviolettem licht. Pflügers Arch Eur J Physiol. 1911;142(1):1–14.

86.   Meyer-Betz F. Untersuchungen über die biologische (photodynamische) Wirkung des Hämatoporphyrins und anderer Derivate des Blut-und

Gallenfarbstoffs. Dtsch Arch Klin Med. 1913;112:476–503.

87.   Policard A. Etude sur les aspects offerts par des tumeurs experimentales examinees a la lumiere de Wood. CR Soc Biol. 1924;91:1423–4.

88.   Auler H, Banzer G. Untersuchungen über die Rolle der Porphyrine bei geschwulstkranken Menschen und Tieren. Z Krebsforsch. 1942 Mar;53(2):65–8.

89.   Figge FHJ, Weiland GS, Manganiello LOJ. Cancer detection and therapy. Affinity of neoplastic, embryonic, and traumatized tissues for porphyrins and metalloporphyrins. Exp Biol Med. 1948;68(3):640–1.

90.   Profio AE, Doiron DR. A feasibility study of the use of fluorescence bronchoscopy for localization of small lung tumours. Phys Med Biol. 1977;22(5):949.

91.   Von Tappeiner H, Jesionek A. Therapeutische versuche mit fluoreszierenden stoffen. Münch Med Wochenschr. 1903;47:2042–4.

92.   Kennedy JC, Pottier RH, Pross DC. Photodynamic therapy with endogenous protoporphyrin IX: basic principles and present clinical experience. J Photochem Photobiol B. 1990 Jun;6(1–2):143–8.

93.   Scott JJ. The metabolism of a-aminolevulinic acid. In: Ciba Foundation Symposium on Porphyrin Biosynthesis and Metabolism GEW Wolstenholme and ECP Millar, editors J & G Churchill Ltd, London. 1955.

94.   Jarret A, Rimington C, Willoughby DA. Delta-Aminolaevulic acid and porphyria. Lancet (London, England). 1956 Jan;270(6908):125–7.

95.   Berlin NI, Neuberger A, Scott JJ. The metabolism of δ-aminolaevulic acid. 1. Normal pathways, studied with the aid of 15N. Biochem J. 1956;64(1):80.

96.   Dailey HA, Smith A. Differential interaction of porphyrins used in photoradiation therapy with ferrochelatase. Biochem J. 1984;223(2):441–5.

97.   Wilson BC, Patterson MS, Burns DM. Effect of photosensitizer concentration in tissue on the penetration depth of photoactivating light. Lasers Med Sci. 1986;1(4):235–44.

98.   van der Putten WJM, van Gemert MJC. A modelling approach to the detection of subcutaneous tumours by haematoporphyrin-derivative fluorescence. Phys Med Biol. 1983 Jun;28(6):639–45.

99.   af Klinteberg C, Nilsson AM, Wang-Nordman I, Andersson-Engels S, Svanberg S, Svanberg K. Laser-induced fluorescence diagnostics of basal cell carcinomas of the skin following topical ALA application. In: BiOS Europe'96. International Society for Optics and Photonics; 1996. p. 32–40.

100.   Andersson-Engels S, Berg R, Svanberg K, Svanberg S. Multi-colour fluorescence imaging in connection with photodynamic therapy of delta-amino levulinic acid (ALA) sensitised skin malignancies. Bioimaging. 1995;3(3):134–43.

101.   Andersson-Engels S, Johansson J, Svanberg S. Medical diagnostic system based on simultaneous multispectral fluorescence imaging. Appl Opt. 1994;33(34):8022–9.

102.   Sterenborg H, Motamedi M, Wagner Jr RF, Duvic M, Thomsen S, Jacques SL. In vivo fluorescence spectroscopy and imaging of human skin tumours. Lasers Med Sci. 1994;9(3):191–201.

103.   Andersson-Engels S, Canti G, Cubeddu R, Eker C, af Klinteberg C, Pifferi A, et al. Preliminary evaluation of two fluorescence imaging methods for the detection and the delineation of basal cell carcinomas of the skin. Lasers Surg Med. 2000;26(1):76–82.

104.   Kleinpenning MM, Wolberink EW, Smits T, Blokx WAM, Van De Kerkhof PCM, Van Erp PEJ, et al. Fluorescence diagnosis in actinic keratosis and squamous cell carcinoma. Photodermatol Photoimmunol Photomed. 2010 Dec 23;26(6):297–302.

105.   Smits T, van Laarhoven AIM, Staassen A, van de Kerkhof PCM, van Erp PEJ, Gerritsen M-JP. Induction of protoporphyrin IX by aminolaevulinic acid in actinic keratosis, psoriasis and normal skin: preferential porphyrin enrichment in differentiated cells. Br J Dermatol. 2009 Apr;160(4):849–57.

106.   Kleinpenning MM, Kanis JH, Smits T, van Erp PEJ, van de Kerkhof P, Gerritsen

RMJP. The effects of keratolytic pretreatment prior to fluorescence diagnosis and photodynamic therapy with aminolevulinic acid-induced porphyrins in psoriasis. J Dermatolog Treat. 2010 Jul;21(4):245–51.

107.	Smits T, Robles CA, van Erp PE, van de Kerkhof PC, Gerritsen M-JP. Correlation Between Macroscopic Fluorescence and Protoporphyrin IX Content in Psoriasis and Actinic Keratosis Following Application of Aminolevulinic Acid. J Invest Dermatol. 2005 Oct;125(4):833–9.

108.	Kleinpenning MM, Smits T, Ewalds E, van Erp PEJ, van de Kerkhof PCM, Gerritsen MJP. Heterogeneity of fluorescence in psoriasis after application of 5-aminolaevulinic acid: an immunohistochemical study. Br J Dermatol. 2006 Sep;155(3):539–45.

109.	van der Beek N, de Leeuw J, Demmendal C, Bjerring P, Neumann HAM. PpIX fluorescence combined with auto-fluorescence is more accurate than PpIX fluorescence alone in fluorescence detection of non-melanoma skin cancer: an intra-patient direct comparison study. Lasers Surg Med. 2012 Apr;44(4):271–6.

110.	Ackerman G. Photophysikalische Grundlagen zur Fluoreszensdiagnostiek von Tumoren der Haut. Regensburg; 2001. 190 p.

111.	Na R, Stender I-M, Wulf HC. Can autofluorescence demarcate basal cell carcinoma from normal skin? A comparison with protoporphyrin IX fluorescence. Acta Derm Venereol. 2001;81(4):246–9.

112.	Brancaleon L, Durkin AJ, Tu JH, Menaker G, Fallon JD, Kollias N. In vivo fluorescence spectroscopy of nonmelanoma skin cancer. Photochem Photobiol. 2001;73(2):178–83.

113.	Lycette R, Leslie R. Fluorescence of malignant tissue. Lancet. 1965;286(7409):436.

114.	Wagnieres GA, Star WM, Wilson BC, Wagnières GA, Star WM, Wilson BC. In vivo fluorescence spectroscopy and imaging for oncological applications. Photochem Photobiol. 1998 Nov;68(5):603–32.

115.	Richards-Kortum R, Sevick-Muraca E. Quantitative optical spectroscopy for

tissue diagnosis. Annu Rev Phys Chem. 1996;47(1):555–606.

116. Abels C, Heil P, Dellian M, Kuhnle GE, Baumgartner R, Goetz AE. In vivo kinetics and spectra of 5-aminolaevulinic acid-induced fluorescence in an amelanotic melanoma of the hamster. Br J Cancer. 1994;70(5):826.

117. van der Veen N. Mechanism and Optimization of PDT using ALA induced PpIX. Erasmus MC: University Medical Center Rotterdam; 2000. p. 152.

118. de Leeuw J, de Vijlder HC, Bjerring P, Neumann H a M. Liposomes in dermatology today. J Eur Acad Dermatol Venereol. 2009 May;23(5):505–16.

119. Schneider C, Johnson SP, Gurusamy K, Cook RJ, Desjardins AE, Hawkes DJ, et al. Identification of liver metastases with probe-based confocal laser endomicroscopy at two excitation wavelengths. Lasers Surg Med. 2016 Dec 1;n/a-n/a.

120. Saarnak AE. Evaluation of fluorescence measurement techniques for tumour detection in vivo. Amsterdam; 1999. 127 p.

121. Welch AJ, Gardner C, Richards-Kortum R, Chan E, Criswell G, Pfefer J, et al. Propagation of fluorescent light. Lasers Surg Med. 1997;21(2):166–78.

122. Drezek R, Sokolov K, Utzinger U, Boiko I, Malpica A, Follen M, et al. Understanding the contributions of NADH and collagen to cervical tissue fluorescence spectra: modeling, measurements, and implications. J Biomed Opt. 2001;6(4):385–96.

123. Valentine RM, Brown CTA, Moseley H, Ibbotson S, Wood K. Monte Carlo modeling of in vivo protoporphyrin IX fluorescence and singlet oxygen production during photodynamic therapy for patients presenting with superficial basal cell carcinomas. J Biomed Opt. 2011;16(4):48002.

124. Liu B, Farrell TJ, Patterson MS. Comparison of photodynamic therapy with different excitation wavelengths using a dynamic model of aminolevulinic acid-photodynamic therapy of human skin. J Biomed Opt. 2012 Aug 1;17(8):088001–1.

125. Liu B, Farrell TJ, Patterson MS. A dynamic model for ALA-PDT of skin: simulation of temporal and spatial distributions of ground-state oxygen, photosensitizer and singlet oxygen. Phys Med Biol. 2010;55(19):5913.

126. Bashkatov AN, Genina EA, Tuchin V V. Optical Properties of Skin Subcutaneous, and Muscle Tissues: A Review. J Innov Opt Health Sci. 2011 Jan 21;4(1):9–38.

127. Tom Alexander Middelburg. Photodynamic therapy of skin using porphyrin precursors -- optical monitoring, vascular effects and personalized medicine. Rotterdam; 2014.

128. Veenstra KA. Long term dynamics of proteins and peptides. Groningen; 2002. 184 p.

129. Van Gemert MJC, Jacques SL, Sterenborg HJCM, Star WM. Skin optics. IEEE Trans Biomed Eng. 1989 Dec;36(12):1146–54.

130. Newell B, Bedlow AJ, Cliff S, Drysdale SB, Stanton AWB, Mortimer PS. Comparison of the microvasculature of basal cell carcinoma and actinic keratosis using intravital microscopy and immunohistochemistry. Br J Dermatol. 2003;149(1):105–10.

131. Mackenzie KA, Miller AP, Hock BD, Gardner J, Simcock JW, Roake JA, et al. Angiogenesis and host immune response contribute to the aggressive character of non-melanoma skin cancers in renal transplant recipients. Histopathology. 2011;58(6):875–85.

132. Arits AHMM, Mosterd K, Essers BA, Spoorenberg E, Sommer A, De Rooij MJM, et al. Photodynamic therapy versus topical imiquimod versus topical fluorouracil for treatment of superficial basal-cell carcinoma: a single blind, non-inferiority, randomised controlled trial. Lancet Oncol. 2013 Jun;14(7):647–54.

133. Roozeboom MH, Nelemans PJ, Mosterd K, Steijlen PM, Arits AHMM, Kelleners-Smeets NWJ. Photodynamic therapy vs. topical imiquimod for treatment of superficial basal cell carcinoma: a subgroup analysis within a noninferiority randomized controlled trial. Br J Dermatol. 2015 Mar;172(3):739–45.

134. de Haas ERM, de Bruijn HS, Sterenborg HJCM, Neumann HAM, Robinson DJ.

Microscopic distribution of protoporphyrin (PpIX) fluorescence in superficial basal cell carcinoma during light-fractionated aminolaevulinic acid photodynamic therapy. Acta Derm Venereol. 2008 Jan;88(6):547–54.

135. Tessari G, Girolomoni G. Nonmelanoma skin cancer in solid organ transplant recipients: update on epidemiology, risk factors, and management. Dermatologic Surg. 2012;38(10):1622–30.

136. Wheless L, Jacks S, Mooneyham Potter KA, Leach BC, Cook J. Skin cancer in organ transplant recipients: More than the immune system. J Am Acad Dermatol. 2014 Aug;71(2):359–65.

137. Dougherty TJ, Potter WR. Of what value is a highly absorbing photosensitizer in PDT? J Photochem Photobiol B Biol. 1991;8(2):223.

138. Pathak MA, Jimbow K, Szabo G, Fitzpatrick TB. Sunlight and melanin pigmentation. In: Smith KC, editor. Photochemical and photobiological reviews. Plenum Press; 1976. p. 211–39.

139. Jacobs LC. Genetic Determinants of Skin Color, Aging, and Cancer. Rotterdam: Erasmus University Rotterdam; 2015.

140. Gambichler T, Moussa G, Altmeyer P. A pilot study of fluorescence diagnosis of basal cell carcinoma using a digital flash light-based imaging system. Photodermatol Photoimmunol Photomed. 2008 Apr;24(2):67–71.

141. van der Beek N, Bjerring P, Neumann HAM. The choice and measurement of fluence in photodynamic therapy for superficial basal cell carcinoma. Br J Dermatol. 2015 Sep 23;173(4):1105–6.

142. Tyrrell JS, Campbell SM, Curnow A. The relationship between protoporphyrin IX photobleaching during real-time dermatological methyl-aminolevulinate photodynamic therapy (MAL-PDT) and subsequent clinical outcome. Lasers Surg Med. 2010;42(7):613–9.

143. De Haas ERM. ALA-PDT; the Treatment of Non-Melanoma Skin Cancer Re-illuminated. Rotterdam; 2007. 183 p.

144. Erceg A, de Jong EMJG, van de Kerkhof PCM, Seyger MMB. The efficacy of pulsed dye laser treatment for inflammatory skin diseases: A systematic review. J Am Acad Dermatol. 2013 Oct;69(4):609–615.e8.

145. de Leeuw J, Tank B, Bjerring PJ, Koetsveld S, Neumann M. Concomitant treatment of psoriasis of the hands and feet with pulsed dye laser and topical calcipotriol, salicylic acid, or both: a prospective open study in 41 patients. J Am Acad Dermatol. 2006 Feb;54(2):266–71.

146. De Leeuw J, Van Lingen RG, Both H, Tank B, Nijsten T, Martino Neumann HA. A comparative study on the efficacy of treatment with 585 nm pulsed dye laser and ultraviolet B-TL01 in plaque type psoriasis. Dermatol Surg. 2009 Jan;35(1):80–91.

147. Bovenschen HJ, Erceg A, Van Vlijmen-Willems I, Van De Kerkhof PCM, Seyger MMB. Pulsed dye laser versus treatment with calcipotriol/betamethasone dipropionate for localized refractory plaque psoriasis: effects on T-cell infiltration, epidermal proliferation and keratinization. J Dermatolog Treat. 2007;18(1):32–9.

148. Racz E, Prens EP, Kurek D, Kant M, de Ridder D, Mourits S, et al. Effective treatment of psoriasis with narrow-band UVB phototherapy is linked to suppression of the IFN and Th17 pathways. J Invest Dermatol. 2011 Jul;131(7):1547–58.

149. Hern S, Allen MH, Sousa AR, Harland CC, Barker JN, Levick JR, et al. Immunohistochemical evaluation of psoriatic plaques following selective photothermolysis of the superficial capillaries. Br J Dermatol. 2001 Jul;145(1):45–53.

150. Hern S, Stanton AWB, Mellor RH, Harland CC, Levick JR, Mortimer PS. In vivo quantification of the structural abnormalities in psoriatic microvessels before and after pulsed dye laser treatment. Br J Dermatol. 2005 Mar 1;152(3):505–11.

151. Rácz E, de Leeuw J, Baerveldt EM, Kant M, Neumann HAM, van der Fits L, et al. Cellular and molecular effects of pulsed dye laser and local narrow-band UVB

therapy in psoriasis. Lasers Surg Med. 2010 Mar;42(3):201–10.

152.   Hugh JM, Newman MD, Weinberg JM. The Pathophysiology of Psoriasis. In: Weinberg JM, Lebwohl M, editors. Advances in Psoriasis. Springer; 2014. p. 9–19.

153.   Bolognia J, Jorizzo JL, Schaffer JF, editors. Dermatology. 3rd ed. London: Elsevier Saunders,; 2012.

154.   Springate DA, Parisi R, Kontopantelis E, Reeves D, Griffiths CEM, Ashcroft DM. Incidence, prevalence and mortality of patients with psoriasis: a UK population-based cohort study. Br J Dermatol. 2016 Aug;

155.   Koek MBG, Buskens E, Steegmans PHA, van Weelden H, Bruijnzeel-Koomen CAFM, Sigurdsson V. UVB phototherapy in an outpatient setting or at home: a pragmatic randomised single-blind trial designed to settle the discussion. The PLUTO study. BMC Med Res Methodol. 2006;6:39.

156.   Stern RS, Thibodeau LA, Kleinerman RA, Parrish JA, Fitzpatrick TB. Risk of cutaneous carcinoma in patients treated with oral methoxsalen photochemotherapy for psoriasis. N Engl J Med. 1979 Apr;300(15):809–13.

157.   Ozawa M, Ferenczi K, Kikuchi T, Cardinale I, Austin LM, Coven TR, et al. 312-nanometer ultraviolet B light (narrow-band UVB) induces apoptosis of T cells within psoriatic lesions. J Exp Med. 1999 Feb;189(4):711–8.

158.   Salem SAM, Barakat MAE-T, Morcos CMZM. Bath psoralen+ultraviolet A photochemotherapy vs. narrow band-ultraviolet B in psoriasis: a comparison of clinical outcome and effect on circulating T-helper and T-suppressor/cytotoxic cells. Photodermatol Photoimmunol Photomed. 2010 Oct;26(5):235–42.

159.   Moodycliffe AM, Kimber I, Norval M. Role of tumour necrosis factor-alpha in ultraviolet B light-induced dendritic cell migration and suppression of contact hypersensitivity. Immunology. 1994 Jan;81(1):79–84.

160.   el-Ghorr AA, Norval M. Biological effects of narrow-band (311 nm TL01) UVB irradiation: a review. J Photochem Photobiol B. 1997 Apr;38(2–3):99–106.

161. Tjioe M, Smits T, van de Kerkhof PCM, Gerritsen MJP. The differential effect of broad band vs narrow band UVB with respect to photodamage and cutaneous inflammation. Exp Dermatol. 2003 Dec;12(6):729–33.

162. Hearn RMR, Kerr AC, Rahim KF, Ferguson J, Dawe RS. Incidence of skin cancers in 3867 patients treated with narrow-band ultraviolet B phototherapy. Br J Dermatol. 2008 Sep;159(4):931–5.

163. Weischer M, Blum A, Eberhard F, Rocken M, Berneburg M. No evidence for increased skin cancer risk in psoriasis patients treated with broadband or narrowband UVB phototherapy: a first retrospective study. Acta Derm Venereol. 2004;84(5):370–4.

164. Archier E, Devaux S, Castela E, Gallini A, Aubin F, Le Maitre M, et al. Carcinogenic risks of psoralen UV-A therapy and narrowband UV-B therapy in chronic plaque psoriasis: a systematic literature review. J Eur Acad Dermatol Venereol. 2012 May;26 Suppl 3:22–31.

165. Ryu HH, Choe YS, Jo S, Youn J Il, Jo SJ. Remission period in psoriasis after multiple cycles of narrowband ultraviolet B phototherapy. J Dermatol. 2014 Jul;41(7):622–7.

166. Fragoulakis V, Raptis E, Vitsou E, Maniadakis N. Annual biologic treatment cost for new and existing patients with moderate to severe plaque psoriasis in Greece. Vol. 7, ClinicoEconomics and Outcomes Research: CEOR. 2015. p. 73–83.

167. Katugampola GA, Rees AM, Lanigan SW. Laser treatment of psoriasis. Br J Dermatol. 1995 Dec 1;133(6):909–13.

168. Ros AM, Garden JM, Bakus AD, Hedblad MA. Psoriasis response to the pulsed dye laser. Lasers Surg Med. 1996 Jan 1;19(3):331–5.

169. Erceg A, Bovenschen HJ, van de Kerkhof PCM, Seyger MMB. Efficacy of the pulsed dye laser in the treatment of localized recalcitrant plaque psoriasis: a comparative study. Br J Dermatol. 2006 Jul;155(1):110–4.

170. van Lingen RG, de Jong EMGJ, van Erp PEJ, van Meeteren WSEC, van De Kerkhof PCM, Seyger MMB. Nd: YAG laser (1,064 nm) fails to improve localized plaque

type psoriasis: a clinical and immunohistochemical pilot study. Eur J Dermatol. 2008;18(6):671–6.

171. Nast A, Boehncke W-H, Mrowietz U, Ockenfels H-M, Philipp S, Reich K, et al. S3 - Guidelines on the treatment of psoriasis vulgaris (English version). Update. J Dtsch Dermatol Ges. 2012 Mar;10 Suppl 2:S1-95.

172. Menter A, Korman NJ, Elmets CA, Feldman SR, Gelfand JM, Gordon KB, et al. Guidelines of care for the management of psoriasis and psoriatic arthritis: Section 5. Guidelines of care for the treatment of psoriasis with phototherapy and photochemotherapy. J Am Acad Dermatol. 2010 Jan;62(1):114–35.

173. Zweegers J, de Jong EMGJ, Nijsten TEC, de Bes J, te Booij M, Borgonjen RJ, et al. Summary of the Dutch S3-guidelines on the treatment of psoriasis 2011. Dutch Society of Dermatology and Venereology. Dermatol Online J. 2014 Mar;20(3).

174. Braverman IM, Yen A. Microcirculation in psoriatic skin. J Invest Dermatol. 1974 May;62(5):493–502.

175. Braverman IM, Sibley J. Role of the microcirculation in the treatment and pathogenesis of psoriasis. J Invest Dermatol. 1982 Jan;78(1):12–7.

176. Braverman IM. Electron microscopic studies of the microcirculation in psoriasis. J Invest Dermatol. 1972 Jul;59(1):91–8.

177. Davis MJ, Lawler JC. The capillary circulation of the skin; some normal and pathological findings. AMA Arch Derm. 1958 Jun;77(6):690–703.

178. Braverman IM, Yen A. Ultrastructure of the Capillary Loops in the Dermal Pappilae of Psoriasis. J Invest Dermatol. 1977 Jan;68(1):53–60.

179. Rowe L. Volume of epidermis and dermal papillae in psoriasis, actinic keratoses, and lentigo. J Invest Dermatol. 1966 Apr;46(4):374–7.

180. Ryan TJ. Microcirculation in psoriasis: Blood vessels, lymphatics and tissue fluid. Pharmacol Ther. 1980 Jan;10(1):27–64.

181. Leong TT, Fearon U, Veale DJ. Angiogenesis in psoriasis and psoriatic arthritis: clues to disease pathogenesis. Curr Rheumatol Rep. 2005 Aug;7(4):325–9.

182. Creamer D, Sullivan D, Bicknell R, Barker J. Angiogenesis in psoriasis. Angiogenesis. 2002;5(4):231–6.

183. Heidenreich R, Röcken M, Ghoreschi K. Angiogenesis drives psoriasis pathogenesis. Int J Exp Pathol. 2009 Jun;90(3):232–48.

184. Hendriks AGM, Steenbergen W, Zeeuwen PLJM, Schalkwijk J, Hondebrink E, Klitsie MAJ, et al. Perfusion Intensity Correlates with Expression Levels of Psoriasis-Related Genes and Proteins. Skin Pharmacol Physiol. 2015;28(6):296–306.

185. Farber EM, Lanigan SW, Boer J. The role of cutaneous sensory nerves in the maintenance of psoriasis. Int J Dermatol. 1990 Jan;29(6):418–20.

186. Naukkarinen A, Nickoloff BJ, Farber EM. Quantification of cutaneous sensory nerves and their substance P content in psoriasis. J Invest Dermatol. 1989 Jan;92(1):126–9.

187. Schmidt R, Schmelz M, Ringkamp M, Handwerker HO, Torebjörk HE. Innervation territories of mechanically activated C nociceptor units in human skin. J Neurophysiol. 1997 Nov;78(5):2641–8.

188. Schmelz M, Schmidt R, Bickel A, Torebjörk HE, Handwerker HO. Innervation territories of single sympathetic C fibers in human skin. J Neurophysiol. 1998 Apr;79(4):1653–60.

189. Kubanov AA, Katunina OR, Chikin V V. Expression of Neuropeptides, Neurotrophins, and Neurotransmitters in the Skin of Patients with Atopic Dermatitis and Psoriasis. Bull Exp Biol Med. 2015 Jul;159(3):318–22.

190. Zhu TH, Nakamura M, Farahnik B, Abrouk M, Lee K, Singh R, et al. The Role of the Nervous System in the Pathophysiology of Psoriasis: A Review of Cases of Psoriasis Remission or Improvement Following Denervation Injury. Am J Clin Dermatol. 2016 Mar 2;

191. Farber EM, Nickoloff BJ, Recht B, Fraki JE. Stress, symmetry, and psoriasis: possible role of neuropeptides. J Am Acad Dermatol. 1986 Feb;14(2 Pt 1):305–11.

192. Weddell G, Cowan MA, Palmer E, Ramaswamy S. Psoriatic Skin. Arch Dermatol. 1965;91:252–66.

193. Williams PL, Wendell-Smith CP. Some additional parametric variations between peripheral nerve fibre populations. J Anat. 1971 Sep;109(Pt 3):505–26.

194. Canavese M, Altruda F, Ruzicka T, Schauber J. Vascular endothelial growth factor (VEGF) in the pathogenesis of psoriasis--a possible target for novel therapies? J Dermatol Sci. 2010 Jun;58(3):171–6.

195. Yamaguchi J, Aihara M, Kobayashi Y, Kambara T, Ikezawa Z. Quantitative analysis of nerve growth factor (NGF) in the atopic dermatitis and psoriasis horny layer and effect of treatment on NGF in atopic dermatitis. J Dermatol Sci. 2009 Jan;53(1):48–54.

196. Saraceno R, Kleyn CE, Terenghi G, Griffiths CEM. The role of neuropeptides in psoriasis. Br J Dermatol. 2006 Nov;155(5):876–82.

197. Jiang WY, Raychaudhuri SP, Farber EM. Double-labeled immunofluorescence study of cutaneous nerves in psoriasis. Int J Dermatol. 1998 Aug;37(8):572–4.

198. Mikami N, Watanabe K, Hashimoto N, Miyagi Y, Sueda K, Fukada S, et al. Calcitonin gene-related peptide enhances experimental autoimmune encephalomyelitis by promoting Th17-cell functions. Int Immunol. 2012 Nov;24(11):681–91.

199. Liakou AI, Nyengaard JR, Bonovas S, Knolle J, Makrantonaki E, Zouboulis CC. Marked Reduction of the Number and Individual Volume of Sebaceous Glands in Psoriatic Lesions. Dermatology. 2016 Jan;232(4):415–24.

200. Cameron JB, Van Voorhees AS. History of Psoriasis. In: Weinberg JM, Lebwohl M, editors. Advances in Psoriasis. London: Springer London; 2014. p. 1–7.

201. Lynde CW, Poulin Y, Vender R, Bourcier M, Khalil S. Interleukin 17A: toward a new understanding of psoriasis pathogenesis. J Am Acad Dermatol. 2014 Jul;71(1):141–50.

202. Gordon KB, Blauvelt A, Papp KA, Langley RG, Luger T, Ohtsuki M, et al. Phase 3

Trials of Ixekizumab in Moderate-to-Severe Plaque Psoriasis. N Engl J Med. 2016 Jul;375(4):345–56.

203. Dennehy EB, Zhang L, Amato D, Goldblum O, Rich P. Ixekizumab Is Effective in Subjects With Moderate to Severe Plaque Psoriasis With Significant Nail Involvement: Results From UNCOVER 3. J Drugs Dermatol. 2016 Aug;15(8):958–61.

204. Vallat VP, Gilleaudeau P, Battat L, Wolfe J, Nabeya R, Heftler N, et al. PUVA bath therapy strongly suppresses immunological and epidermal activation in psoriasis: a possible cellular basis for remittive therapy. J Exp Med. 1994 Jul 1;180(1):283–96.

205. Dewing SB. Remission of psoriasis associated with cutaneous nerve section. Arch Dermatol. 1971 Aug;104(2):220–1.

206. Perlman HH. Remission of psoriasis vulgaris from the use of nerve-blocking agents. Arch Dermatol. 1972 Jan;105(1):128–9.

207. Farber EM, Peterson JB. Variations in the natural history of psoriasis. Calif Med. 1961 Jul;95:6–11.

208. Raychaudhuri SK, Raychaudhuri SP, Weltman H, Farber EM. Effect of nerve growth factor on endothelial cell biology: proliferation and adherence molecule expression on human dermal microvascular endothelial cells. Arch Dermatol Res. 2001 Jun;293(6):291–5.

209. Raychaudhuri SP, Jiang WY, Farber EM. Psoriatic keratinocytes express high levels of nerve growth factor. Acta Derm Venereol. 1998 Mar;78(2):84–6.

210. Farber EM, Rein G, Lanigan SW. Stress and psoriasis. Psychoneuroimmunologic mechanisms. Int J Dermatol. 1991 Jan;30(1):8–12.

211. Kumar B, Raychaudhuri SP, Vossough S, Farber EM. The rare coexistence of leprosy and psoriasis. Int J Dermatol. 1992 Aug;31(8):551–4.

212. Wahba A, Dorfman M, Sheskin J. Psoriasis and other common dermatoses in leprosy. Int J Dermatol. 1980 Mar;19(2):93–5.

213. Pavithran K. Psoriasis developing in a patch of leprosy as a Koebner phenomenon. Indian J Lepr. 1992 Jan;64(2):197–9.

214. Azimi E, Lerner EA, Elmariah SB. Altered manifestations of skin disease at sites affected by neurological deficit. Br J Dermatol. 2015 Apr;172(4):988–93.

215. Bernstein JE. Capsaicin and substance P. Clin Dermatol. 1991 Jan;9(4):497–503.

216. Bernstein JE, Parish LC, Rapaport M, Rosenbaum MM, Roenigk HH. Effects of topically applied capsaicin on moderate and severe psoriasis vulgaris. J Am Acad Dermatol. 1986 Sep 9;15(3):504–7.

217. Zachariae R, Oster H, Bjerring P, Kragballe K. Effects of psychologic intervention on psoriasis: a preliminary report. J Am Acad Dermatol. 1996 Jun;34(6):1008–15.

218. Ostrowski SM, Belkadi A, Loyd CM, Diaconu D, Ward NL. Cutaneous denervation of psoriasiform mouse skin improves acanthosis and inflammation in a sensory neuropeptide-dependent manner. J Invest Dermatol. 2011 Jul;131(7):1530–8.

219. Xia Y-P, Li B, Hylton D, Detmar M, Yancopoulos GD, Rudge JS. Transgenic delivery of VEGF to mouse skin leads to an inflammatory condition resembling human psoriasis. Blood. 2003 Jul 1;102(1):161–8.

220. Schmidt R, Schmelz M, Weidner C, Handwerker HO, Torebjörk HE. Innervation territories of mechano-insensitive C nociceptors in human skin. J Neurophysiol. 2002 Oct;88(4):1859–66.

221. O' Donnell DR, Prasad A, Brull R. Antiinflammatory effect of peripheral nerve blockade. Vol. 110, Anesthesiology. United States; 2009. p. 1189; author reply 1189.

222. Martin F, Martinez V, Mazoit JX, Bouhassira D, Cherif K, Gentili ME, et al. Antiinflammatory effect of peripheral nerve blocks after knee surgery: clinical and biologic evaluation. Anesthesiology. 2008 Sep;109(3):484–90.

223. Roosterman D, Goerge T, Schneider SW, Bunnett NW, Steinhoff M. Neuronal control of skin function: the skin as a neuroimmunoendocrine organ. Physiol Rev. 2006 Oct 1;86(4):1309–79.

224. Chiu IM, von Hehn CA, Woolf CJ. Neurogenic inflammation and the peripheral nervous system in host defense and immunopathology. Nat Neurosci. 2012 Aug;15(8):1063–7.

225. Andersson U, Tracey KJ. Neural reflexes in inflammation and immunity. J Exp Med. 2012 Jun 4;209(6):1057–68.

226. Brogden KA, Guthmiller JM, Salzet M, Zasloff M. The nervous system and innate immunity: the neuropeptide connection. Nat Immunol. 2005 Jun;6(6):558–64.

227. Luger TA. Neuromediators--a crucial component of the skin immune system. J Dermatol Sci. 2002 Nov;30(2):87–93.

228. Lambrecht BN. Immunologists getting nervous: neuropeptides, dendritic cells and T cell activation. Respir Res. 2001;2(3):1–6.

229. Darsow U, Ring J. Neuroimmune interactions in the skin. Curr Opin Allergy Clin Immunol. 2001 Oct;1(5):435–9.

230. Schaffer M, Beiter T, Becker HD, Hunt TK. Neuropeptides: mediators of inflammation and tissue repair? Arch Surg. 1998 Oct;133(10):1107–16.

231. Ding W, Stohl LL, Wagner JA, Granstein RD. Calcitonin gene-related peptide biases Langerhans cells toward Th2-type immunity. J Immunol. 2008 Nov 1;181(9):6020–6.

232. Gullo CA, Macary P, Graner M. The Role of Heat Shock Proteins in the Elicitation of Immune Responses. In: Asea AAA, Maio A De, editors. Heat Shock Proteins: Potent Mediators of Inflammation and Immunity. Dordrecht: Springer; 2007. p. 173–87.

233. Mailhos C, Howard MK, Latchman DS. Heat shock protects neuronal cells from programmed cell death by apoptosis. Neuroscience. 1993 Aug;55(3):621–7.

234. Ishima T, Iyo M, Hashimoto K. Neurite outgrowth mediated by the heat shock protein Hsp90α: a novel target for the antipsychotic drug aripiprazole. Transl Psychiatry. 2012 Jan;2:e170.

235. Yenari MA, Giffard RG, Sapolsky RM, Steinberg GK. The neuroprotective

potential of heat shock protein 70 (HSP70). Mol Med Today. 1999 Dec;5(12):525–31.

236. Turturici G, Sconzo G, Geraci F. Hsp70 and its molecular role in nervous system diseases. Biochem Res Int. 2011 Jan;2011:618127.

237. Chen Y, Voegeli TS, Liu PP, Noble EG, Currie RW. Heat shock paradox and a new role of heat shock proteins and their receptors as anti-inflammation targets. Inflamm Allergy Drug Targets. 2007 Jun;6(2):91–100.

238. Prieto VG, Diwan AH, Shea CR, Zhang P, Sadick NS. Effects of intense pulsed light and the 1,064 nm Nd:YAG laser on sun-damaged human skin: histologic and immunohistochemical analysis. Dermatol Surg. 2005 May;31(5):522–5.

239. Laubach H-J, Tannous Z, Anderson RR, Manstein D. Skin responses to fractional photothermolysis. Lasers Surg Med. 2006 Feb;38(2):142–9.

240. Beckham JT, Mackanos MA, Crooke C, Takahashi T, O'Connell-Rodwell C, Contag CH, et al. Assessment of cellular response to thermal laser injury through bioluminescence imaging of heat shock protein 70. Photochem Photobiol. 2004 Jan;79(1):76–85.

241. Polla BS, Anderson RR. Thermal injury by laser pulses: Protection by heat shock despite failure to induce heat-shock response. Lasers Surg Med. 1987 Jan 1;7(5):398–404.

242. Souil E, Capon A, Mordon S, Dinh-Xuan AT, Polla BS, Bachelet M. Treatment with 815-nm diode laser induces long-lasting expression of 72-kDa heat shock protein in normal rat skin. Br J Dermatol. 2001 Feb;144(2):260–6.

243. Nijhuis E. Hyperthermia-induced apoptosis. Hengelo: PrintPartners Ipskamp, Enschede; 2008. 138 p.

244. Rylander MN, Feng Y, Bass J, Diller KR. Thermally induced injury and heat-shock protein expression in cells and tissues. Ann N Y Acad Sci. 2005 Dec;1066:222–42.

245. Rylander MN, Feng Y, Bass J, Diller KR. Heat shock protein expression and injury optimization for laser therapy design. Lasers Surg Med. 2007 Oct;39(9):731–46.

246. Dwyer PJ, Anderson RR, DiMarzio CA. Mapping blood oxygen saturation using a multi-spectral imaging system. In: Vo-Dinh T, Lieberman RA, Vurek GG, Katzir A, editors. BiOS '97, Part of Photonics West. International Society for Optics and Photonics; 1997. p. 270–80.

247. Kim TG, Roh HJ, Cho SB, Lee JH, Lee SJ, Oh SH. Enhancing effect of pretreatment with topical niacin in the treatment of rosacea-associated erythema by 585-nm pulsed dye laser in Koreans: a randomized, prospective, split-face trial. Br J Dermatol. 2011 Mar;164(3):573–9.

248. Craighead DH, Alexander LM. Topical menthol increases cutaneous blood flow. Microvasc Res. 2016 Sep;107:39–45.

249. Moretti G, Ellis RA, Mescon H. Vascular patterns in the skin of the face. J Invest Dermatol. 1959 Sep;33:103–12.

250. Qin J, Jiang J, An L, Gareau D, Wang RK. In vivo volumetric imaging of microcirculation within human skin under psoriatic conditions using optical microangiography. Lasers Surg Med. 2011 Feb;43(2):122–9.

251. Burton AC. Relation of structure to function of the tissues of the wall of blood vessels. Physiol Rev. 1954 Oct;34(4):619–42.

252. Anderson RR, Parrish JA. The optics of human skin. J Invest Dermatol. 1981 Jul;77(1):13–9.

253. Zijlstra WG, Buursma A, Assendelft OW van. Visible and Near Infrared Absorption Spectra of Human and Animal Haemoglobin. Taylor & Francis; 2000. 368 p.

254. Friebel M, Roggan A, Müller G, Meinke M. Determination of optical properties of human blood in the spectral range 250 to 1100 nm using Monte Carlo simulations with hematocrit-dependent effective scattering phase functions. J Biomed Opt. 2006 Jan;11(3):34021.

255. Town G, Ash C, Eadie E, Moseley H. Measuring key parameters of intense pulsed light (IPL) devices. J Cosmet Laser Ther. 2007 Sep;9(3):148–60.

256. Duck FA. Physical properties of tissue. The University Press; 1990. 357 p.

257. Webb RC, Pielak RM, Bastien P, Ayers J, Niittynen J, Kurniawan J, et al. Thermal transport characteristics of human skin measured in vivo using ultrathin conformal arrays of thermal sensors and actuators. PLoS One. 2015;10(2):e0118131.

258. Hulsbergen Henning JP, Gemert MJC van, Lahaye CTW. Clinical and Histological Evaluation of Portwine Stain Treatment With a Microsecond-Pulsed Dye-Laser at 577 NM. Lasers Surg Med. 1984;4:375–80.

259. Kimel S, Svaasand LO, Cao D, Hammer-Wilson MJ, Nelson JS. Vascular response to laser photothermolysis as a function of pulse duration, vessel type, and diameter: implications for port wine stain laser therapy. Lasers Surg Med. 2002 Jan;30(2):160–9.

260. Altshuler GB, Anderson RR, Manstein D, Zenzie HH, Smirnov MZ. Extended theory of selective photothermolysis. - PubMed - NCBI [Internet]. Vol. 29, Lasers in surgery and medicine. 2001 [cited 2015 Oct 3]. p. 416–32. Available from: https://ccz1m01ce59egikdl-l5kiz.sec.amc.nl/pubmed/11891730

261. Anderson RR, Parrish JA. Selective photothermolysis: precise microsurgery by selective absorption of pulsed radiation. Science. 1983 May 29;220(4596):524–7.

262. Diller KR, Klutke G-A. Accuracy analysis of the Henriques model for predicting thermal burn injury. Am Soc Mech Eng Heat Transf Div. 1993;268:117–23.

263. Brown SL, Hunt JW, Hill RP. Differential thermal sensitivity of tumour and normal tissue microvascular response during hyperthermia. Int J Hyperth. 1992 Jan 9;8(4):501–14.

264. Goh CL, Khoo L. Laser Doppler perfusion imaging (LDPI) and transepidermal water loss (TEWL) values in psoriatic lesions treated with narrow band UVB phototherapy. Dermal vascularity may be useful indicator of psoriatic activity. Ann Acad Med Singapore. 2004 Jan;33(1):75–9.

265. Hendriks AGM, van de Kerkhof PCM, de Jonge CS, Lucas M, Steenbergen W,

Seyger MMB. Clearing of psoriasis documented by laser Doppler perfusion imaging contrasts remaining elevation of dermal expression levels of CD31. Skin Res Technol. 2015 Aug;21(3):340–5.

266. Hendriks AGM, Steenbergen W, Hondebrink E, van Hespen JCG, van de Kerkhof PCM, Seyger MMB. Whole field laser Doppler imaging of the microcirculation in psoriasis and clinically unaffected skin. J Dermatolog Treat. 2014 Feb;25(1):18–21.

267. van Gemert MJ, Welch AJ, Amin AP. Is there an optimal laser treatment for port wine stains? Lasers Surg Med. 1986 Jan;6(1):76–83.

268. van Gemert MJ, Smithies DJ, Verkruysse W, Milner TE, Nelson JS. Wavelengths for port wine stain laser treatment: influence of vessel radius and skin anatomy. Phys Med Biol. 1997 Jan;42(1):41–50.

269. van Gemert MJ, Welch AJ, Pickering JW, Tan OT, Gijsbers GH. Wavelengths for laser treatment of port wine stains and telangiectasia. Lasers Surg Med. 1995 Jan;16(2):147–55.

270. Nymann P, Hedelund L, Haedersdal M. Long-pulsed dye laser vs. intense pulsed light for the treatment of facial telangiectasias: a randomized controlled trial. J Eur Acad Dermatol Venereol. 2010 Feb;24(2):143–6.

271. Ritossa F. A new puffing pattern induced by temperature shock and DNP in drosophila. Experientia. 1962;18(12):571–3.

272. Trautinger F. Heat shock proteins in the photobiology of human skin. J Photochem Photobiol B. 2001 Oct;63(1–3):70–7.

273. Morris SD. Heat shock proteins and the skin. Clin Exp Dermatol. 2002 May;27(3):220–4.

274. Lancaster GI, Febbraio MA. Mechanisms of stress-induced cellular HSP72 release: implications for exercise-induced increases in extracellular HSP72. Exerc Immunol Rev. 2005 Jan;11:46–52.

275. Asea A. Mechanisms of HSP72 release. J Biosci. 2007 Apr;32(3):579–84.

276. Wachstein J, Tischer S, Figueiredo C, Limbourg A, Falk C, Immenschuh S, et al. HSP70 enhances immunosuppressive function of CD4(+)CD25(+)FoxP3(+) T regulatory cells and cytotoxicity in CD4(+)CD25(-) T cells. PLoS One. 2012 Jan;7(12):e51747.

277. Bovenschen HJ, van de Kerkhof PC, van Erp PE, Woestenenk R, Joosten I, Koenen HJPM. Foxp3+ regulatory T cells of psoriasis patients easily differentiate into IL-17A-producing cells and are found in lesional skin. J Invest Dermatol. 2011 Sep;131(9):1853–60.

278. Koike T, Uno S, Ishizawa M, Takahashi H, Ikeda K, Yokota S, et al. The heat shock protein inhibitor KNK437 induces neurite outgrowth in PC12 cells. Neurosci Lett. 2006 Dec 27;410(3):212–7.

279. Amin V, Cumming D V, Latchman DS. Over-expression of heat shock protein 70 protects neuronal cells against both thermal and ischaemic stress but with different efficiencies. Neurosci Lett. 1996 Mar 8;206(1):45–8.

280. Amin V, Cumming D V, Coffin RS, Latchman DS. The degree of protection provided to neuronal cells by a pre-conditioning stress correlates with the amount of heat shock protein 70 it induces and not with the similarity of the subsequent stress. Neurosci Lett. 1995 Nov 17;200(2):85–8.

281. Raychaudhuri SP, Raychaudhuri SK. Role of NGF and neurogenic inflammation in the pathogenesis of psoriasis. Prog Brain Res. 2004 Jan;146:433–7.

282. Raychaudhuri SP, Jiang W-Y, Raychaudhuri SK. Revisiting the Koebner phenomenon: role of NGF and its receptor system in the pathogenesis of psoriasis. Am J Pathol. 2008 Apr;172(4):961–71.

283. Calabrese V, Scapagnini G, Ravagna A, Giuffrida Stella AM, Butterfield DA. Molecular Chaperones and Their Roles in Neural Cell Differentiation. Dev Neurosci. 2002;24(1):1–13.

284. Al-Masaud AS, Wood EJ, Cunliffe WJ, Holland DB. Are stress proteins induced during PUVA therapy? Br J Dermatol. 1996 May;134(5):892–9.

285. Trautinger F, Kindås-Mügge I, Knobler RM, Hönigsmann H. Stress proteins in the

cellular response to ultraviolet radiation. J Photochem Photobiol B. 1996 Sep;35(3):141–8.

286. Wilson N, McArdle A, Guerin D, Tasker H, Wareing P, Foster CS, et al. Hyperthermia to normal human skin in vivo upregulates heat shock proteins 27, 60, 72i and 90. J Cutan Pathol. 2000 Apr;27(4):176–82.

287. Narbutt J, Olejniczak I, Sobolewska-Sztychny D, Sysa-Jedrzejowska A, Slowik-Kwiatkowska I, Hawro T, et al. Narrow band ultraviolet B irradiations cause alteration in interleukin-31 serum level in psoriatic patients. Arch Dermatol Res. 2013 Apr;305(3):191–5.

288. Tintle S, Shemer A, Suarez-Farinas M, Fujita H, Gilleaudeau P, Sullivan-Whalen M, et al. Reversal of atopic dermatitis with narrow-band UVB phototherapy and biomarkers for therapeutic response. J Allergy Clin Immunol. 2011 Sep;128(3):583–4.

289. Johnson-Huang LM, Suarez-Farinas M, Sullivan-Whalen M, Gilleaudeau P, Krueger JG, Lowes MA. Effective narrow-band UVB radiation therapy suppresses the IL-23/IL-17 axis in normalized psoriasis plaques. J Invest Dermatol. 2010 Nov;130(11):2654–63.

290. Haedersdal M, Togsverd-Bo K, Wiegell SR, Wulf HC. Long-pulsed dye laser versus long-pulsed dye laser-assisted photodynamic therapy for acne vulgaris: A randomized controlled trial. J Am Acad Dermatol. 2008 Mar;58(3):387–94.

291. Cao Y, Ohwatari N, Matsumoto T, Kosaka M, Ohtsuru A, Yamashita S. TGF-beta1 mediates 70-kDa heat shock protein induction due to ultraviolet irradiation in human skin fibroblasts. Pflugers Arch. 1999 Aug;438(3):239–44.

292. Higgins E, Ralph N, Ryan S, Koik N, Honari B, Lally A, et al. A randomised half body prospective study of low and medium dose regimens using the 308 nm excimer laser in the treatment of localised psoriasis. J Dermatolog Treat. 2016 Sep 29;1–6.

293. Hofer A, Fink-Puches R, Kerl H, Wolf P. Comparison of phototherapy with near vs. far erythemogenic doses of narrow-band ultraviolet B in patients with

psoriasis. Br J Dermatol. 1998 Jan;138(1):96–100.

294. Kunisada M, Kumimoto H, Ishizaki K, Sakumi K, Nakabeppu Y, Nishigori C. Narrow-band UVB induces more carcinogenic skin tumors than broad-band UVB through the formation of cyclobutane pyrimidine dimer. J Invest Dermatol. 2007 Dec;127(12):2865–71.

295. Aufiero BM, Talwar H, Young C, Krishnan M, Hatfield JS, Lee HK, et al. Narrow-band UVB induces apoptosis in human keratinocytes. J Photochem Photobiol B. 2006 Feb;82(2):132–9.

296. Gu X, Nylander E, Coates PJ, Nylander K. Oxidation reduction is a key process for successful treatment of psoriasis by narrow-band UVB phototherapy. Acta Derm Venereol. 2015 Feb;95(2):140–6.

297. Batycka-Baran A, Besgen P, Wolf R, Szepietowski JC, Prinz JC. The effect of phototherapy on systemic inflammatory process in patients with plaque psoriasis. J Photochem Photobiol B. 2016 Aug;161:396–401.

298. Tan ST, Bialostocki A, Armstrong JR. Pulsed dye laser therapy for rosacea. Br J Plast Surg. 2004 Jun;57(4):303–10.

299. de Leeuw J, van der Beek N, Bjerring P, Neumann HAM. Photodynamic therapy of acne vulgaris using 5-aminolevulinic acid 0.5% liposomal spray and intense pulsed light in combination with topical keratolytic agents. J Eur Acad Dermatol Venereol. 2010 Apr;24(4):460–9.

300. Sommer S, Sheehan-Dare RA. The Koebner phenomenon in vitiligo following treatment of a port-wine stain naevus by pulsed dye laser. Br J Dermatol. 1998 Jan;138(1):200–1.

301. Asea A. Stress proteins and initiation of immune response: chaperokine activity of hsp72. Exerc Immunol Rev. 2005 Jan;11:34–45.

302. Asea AAA, Maio A De, editors. Heat Shock Proteins: Potent Mediators of Inflammation and Immunity. Dordrecht: Springer Netherlands; 2007. (Heat Shock Proteins; vol. 1).

303. Kakeda M, Arock M, Schlapbach C, Yawalkar N. Increased expression of heat shock protein 90 in keratinocytes and mast cells in patients with psoriasis. J Am Acad Dermatol. 2014 Apr;70(4):683–690.e1.

304. Stenderup K, Rosada C, Gavillet B, Vuagniaux G, Dam TN. Debio 0932, a new oral Hsp90 inhibitor, alleviates psoriasis in a xenograft transplantation model. Acta Derm Venereol. 2014 Nov;94(6):672–6.

305. Wu L, Wang C, Boisson B, Misra S, Rayman P, Finke JH, et al. The differential regulation of human ACT1 isoforms by Hsp90 in IL-17 signaling. J Immunol. 2014 Aug 15;193(4):1590–9.

306. Lehner T, Wang Y, Whittall T, Bergmeier LA, Babaahmady K, Kelly C. Hsp-Induced Stimulation of Immune Responses. In: Heat Shock Proteins: Potent Mediators of Inflammation and Immunity. Dordrecht: Springer Netherlands; 2007. p. 159–72.

307. Esteva A, Kuprel B, Novoa RA, Ko J, Swetter SM, Blau HM, et al. Dermatologist-level classification of skin cancer with deep neural networks. Nature. 2017 Feb 2;542(7639):115–8.

308. Jorgensen GF, Hedelund L, Haedersdal M. Long-pulsed dye laser versus intense pulsed light for photodamaged skin: a randomized split-face trial with blinded response evaluation. Lasers Surg Med. 2008 Jul;40(5):293–9.

309. Nymann P, Hedelund L, Haedersdal M. Intense pulsed light vs. long-pulsed dye laser treatment of telangiectasia after radiotherapy for breast cancer: a randomized split-lesion trial of two different treatments. Br J Dermatol. 2009 Jun;160(6):1237–41.

310. Campbell CL, Wood K, Brown CTA, Moseley H. New insights into photodynamic therapy treatment through the use of 3D Monte Carlo radiation transfer modelling. In: Choi B, Kollias N, Zeng H, Kang HW, Wong BJF, Ilgner JF, et al., editors. SPIE BiOS. International Society for Optics and Photonics; 2016. p. 96890Q.

311. Bjerring P, Christiansen K, Troilius A, Bekhor P, de Leeuw J. Skin fluorescence controlled photodynamic photorejuvenation (wrinkle reduction). Lasers Surg

Med. 2009;41(5):327–36.

312. Simon M, L'Heveder G, Genestet S, Misery L. Efficacy of capsaicin in the treatment of acne in one case: new pathophysiological perspectives. J Eur Acad Dermatology Venereol. 2010;24(7):857.

7. Acknowledgements

First and foremost, my gratitude goes to prof. Kelvin Donne. Thank you for accepting me as your student. My background didn't make me the most obvious candidate for research which, initially in part and later in full, is based on the application of computational methods. In particular since a small pond separates Hilversum from Swansea, which was bound to have an effect on supervision. Yet, you could see beyond my formal training and the geographical difficulties that could arise. You provided me with the necessary environment and support to conduct my research, and allowed me to use the software you, with previous students, had developed and refined for over more than two decades. Without your additions to the code, which tailored the software to my needs, the work contained in this book would have been of less quality. Our meetings were intense and consumed a significant amount of your time: Although in the morning we started at the faculty, the sessions were not seldom concluded late in the evening at your home. That to me is another example of your commitment to your students: Like the professors of long ago, you show an exceptional hospitality by welcoming us at your home and allowing us to enrich ourselves with your knowledge. Our discussions not seldom extended beyond the topic of laser-tissue interactions and formed lessons well in extent of the topic of the research. Thank you.

I'm indebted to the University of Wales and the University of Wales TSD for giving me the opportunity to pursue the research that is contained in this thesis. Special thanks go to Dr. Tim Bashford in particular. Tim, your contributions to the code and the increase in performance that resulted from them has allowed me to apply a much broader scope than would have otherwise been possible.

Furthermore, my gratitude goes to the two examiners, prof. Martin J.C. Van Gemert and dr. A. Marotin. Thank you for your time and effort while thoroughly reviewing of the manuscript, as well as your comments during the viva. Both the manuscript and myself have truly benefited from your insights and remarks.

Two persons who deserve separate mention: Prof. Peter Bjerring and prof. H.A. Martino Neumann. Over more than a few years you have granted me the privilege to benefit from your knowledge on dermatology, light therapy and related topics. You where always willing to answer my questions and patiently taught me what I needed or wanted

to learn. The advice you gave me has been instrumental to my understanding of light based therapies in dermatology. I would not be where I am today if it weren't for you.

Furthermore, I'd like to thank my colleagues at ZBC Multicare, an independent treatment centre for dermatology. Your continuous determination to provide patients with those treatments which are best suited to their needs, with a particular emphasis on light based therapies, has served both as an inspiration and benchmark for the research presented in this thesis. Thank you for your interest and your willingness to discuss my ideas, providing me with the feedback needed to validate the results of the calculations and refine the experiments were necessary.

I would never have been able to complete the thesis without the unwavering support from my parents and family. Mom and dad: you have stimulated me to look beyond the obvious, ask questions, walk the path less travelled and persist in the face of adversity. I knew I could always count on you when needed. Thank you for providing a sense of security and peace of mind so dire needed in the pursuit of scientific knowledge.

Last but not least my gratitude goes to my wife and children. Dear Suzanne, Lieke and Charlotte, although my work and this research has kept me from you more than you perhaps liked, the love and kindness I found at home has always provided me with peace of mind and encouragement. Thank you for filling my heart with joy and bringing a smile to my face. I hope that this work forms an inspiration for you to make the most of yourself, to stay curious, to never stop asking why, to dream the impossible, to push the boundaries of ignorance, and above all to have fun regardless of the required effort.